Reactivity of Co(III)-peroxo Complexes with NO and Co(II)-nitrosyl with H_2O_2: Putative Formation of Co-peroxynitrite

A dissertation submitted to the Indian Institute of Technology Guwahati as Partial fulfillment for the degree of Doctor of Philosophy in Chemistry

Submitted by

Bapan Samanta

(Roll No. 186122005)

Supervisor

Prof. Biplab Mondal

Department of Chemistry

Indian Institute of Technology Guwahati

Assam, India

June, 2024

Dedicated to the Memory

of

my Father

STATEMENT

I hereby declare that this thesis entitled "**Reactivity of Co(III)-peroxo Complexes with NO and Co(II)-nitrosyl with H_2O_2: Putative Formation of Co-peroxynitrite**" is the outcome of research work carried out by me under the supervision of Prof. Biplab Mondal in the Department of Chemistry, Indian Institute of Technology Guwahati, India.

In keeping with the general practice of reporting scientific observations, due acknowledgements have been made wherever the work described is based on the findings of other investigators.

Bapan Samanta

June, 2024 **Bapan Samanta**

IIT Guwahati

भारतीय प्रौद्योगिकी संस्थान गुवाहाटी
INDIAN INSTITUTE OF TECHNOLOGY GUWAHATI
North Guwahati, Assam – 781039, India

Dr. Biplab Mondal
Professor
Department of Chemistry

Phone : + 91-361-258-2317
Fax: + 91-361-258-2349
E-mail: biplab@iitg.ac.in

Certificate

This is to certify that **Mr. Bapan Samanta** has been working under my supervision since July, 2018 as a regular Ph.D. student in the Department of Chemistry, Indian Institute of Technology Guwahati. I am forwarding his thesis entitled "**Reactivity of Co(III)-peroxo Complexes with NO and Co(II)-nitrosyl with H_2O_2: Putative Formation of Co-peroxynitrite**" being submitted for the Ph.D. degree.

I certify that he has fulfilled all the requirements according to the rules of this Institute regarding the investigations embodied in his thesis and this work has not been submitted elsewhere for a degree.

June, 2024 **Biplab Mondal**

Acknowledgement

The research work that I had carried out throughout the past six years has been systematically placed into order in the form of this thesis. But there were many individuals behind the scenes, whose direct or indirect contribution has significantly influenced this thesis in various ways.

First, I must acknowledge the gracious presence of my supervisor, Prof. Biplab Mondal, during this most constructive period of my life. I believe that your guidance is the most instrumental input that has transformed me the best human. Your friendly approach and ever-presence for any kind of discussions is highly appreciated. Your rich guidance shall remain etched into me as a star, so that so it will shine my career throughout years to come. We experienced together all the ups and downs. I must be grateful for your moral support that made me more adamant to deal with the any challenges of my career. I shall remain indebted to you forever, for my success and achievement is the result of your support, guidance and motivation.

I am thankful to my doctoral committee members, Prof. Gopla Das sir, Dr. Kalyan Raidongia sir, Dr. Sunanda Chatterjee mam for their valuable tips and advices for the betterment of my research work.

Also I would like to thank all the teaching and non-teaching staff of the Department of Chemistry for their consistent help and support and IITG for the financial support. I acknowledge Central Instruments Facility (CIF) and Department of Chemistry for providing instrument facilities. Due acknowledge to IIT Guwahati for financial support and all the facilities.

I should thank all of my teachers whom I learnt since my childhood, I would not have been here without their guidance, blessing and support. Special mention from my graduation and masters days, viz. Chandrakanta Bandyopadhaya sir, Subhabrata Banerjee sir, Alakananda Hajra sir, Bijoy Krishna Dolui sir, Pranab Sarkar sir, Asim Kumar Das sir.

I have spent my most wonderful time in the CHEL004 lab. I extend my gratitude to my ever-helpful and cooperative seniors and labmates Dibya da, Baishakhi-di, Rakesh da, Shankhadeep, Riya, Sayani, Bristi, Mrinmoy and Risha for always being there and bearing

with me the good and bad times. Special thanks to Dibya da, Rakesh da and Riya for their assistance and camaraderie during the challenging moment of this journey. I would also like to thank all the project students whom I worked together.

I would also like to thank all my friends, Biswanath da, Bitan, Samir, Sujit, Abhishek, Sukdeb, Altaf, Prangobinda, Jitendra, Sandeep for their love and support. The list is endless…..thanks to one and all.

I owe my deepest gratitude to my betterhalf for her unwavering support and understanding of my goals and aspirations. Her patience, love and support has been source of my strength and it will continue to inspire me throughout my life. These few words are not enough to fully express my gratitude to Sanghamita.

Last but never the least, my family and loved ones. I feel profoundly fortunate to have the love and support of my parents, Late Shri Nepal Chandra Samanta and Smt. Mamoni Samanta, the blessings and affection from my grand-mother, Smt. Sandhya Rani Jana and support from my brother, Rahul Samanta. They have always been my side. I can never imagine reaching this stage without their endless support, motivation and sacrifices. I would also like to thank Shri Narayan Chandra Mondal for always believing in me.

I feel fortunate to have so many well-wishers around that it is difficult for me to name them all. I sincerely thank each of them for making me the person I am.

Bapan Samanta

Indian Institute of Technology Guwahati

List of Abbreviations

Abbreviations	Full name
NO	Nitric oxide
NO_2	Nitrogen dioxide
NO_2^-	Nitrite ion
NO_3^-	Nitrate ion
$ONOO^-$	Peroxynitrite ion
O_2	Oxygen
O_2^-	Superoxide ion
H_2O_2	Hydrogen peroxide
NEt_3	Triethylamine
BM	Bohr Magneton
ESI-mass	Electrospray Ionization Mass Spectrometry
UV-vis	UltraViolet-Visible Spectroscopy
NMR	Nuclear Magnetic Resonance
SC-XRD	Single-Crystal X-ray Diffraction
EPR	Electron Paramagnetic Resonance Spectroscopy
FT-IR	Fourier Transform Infrared Spectroscopy
ATR FT-IR	Attenuated Total Reflectance-Fourier Transform Infrared Spectroscopy
L1	*Bis*(3,5-dimethylpyrazolyl)methane
L2	*Tris*(3,5-dimethylpyrazol-1-yl-methyl)amine

L3	N^1,N^1-*bis*((3,5-dimethyl-1-pyrazol-1-yl)methyl)-N^2,N^2-dimethylethane-1,2-diamine
$TTMPP^{2-}$	5,10,15,20-*tetrakis*(3,4,5-trimethoxyphenyl) porphyrinate
L_a	Ortho-difluro substituted tetraarylporphyrinate
12-TMC	1,4,7,10-tetramethyl-1,4,7,10-tetraazacyclododecane
13-TMC	1,4,7,10-tetramethyl-1,4,7,10-tetraazacyclotridecane
14-TMC	1,4,8,11-tetramethyl-1,4,8,11-tetraazacyclotetradecane
BPI	*Bis*(pyridylimino)isoindol
Iz	*Bis*(2-ethyl-4-methyl-imidazol-5-yl)methane
Cl_4TPP^{2-}	5,10,15,20-*tetrakis*(4-chlorophenyl)porphyrinate
F_8TPP^{2-}	5,10,15,20-*tetrakis*(2,6-diflurophenyl)porphyrinate
$F_{20}TPP^{2-}$	5,10,15,20-*tetrakis*(pentaflurophenyl)porphyrinate
$TMPP^{2-}$	5,10,15,20-*tetrakis*(4-methoxyphenyl)porphyrinate
$UN\text{-}O^-$	2-(*bis*(2-(pyridin-2-yl)ethyl)amino)-6-((*bis*(2-(pyridin-2-yl)ethyl)amino)methyl)phenolate
N3PY	N^1,N^2-dimethyl-N^1-(2-(methyl(pyridin-ylmethyl) amino) ethyl)-N^2-(pyridin-2-ylmethyl)ethane-1-diamine
3PYENMe	N^1-methyl-N^1,N^2,N^2-*tris*(pyridine-2-ylmethyl)ethane-1,2-diamine

Contents

Synopsis

The thesis entitled "**Reactivity of Co(III)-peroxo Complexes with NO and Co(II)-nitrosyl with H_2O_2: Putative Formation of Co-peroxynitrite**" is divided into five chapters.

Chapter 1: Introduction

Nitric oxide (NO) is a diatomic colorless gas. Presence of one unpaired electron in the π* orbital makes it reactive in nature. NO is a signaling molecule. It regulates many biophysical processes such as neurotransmission, vasodilation and defense mechanism of the immune system etc. in mammalian biology.[1-4] Nitric oxide synthase (NOS) enzymes produce NO *via* oxidation of L-arginine to L-citrulline.[5,6] Excess production of NO can have detrimental effect *via* the formation of secondary reactive nitrogen species like nitrogen dioxide (NO_2) and peroxynitrite ($ONOO^-$), which leads to the oxidative and nitrosative stress.[7,8] When NO is produced in excess, it reacts with superoxide ion in a diffusion control reaction to form peroxynitrite anion. It plays a vital role in chemical modification of lipids, proteins and nucleic acids etc.[9-11] For instance, it leads to the protein tyrosine ring nitration.[12,13]

Nitric oxide dioxygenase (NOD) enzymes regulate the concentration of NO in biological systems. In NOD, a [Fe^{III}-O_2^-] complex reacts with NO to give biologically benign nitrate (NO_3^-).[14-16] This reaction has been proposed to proceed *via* the putative formation of peroxynitrite intermediate. This intermediate then decomposes to a [Fe^{IV}=O] species and NO_2 *via* the homolytic cleavage of the O-O bond of the proposed peroxynitrite intermediate followed by recombination which results in nitrate anion.

Transition metal ions are known to catalyze the formation and decomposition of peroxynitrite anions. Metal-peroxynitrite complexes are proposed to form in two pathways. Either in the reaction of metal nitrosyls with oxygen and reactive oxygen species such as superoxide (O_2^-)

and hydrogen peroxide (H_2O_2) or in the reaction of metal superoxo/peroxo complexes with NO.[17-24] For example, a Co(III)-peroxo complex, $[Co^{III}(Iz)_2(O_2^{2-})]^+$ {Iz = *bis*(2-ethyl-4-methyl-imidazol-5-yl)methane}, on reaction with NO resulted in corresponding nitrate complex through the formation of putative Co(II)-peroxynitrite intermediate.[23]

Our group reported a Cu-nitrosyl complex, $[Cu(Iz)_2(NO)](ClO_4^-)_2$, using the same ligand framework which reacts with H_2O_2 to form a corresponding Cu(I)-nitrate complex *via* a Cu(I)-peroxynitrite intermediate.[20]

The present thesis originates from our interest to explore the reactivity of the metal-peroxo complexes with NO and the reaction of metal-nitrosyl with reactive oxygen species. Thus, the subsequent chapters of this thesis describe the reactions of Co(III)-peroxo complexes of various ligand framework with NO gas where the involvement of peroxynitrite intermediates were observed. The change of reactivity pattern with ligand denticity has been studied. The last chapter describes the reaction of a Co-nitrosyl complex with H_2O_2 which presumably results in the corresponding peroxynitrite intermediate.

Chapter 2: Reaction of a Co(III)-peroxo Complex with Nitric Oxide: Putative Formation of a Peroxynitrite Intermediate

A Co(II)-complex, **2.1** was synthesized and characterized spectroscopically as well as structurally. The perspective ORTEP view is shown in figure **S1**. This complex **2.1** in the presence of H_2O_2 followed by NEt_3 in acetonitrile solution at -40 °C afforded corresponding Co(III)-peroxo intermediate, $[Co^{III}(L1)_2(O_2^{2-})]^+$, **2a** (Scheme **S1**). It showed an absorption band at 375 nm ($\epsilon/M^{-1}cm^{-1}$, 856) in UV-visible spectroscopic study (Figure **S1**). It was silent in the X-band EPR study as expected for a low spin Co(III) centre. The ESI-mass spectrum of the intermediate displayed a molecular ion peak at m/z 499.172, which is attributed to the mass of $[Co^{III}(L1)_2(O_2^{2-})]^+$ (Calcd. 499.198) (Figure **S2**).

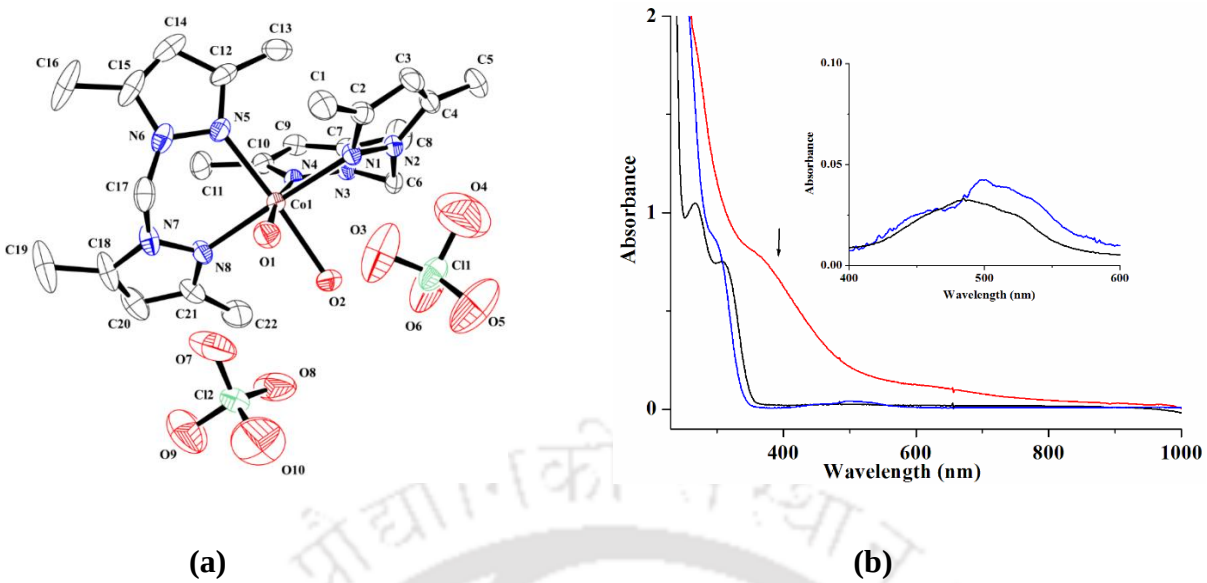

Figure S1. (a) ORTEP diagram of complex **2.1** (35% thermal ellipsoid plot, H-atoms are omitted for clarity). (b) UV-visible spectra of the reaction of complex **2.1** with H_2O_2 followed by NO, in acetonitrile at -40 °C [complex **2.1** (black), after addition of H_2O_2 (red) and after addition of NO (blue)].

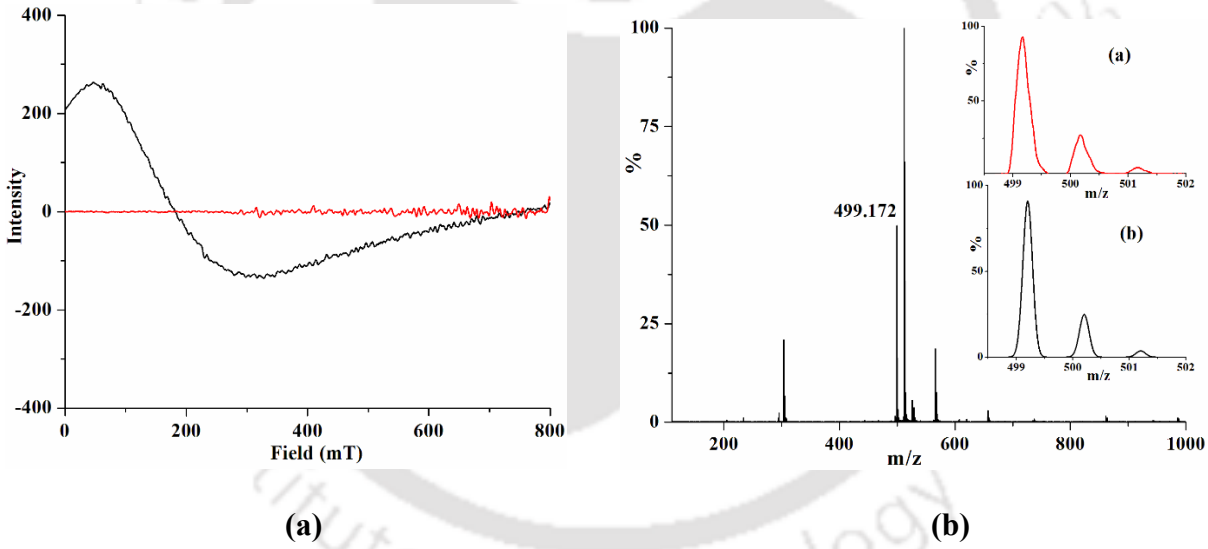

Figure S2. (a) X-band EPR study of the reaction of complex **2.1** (black) with H_2O_2 followed by NEt_3 in acetonitrile at 77 K [red, after the addition of H_2O_2]. (b) ESI-mass spectrum of Co(III)-peroxo intermediate in acetonitrile [Inset: (a) experimental and (b) simulated isotopic distribution pattern].

When NO gas was added into the freshly prepared Co(III)-peroxo solution at -40 °C followed by warming up to room temperature, the formation of the corresponding nitrate complex, $[Co^{III}(L1)_2(NO_3^-)]^+$, **2.2** was observed (Scheme **S1**). The ORTEP diagram of complex **2.2** is shown in figure **S3**.

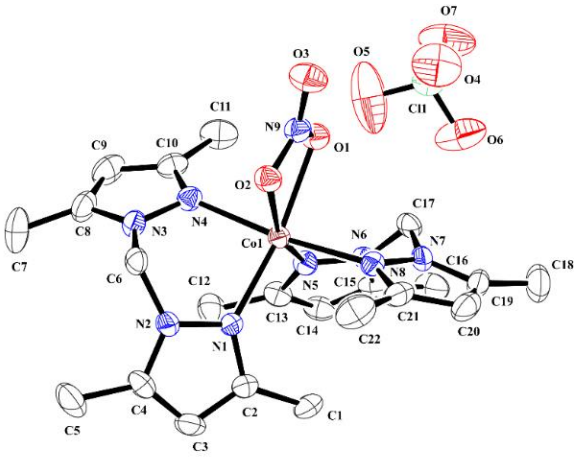

Figure S3. ORTEP diagram of complex **2.2** [35% thermal ellipsoid plot, solvent molecule and H-atoms are omitted for clarity].

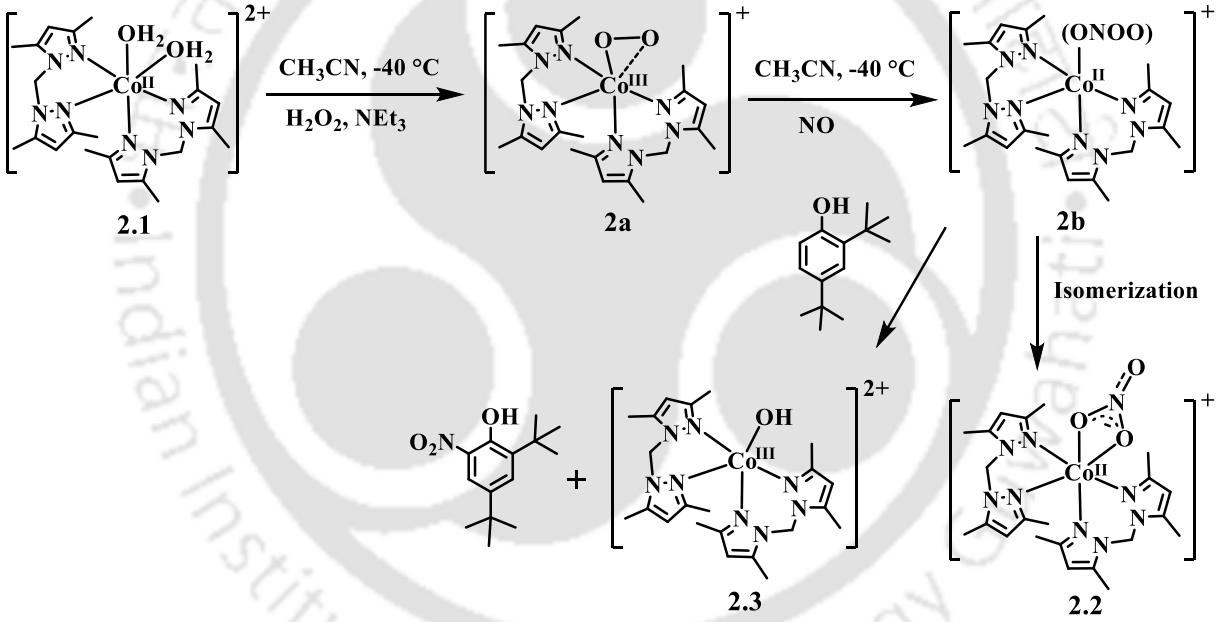

Scheme S1. Overall reactions.

Due to the thermal instability of the peroxynitrite intermediate, direct spectroscopic evidence was not found. Hence, chemical evidence was sought for the formation of peroxynitrite intermediate.[19-22] When NO gas was added to the freshly generated Co(III)-peroxo solution at -40 °C in the presence of 2,4-di-*tert*-butylphenol, corresponding nitrophenol was obtained along with Co(III)-hydroxo complex, **2.3** (Scheme **S1**). However, when 2,4-di-*tert*-butyl

phenol was added after addition of NO gas into the solution of Co(III)-peroxo complex, no phenol ring nitration was observed owing to the first isomerization of the peroxynitrite complex to nitrate.

Hence, a Co(II)-complex, **2.1** having a bidentate ligand framework was synthesized and characterized. Complex **2.1** in the presence of H_2O_2 afforded Co(III)-peroxo species. This upon reaction with NO gas resulted in corresponding nitrate complex, **2.2** *via* a peroxynitrite intermediate.

Chapter 3: Reaction of a Co(III)-peroxo Complex of Symmetric Tetradentate Ligand Framework with Nitric Oxide: Putative Formation of a Peroxynitrite Intermediate

Complex **3.1**, $[Co^{II}(L2)(CH_3CN)]^{2+}$ with a tripodal tetradentate ligand framework was synthesized having perchlorate as counter anion. It was prepared by constant stirring of a mixture of Co(II)-perchlorate hexahydrate and the ligand **L2** in equivalent amount in acetonitrile. It was then characterized both spectroscopically and structurally. Structural studies confirmed that the cobalt centre is coordinated to four nitrogen atoms from the ligand and one acetonitrile molecule in a distorted trigonal bipyramidal geometry (Figure **S4**). The reaction of complex **3.1** with H_2O_2 in acetonitrile solution at -40 °C leads to the formation of corresponding Co(III)-peroxo intermediate, **3a** (Scheme **S2**). In UV-visible spectral monitoring, the characteristic absorption band for Co(III)-peroxo species appeared at 340 nm (Figure **S4**).

The EPR silent nature of this intermediate suggests the +3 oxidation state of the cobalt centre (Figure **S5**). In ESI-mass spectrum this intermediate species in acetonitrile solution displayed a molecular ion peak at m/z 432.157 (Calcd. 432.156 for $[Co^{III}(L2)(O_2^{2-})]^+$) (Figure **S5**).

Reaction of NO gas with freshly generated Co(III)-peroxo species in acetonitrile solution at

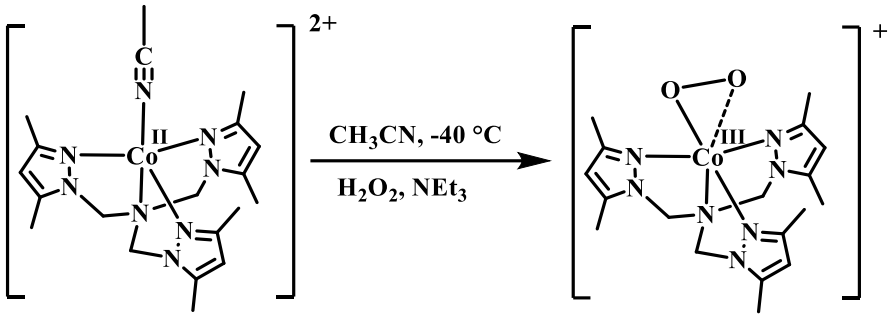

Scheme S2.

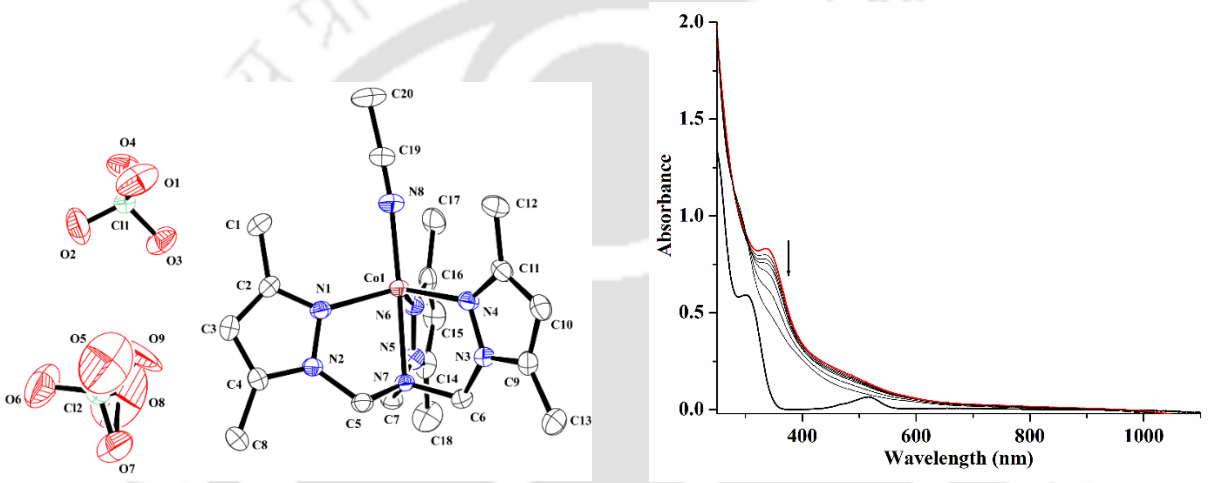

(a) **(b)**

Figure S4. (a) ORTEP diagram of complex **3.1** [35% thermal ellipsoid plot, solvent molecule and H-atoms are omitted for clarity]. (b) UV-visible spectra of the reaction of complex **3.1** with H_2O_2 in acetonitrile at −40 °C [Complex **3.1** (black), after addition of H_2O_2 (red)].

-40 °C resulted in the corresponding nitrate complex, **3.2** (Scheme **S3**). ORTEP diagram of complex **3.2** is shown in figure S6. The crystal structure of complex **3.2** revealed that the cobalt centre is bonded to four nitrogen atoms from the ligand and one nitrate group in a distorted trigonal bipyramidal geometry. This reaction presumably proceeds through the formation of the corresponding peroxynitrite intermediate.

However, no spectroscopic evidence was observed due to the thermal instability of the peroxynitrite intermediate. As a characteristic test, precooled acetonitrile solution of 2,4-di-

tert-butylphenol was added to the freshly prepared Co(III)-peroxo species in acetonitrile solution at -40 °C followed by addition of NO gas and 2,4-di-*tert*-butyl-6-nitrophenol along with Co(III)-hydroxo complex were obtained. Formation of nitration product suggests the involvement of peroxynitrite intermediate in the course of the reaction.

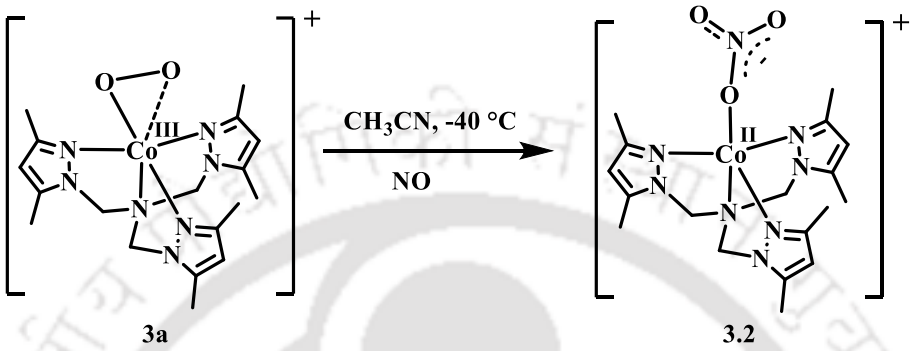

Scheme S3.

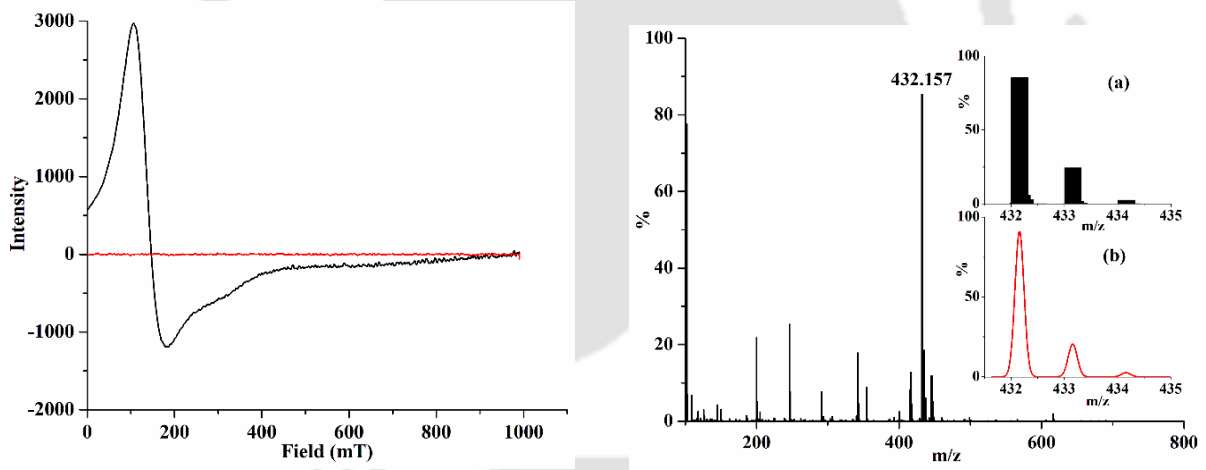

(a) **(b)**

Figure S5. (a) X-band EPR spectral monitoring of the reaction of complex **3.1** (black) with H_2O_2 in acetonitrile at 77 K [red, after the addition of H_2O_2]. (b) ESI-mass spectrum of Co(III)-peroxo intermediate, **3a** in acetonitrile [Inset: (a) experimental (b) simulated isotopic distribution pattern].

Thus, a Co(III)-peroxo species was generated in the reaction of a Co(II)-complex with H_2O_2 in the presence of NEt_3. This peroxo species upon reaction with NO gas results in the corresponding nitrate complex, **3.2** *via* a putative peroxynitrite intermediate.

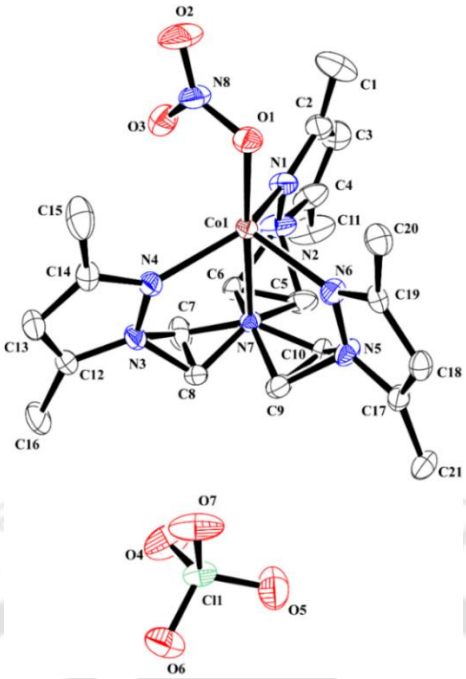

Figure S6. ORTEP diagram of complex **3.2** (35% thermal ellipsoid plot, solvent molecule and H-atoms are omitted for clarity).

Chapter 4: Reaction of a Co(III)-peroxo Complex of an Assymetric Tetradentate ligand with Nitric Oxide: Putative Formation of a Peroxynitrite Intermediate

In this chapter, an assymetric tetradentate tripodal ligand has been used. A Co(II)-complex, $[Co^{II}(L3)(CH_3CN)]^{2+}$, **4.1**, having tetradentate ligand L3 has been synthesized and characterized using various spectroscopic techniques as well as single X-ray crystal structure determination. The ORTEP diagram of complex **4.1** is shown in figure S7. The crystal structure of complex **4.1** revealed that the cobalt centre is coordinated to four nitrogen atoms from the ligand and one acetonitrile molecule in a distorted trigonal bipyramidal geometry.

Complex **4.1** in acetonitrile solution at -40 °C in the presence of H_2O_2 and NEt_3 leading to an intermediate species, $[Co^{III}(L3)(O_2^{2-})]^{+}$, **4a** (Scheme **S4**). Thermal instability precluded its isolation and further characterization. In UV-visible spectroscopic monitoring, the appearance

of the transient absorption band at 440 nm suggests the formation of Co(III)-peroxo complex (Figure **S7**). The intensity of the band decreases with time suggesting the instability of peroxo

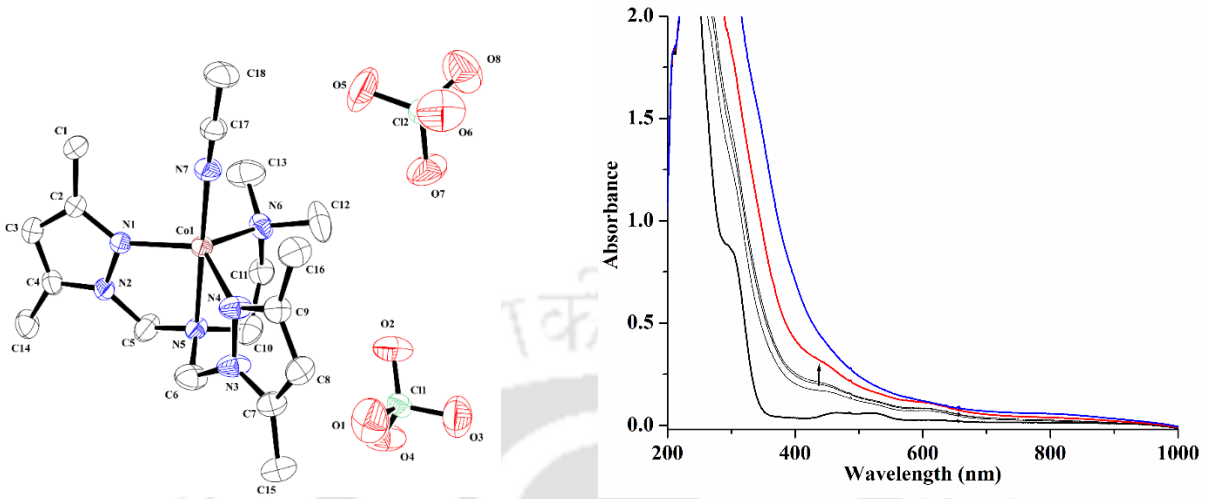

(a) **(b)**

Figure S7. (a) ORTEP diagram of complex **4.1** [35% thermal ellipsoid plot, solvent molecule and H-atoms are omitted for clarity]. (b) UV-visible spectra of the reaction of complex **4.1** with H_2O_2 in acetonitrile at -40 °C [complex **4.1** (black), after addition of H_2O_2 (red), final (blue)].

complex. In X-band EPR spectroscopy, the intermediate **4a** was silent as expected for Co(III)-peroxo species having low spin Co(III)-centre (Figure **S8**). In ESI-mass spectrometry, this intermediate **4a** displayed molecular ion peak at m/z 395.162, which is attributed to the mass of $[Co^{III}(L3)(O_2^{2-})]^+$ (Calcd. 395.160).

When NO gas was bubbled into the freshly generated Co(III)-peroxo intermediate, **4a** $[Co^{III}(L3)(O_2^{2-})]^+$ in dry and degassed acetonitrile solution at -40 °C followed by warm up to room temperature, formation of the corresponding nitrite complex **4.2,** $[Co^{II}(L3)(NO_2^-)]^+$ was observed along with molecular oxygen (Scheme **S5**). The formation of molecular oxygen was confirmed by the alkaline pyrogallol test. The ORTEP diagram of complex **4.2** is shown in figure **S9**. The crystal structure of complex **4.2** revealed that cobalt centre is coordinated to four nitrogen atoms from the ligand in a distorted octahedral geometry where one nitrite group is bonded in a η^2-O fashion.

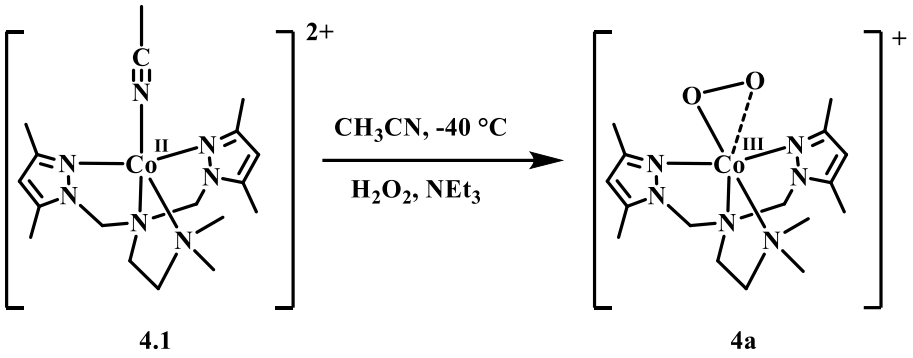

Scheme S4.

The reaction is proposed to proceed through the formation of the corresponding peroxynitrite intermediate. However, due to transient nature of peroxynitrite intermediate, direct spectroscopic evidence was not observed. Hence, the chemical evidence was sought to establish the involvement of the peroxynitrite intermediate in the course of the reaction. When NO gas was added to the freshly generated complex **4a** in acetonitrile at -40 °C in the presence of 2,4-di-*tert*-butylphenol, ring nitration was observed (*ca*. 60%) along with formation of

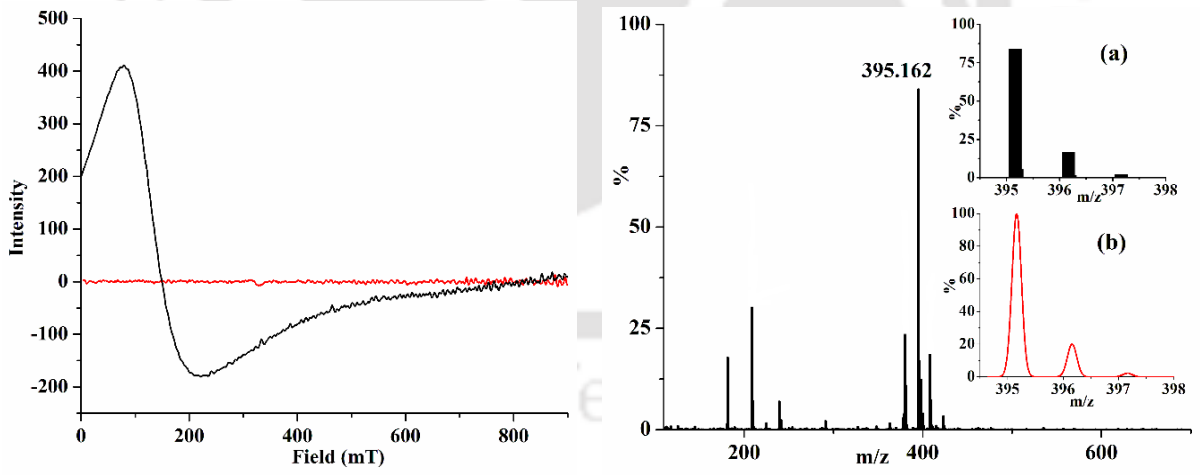

(a) **(b)**

Figure S8. (a) X-band EPR spectral monitoring of the reaction of complex **4.1** (black) with H_2O_2 in acetonitrile at 77 K [red, after the addition of H_2O_2]. (b) ESI-mass spectrum of Co(III)-peroxo intermediate, **4a** in acetonitrile [Inset: (a) experimental (b) simulated isotopic distribution pattern].

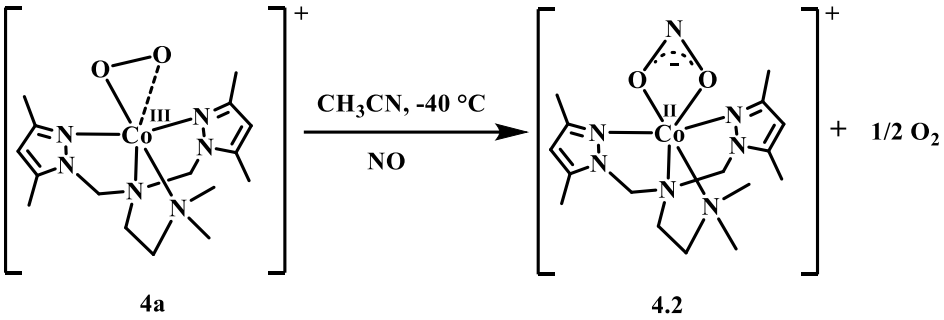

Scheme S5.

Co(III)-hydroxide complex **4.3**, indicating the involvement of the peroxynitrite intermediate in the course of the reaction.

In conclusion, a cobalt(II) complex, **4.1** has been synthesized. The reaction of complex **4.1** with H_2O_2 in the presence of NEt_3 in acetonitrile solution at -40 °C afforded corresponding

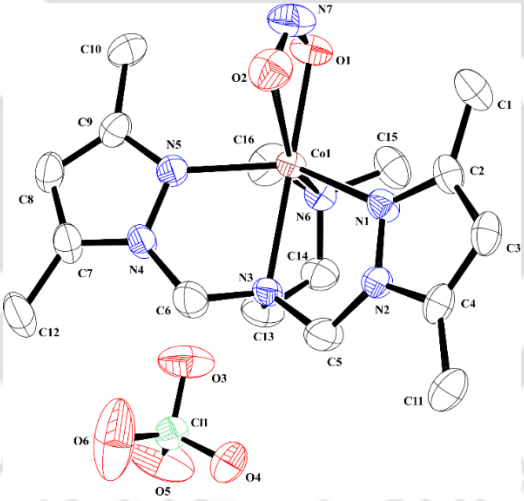

Figure S9. ORTEP diagram of complex **4.2** (35% thermal ellipsoid plot, solvent molecule and H-atoms are omitted for clarity).

Co(III)-peroxo, **4a** intermediate. This intermediate in the presence of NO gas yielded nitrite complex, **4.2**. Characteristic phenol ring nitration reaction suggests the involvement of a peroxynitrite intermediate in the course of the reaction.

Chapter 5: Reaction of a Nitrosyl Complex of Co(II)-porphyrin with Hydrogen Peroxide: Formation of a Porphyrin Radical Cation

The precursor complex, [Co^{II}($TTMPP^{2-}$)], **5.1a** was synthesized by following a reported procedure.[25] Complex **5.1a** was characterized spectroscopically using UV-visible, FT-IR, EPR spectroscopy and ESI-mass spectrometry. The single crystal structure of complex **5.1a** shows square planar geometry around the cobalt centre (Figure **S10**). The reaction of complex **5.1a** with H_2O_2 was carried out in order to generate the corresponding peroxo species. However, no spectroscopic evidences was obtained in support of the formation of it. Hence, the corresponding nitrosyl complex was prepared to study it's reactivity with H_2O_2. The nitrosyl complex [Co($TTMPP^{2-}$)(NO)], **5.1** was synthesized by addition of NO gas in the degassed dichloromethane solution of complex **5.1a**. It was isolated as red solid and characterized spectroscopically as well as structurally. The perspective ORTEP view of complex **5.1** shows that the cobalt center is coordinated to four nitrogen atoms of porphyrin ring and NO group is bonded axially to result in a square pyramidal geometry (Figure **S10**). The N-O bond lengths is 1.218(9) Å and Co-N-O bond angle is 141.6(6)° which matches well with the reported complexes.[23] The FT-IR spectrum of complex **5.1** shows nitrosyl stretching frequency at 1675 cm^{-1}. This value matches well with the other reported analogues complexes.[23] Owing to the antiferromagnetic coupling between NO group and Co(II)-centre, complex **5.1** becomes EPR silent. It shows well resolved ^{1}H-NMR spectrum confirming the diamagnetic nature.

The reaction of 1.5 mole equivalent H_2O_2 with complex **5.1** in dichloromethane:acetonitrile (1:4, v/v) solution yielded the corresponding nitrite complex, [Co^{III}($TTMPP^{2-}$)(NO_2^-)], **5.2** as final product (Scheme **S6**). Complex **5.2** was isolated and characterized spectroscopically as well as structurally. FT-IR spectrum of complex **5.2** shows a strong stretching frequency at 1259 cm^{-1}, suggesting the presence of nitrite group. This is further confirmed by ESI-mass spectrometric analysis. Its shows a molecular ion peak at 1077.282 (Calcd. 1077.284 for

[Co^{III}($TTMPP^{2-}$)(NO_2^-)]). The EPR silent nature and well resolved ^{1}H-NMR spectrum of complex **5.2** suggest that the cobalt centre is in +3 oxidation state.

In UV-visible spectroscopy, complex **5.1** in dichloromethane:acetonitrile (1:4, v/v) solution shows characteristic soret band at 418 nm and Q band at 537 nm at -40 °C. Addition of precooled 1.5 mole equivalent H_2O_2 to this solution shows immediate shift of the soret band maxima to 434 nm and Q band at 543 nm. The absorption band at 434 nm was further shifted to 458 nm with a quenching of intensity. A new set of absorption bands appeared at 712, 818 and 926 nm. Here, the transient absorptions at 434 nm and 542 nm are attributed to a [Co^{IV}=O] species.[26] This rapidly isomerizes to corresponding porphyrin radical cation complex as evidenced by the quenching of the soret band in UV-visible spectroscopy (Figure **S11**)[27]. In X-band EPR spectroscopic analysis of the frozen reaction mixture of complex **5.1** and H_2O_2 in

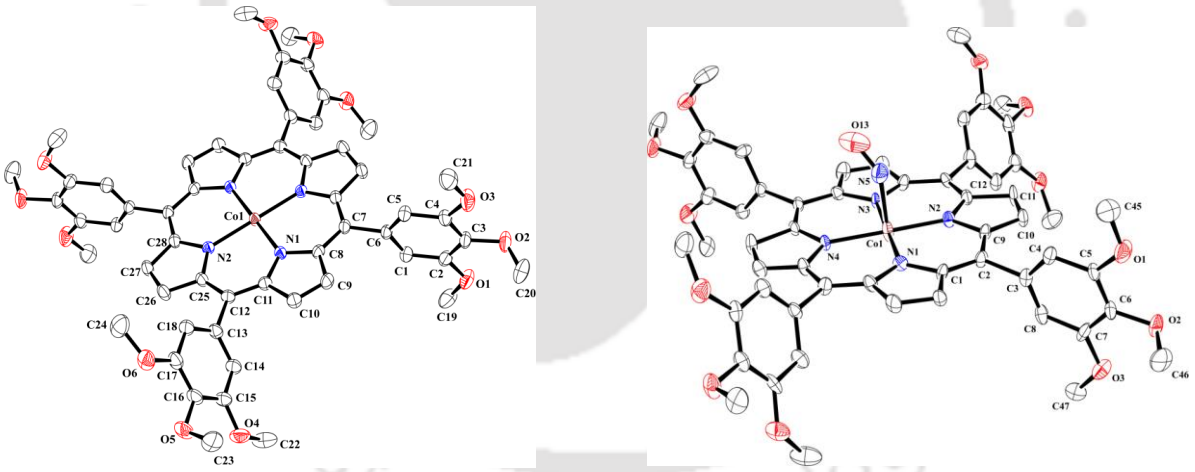

(a) **(b)**

Figure S10. ORTEP diagram of complex (a) **5.1a** and (b) **5.1** [35% thermal ellipsoid plot, solvent molecule and H-atoms are omitted for clarity].

dichloromethane:acetonitrile (1:4, v/v) solution shows a sharp isotropic signal at g ~ 2.001 which confirms the generation of a radical species in the reaction mixture. When this reaction mixture brought to room temperature, the signal was disappeared due to the formation of

complex **5.2** (Figure **S11**). The ESI-mass spectrum of the reaction mixture displays a peak at 1048.29 which is assignable to the [Co^{III}(TTMPP^{2-})(O)] moiety (Calcd. 1047.21).

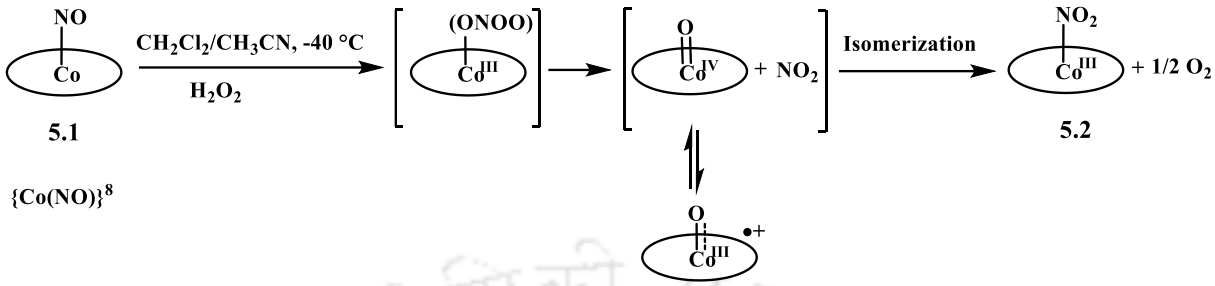

Scheme S6.

To confirm the formation of peroxynitrite intermediate in the reaction medium, complex **5.1,** are allowed to react with H_2O_2 in the presence of 2,4-di-*tert*-butylphenol. Appreciable amount

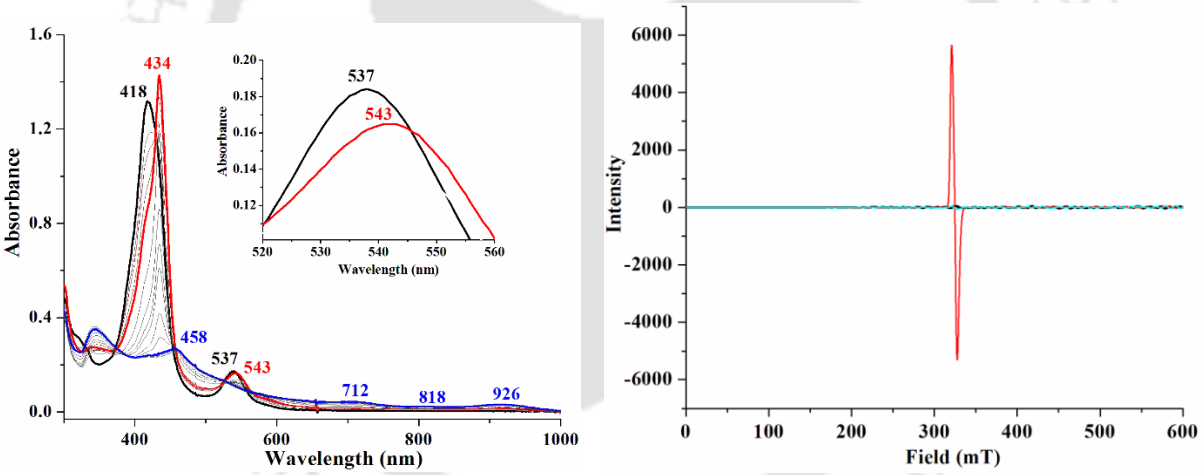

Figure S11. (a) UV-visible spectral monitoring of the reaction of complex **5.1** with H_2O_2 [complex **5.1** (black), after addition of H_2O_2 (red), final product (blue) in dichloromethane:acetonitrile (1:4, v/v) solution at -40 ºC]. (b) X-band EPR spectral monitoring of the reaction of complex **5.1** with H_2O_2 in dichloromethane:acetonitrile (1:4, v/v) solution at 77 K [complex **5.1** (black), intermediate (red) and complex **5.2** (green)].

of (*ca*. 60%) 2,4-di-*tert*-butyl-6-nitrophenol and corresponding Co(III)-hydroxide were obtained from the final reaction mixture.

Thus, the nitrosyl complex, **5.1** reacts with H_2O_2 to give corresponding nitrite complex **5.2**. Involvement of the corresponding Co(III)-peroxynitrite intermediate was presumed during the reaction.

References

1. Ignarro, L. J. *Nitric Oxide: Biology and Pathobiology*; Ed.; Academic Press: San Diego, **2000**.
2. Fang, F. C. *Nitric Oxide and Infection*; Ed., Kluwer Academic/ Plenum Publishers: New York, **1999**.
3. Bourassa, J. L.; Ives, E. P.; Marqueling, A. L.; Shimanovich, R.; Groves, J. T. *J. Am. Chem. Soc*. **2001**, *123*, 5142.
4. (a) Lehnert, N.; Kim, E.; Dong, H. T.; Harland, J. B.; Hunt, A. P.; Manickas, E. C.; Oakley, K. M.; Pham, J.; Reed, G. C.; Alfaro, V. S. *Chem. Rev*. **2021**, *121*, 14682. (b) Gantner, B. N.; Lafond, K. M.; Bonini, M. G. *Redox. Biol*. **2020**, *34*, 101550. (c) Horst, G.; Marletta, M. A. *Nitric Oxide*, **2018**, *77*, 65.
5. Marietta, M. A.; Yoon, P. S.; Iyengar, R.; Leaf, C. D.; Wishnok, J. S. *Biochemistry,* **1988**, *27,* 8706.
6. (a) Stuehr, D. J. *Annu. Rev. Pharmacol. Toxicol*. **1997**, *37*, 339. (b) Gorren, A. C. F.; Mayer, B. *Biochim. Biophys. Acta, Gen. Subj*. **2007**, *1770*, 432. (c) Santolini, J. *J. Inorg. Biochem*. **2011**, *105*, 127. (d). Childers, K. C.; Garcin, E. D. eLS, John Wiley & Sons, Ltd. *Chichester*, **2017**, 1.
7. Pacher, P.; Beckman, J. S.; Liaudet, L. *Physiol. Rev*. **2007**, *87*, 315.
8. Beckman, J. S.; Koppenol, W. H. *Am. J. Physiol*. **1996**, *271*, 1424.
9. Radi, R. *Chem. Res. Toxicol*. **1998**, *11*, 720.
10. Szabo, C.; Ischiropoulos, H.; Radi, R. *Nat. rev. drug. Discov*. **2007**, *6*, 662.

11. (a) Beal, M. F. *Free Radic. Biol. Med*. **2002**, *32*, 797. (b) Radi, R.; Cassina, A.; Hodara, R.; Quijano, C.; Castro, L. *Free Radic. Biol. Med*. **2002**, *33*, 1451.
12. Beckman, J. S.; Ischiropoulos, H.; Zhu, L.; Woerd, M.; Smith, C.; Chen, J.; Harriso, J.; Martin, J. C.; Tsai, M. *Arch. Biochem. Biophys*. **1992**, *298*, 438.
13. Beckmann, J. S.; Ye, Y. Z.; Anderson, P. G.; Chen, J.; Accavitti, M. A.; Tarpey, M. M.; White, C. R. *J. Biol. Chem.* **1994**, *375*, 81.
14. Balagopalakrishna, C.; Abugo, O. O.; Horsky, J.; Manoharan, P. T.; Nagababu, E.; Rifkind, J. M. *Biochemistry*, **1998**, *37*, 13194.
15. Singha, A.; Das, P. K.; Dey, A. *Inorg. Chem*. **2019**, *58*, 10704.
16. Yan, J. J.; Kroll, T.; Baker, M. L.; Wilson, S. A.; Decréau, R.; Lundberg, M.; Sokaras, D.; Glatzel, P.; Hedman, B.; Hodgson, K. O.; Solomon, E. I. *Proc. Natl. Acad. Sci. U. S. A*. **2019**, *116*, 2854.
17. Cao, R.; Elrod, L. T.; Lehane, R. L.; Kim, E.; Karlin, K. D. *J. Am. Chem. Soc*. **2016**, *138*, 16148.
18. Gogoi, K.; Saha, S.; Mondal, B.; Deka, H.; Ghosh, S.; Mondal, B. *Inorg. Chem*. **2017**, *56*, 14438.
19. Mazumdar, R.; Mondal, B.; Saha, S.; Samanta, B.; Mondal, B. *J. Inorg. Biochem*. **2022**, *228*, 111698.
20. Kalita, A.; Kumar, P.; Mondal, B. *Chem. Commun*. **2012**, *48*, 4636.
21. Schopfer, M. P.; Mondal, B.; Lee, D. H.; Sarjeeant, A. A. N.; Karlin, K. D. *J. Am. Chem. Soc*. **2009**, *131*, 11304.
22. Yokoyama, A.; Cho, K. B.; Karlin, K. D.; Nam, W. *J. Am. Chem. Soc*. **2013**, *135*, 14900.
23. Saha, S.; Ghosh, S.; Gogoi, K.; Deka, H.; Mondal, B.; Mondal, B. *Inorg. Chem*. **2017**, *56*, 10932.

24. Yokoyama, A.; Han, J. E.; Cho, J.; Kubo, M.; Ogura, T.; Siegler, M. A.; Karlin, K. D.; Nam, W. *J. Am. Chem. Soc*. **2012**, *134*, 15269.

25. Kadish, K. M.; Araullo, M. C.; Han, B. C.; Franzen, M. M. *J. Am. Chem. Soc*. **1990**, *112*, 8364.

26. Mazumdar, R.; Saha, S.; Samanta, B.; Ghosh, R.; Maity, S. *Dalton Trans.* **2023**, *52*, 7917.

27. (a) Dey, S.; Sil, D.; Rath, S. P. *Angew. Chem*. **2016**, *128*, 1008. (b) Hong, S.; Pfaff, F. F.; Kwon, E.; Wang, Y.; Seo, M. S.; Bill, E.; Ray, K.; Nam, W. *Angew. Chem. Int. Ed.*, **2014**, *53*, 10403. (c) Ikezaki, A.; Takahashi; Nakamura, M. *Chem. Commun*. **2013**, *49*, 3098. (d) Ichimori, K.; Nishiguchi, H. O.; Hirota, N.; Yamamoto, K. *Bull. Chem. Soc. Jpn*. **1985**, *58*, 623.

Chapter 1

Introduction

1.1 General aspect of peroxynitrite ion

Nitric oxide (NO) is a colorless, diatomic gas. Having one unpaired electron in the π* orbital renders it reactive in nature. Since a long time NO has been used as a ligand and because of its redox active nature, it shows different oxidation states such as NO^+, $NO^\bullet$, NO^-, upon coordination to transition metal centre.[1-5] In mammalian biology, NO is generated by nitric oxide synthase enzymes *via* the oxidation of L-arginine into citrulline and NO.[6,7] It has been found that NO regulates various physiological processes like blood flow, neurotransmission and immune response etc.[8-10] However when NO is produced in excess, it reacts with superoxide ion (O_2^-) in a diffusion controlled rate to yield peroxynitrite anion ($ONOO^-$) (Eq. **1.1**).[11,12] Peroxynitrite can also form through the reaction of H_2O_2 and nitrite (NO_2^-) in the presence of peroxidase enzymes.[13,14] Peroxynitrite having half-life less than 10 ms, causes oxidative and nitrosative stress. It mediates oxidation and nitrosation of biomolecules, causing a diverse chemical modification of lipids, proteins and nucleic acids etc.[11,15-17] For example, it reacts directly with thiols through a two-electron oxidation process to produce a disulfide.[18] Protonated form of peroxynitrite, due to its transient nature, homolytically cleaves to OH and NO_2 radicals. NO_2 reacts with sugar to give polymerization and fragmentation products.[15-17] It also affects the DNA bases such as guanine, where oxidation of guanine converts to 8-nitro guanine.[16-17] Whereas, hydroxyl radical damages the DNA strand. Peroxynitrite can also reacts with CO_2 to form a transient species nitroso-peroxocarbonate ($ONOOCO_2^-$).[19] This species decomposed to NO_2 and $CO_3^{\bullet-}$ radicals which act as one electron oxidizing agent.

$$NO + O_2^- \longrightarrow ONOO^- \qquad \text{(Eq. 1.1)}$$

An essential component of peroxynitrite-mediated toxicity is the nitration of protein tyrosine residues.[20-22] It does not directly interact with tyrosine, rather it first decomposes to NO_2 radical which finally gives rise to nitration product.[23] This nitration of phenol ring takes place in two steps. First one H atom of tyrosine is abstracted by physiologically active oxidants like $CO_3^{\bullet-}$ or metal-oxo to form a tyrosyl radical. Then this radical in the presence of NO_2 converted to 3-nitro tyrosine. The formation of 3,3'-dityrosine through the dimerization of tyrosyl radicals hinders the normal function of proteins.[23]

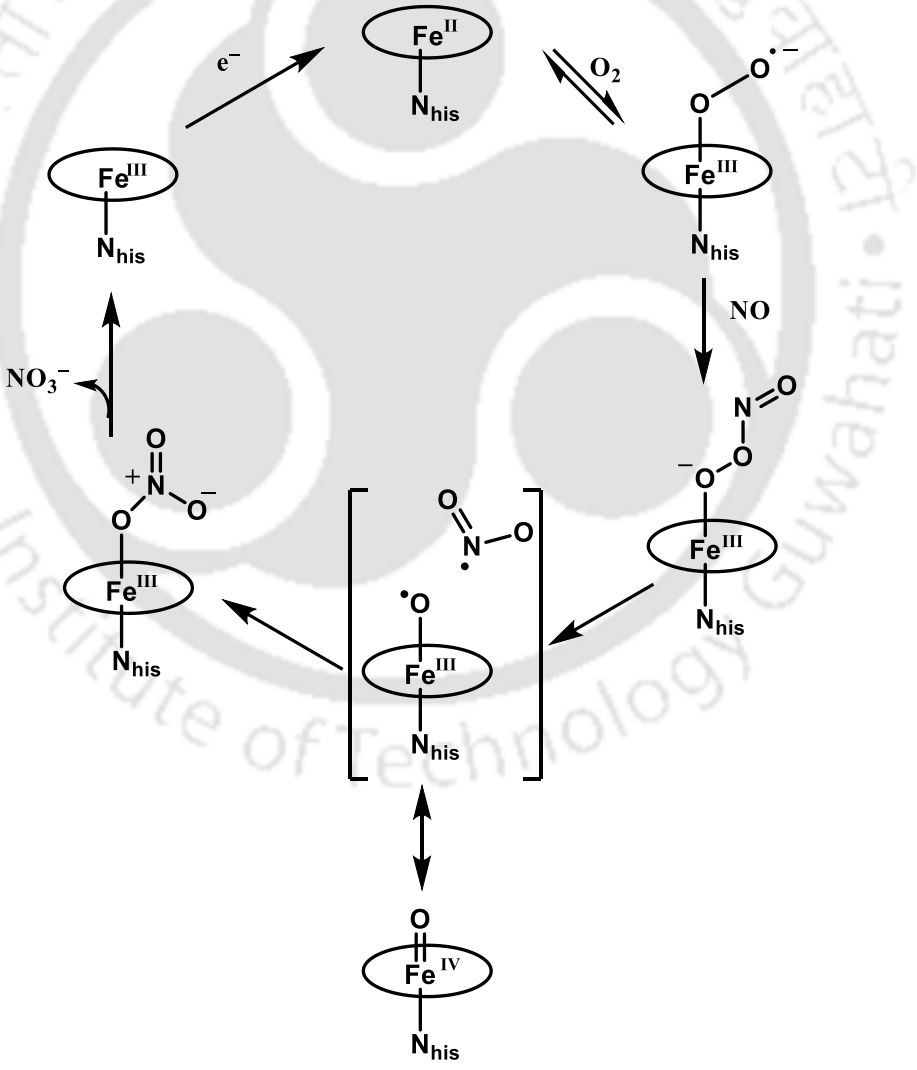

Scheme 1.1 Proposed mechanism for the nitric oxide dioxygenase (NOD) activity.

Nitric oxide dioxygenase enzymes (NODs) control the overproduction of NO *in vivo* by transforming it into the biologically benign nitrate (NO_3^-) ion.[24-32] In this process, it is proposed that an Fe(III)-superoxide species reacts with NO to form a Fe(III)-peroxynitrite intermediate. This intermediate is short lived and rapidly isomerizes to Fe(III)-nitrate complex (Scheme **1.1**).

1.2 Literature study

1.2.1 Reaction of metal-nitrosyl complexes with reactive oxygen species

The formation of metal-peroxynitrite was first reported by Basolo and Clarkson.[33] A cobalt nitrosyl complex on ethylenediamine ligand framework upon reaction with molecular oxygen results in corresponding nitrite complex. It has been proposed that the reaction proceeds through the formation of corresponding peroxynitrite intermediate though no evidence was given (Scheme **1.2**).

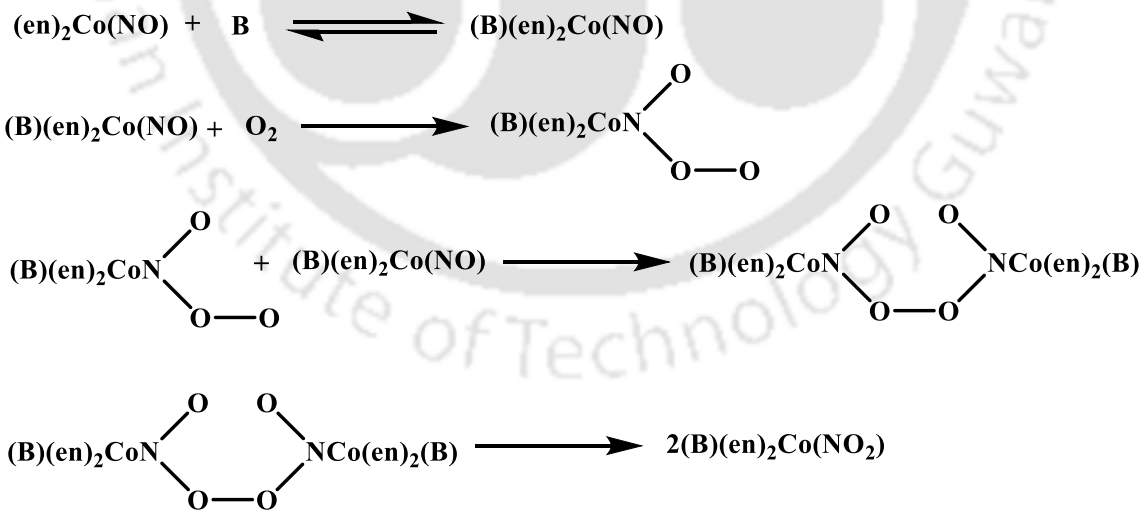

B = nitrogen or phosphorus base
en = ethylenediamine

Scheme 1.2

The Karlin group described a mixed valent di-copper nitrosyl system $[Cu^{I,II}_2(UN\text{-}O^-)(NO)]^{2+}$, {UN-$O^-$ = 2-(*bis*(2-(pyridin-2-yl)ethyl)amino)-6-((*bis*(2-(pyridin-2-yl)ethyl)amino)methyl) phenolate}, which reacts with O_2 in dichloromethane solution at -80 ºC to form a one electron oxidized species $[Cu^{II}_2(UN\text{-}O^-)(O_2^-)(NO)]^{2+}$. In the next step, the generation of a peroxynitrite intermediate was proposed (Scheme **1.3**).[34]

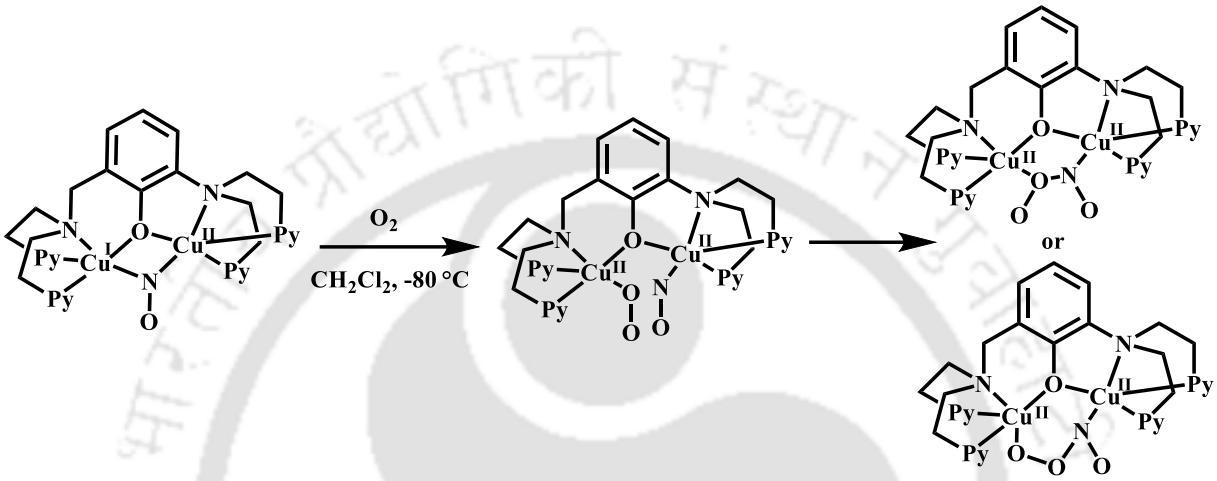

Scheme 1.3

A Co-nitrosyl complex, [Co(BPI)(NO)(OAc)], {BPI = *bis*(pyridylimino)isoindol} was reported which upon exposure to O_2, transformed into its corresponding nitrite complex, $[Co^{III}(BPI)(NO_2^-)(OAc)]$ (Scheme **1.4**).[35] In this instance, a six-coordinated intermediate species $[Co^{III}(BPI)(NO)(O_2^-)(OAc)]$, was observed during the reaction. The formation of a Co-peroxynitrite intermediate was presumed.

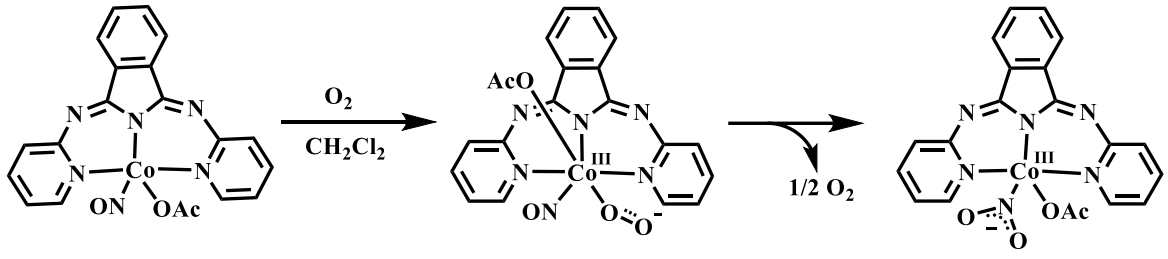

Scheme 1.4

In another report, a Co-nitrosyl complex, $[Co(F_{20}TPP^{2-})(NO)]$, {$F_{20}TPP^{2-}$ = 5,10,15,20-*tetrakis*(pentaflurophenyl)porphyrinate} was shown to afford the corresponding $[Co^{III}(F_{20}TPP^{2-})(NO_2^-)]$ complex in the presence of superoxide ion in dichloromethane at -40 °C. The involvement of a Co(II)-peroxynitrite intermediate was proposed. Spectroscopic analyses suggested the formation of $[Co(F_{20}TPP^{2-})(NO)(O_2^-)]$ species in the reaction medium (Scheme **1.5**).[36]

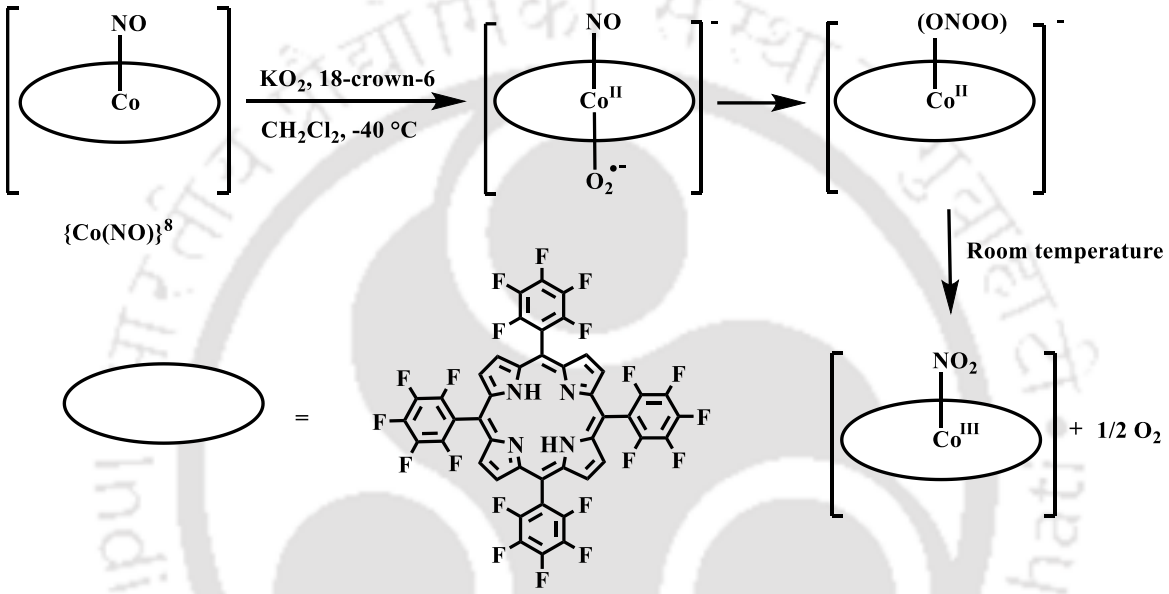

Scheme 1.5

A Cu-nitrosyl complex, $[Cu(Iz)_2(NO)](ClO_4^-)_2$ {Iz = *bis*(2-ethyl-4-methyl-imidazol-5-yl)methane} was reported to react with H_2O_2 in acetonitrile at -20 °C to result in the corresponding Cu(I)-nitrate complex $[Cu^I(Iz)_2(NO_3^-)]$ *via* a Cu(I)-peroxynitrite intermediate (Scheme **1.6**).[37] The generation of the Cu(I)-peroxynitrite was confirmed through the characteristic phenol ring nitration test. The $[Cu^I(Iz)_2(NO_3^-)]$ complex was converted to the corresponding $[Cu^{II}(Iz)_2(NO_3^-)]$ in the presence of O_2.

Nam group published two Co-nitrosyl complexes, $[Co(12\text{-}TMC)(NO)]^{2+}$ and $[Co(13\text{-}TMC)(NO)]^{2+}$, {12-TMC = 1,4,7,10-tetramethyl-1,4,7,10-tetraazacyclododecane) and

(13-TMC = 1,4,7,10-tetramethyl-1,4,7,10-tetraazacyclotridecane} which did not react with molecular oxygen but reacted with superoxide, resulting in the formation of the respective Co(II)-nitrite complexes and O_2 (Scheme **1.7**).[38] Co(II)-peroxynitrite intermediate was

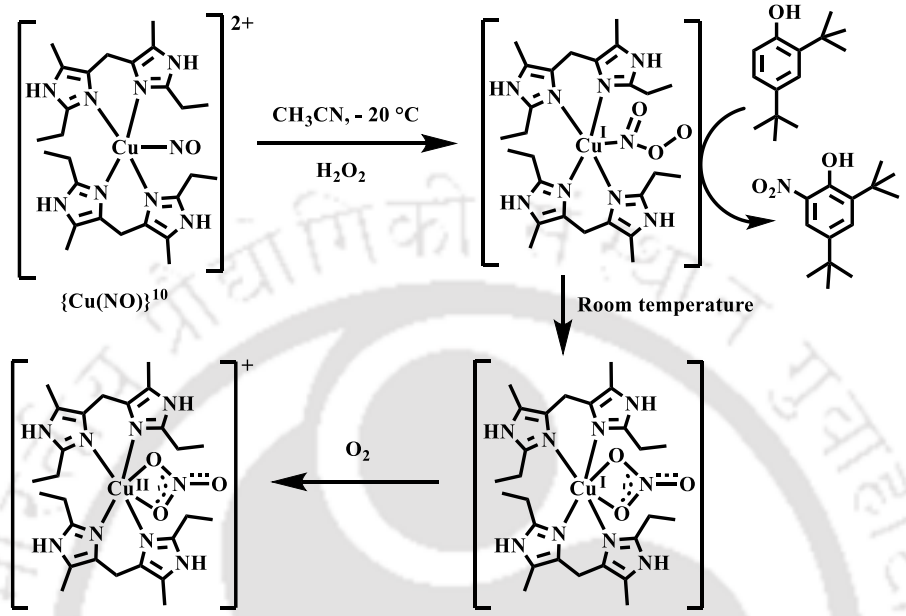

Scheme 1.6

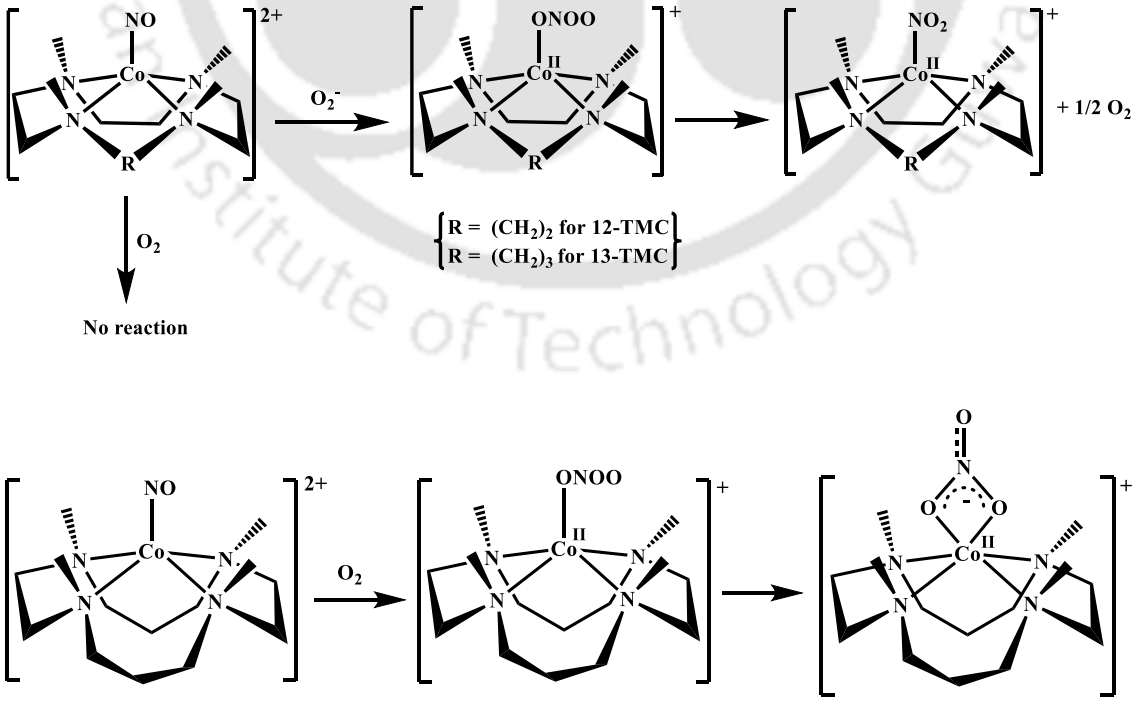

Scheme 1.7

suggested to be involved in the reaction. In another study, a Co-nitrosyl complex of 14-TMC {14-TMC = 1,4,8,11-tetramethyl-1,4,8,11-tetraazacyclotetradecane} ligand framework, upon exposure to molecular oxygen, produced the corresponding Co(II)-nitrate complex *via* a proposed Co(II)-peroxynitrite intermediate. (Scheme **1.7**).[39]

Our group recently reported two Co-nitrosyl complexes, [Co(Cl_4TPP^{2-})(NO)] and [Co(F_8TPP^{2-})(NO)], {Cl_4TPP^{2-} = 5,10,15,20-*tetrakis*(4′-chlorophenyl)porphyrinate} and {F_8TPP^{2-} = 5,10,15,20-*tetrakis*(2,6-difluorophenyl)porphyrinate} which reacts with H_2O_2, giving rise to the corresponding Co(III)-nitrite and Co(III)-nitrate complexes, respectively (Scheme **1.8**).[40,41] In both instances, the formation of a proposed Co(III)-peroxynitrite

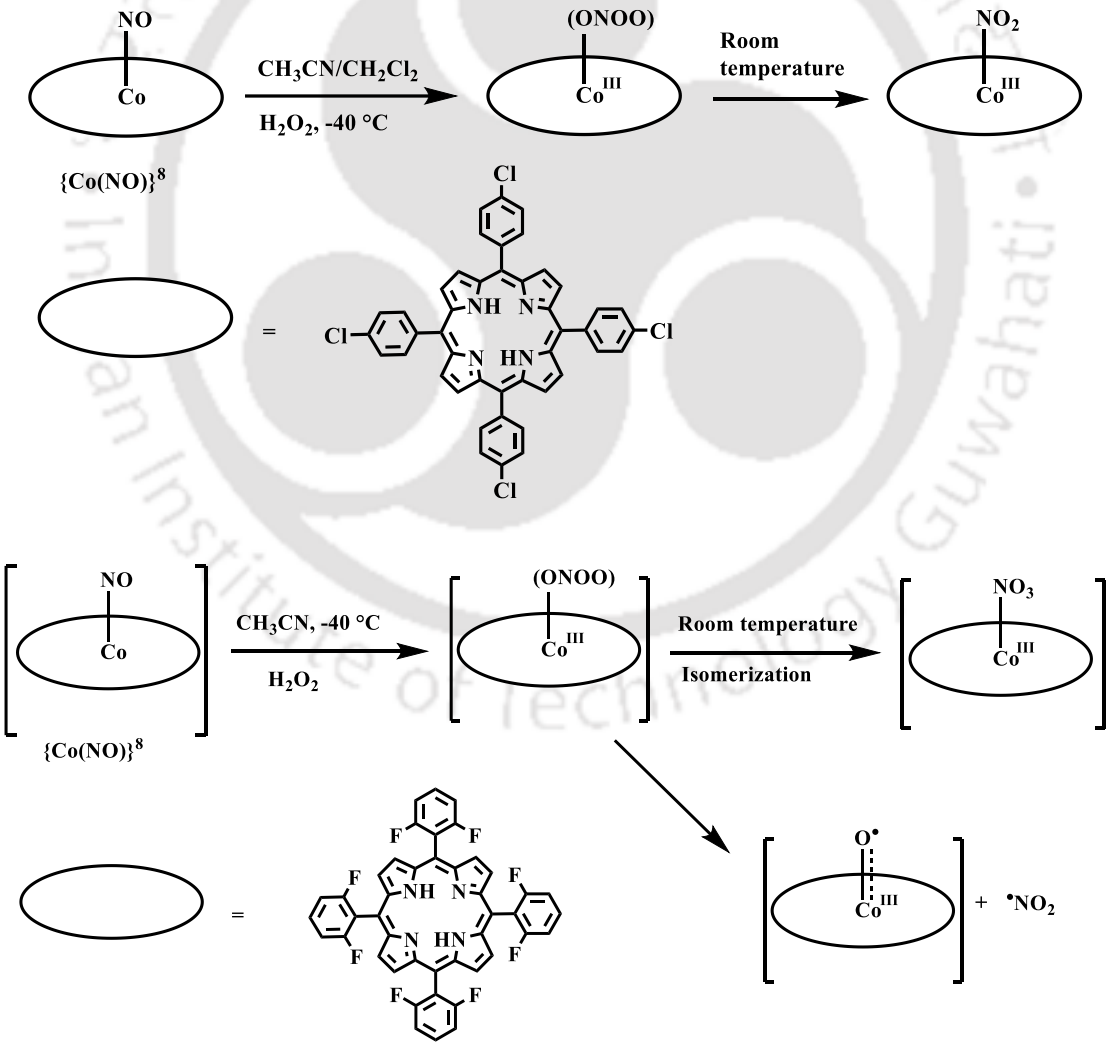

Scheme 1.8

intermediate was suggested. In the second case, genaration of a cobalt-oxyl radical species [Co^{III}-$O^{\bullet}$] was detected spectroscopically which is formed through the homolytic decomposition of the O-O bond of the proposed peroxynitrite moiety.

A Mn-nitrosyl complex, [Mn($F_{20}TPP^{2-}$)(NO)] of {Mn(NO)}^{6} configuration, reacted with superoxide ion to form [Mn^{III}($F_{20}TPP^{2-}$)(NO_3^-)] complex *via* a proposed Mn(III)-peroxynitrite intermediate (Scheme **1.9**).[42] Here, involvement of Mn(IV)-oxo species was observed which formed after the homolytic decomposition of the O-O bond of peroxynitrite. UV-visible, EPR spectroscopy and ESI-mass spectrometry suggested the formation of [Mn^{IV}=O] species in the reaction.

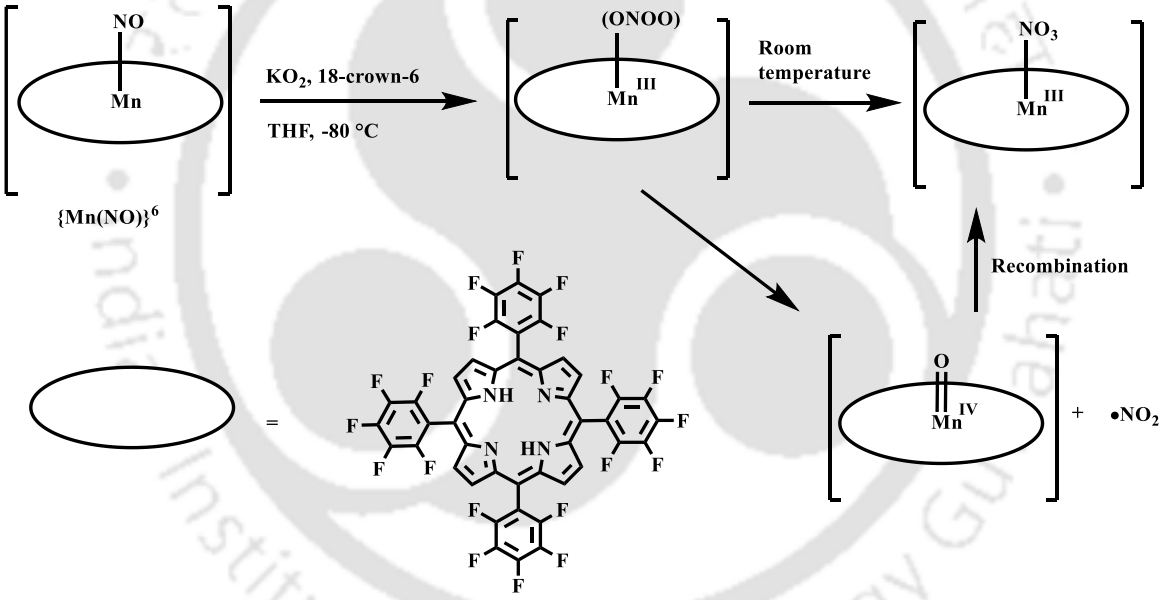

Scheme 1.9

Another Mn-nitrosyl complex, [Mn($TMPP^{2-}$)(NO)], {$TMPP^{2-}$ = 5,10,15,20-*tetrakis*(4-methoxyphenyl)porphyrinate} upon reacting with superoxide ion resulted in the formation of corresponding [Mn^{III}-OH] and NO_2. Here putative formation of the peroxynitrite was proposed (Scheme **1.10**).[43] Formation of high valent [Mn^{IV}=O] was also evidenced by spectroscopic analysis.

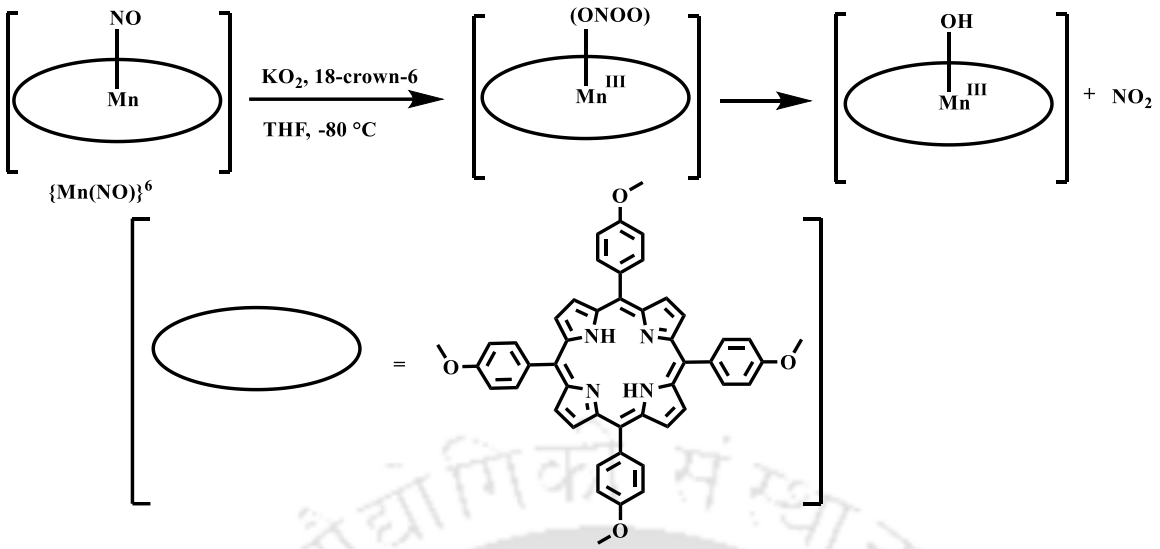

Scheme 1.10

1.2.2 Reaction of metal-superoxo complexes with NO

Karlin group reported a superoxo complex of Fe(III)-porphyrinate, $[Fe^{III}(F_8TPP^{2-})(thf)(O_2^{-})]$, {$F_8$ = an ortho-difluoro substituted tetraarylporphyrinate} which reacts with NO gas to yield corresponding nitrate complex, $[Fe^{III}(F_8TPP^{2-})(thf)(NO_3^{-})]$ *via* a proposed peroxynitrite intermediate (Scheme **1.11**).[44]

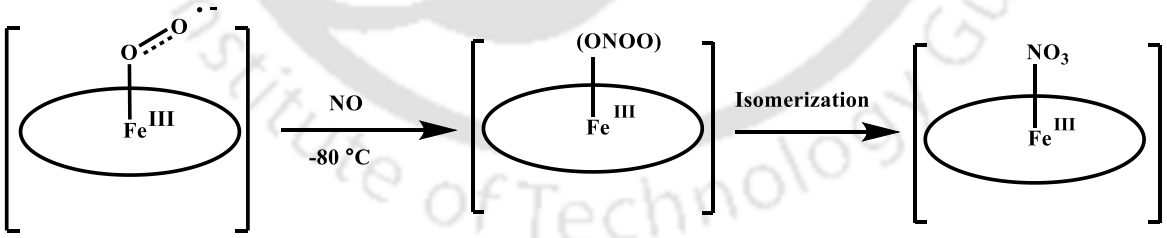

Scheme 1.11

Nam group reported a superoxo complex of Cr(III), $[Cr^{III}(14\text{-TMC})(O_2^{-})(Cl)]^{+}$ having 14-TMC ligand framework, upon reaction with NO results in the corresponding Cr(III)-nitrite complex, $[Cr^{III}(14\text{-TMC})(NO_2^{-})(Cl)]^{+}$. Involvement of a Cr(III)-peroxynitrite intermediate

was proposed in this case. Formation of Cr(IV)-oxo species was also proposed during the reaction (Scheme **1.12**).[45]

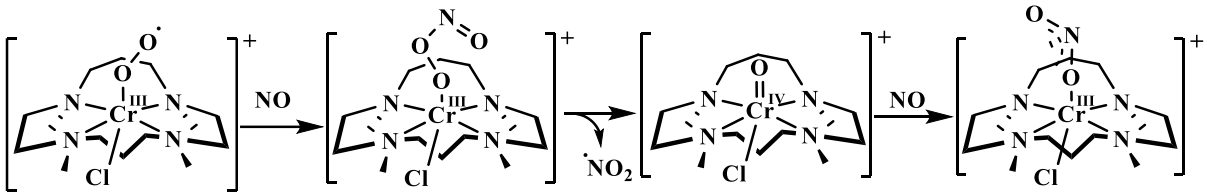

Scheme 1.12

1.2.3 Reaction of metal-peroxo complexes with NO

Our group reported a Co(III)-peroxo complex, $[Co^{III}(Iz)_2(O_2^{2-})]^+$ {Iz = *bis*(2-ethyl-4-methylimidazol-5-yl)methane}, which yields the corresponding $[Co^{II}(Iz)_2(NO_3^-)]^+$ complex upon reaction with NO in methanol solution at -40 °C (Scheme **1.13**).[46] Formation of a Co(II)-peroxynitite intermediate was evidenced through the characteristic phenol ring nitration test.

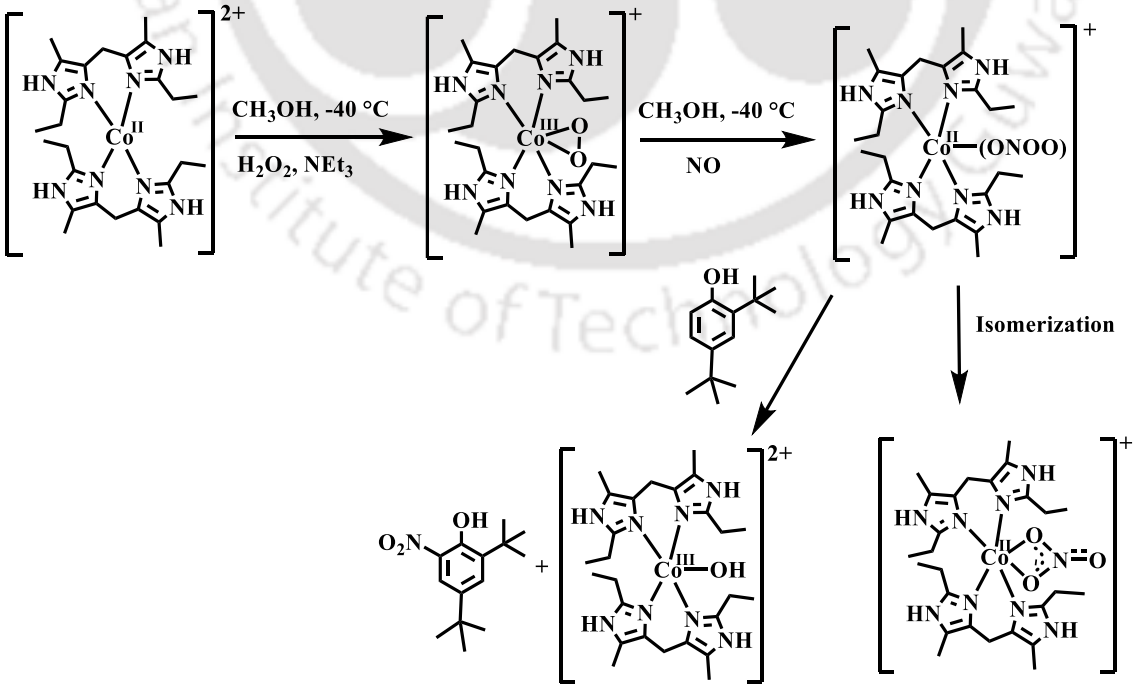

Scheme 1.13

A Cr(IV)-peroxo complex, $[Cr^{IV}(12\text{-}TMC)(O_2^{2-})(Cl)]^+$ bearing 12-TMC ligand framework, upon reaction with NO results in Cr(III)-nitrate complex, $[Cr^{III}(12\text{-}TMC)(NO_3^-)(Cl)]^+$ *via* a Cr(III)-peroxynitrite intermediate (Scheme **1.14**).[47] Involvement of Cr(IV)-oxo species and NO_2 was shown to form by homolytic cleavage of the O-O bond of peroxynitrite.

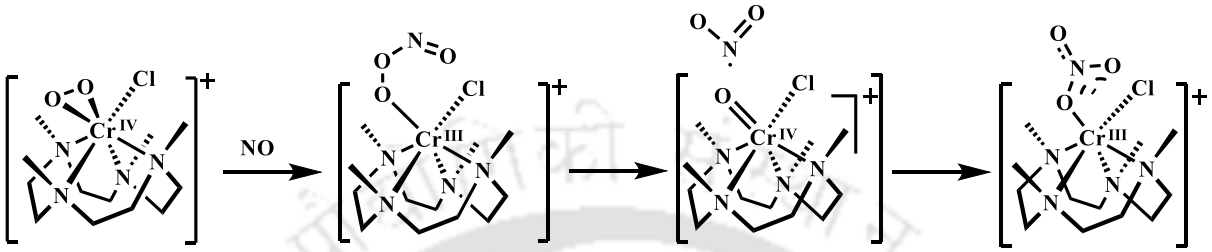

Scheme 1.14

Kumar group reported a Ni(III)-peroxo complex, $[Ni^{III}(12\text{-}TMC)(O_2^{2-})]^+$ which upon reaction with NO leads to the corresponding Ni(II)-nitrate complex, $[Ni^{II}(12\text{-}TMC)(NO_3^-)]^+$ (Scheme **1.15**). It was proposed that the reaction is going through a peroxynitrite intermediate.[48]

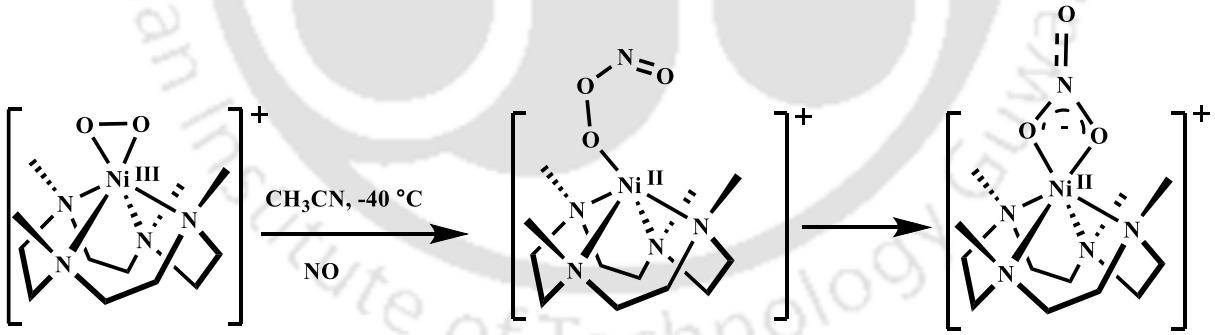

Scheme 1.15

They also reported two more Mn(III)-peroxo complexes, $[Mn^{III}(3PYENMe)(O_2^{2-})]^+$ and $[Mn^{III}(N3PY)(O_2^{2-})]^+$ {3PYENMe = N^1-methyl-N^1,N^2,N^2-*tris*(pyridin-2-ylmethyl)ethane-1,2-diamine}, {N3PY = N^1,N^2-dimethyl-N^1-(2-(methyl(pyridin-2-ylmethyl)amino)ethyl)-N^2-

(pyridin-2-ylmethyl)ethane-1,2-diamine}, having pentadentate ligand framework gives corresponding Mn(II)-nitrate complexes, $[Mn^{II}(3PYENMe)(NO_3^-)]^+$ and $[Mn^{II}(N3PY)(NO_3^-)]^+$, respectively in the presence of NO (Scheme **1.16**). In both the cases, nitration of phenol ring confirms the involvement of Mn(II)-peroxynitrite intermediate during the reaction.[49]

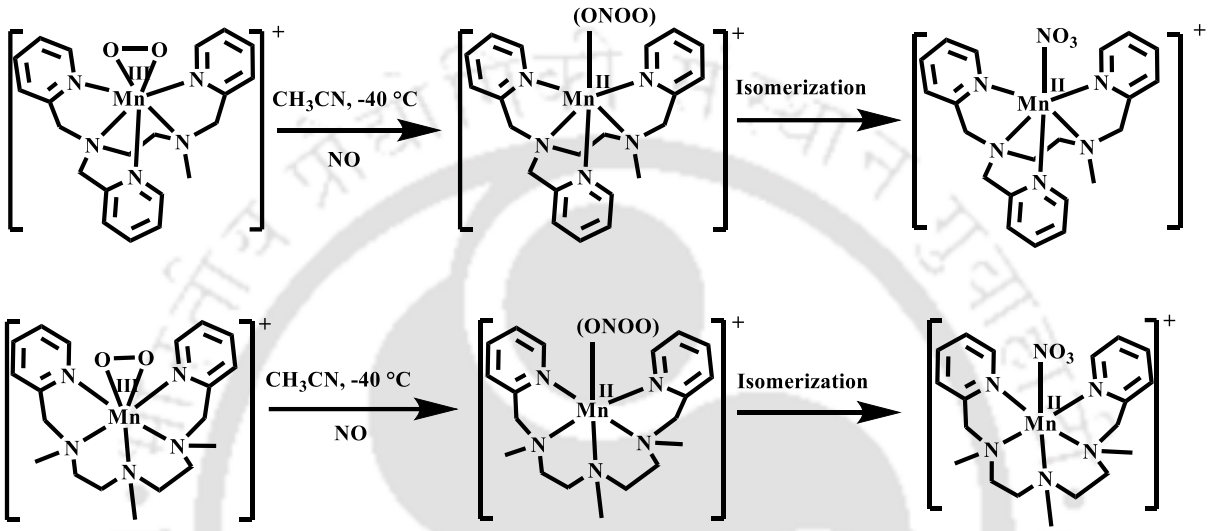

Scheme 1.16

1.3 Scope of the thesis

This thesis work stems from our curiosity to identify the metal-peroxynitrite intermediate in reactions of metal-nitrosyl complexes with H_2O_2 and metal-peroxo complexes with nitric oxide. Direct spectroscopic characterization of metal peroxynitrite are still elusive. Moreover, the formation of high-valent metal-oxo through the decomposition of the metal peroxynitrite's O-O bond is not well-documented. Hence, the objectives of the thesis are:

1. Preparation and characterization of metal-peroxo and metal-nitrosyl complexes having non-heme and heme ligand framework, respectively.

2. Study of the reaction of these metal-peroxo or metal-nitrosyl complexes with nitric oxide gas and H_2O_2, respectively, to understand the reaction pathway and any intermediate involved.
3. Investigate the decomposition pathways of metal-peroxynitrites and detection of the metal-oxo species through the decomposition of the O-O bond of unstable metal-peroxynitrite intermediate during the reaction.

1.4 References

1. Jorgensen, C. K. *Coord. Chem. Rev*. **1966**, *1*, 164.
2. Mingos, D. M. P. *J. Organomet. Chem*. **2014**, *751*, 153.
3. Greenwood, N. N.; Earnshaw, A. Chemistry of the Elements; 2nd Ed.; Elsevier, **2012**, *412*, 445.
4. Ford, P. C.; Lorkovic, I. M. *Chem. Rev*. **2002**, *102*, 993.
5. Laane, J.; Ohlsen, J. R. *Inorg. Chem*. **2007**, *27*, 465.
6. Marietta, M. A.; Yoon, P. S.; Iyengar, R.; Leaf, C. D.; Wishnok, J. S. *Biochemistry*, **1988**, *27*, 8706.
7. (a) Stuehr, D. J. *Annu. Rev. Pharmacol. Toxicol*. **1997**, *37*, 339. (b) Gorren, A. C. F.; Mayer, B. *Biochim. Biophys. Acta, Gen. Subj*. **2007**, *1770*, 432. (c) Santolini, J. *J. Inorg. Biochem*. **2011**, *105*, 127. (d) Childers, K. C.; Garcin, E. D. eLS, John Wiley & Sons, Ltd. Chichester, **2017**, 1.
8. Gantner, B. N.; Lafond, K. M.; Bonini, G. M. *Redox Biology*, **2020**, *34*, 101550.
9. Ignarro, L. J. *Nitric Oxide: Biology and Pathobiology*; Ed.; Academic Press: San Diego, **2000**.
10. (a) Furchgott, R. F. *Angew. Chem. Int. Ed*. **1999**, *38*, 1870. (b) Ignaro, L. J. *Angew. Chem. Int. Ed*. **1999**, *38*, 1882.

11. Pacher, P.; Beckman, J. S.; Liaudet, L. *Physiol. Rev*. **2007**, *87*, 315.

12. Beckman, J. S.; koppenol, W. H. *Am. J. Physiol*. **1996**, *271*, 1424.

13. Vliet, A.; Eiserich, J. P.; Halliwell, B.; Cross, C. E. *J. Biol. Chem*. **1997**, *272*, 7617.

14. Qiao, L.; Lu, Y.; Liu, B.; Girault, H. H. *J. Am. Chem. Soc*. **1997**, *272*, 7617.

15. Radi, R. *Chem. Res. Toxicol*. **1998**, *11*, 720.

16. Szabo, C.; Ischiropoulos, H.; Radi, R. *Nat. Rev. Drug. Discov*. **2007**, *6*, 662.

17. (a) Beal, M. F. *Free Radic. Biol. Med*. **2002**, *32*, 797. (b) Radi, R.; Cassina, A.; Hodara, R.; Quijano, C.; Castro, L. *Free Radic. Biol. Med*. **2002**, *33*, 1451.

18. Redi, R.; Beckman, J. S.; Bush, K. M. *J. Biol. Chem*. **1991**, *266*, 4244.

19. (a) Lymar, S. V.; Hurst, J. K. *J. Am. Chem. Soc*. **1995**, *117*, 8867. (b) Denicola, A.; Freeman, B. A.; Trujillo, M.; Radi, R. *Arch. Biochem. Biophys*. **1996**, *333*, 49.

20. Beckman, J. S.; Ischiropoulos, H.; Zhu, L.; Woerd, M.; Smith, C.; Chen, J.; Harriso, J.; Martin, J. C.; Tsai, M. *Arch. Biochem. Biophys*. **1992**, *298*, 438.

21. Beckmann, J. S.; Ye, Y. Z.; Anderson, P. G.; Chen, J.; Accavitti, M. A.; Tarpey, M. M.; White, C. R. *J. Biol. Chem.* **1994**, *375*, 81.

22. Herold, S.; Koppenol, W. H. *Coord. Chem. Rev*. **2005**, *249*, 499.

23. Radi, R. *J. Biol. Chem*. **2013**, *288*, 26464.

24. Olson, J. S.; Foley, E. W.; Rogge, C.; Tsai, A. L.; Doyle, M. P.; Lemon, D. D. *Free Radic. Biol. Med*. **2004**, *36*, 685.

25. Gardner, P. R.; Gardner, A. M.; Brashear, W. T.; Suzuki, T.; Hvitved, A. N.; Setchell, K. D. R.; Olson, J. S. J. *Inorg. Biochem*. **2006**, *100*, 542.

26. Weiss, J. J. *Nature*, **1964**, *202*, 83.

27. Wittenberg, J. B.; Wittenberg, B. A.; Peisach, J.; Blumberg, W. E. *Proc. Natl. Acad. Sci. U. S. A*. **1970**, *67*, 1846.

28. Balagopalakrishna, C.; Abugo, O.; Horsky, J.; Manoharan, P. T.; Nagababu, E.;

Rifkind, J. M. *Biochemistry*, **1998**, *37*, 13194.

29. Singha, A.; Das, P. K.; Dey, A. *Inorg. Chem*. **2019**, *58*, 10704.
30. Yan, J. J.; Kroll, T.; Baker, M. L.; Wilson, S. A.; Decréau, R.; Lundberg, M.; Sokaras, D.; Glatzel, P.; Hedman, B.; Hodgson, K. O.; Solomon, E. I. *Proc. Natl. Acad. Sci. U. S. A*. **2019**, *116*, 2854.
31. Shaik, S.; Chen, H. *J. Biol. Inorg. Chem*. **2011**, *16*, 841.
32. (a) Tocheva, E. I.; Rosell, F. I.; Mauk, A. G.; Murphy, M. E. *Science*, **2004**, *304*, 867. (b) Cooper, C. E.; Torres, J.; Sharpe, M. A.; Wilson, M. T. *FEBS Lett*. **1997**, *414*, 281.
33. (a) Clarkson, S. G.; Basolo, F. J. *Chem. Soc. Chem. Commun*. **1972**, *11*, 670. (b) Clarkson, S. G.; Basolo, F. *Inorg. Chem*. **1973**, *12*, 1528.
34. Cao, R.; Elrod, L. T.; Lehane, R. L.; Kim, E.; Karlin, K. D. *J. Am. Chem. Soc*. **2016**, *138*, 16148.
35. Gogoi, K.; Saha, S.; Mondal, B.; Deka, H.; Ghosh, S.; Mondal, B. *Inorg. Chem*. **2017**, *56*, 14438.
36. Mazumdar, R.; Mondal, B.; Saha, S.; Samanta, B.; Mondal, B. *J. Inorg. Biochem*. **2022**, *228*, 111698.
37. Kalita, A.; Kumar, P.; Mondal, B. *Chem. Commun*. **2012**, *48*, 4636.
38. Kumar, P.; Lee, Y. M.; Park, Y. J.; Siegler, M. A.; Karlin, K. D.; Nam, W. *J. Am. Chem. Soc*. **2015**, *137*, 4284.
39. Kumar, P.; Lee, Y. M.; Hu, L.; Chen, J.; Park, Y. J.; Yao, J.; Chen, H.; Karlin, K. D.; Nam, W. *J. Am. Chem. Soc*. **2016**, *138*, 7753.
40. Saha, S.; Gogoi, K.; Mondal, B.; Ghosh, S.; Deka, H.; Mondal, B. *Inorg. Chem*. **2017**, *56*, 7781.
41. Mondal, B.; Saha, S.; Borah, D.; Mazumdar, R.; Mondal, B. *Inorg. Chem*. **2019**, *58*,

1234.

42. Mondal, B.; Borah, D.; Mazumdar, R.; Mondal, B. *Inorg. Chem*. **2019**, *58*, 14701.
43. Mazumdar, R.; Saha, S.; Samanta, B.; Ghosh, R.; Maity, S.; Mondal, B. *Dalton Trans*. **2023**, *52*, 7917.
44. Schopfer, M. P.; Mondal, B.; Lee, D. H.; Sarjeeant, A. N.; Karlin, K. D. *J. Am. Chem. Soc*. **2009**, *131*, 11304.
45. Yokoyama, A.; Cho, K. B.; Karlin, K. D.; Nam, W. *J. Am. Chem. Soc*. **2013**, *135*, 14900.
46. Saha, S.; Ghosh, S.; Gogoi, K.; Deka, H.; Mondal, B.; Mondal, B. *Inorg. Chem*. **2017**, *56*, 10932.
47. Yokoyama, A.; Han, J. E.; Cho, J.; Kubo, M.; Ogura, T.; Siegler, M. A.; Karlin, K. D.; Nam, W. *J. Am. Chem. Soc*. **2012**, *134*, 15269.
48. Yenuganti, M.; Das, S.; Kulbir.; Ghosh, S.; Bhardwaj, P.; Pawar, S. S.; Sahoo, S. C.; Kumar, P. *Inorg. Chem. Front*. **2020**, *7*, 4872.
49. Das, S.; Keerthi, A. C. S.; Kulbir.; Singh, S.; Roy, S.; Singh, R.; Ghosh, S.; Kumar, P. *Dalton Trans*. **2023**, *52*, 5095.

Chapter 2

Reaction of a Co(III)-peroxo Complex with Nitric Oxide: Putative Formation of a Peroxynitrite Intermediate

Abstract

A Co(II) complex, $[Co^{II}(L1)_2(H_2O)_2](ClO_4^-)_2$, **2.1** having bidentate ligand **L1** [L1 = *bis*(3,5-dimethylpyrazolyl)methane] has been synthesized. Complex **2.1** in acetonitrile solution at -40 °C in the presence of H_2O_2 and NEt_3 afforded the corresponding Co(III)-peroxo species, $[Co^{III}(L1)_2(O_2^{2-})]^+$ as a transient intermediate, **2a**. Thermal instability precluded it's isolation. The addition of NO gas into the freshly prepared $[Co^{III}(L1)_2(O_2^{2-})]^+$ in acetonitrile at -40 °C resulted in the corresponding Co(II)-nitrate complex, $[Co^{II}(L1)_2(NO_3^-)](ClO_4^-)$, **2.2**. The reaction is proposed to proceed through a putative Co(II)-peroxynitrite intermediate, **2b**. It was evidenced by the characteristic phenol ring nitration reaction.

2.1 Introduction

Nitric oxide (NO) is a highly reactive diatomic molecule due to the presence of an unpaired electron in π* orbital. At a very low concentration, NO controls several physiological processes like neurotransmission, vasodilation and defensive immune system etc.[1-8] In living organisms, nitric oxide synthase (NOS) produces NO and in biological denitrification processes nitrite reductase enzymes (NiR) generate NO from the reduction of nitrite.[9] Imbalance of NO can cause oxidative and nitrosative stress through the formation of secondary reactive nitrogen species (RNS) such as NO_2 and peroxynitrite.[10-11] The level of NO is controlled by nitric oxide dioxygenase (NOD) which oxidize NO to nitrate (NO_3^-).[12] This conversion is proposed to proceed *via* the formation of peroxynitrite intermediate. *In vivo*, peroxynitrite is formed in a reaction of NO with O_2^- adduct of ferri-heme i.e. [Fe^{III}-O_2^-] proteins in a diffusion controlled rate.[13-15] It is also believed to form in the reaction of nitrite with H_2O_2 in the presence of peroxidase enzymes.[16] *In vitro*, peroxynitrite complexes are reported to form in the reaction of metal nitrosyls with molecular oxygen (O_2) or reactive oxygen species such as superoxide (O_2^-) and hydrogen peroxide (H_2O_2) or in reaction of metal superoxo/peroxo complexes with NO. For instance, Co-nitrosyl complexes, $[Co(12\text{-}TMC)(NO)]^{2+}$ and $[Co(13\text{-}TMC)(NO)]^{2+}$ are reported to react with O_2^- ion to afford Co(II)-nitrite complexes, $[Co^{II}(12\text{-}TMC)(NO_2^-)]^+$ and $[Co^{II}(13\text{-}TMC)(NO_2^-)]^+$, respectively, *via* a presumed Co(II)-peroxynitrite intermediate.[17] Peroxo complex of chromium with same ligand framework, $[Cr^{IV}(12\text{-}TMC)(O_2^{2-})(Cl)]^+$ reacts with NO leading to the formation of a Cr(III)-nitrate complex,[18] $[Cr^{III}(12\text{-}TMC)(NO_3^-)(Cl)]^+$. A [$Cr^{III}$-$O_2^-$] complex, $[Cr^{III}(14\text{-}TMC)(O_2)(Cl)]^+$, upon reaction with NO resulted in a Cr(IV)-oxo species, $[Cr^{IV}(14\text{-}TMC)(O)(Cl)]^+$ and NO_2 *via* the formation of Cr(III)-peroxynitrite intermediate, $[Cr^{III}(14\text{-}TMC)(OONO^-)(Cl)]^+$.[19] Recently, a Ni(III)-peroxo complex, $[Ni^{III}(12\text{-}TMC)(O_2^{2-})]^+$ has been reported to react with NO to result in a Ni(II)-nitrate complex, $[Ni^{II}(12\text{-}TMC)(NO_3^-)]^+$. The involvement of a Ni(II)-peroxynitrite intermediate was presumed in this

reaction.[20] An Fe(III)-peroxynitrite intermediate is presumed to form in the reaction of Fe(III)-peroxo complex, $[Fe^{III}(14\text{-}TMC)(O_2^{2-})]^+$ with NO which results in the corresponding Fe(III)-nitrate analogue, $[Fe^{III}(14\text{-}TMC)(NO_3^-)]^+$.[21] On the other hand, the reaction of a non-heme dinitrosyl iron, $[Fe(NO)_2]$ with O_2 afford Fe(III)-nitrate is proposed to proceed *via* the corresponding peroxynitrite intermediate.[22,23] A mixed valent dicopper μ-nitrosyl complex, $[Cu^{I,II}_2(UN\text{-}O^-)(NO)]^{2+}$ was reported by the Karlin's group to react with O_2 to give peroxynitrite intermediate.[24] It has been demonstrated that Cu-nitrosyl complex, $[Cu(Iz)_2(NO)](ClO_4^-)_2$ reacts with H_2O_2 to form a Cu(I)-nitrate complex and based on chemical evidence, the formation of a Cu(I)-peroxynitrite intermediate was proposed.[25] In a different example, a Co-nitrosyl, [Co(BPI)(NO)(OAc)], has been shown to give Co(III)-nitrite complex on its reaction with O_2 *via* a Co(III)-peroxynitrite intermediate.[26] Though the reaction of heme and non-heme cobalt nitrosyl with $O_2/O_2^-/O_2^{2-}$ are known to form cobalt nitrite/nitrate complex *via* a peroxynitrite intermediate, the examples of the reaction of cobalt-oxy species with NO are very limited. Recently, we have reported that a Co(III)-peroxo complex with imidazole based ligand framework reacts with NO to form a Co(II)-nitrate complex presumably *via* a peroxynitrite intermediate.[27]

This chapter describes a $[Co^{II}(L1)_2(H_2O)_2]^{2+}$ complex, **2.1** which in acetonitrile solution at -40 °C upon reaction with H_2O_2 and NEt_3 resulted Co(III)-peroxo intermediate, **2a**. This intermediate in the presence of NO results in the corresponding Co(II)-nitrate complex, **2.2**. Chemical evidence suggests the involvement of a Co(II)-peroxynitrite species in this reaction.

2.2 Results and Discussion

The ligand **L1** was prepared using 3,5-dimethylpyrazole following a previously reported procedure.[28] It was isolated as pure solid and characterized by using different spectroscopic

techniques (Appendix I, Figures **A1.1-A1.4**). Complex **2.1,** $[Co^{II}(L1)_2(H_2O)_2]^{2+}$ was synthesized with perchlorate as counter anion by constant stirring of a mixture of cobalt(II) perchlorate hexahydrate and the ligand **L1** in 1:2 mole equivalent in acetonitrile. It was characterized by UV-visible, FT-IR, EPR, and ESI-mass spectrometry as well as by the single-crystal X-ray structure determination (Appendix I, Figures **A1.5-A1.8**). The perspective ORTEP view of complex **2.1** is shown in figure 2.1. The crystallographic data and other metric parameters are listed in tables (Appendix I, Tables **A1.1-A1.3**). Crystal structure of complex **2.1** revealed that the Co(II)-center is bonded with four nitrogen atoms from two units of ligand and two water molecules in a distorted octahedral geometry. Two perchlorate ions are present

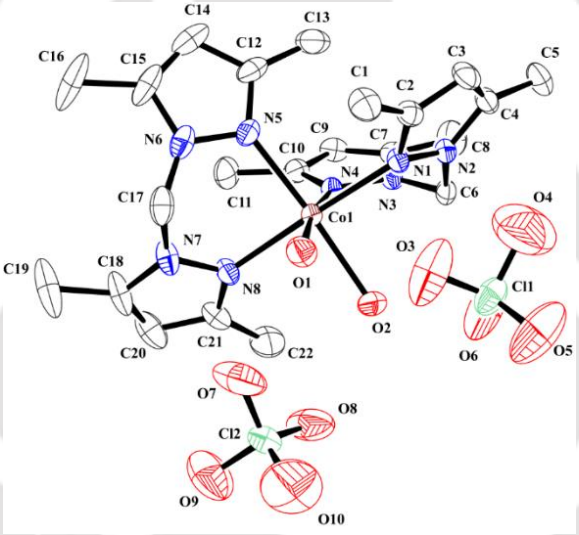

Figure 2.1. ORTEP diagram of complex **2.1** [35% thermal ellipsoid plot, H-atoms are omitted for clarity].

in the outside of the coordination sphere to satisfy the charge of the metal center (Figure **2.1**). The Co-N bond distances are within the range of reported values in analogous compounds (Appendix I, Tables **A1.1-A1.3**).[29] It would be worth mentioning here that analogous imidazole based ligand, Iz, {Iz = *bis*(2-ethyl-4-methylimidazole-5-yl)methane}, affords a distorted tetrahedral geometry to the Co(II)-center.[27]

Complex **2.1**, in acetonitrile solution exhibited an absorption band at 485 nm, ($\epsilon/M^{-1}cm^{-1}$, 50) along with other intra-ligand transitions at 317 nm ($\epsilon/M^{-1}cm^{-1}$, 1230) and 268 nm ($\epsilon/M^{-1}cm^{-1}$, 1830) (Appendix I, Figure **A1.6**). X-band EPR spectrum of complex **2.1** was recorded at 77 K and an axial spectrum was observed for a Co(II)-center with 3/2 spin state (Appendix I, Figure **A1.8**).[30] The magnetic moment (μ_B) of the complex was measured 4.34 BM as expected for Co(II)-octahedral complexes.[31]

A dry and degassed acetonitrile solution of complex **2.1** at -40 °C, upon addition of 1.5 mole equivalent of freshly estimated H_2O_2 followed by 1 mole equivalent of NEt_3 resulted in a thermally unstable purple color intermediate **2a,** $[Co^{III}(L1)_2(O_2^{2-})]^+$ (Scheme **2.1**). It was found to decompose readily with increasing temperature. In UV-visible spectroscopic monitoring, a new transient absorption band appeared at 375 nm ($\epsilon/M^{-1}cm^{-1}$, 856) (Figure **2.2**). The intensity

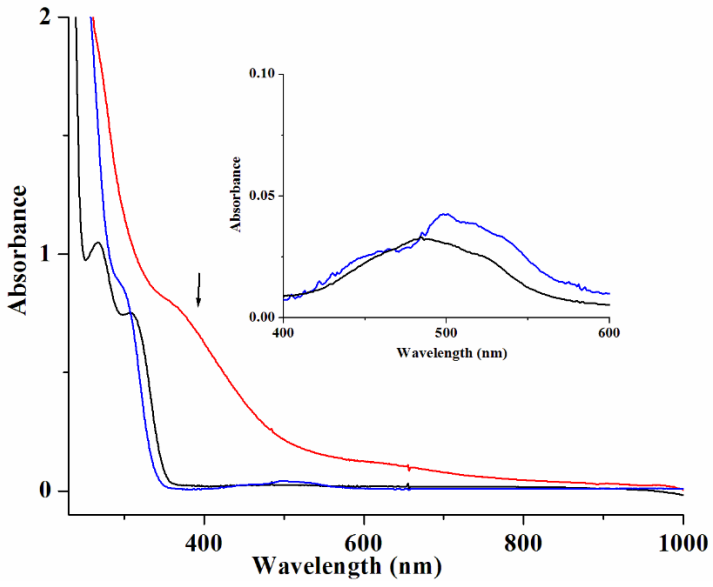

Figure 2.2. UV-visible spectra of the reaction of complex **2.1** with H_2O_2 followed by NO, in acetonitrile at -40 °C. [complex **2.1** (black), after addition of H_2O_2 followed by NEt_3 (red) and after addition of NO (blue)].

of the band decreases with time suggesting it's unstable nature. This is attributed to corresponding Co(III)-peroxo complex. In case of Co(II)-complex of *bis*(2-ethyl-4-

methylimidazole-5-yl)methane ligand, the reaction of H_2O_2 in the presence of NEt_3 also resulted in the corresponding Co(III)-peroxo species.[27] It should be noted that the side-on peroxo complexes of transition metal ions are found to show absorption in the range of 340 nm to 470 nm in UV-visible spectroscopy.[32] For instance, the side-on peroxo complexes $[Co^{III}(12\text{-}TMC)(O_2^{2-})]^+$, $[Co^{III}(TMC)(O_2^{2-})]^+$, $[Co^{III}(15\text{-}TMC)(O_2^{2-})]^+$ were reported to absorb at 350 nm, 436 nm and 464 nm, respectively.[33] Whereas $[Co^{III}(Iz)_2(O_2^{2-})]^+$ was found to absorb at 452 nm ($\epsilon/M^{-1}cm^{-1}$, 890).[27] On the other hand, end-on peroxo complexes of Co(III) were reported to absorb in the range of 485 to 580 nm.[34]

In X-band EPR spectroscopy, the intermediate **2a**, was found to be silent as expected for Co(III)-peroxo species having low spin Co(III)-center (Figure **2.3**).[33] In ESI-mass spectrometry, this intermediate **2a** displayed molecular ion peak at 499.172, which is attributed to the mass of $[Co^{III}(L1)_2(O_2^{2-})]^+$ (Calcd. 499.198). The observed isotropic distribution pattern matches well with the simulated one (Figure **2.4**). Unfortunately, attempts to record the

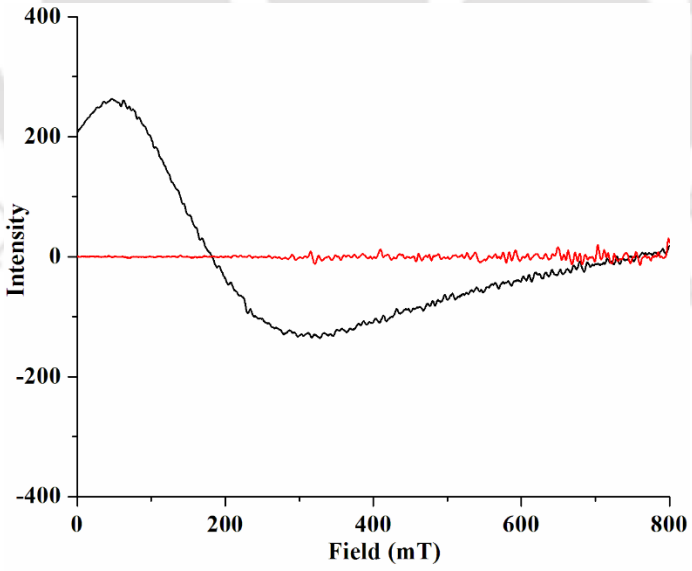

Figure 2.3. X-band EPR spectral monitoring of the reaction of complex **2.1** with H_2O_2 followed by NEt_3 in acetonitrile at 77 K [complex **2.1** (black), after addition of H_2O_2, intermediate **2a** (red)].

FT-IR spectrum of the intermediate **2a** were unsuccessful owing to its thermal instability. It is

to be noted that in the presence of the base, there is a possibility of the formation of Co(IV)-oxo species.[35] However, it is well-known that cobalt being a later first row transition metal, Co(IV)-oxo is relatively rare owing to their electronic instability, which is known as oxo wall.[35] In addition, Co(IV)-oxo species are known to initiate oxygen atom transfer (OAT) to the suitable substrates.[36,37] In the present case, no trace of OAT was observed in the presence of substrates like fluorine etc. Considering all these, it is logical to rule out the possibility of formation of Co(IV)-oxo species.

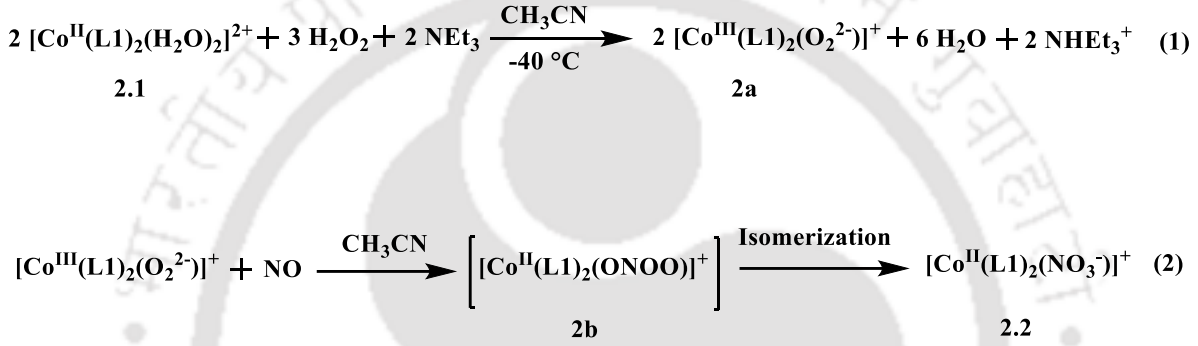

Scheme 2.1. Reaction of complex **2.1** with H_2O_2 followed by addition of NEt_3 and NO in acetonitrile at -40 °C.

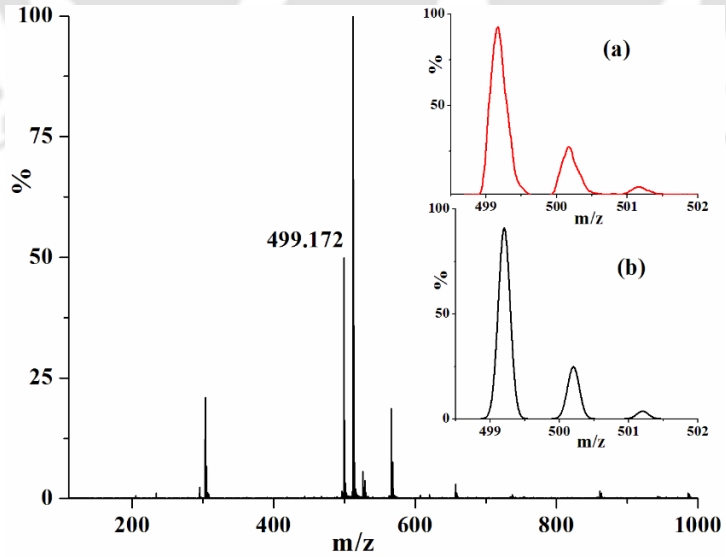

Figure 2.4. ESI-mass spectrum of Co(III)-peroxo intermediate, **2a** in acetonitrile. [Inset: (a) experimental and (b) simulated isotopic distribution pattern].

Upon bubbling of NO gas to the freshly generated Co(III)-peroxo intermediate, **2a** in dry and degassed acetonitrile solution at -40 °C followed by warming up to room temperature formation of complex **2.2**, $[Co^{II}(L1)_2(NO_3^-)](ClO_4^-)$ was observed. It was isolated as solid and characterized by different spectroscopic methods as well as by the single-crystal X-ray structure determination (Appendix I, Figure **A1.9-A1.11**). The ORTEP diagram is shown in figure 2.5. Crystallographic data, important bond distances and bond angles are listed in the appendix (Appendix I, Tables **A1.1-A1.3**). The crystal structure of complex **2.2** revealed a distorted octahedral geometry around the Co(II)-centre. Here four nitrogen atoms from two units of ligand and a nitrate group (NO_3^-) is coordinated to the metal. In FT-IR spectrum complex **2.2** shows a strong band at 1384 cm^{-1} which corresponds to NO_3^- stretching (Appendix I, Figure **A1.9**). This matched well with the earlier reported value.[38]

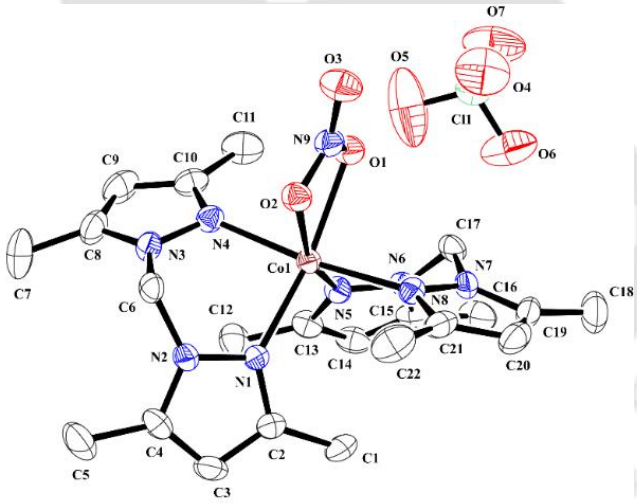

Figure 2.5: ORTEP diagram of complex **2.2** [35% thermal ellipsoid plot, solvent molecule and H-atoms are omitted for clarity].

The formation of complex **2.2** as the final decomposition product in the reaction of Co(III)-peroxo species, **2a** with NO suggests the putative formation of peroxynitrite ($ONOO^-$) intermediate in the course of the reaction. Since, NO_3^- is the common isomerization product of peroxynitrite ($ONOO^-$). Since direct spectral evidence were not obtained in favor of the formation of peroxynitrite intermediate, chemical evidence was sought to establish it's

involvement in the reaction. The nitration of phenol ring has been extensively used as an evidence for the formation of metal-peroxynitrite intermediate.[38] When NO was added to the freshly generated complex **2a** in acetonitrile at -40 °C in the presence of 2,4-di-*tert*-butyl phenol, ring nitration was observed (*ca*. 65%) along with formation of Co(III)-hydroxide complex, **2.3**. 2,4-di-*tert*-butyl-6-nitrophenol and complex **2.3** were purified using silica gel column chromatography using chloroform/methanol as eluent and spectroscopic characterization were done (Appendix I, Figures **A1.12-A1.19**). In contrary, when the external phenol was added after the addition of NO gas into the solution of **2a**, only complex **2.2** was formed and the formation of 2,4-di-*tert*-butyl-6-nitrophenol was not observed. This suggests

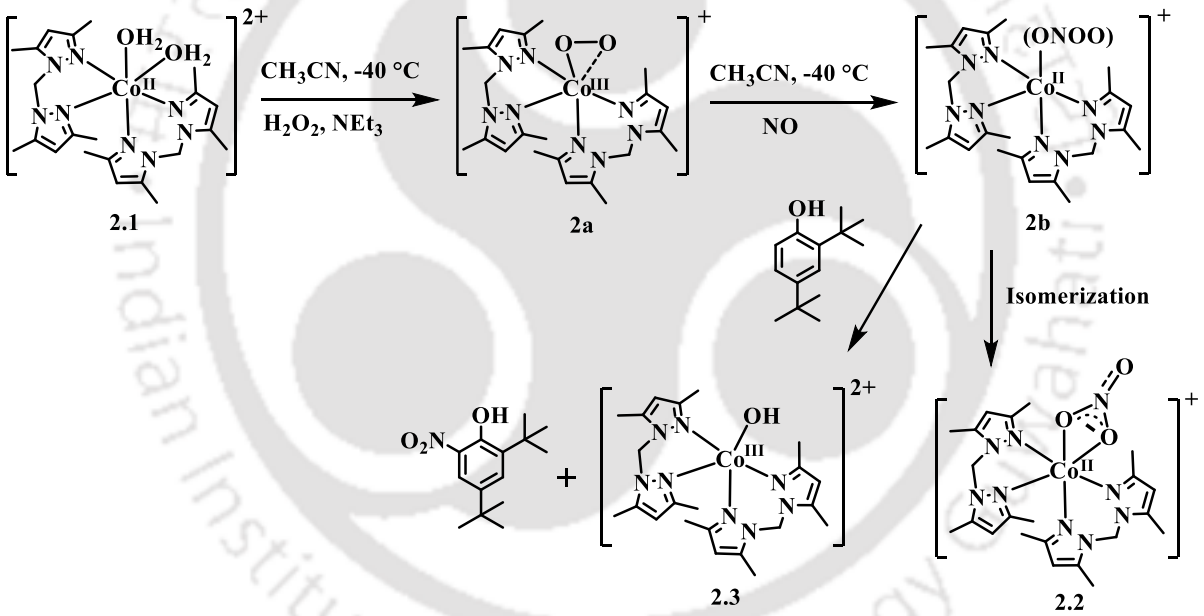

Scheme 2.2. Overall reactions.

that the reaction proceeds through a presumed peroxynitrite intermediate.[38] In this reaction the formation of corresponding Co(II)-hydroxide is expected which was evidenced in X-band EPR study of the reaction mixture (Appendix I, Figure **A1.20**).[39] However, work up and isolation afforded Co(III)-hydroxide as final product probably due to the air/moisture sensitivity of Co(II)-complex. It was worth mentioning that the reaction of complex **2.2** with externally

added phenol does not result in the formation of 2,4-di-*tert*-butyl-6-nitrophenol.

2.3 Experimental Section

2.3.1 Materials and methods

All the reagents were purchased from commercial sources and used as it is without further purification unless specified. Acetonitrile was stored over calcium hydride overnight followed by distillation with P_2O_5 under N_2. All the reactions were performed under inert atmosphere except mentioned differently. Deoxygenation of solvents and solutions were effected by consecutive vacuum/Ar purge cycles. UV–visible spectra were taken on an Agilent Cary 8454 spectrophotometer. FT-IR spectra were recorded as KBr pellets or in a KBr cell using a PerkinElmer spectrophotometer. ^{1}H, ^{13}C-NMR studies were recorded using Bruker Avance III on a 500 MHz Varian FT-NMR spectrophotometers. X-band EPR spectra were recorded on a JES-FA200 EPR spectrophotometer with microwave power, 0.998 mW; microwave frequency, 9.14 GHz; and modulation amplitude, 2.

The X-ray quality crystals were grown using diffusion followed by slow evaporation method. The intensity data were collected using a Bruker SMART APEX-II CCD diffractometer, equipped with a fine focus 1.75 kW sealed tube Mo Kα radiation (λ = 0.71073 Å), with increasing ω (width of 0.3° per frame) at a scan speed of 3 s/frame. The SMART software was used for data acquisition. Data integration and reduction were undertaken with SAINT and XPREP software.[40] Structures were solved by direct methods using SHELXL[41a] and refined with full-matrix least-squares on F^2 using SHELXL-2019/1.[41b] Structural illustrations were drawn with ORTEP-3 for Windows.[41c]

2.3.2 Syntheses

[*Bis*(3,5-dimethylpyrazolyl)methane], L1

3,5-dimethylpyrazole (5 g, 52 mmol) was dissolved in 50 mL of dimethyl sulfoxide and finely powdered KOH (5.84 g, 104 mmol) was added to it. This suspension was stirred vigorously for 1 h at 80 °C. After that 1.67 mL dichloromethane in 10 mL dimethyl sulfoxide was added dropwise and allowed to stirred for another 4 h. This reaction mixture was poured into 200 mL of cold water to precipitate out the pure ligand **L1**. Yield: 4.35 g (*ca*. 82%). Elemental analyses for $C_{11}H_{16}N_4$. Calcd. (%): C, 64.68; H, 7.90; N, 27.43, Found (%): C, 64.55; H, 7.98; N, 27.62. FT-IR (in KBr): 1557, 1464, 1419, 1382, 1354, 1313, 1267, 1139, 1035, 970, 953, 811, 776, 712, 673, 628 and 469 cm^{-1}. ^{1}H-NMR (500 MHz, $CDCl_3$): $\delta_{ppm,}$ 6.01 (s, 1H), 5.74 (s, 1H), 2.17 (s, 3H), 2.14 (s, 3H). ^{13}C-NMR (125 MHz, $CDCl_3$): $\delta_{ppm,}$ 148.2, 140.3, 106.3, 60.4, 13.4. ESI-mass (m/z): Calcd.: 204.137, Found: 205.153 (M+1).

Complex 2.1, $[Co^{II}(L1)_2(H_2O)_2](ClO_4^-)_2$

15 mL acetonitrile solution of ligand **L1** (408 mg, 2 mmol) was added drop wise to the 15 mL acetonitrile solution of Co(II)-perchlorate hexahydrate (366 mg, 1 mmol). This mixture was stirred for 4 h at room temperature. The volume was reduced to 5 mL and benzene (25 mL) was added to precipitate out the complex **2.1**. Pink crystals of complex **2.1** were obtained from acetonitrile solution by layering with benzene. Yield: 632 mg (*ca*. 90%). Elemental analyses for $C_{22}H_{36}Cl_2N_8O_{10}Co$. Calcd. (%): C, 37.62; H, 5.17; N, 15.95; Found (%): C, 37.54; H, 5.09; N, 16.09. FT-IR (in KBr): 1558, 1465, 1422, 1371, 1279, 1097, 1040, 929, 829, 810, 789, 705, 679, 662, 620, 493 and 477 cm^{-1}. UV-visible (CH_3CN): 268 nm (ϵ/M^{-1} cm^{-1}, 1830), 317 nm (ϵ/M^{-1} cm^{-1},1230) and 485 nm (ϵ/M^{-1} cm^{-1}, 51). $\mu_{obs.}$: 4.34 BM. X-band EPR (CH_3CN, 77 K): g ~ 4.2. Crystal data: CCDC No. 2279868. $C_{22}H_{36}N_8O_{10}Cl_2Co$, M = 702.42, monoclinic

(P21/c), a = 12.8427(6), b = 12.6406(6), c = 20.2239(9) Å, α = 90°, β = 106.4850(10)°, γ = 90°, V = 3148.2(3) $Å^3$, Z = 4, D_c = 1.482 g cm^{-3}, μ = 0.778 mm^{-1}, T = 296(2) K, 5534 reflections, 4352 independent, R(F) = 0.0560 [I>2δ(I)], R(int) = 0.0736, wR(F^2) = 0.1757 (all data), GOF = 1.013.

2.3.3 Reaction of complex 2.1 with H_2O_2

Complex **2.1** (702 mg, 1 mmol) was dissolved in 10 mL of dry and degassed acetonitrile and kept it at -40 °C for 4 h. To this solution, pre-cooled 1.5 mole equivalent of H_2O_2 (37% v/v, 0.7 mL) was added followed by 1 mole equivalent NEt_3. The color of the reaction mixture changed to purple from pink and afforded intermediate, **2a**. UV-visible (CH_3CN): 375 nm (ϵ/$M^{-1}cm^{-1}$, 856), 630 nm (ϵ/$M^{-1}cm^{-1}$, 95). ESI-mass (m/z): Calcd.: 499.198 for $[Co^{III}(L1)_2(O_2)]^+$, Found: 499.172.

Complex 2.2, $[Co^{II}(L1)_2(NO_3^-)](ClO_4^-)$

NO gas was bubbled to the freshly prepared Co(III)-peroxo species, **2a** in acetonitrile solution at -40 °C and stirred for 30 min. It was then brought to room temperature and allowed to stir for 30 min. The excess NO gas was removed by applying few cycles of vacuum and Ar. The reaction mixture was then kept for slow evaporation and brown crystals of complex **2.2** were obtained after 5 d. Yield: 440 mg (*ca*. 70%). Elemental analyses for $C_{22}H_{32}ClN_9O_7Co$. Calcd. (%): C, 42.01; H, 5.13; N, 20.04. Found (%): C, 42.06; H, 5.04; N, 20.11. FT-IR (in KBr): 1639, 1558, 1486, 1465, 1422, 1384, 1287, 1121, 1100, 1084, 1045, 835, 803, 705, 681 and 624 cm^{-1}. UV-visible (CH_3CN): 295 (ϵ/M^{-1} cm^{-1}, 1785), 450 (ϵ/M^{-1} cm^{-1}, 49), 498 (ϵ/M^{-1} cm^{-1}, 55) and 517 nm (ϵ/M^{-1} cm^{-1}, 62). $\mu_{obs.}$: 4.36 BM. Crystal data: CCDC No. 2279867. $C_{24}H_{35}N_{10}O_7ClCo$, M = 670.00, monoclinic (P21/c), a = 14.7963(8), b = 8.2883(4), c = 25.5819(13) Å, α = 90°, β = 94.607(2)°, γ = 90°, V = 3127.1(3) $Å^3$, Z = 4, D_c = 1.423 g cm^{-3},

μ = 0.692 mm^{-1}, T = 296(2) K, 5508 reflections, 4464 independent, R(F) = 0.0532 [I>2δ(I)], R(int) = 0.0703, wR(F^2) = 0.1236 (all data), GOF = 1.102.

2.3.4 Reaction of complex 2.1 with H_2O_2 followed by NEt_3 and NO in the presence of 2,4-di-*tert*-butylphenol

Dry and degassed acetonitrile solution (10 mL) of complex **2.1** (702 mg, 1mmol) was kept at -40 °C for 2 h. To this, precooled 1.5 mole equivalent H_2O_2 (37% v/v, 0.7 mL) followed by 1 mole equivalent of NEt_3 was added to afford Co(III)-peroxo intermediate, **2a**. To this intermediate **2a**, 2 mL precooled acetonitrile solution containing 2,4-di-*tert*-butylphenol (1.03 g, 5 mmol) was added followed by NO. This reaction mixture was allowed to stir for 1 h at -40 °C and warmed up to room temperature. Excess NO gas was removed by purging Ar. 2,4-di-*tert*-butyl-6-nitrophenol and complex **2.3** were isolated using column chromatography.

2,4-di-*tert*-butyl-6-nitrophenol

Yield: 145 mg (*ca*. 58%). Elemental analyses for $C_{14}H_{21}NO_3$. Calcd. (%): C, 66.91; H, 8.42; N, 5.57. Found (%): C, 66.85; H, 8.38; N, 5.68. FT-IR (in KBr): 1542, 1481, 1463, 1407, 1363, 1315, 1276, 1259, 1238, 1203, 1180, 1139, 1112, 1097, 1022, 923, 887, 865, 852, 819, 806, 773, 748 and 723 cm^{-1}. ^{1}H-NMR (500 MHz, $CDCl_3$): $\delta_{ppm,}$ 11.45 (s, 1H), 7.96 (d, 1H), 7.65-7.64 (d, 1H), 1.45 (s, 9H), 1.32 (s, 9H). ^{13}C-NMR (125 MHz, $CDCl_3$): $\delta_{ppm,}$ 153.2, 142.2, 140.1, 133.9, 132.8, 119.1, 35.9, 34.7, 31.3, 29.6. ESI-mass (m/z): Calcd.: 251.15, Found: 250.16 (M-1).

Complex 2.3, $[Co^{III}(L1)_2(OH)](ClO_4^-)_2$

Yield: 342 mg (*ca*. 50%). Elemental analyses for $C_{22}H_{33}Cl_2N_8O_9Co$. Calcd. (%): C, 38.67; H, 4.87; N, 16.40. Found (%): C, 38.58; H, 4.79; N, 16.31. FT-IR (in KBr): 1635, 1559, 1467, 1424, 1391, 1285, 1109, 1042, 906, 835, 683 and 625 cm^{-1}. UV-visible (CH_3CN): 294 nm

(ϵ/M^{-1} $cm^{-1,}$ 1204), 415 nm (ϵ/M^{-1} cm^{-1}, 140) and 513 nm (ϵ/M^{-1} cm^{-1}, 73). ESI-mass (m/z): Calcd.: 233.604, Found: 233.620 (M/2).

2.4 Conclusion

Thus, a Co(II)-complex bearing pyrazole based bidentate ligand (*bis*(3,5-dimethylpyrazolyl)methane), **2.1** has been synthesized and characterized spectroscopically as well as structurally. In acetonitrile solution at -40 °C temperature, complex **2.1** reacts with H_2O_2 in the presence of NEt_3 to result in the corresponding Co(III)-peroxo intermediate, **2a**. It is thermally unstable and decomposes rapidly. Addition of NO gas to the freshly prepared acetonitrile solution of Co(III)-peroxo intermediate, **2a** at -40 °C leads to the formation of the corresponding Co(II)-nitrate complex, **2.2**. It is proposed that the reaction proceeds *via* a Co(II)-peroxinitrite intermediate, **2b** which is evidenced by the characteristic phenol ring nitration reaction.

2.5 References

1. Goyal, R. K.; Hirano, I. *N. Engl. J. Med*. **1996**, *334*, 1106.
2. Stark, M. E.; Szurszewski, J. H. *Gastroenterology*, **1992**, *103*, 1928.
3. Jaffrey, S. R.; Snyder, S. H. *Annu. Rev. Cell. Dev. Biol*. **1995**, *11*, 417.
4. Bogdan, C. *Nat. Immunol*. **2001**, *2*, 907.
5. Ignarro, L. J. *Nitric Oxide: Biology and Pathobiology*; Ed.; Academic Press: San Diego, **2000**.
6. Fang, F. C. *Nitric Oxide and Infection*; Ed., Kluwer Academic Plenum Publishers: New York, **1999**.
7. Bourassa, J. L.; Ives, E. P.; Marqueling, A. L.; Shimanovich, R.; Groves, J. T. *J. Am.*

Chem. Soc. **2001**, *123*, 5142.

8. (a) Lehnert, N.; Kim, E.; Dong, H. T.; Harland, J. B.; Hunt, A. P.; Manickas, E. C.; Oakley, K. M.; Pham, J.; Reed, G. C.; Alfaro, V. S. *Chem. Rev*. **2021**, *121*, 14682. (b) Gantner, B. N.; Lafond, K. M.; Bonini, M. G. *Redox Biology*, **2020**, *34*, 101550. (c) Horst, G.; Marletta, M. A. *Nitric Oxide*, **2018**, *77*, 65.
9. Averill, B. A. *Chem. Rev*. **1996**, *96*, 2951.
10. Pacher, P.; Beckman, J. S.; Liaudet, L. *Physiol. Rev*. **2007**, *87*, 315.
11. Beckman, J. S.; Koppenol, W. H. *Am. J. Physiol*. **1996**, *271*, 1424.
12. Schopfer, M. P.; Mondal, B.; Lee, D. H.; Sarjeant, A. A. N.; Karlin, K. D. *J. Am. Chem. Soc*. **2009**, *131*, 11304.
13. (a) Pfeiffer, S.; Gorren, A. C. F.; Schmidt, K.; Werner, E. R.; Hansert, B.; Bohle, D. S.; Mayer, B. *J. Biol. Chem*. **1997**, *272*, 3465. (b) Coddington, J. W.; Hurst, J. K.; Lymar, S. V. *J. Am. Chem. Soc*. **1999**, *121*, 2438. (c) Koppenol, W. H.; Bounds, P. L.; Nauser, T.; Kissner, R.; Rüegger, H. *Dalton Trans*. **2012**, *41*, 13779. (d) Lymar, S. V.; Khairutdinov, R. F.; Hurst, J. K. *Inorg. Chem*. **2003**, *42*, 5259. (e) Goldstein, S.; Lind, J.; Merényi, G. *Chem. Rev*. **2005**, *105*, 2457. (f) Molina, C.; Kissner, R.; Koppenol, W. H. *Dalton Trans*. **2013**, *42*, 9898.
14. (a) Schopfer, M. P.; Wang, J.; Karlin, K. D. *Inorg. Chem*. **2010**, *49*, 6267. (b) Ouellet, H.; Ouellet, Y.; Richard, C.; Labarre, M.; Wittenberg, B.; Wittenberg, J.; Guertin, M. *Proc. Natl. Acad. Sci*, *U. S. A*. **2002**, *99*, 5902. (c) Gardner, P. R.; Gardner, A. M.; Martin, L. A.; Salzman, A. L. *Proc. Natl. Acad. Sci. U. S. A*. **1998**, *95*, 10378. (d) Ford, P. C.; Lorkovic, I. M. *Chem. Rev*. **2002**, *102*, 993. (e) Gardner, P. R.; Gardner, A. M.; Brashear, W. T.; Suzuki, T.; Hvitved, A. N.; Setchell, K. D. R.; Olson, J. S. *J. Inorg. Biochem*. **2006**, *100*, 542.
15. Tejero, J. A.; Hunt, P.; Lehnert, J. N.; Stuehr, D. J. *J. Biol. Chem*. **2019**, *294*, 7904.

16. Georg, B. *Redox Biology*, **2019**, *26*, 101291.

17. Kumar, P.; Lee, Y. M.; Park, Y. J.; Siegler, M. A.; Karlin, K. D.; Nam, W. *J. Am. Chem. Soc*. **2015**, 137, 4284.

18. Yokoyama, A.; Han, J. E.; Cho, J.; Kubo, M.; Ogura, T.; Siegler, M. A.; Karlin, K. D.; Nam, W. *J. Am. Chem. Soc*. **2012**, *134*, 15269.

19. Yokoyama, A.; Cho, K. B.; Karlin, K. D.; Nam, W. *J. Am. Chem. Soc*. **2013**, *135*, 14900.

20. Yenuganti, M.; Das, S.; Kulbir.; Ghosh, S.; Bhardwaj, P.; Pawar, S. S.; Sahoo, S. C.; Kumar, P. *Inorg. Chem*. *Front*. **2020**, *7*, 4872.

21. Yokoyama, A.; Han, J. E.; Karlin, K. D.; Nam, W. *Chem. Commun*. **2014**, *50*, 1742.

22. Tran, N. G.; Kalyvas, H.; Skodje, K. M.; Hayashi, T.; Loccoz, P. M.; Callan, P. E.; Shearer, J.; Kirschenbau, L. J.; Kim, E. *J. Am. Chem. Soc*. **2011**, *133*, 1184.

23. Skodje, K. M.; Williard, P. G.; Kim, E. *Dalton Trans*. **2012**, *41*, 7849.

24. Cao, R.; Elrod, L. T.; Lehane, R. L.; Kim, E.; Karlin, K. D. *J. Am. Chem. Soc*. **2016**, *138*, 16148.

25. Kalita, A.; Kumar, P.; Mondal, B. *Chem. Commun*. **2012**, *48*, 4636.

26. Gogoi, K.; Saha, S.; Mondal, B.; Deka, H.; Ghosh, S.; Mondal, B. *Inorg. Chem*. **2017**, *56*, 14438.

27. Saha, S.; Ghosh, S.; Gogoi, K.; Deka, H.; Mondal, B.; Mondal, B. *Inorg. Chem*. **2017**, *56*, 10932.

28. Schepetkin, I.; Potapov, A.; khlebnikov, A.; Lukina, E. A.; Malovichko, G.; Kirpotina, L.; Quinn, M. T. *J. Biol. Inorg. Chem*. **2006**, *11*, 499.

29. Larsen, E.; Kofod, P.; Madsen, A. S.; Song, Y. S. *Inorg. Chem*. **2009**, *48*, 7159.

30. Kuin, Y.; Cox, N.; Lubitz, W.; Schnegg, A.; Rüdiger, O. *Catalysts*. **2019**, *9*, 926.

31. Zarembowwitch, J.; Khan, O. *Inorg. Chem*. **1984**, *23*, 589.

32. Kim, D.; Cho, J.; Lee, Y. M.; Sarangi, R.; Nam, W. *Chem. Eur. J*. **2013**, *19*, 14112.

33. (a) Jo, Y.; Annaraj, J.; Seo, M. S.; Lee, Y. M.; Kim, S. Y.; Cho, J.; Nam, W. *J. Inorg. Biochem*. **2008**, *102*, 2155. (b) Cho, J.; Sarangi, R.; Kang, H. Y.; Lee, J. Y.; Kubo, M.; Ogura, T.; Solomon, E. I.; Nam, W. *J. Am. Chem. Soc*. **2010**, *132*, 16977.

34. Wang, C. C.; Chang, H. C.; Lai, Y. C.; Fang, H.; Li, C. C.; Hsu, H. K.; Li, Z. Y.; Lin, T. S.; Kuo, T. S.; Neese, F.; Ye, S.; Chiang, Y. W.; Tsai, M. L.; Liaw, W. F.; Lee, W. Z. *J. Am. Chem. Soc*. **2016**, *138*, 14186.

35. Yang, J.; Dong, H. T.; Seo, M. S.; Larson, V. A.; Lee, Y. M.; Shearer, J.; Lehnert, N.; Nam, W. *J. Am. Chem. Soc.* **2021**, *143*, 16943.

36. Zhang, M.; Respinis, M. D.; Frei, H. *Nat. Chem*. **2014**, *6*, 362.

37. Nguyen, A. I.; Ziegler, M. S.; Burgos, P. O.; Hohne, M. S.; Kim, W.; Bellone, D. E.; Tilley, T. D. *J. Am. Chem. Soc*. **2015**, *137*, 12865.

38. Mondal, B.; Saha, S.; Borah, D.; Mazumdar, R.; Mondal, B. *Inorg. Chem*. **2019**, *58*, 1234.

39. Sheldrick, W. S.; Subramanian, J.; Stelzer, O. *J. Chem. Soc, Dalton Trans*. **1977**, 966.

40. SMART, SAINT and XPREP, Siemens Analytical X-ray Instruments Inc, Madison, Wisconsin, USA. **1995**.

41. (a) Sheldrick, G. M. *Acta Crystallogr. Sect. A Found. Adv.* **2015***, 71,* 3. (b) Sheldrick, G. M. *Acta. Crystallogr. Sect. C Struct. Chem.* **2015**, *71*, 3. (c) Farrugia, L. J. ORTEP-3 for Windows - a version of ORTEP-III with a Graphical User Interface (GUI). *J. Appl. Crystallogr.* **1997**, *30*, 565.

Chapter 3

Reaction of a Co(III)-peroxo Complex of Symmetric Tetradentate Ligand Framework with Nitric Oxide: Putative Formation of a Peroxynitrite Intermediate

Abstract

A Co(II)-complex, $[Co^{II}(L2)(CH_3CN)](ClO_4^-)_2$, **3.1** having a symmetric tetradentate ligand framework **L2** was subjected to react with 1.5 mole equivalent of H_2O_2 followed by 1 mole equivalent of NEt_3 in acetonitrile solution at -40 °C and resulted in the formation of the corresponding Co(III)-peroxo species, $[Co^{III}(L2)(O_2^{2-})]^+$ as transient intermediate, **3a**. When NO gas was added into the freshly generated Co(III)-peroxo species in acetonitrile at -40 °C, yielded the corresponding Co(II)-nitrate complex, $[Co^{II}(L2)(NO_3^-)](ClO_4^-)$, **3.2**. It was characterized by various spectroscopic techniques and single crystal X-ray structure determination. Presumably, this reaction involves the formation of a Co(II)-peroxynitrite intermediate, **3b**. This was confirmed by the characteristic nitration test of the phenol ring.

3.1 Introduction

Nitric oxide (NO) is a heteronuclear diatomic gaseous molecule. It also acts as a signalling molecule and controls various physiological processes such as neurotransmission, vasodilation, defence immune system etc.[1-10] For these processes, NO requires in sub-micromolar concentration. Nitric oxide dioxygenase (NOD) enzyme regulates the amount of NO in biological systems. Excess production of NO leads to toxic effects which cause the oxidative and nitrosative stress.[8] It is proposed that in NOD, a Fe(III)-superoxo complex, $[Fe^{III}(O_2^{-})]$ upon reaction with NO results in biologically atoxic nitrate. This reaction is proposed to proceed through the formation of peroxynitrite intermediate. This peroxynitrite intermediate upon homolytic decomposition of 'O-O' bond results in Fe(IV)-oxo and NO_2 species. Subsequent recombination of these two species give corresponding nitrate complex.[11-13]

NO reactivity of metal-superoxo/peroxo complexes were reported earlier where the involvement of a peroxynitrite intermediate was implicated.[14-21] For example, a $[Fe^{III}(L_a)(O_2^{-})]$ complex reacted with NO to results in the corresponding $[Fe^{III}(L_a)(NO_3^{-})]$ complex, *via* a proposed peroxynitrite intermediate.[11] Peroxo and superoxo complexes of Cr, was reported which react with NO to form the nitrate and nitrite complexes, respectively. In both the cases, the formation of Cr(III)-peroxynitrite was suggested.[19,20] Kumar group reported a peroxo complex of Ni, $[Ni^{III}(12\text{-TMC})(O_2^{2-})]^{+}$ which on reaction with NO resulted in Ni(II)-nitrate complex, $[Ni^{II}(12\text{-TMC})(NO_3^{-})]^{+}$.[22] Formation of the Ni(II)-peroxynitrite was proposed in this case. Mn(III)-peroxo complexes, $[Mn^{III}(3PYENMe)(O_2^{2-})]$ and $[Mn^{III}(N3PY)(O_2^{2-})]$ upon reaction with NO lead to the corresponding Mn(II)-nitrate complexes, $[Mn^{II}(3PYENMe)(NO_3^{-})]$ and $[Mn^{II}(N3PY)(NO_3^{-})]$, respectively.[23] Formation of the

Mn(II)-peroxynitrite intermediates were proposed in both the cases. Our group reported two Co(III)-peroxo complexes, $[Co^{III}(Iz)_2(O_2^{2-})]^+$ and $[Co^{III}(L1)_2(O_2^{2-})]^+$, which in the presence of NO resulted in the corresponding Co(II)-nitrate complexes, $[Co^{II}(Iz)_2(NO_3^-)]^+$ and $[Co^{II}(L1)_2(NO_3^-)]^+$, respectively. Formation of the corresponding Co(II)-peroxynitrite intermediate was proposed in these cases.[21,24]

Reaction involving metal nitrosyls and reactive oxygen species like superoxide and peroxide ion also lead to the corresponding nitrate/nitrite complexes *via* a peroxynitrite intermediate. For example, a non-heme dinitrosyl complex of iron reacted with O_2 and giving rise to the formation of nitrate complex.[25] A Cu-nitrosyl complex reacted with H_2O_2 resulting in Cu(II)-nitrate complex through a proposed Cu(I)-peroxynitrite intermediate.[26] Co-nitrosyl complexes, $[Co(Cl_4TPP^{2-})(NO)]$ and $[Co(F_8TPP^{2-})(NO)]$, upon reaction with H_2O_2 formed the corresponding $[Co^{III}(Cl_4TPP^{2-})(NO_2^-)]$ and $[Co^{III}(F_8TPP^{2-})(NO_3^-)]$ complexes respectively,. The putative formation of Co(II)-peroxynitrite intermediate was proposed in both cases .[27,28]

This chapter describes a Co(II)-complex, $[Co^{II}(L2)(CH_3CN)](ClO_4^-)_2$, **3.1** which upon reaction with H_2O_2 followed by NEt_3 affords Co(III)-peroxo intermediate, $[Co^{III}(L2)(O_2^{2-})](ClO_4^-)$, **3a**. This peroxo complex further reacts with NO to result in the corresponding nitrate complex, $[Co^{II}(L2)(NO_3^-)](ClO_4^-)$, **3.2**. Chemical evidence indicates the formation of Co(II)-peroxynitrite intermediate, **3b** during this reaction.

3.2 Results and Discussion

The ligand, **L2** was synthesized using a procedure reported previously.[29] Ligand **L2** was obtained as pure white solid and characterized spectroscopically (Appendix II, Figures **A2.1-A2.8**). The Co(II)-complex, $[Co^{II}(L2)(CH_3CN)](ClO_4^-)_2$, **3.1** was synthesized by mixing ligand

L2 and Co(II)-perchlorate hexahydrate in equimolar amount in acetonitrile. Complex **3.1** was characterized using spectroscopic techniques as well as structurally (Appendix II, Figures **A2.9-A2.12**). ORTEP diagram of complex **3.1** revealed that the cobalt centre is bonded to four nitrogen atoms from **L2** and one acetonitrile occupying the axial position in a distorted trigonal bipyramidal geometry (Figure **3.1**). Two perchlorate ions remain outside of the coordination sphere to balance the +2 charge of the cobalt centre.

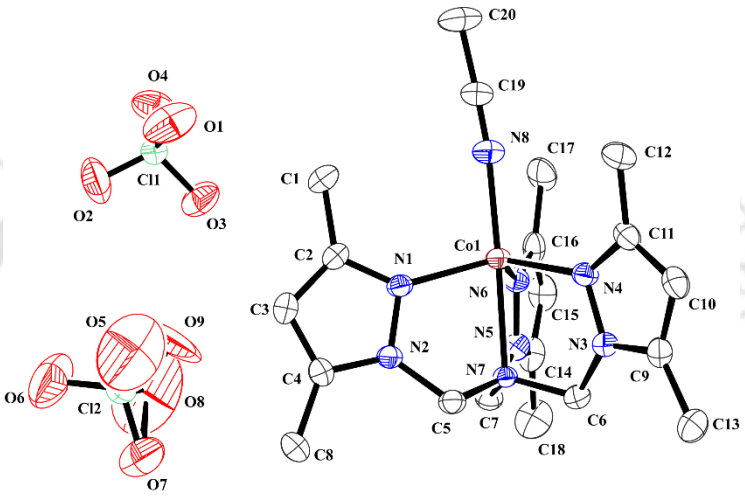

Figure 3.1. ORTEP diagram of complex **3.1** [35% thermal ellipsoid plot, H-atoms are omitted for clarity].

In UV-visible spectroscopy, complex **3.1** showed *d-d* transition bands at 517 nm ($\epsilon/M^{-1}cm^{-1}$, 1.24×10^2) and 468 nm ($\epsilon/M^{-1}cm^{-1}$, 0.95×10^2) along with intraligand charge transfer bands at 219 nm ($\epsilon/M^{-1}cm^{-1}$, 2.23×10^4), 253 nm ($\epsilon/M^{-1}cm^{-1}$, 1.02×10^4) and 304 nm ($\epsilon/M^{-1}cm^{-1}$, 4.29×10^3) in acetonitrile solution (Appendix II, Figure **A2.10**). The complex **3.1** was dissolved in acetonitrile solution and X-band EPR spectrum was recorded at 77 K which showed an axial peak at g ~ 4.55 indicating that cobalt is in +2 oxidation state (Appendix II, Figure **A2.12**). This value is consistent with the other reported Co(II)-complexes.[24]

When dry and degassed acetonitrile solution of complex **3.1** was allowed to react with 1.5 mole equivalent of H_2O_2 followed by 1 mole equivalent of NEt_3 at -40 ºC, resulted in transient

intermediate, **3a** (Scheme **3.1**). In UV-visible spectral monitoring, it was found to absorb at 340 nm which diminishes over time, indicating the unstable nature of the intermediate (Figure **3.2**). This is attributed to the corresponding Co(III)-peroxo species. This value matches with the range (340-470 nm) of other reported analogues.[21,24]

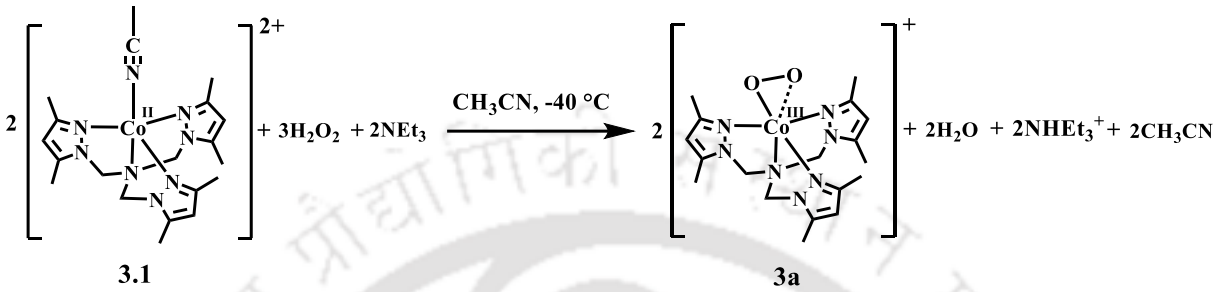

Scheme 3.1. Reaction of complex **3.1** with H_2O_2 followed by NEt_3 in acetonitrile at -40 °C.

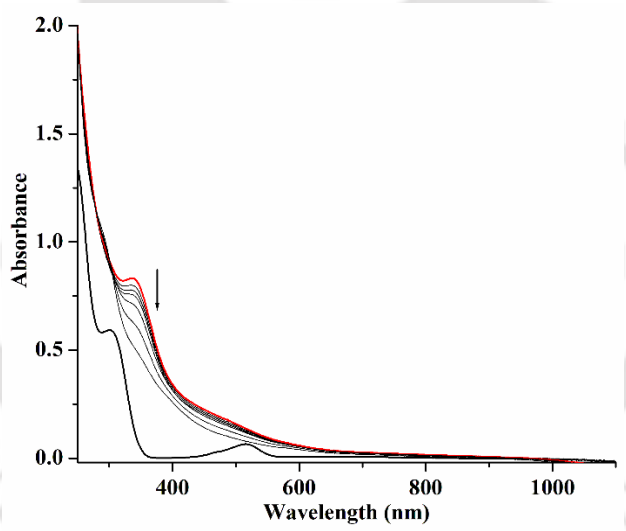

Figure 3.2. UV-visible spectra of the reaction of complex **3.1** with H_2O_2 followed by NEt_3, in acetonitrile at -40 °C [complex **3.1** (black), after the addition of H_2O_2 followed by NEt_3, intermediate **3a** (red)].

In X-band EPR study, the frozen reaction mixture of H_2O_2 and complex **3.1** in acetonitrile results in a EPR silent species which is expected for a low spin Co(III)-peroxo species (Figure **3.3**).

The ESI-mass spectrum of intermediate **3a** in acetonitrile was populated by a molecular ion peak at m/z 432.157 (Figure **3.4**). This corresponds to the mass of $[Co^{III}(L2)(O_2^{2-})]^+$ moiety (Calcd. 432.156). The isotopic distribution pattern is in good agreement with the simulated one.

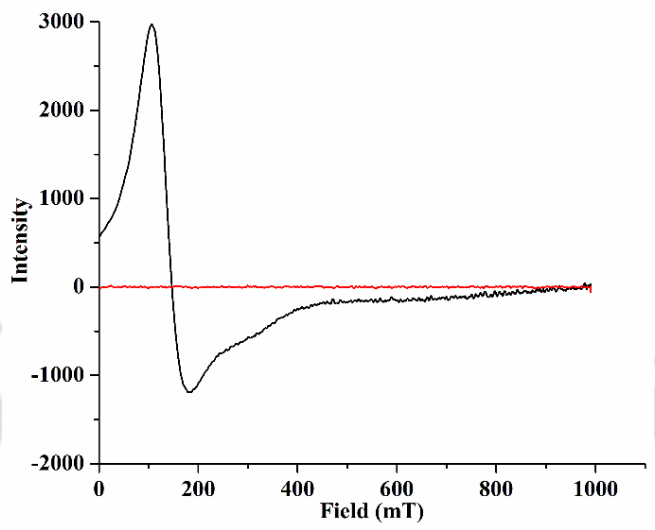

Figure 3.3. X-band EPR spectral monitoring of the reaction of complex **3.1** with H_2O_2 followed by NEt_3 in acetonitrile at 77 K [complex **3.1** (black), after addition of H_2O_2, intermediate **3a** (red)].

Co(III)-peroxo species further reacted with NO gas in dry and degassed acetonitrile solution at -40 ºC followed by warm up to room temperature, giving corresponding nitrate complex,

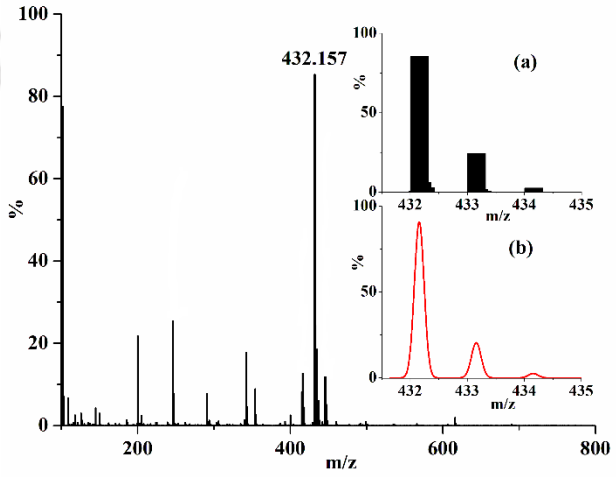

Figure 3.4. ESI-mass spectrum of Co(III)-peroxo intermediate, **3a** in acetonitrile. [Inset: (a) experimental (b) simulated isotopic distribution pattern].

$[Co^{II}(L2)(NO_3^-)]^+$, **3.2**. Complex **3.2** was isolated as a brown crystalline solid and characterized both spectroscopically and structurally (Appendix II, Figures **A2.13-A2.15**). Figure **3.5** displays the ORTEP diagram of complex **3.2**. The important bond lengths and bond angles are listed in the Appendix (Tables **A2.1-A2.3**). Structural study of complex **3.2** confirms that the cobalt center is coordinated to four nitrogen atoms from the ligand and the nitrate group (NO_3^-) in a distorted trigonal bipyramidal geometry (Figure **3.5**). A strong stretching frequency in FT-IR spectrum at 1384 cm^{-1} confirms the presence of nitrate (NO_3^-) group in the complex **3.2** (Appendix II, Figure **A2.13**).

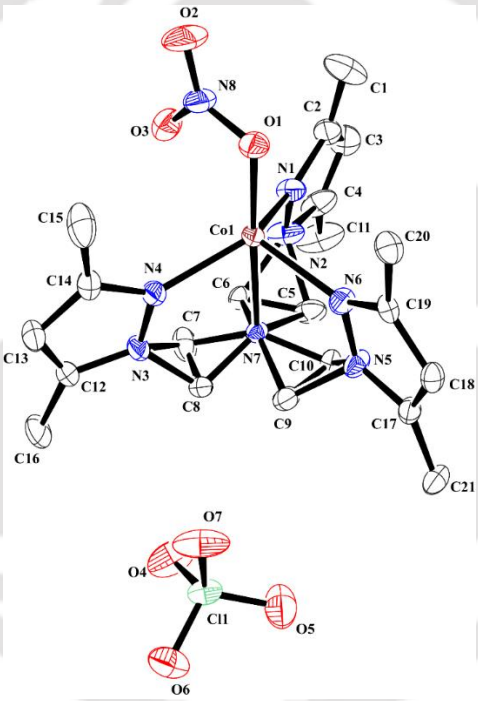

Figure 3.5. ORTEP diagram of complex **3.2** [35% thermal ellipsoid plot, solvent and H-atoms are omitted for clarity].

The final decomposition product, complex **3.2** suggests the involvement of putative peroxynitrite intermediate as peroxynitrite anion ($ONOO^-$) commonly isomerizes to nirate (NO_3^-).[12] Direct spectral evidences were not found due to the unstable nature of the peroxynitrite intermediate. So, we sought for chemical evidences. After the addition of precooled dry and degassed acetonitrile solution of 2,4-di-*tert*-butylphenol to the freshly

prepared Co(III)-peroxo solution followed by the addition of NO, 2,4-di-*tert*-butyl-6-nitrophenol was obtained in significant quantity (*ca*. 65%) along with Co(III)-hydroxo product, **3.3** (Scheme **3.2**). Both were purified by column chromatography and characterized spectroscopically (Appendix II, Figures **A2.16-2.23**). Formation of 2,4-di-*tert*-butyl-6-nitrophenol confirms the involvement of peroxynitrite intermediate.

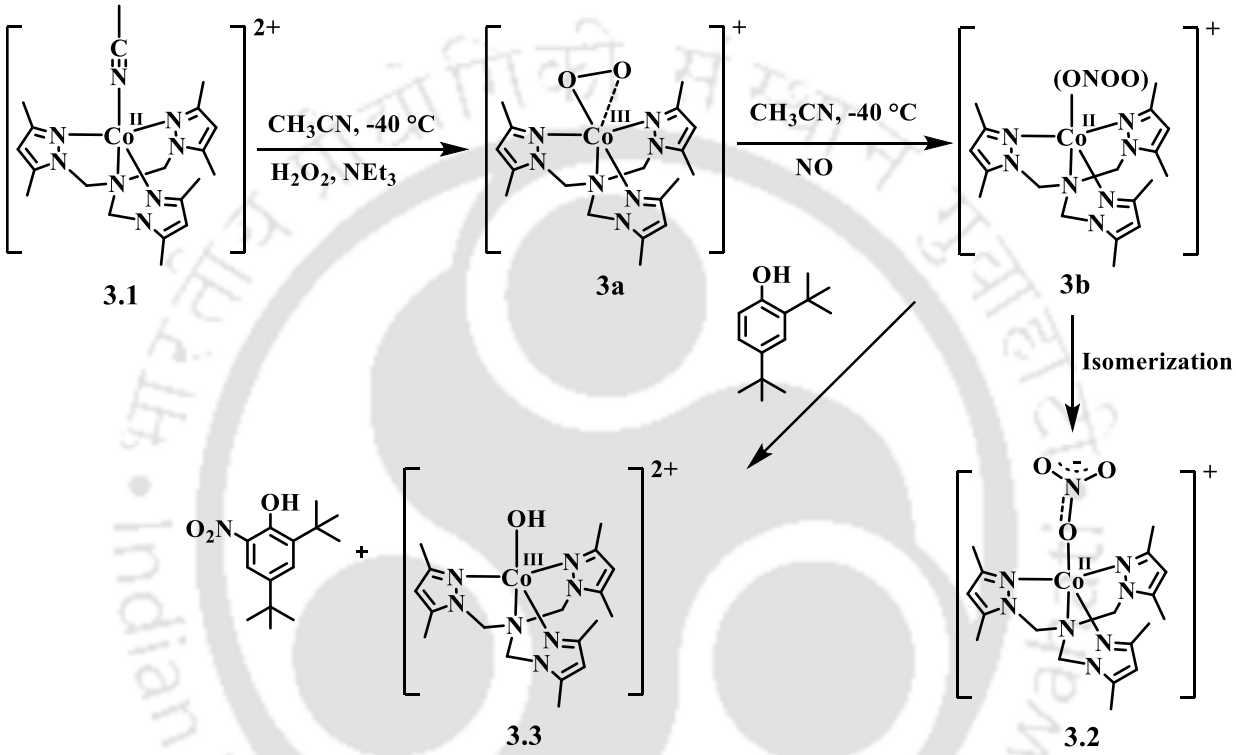

Scheme 2. Overall reactions.

3.3 Experimental Section

3.3.1 Materials and methods

All the reagents were purchased from commercial sources and used as it is without further purification unless specified. Acetonitrile was stored over calcium hydride overnight followed by distillation with P_2O_5 under N_2. All the reactions were performed under inert atmosphere except mentioned differently. Deoxygenation of solvents and solutions were effected by

consecutive vacuum/Ar purge cycles. UV-visible spectra were taken on an Agilent Cary 8454 spectrophotometer. FT-IR spectra were recorded as KBr pellets or in a KBr cell using a PerkinElmer spectrophotometer. ^{1}H, ^{13}C-NMR studies were recorded using Bruker Avance III on a 400 MHz Varian FT-NMR spectrophotometers. X-band EPR spectra were recorded on a JES-FA200 EPR spectrophotometer with microwave power, 0.998 mW; microwave frequency, 9.14 GHz; and modulation amplitude, 2.

Single crystals were grown from acetonitrile solution using slow evaporation technique. The intensity data were collected using a Bruker SMART APEX-II CCD diffractometer, equipped with a fine focus 1.75 kW sealed tube Mo Kα radiation (λ = 0.71073 Å), with increasing ω (width of 0.3° per frame) at a scan speed of 3 s/frame. The SMART software was used for data acquisition. Data integration and reduction were undertaken with SAINT and XPREP software.[30] Structures were solved by direct methods using SHELXL[31a] and refined with full-matrix least-squares on F^2 using SHELXL-2019/1.[31b] Structural illustrations were drawn with ORTEP-3 for Windows.[31c]

3.3.2 Syntheses

Tris(3,5-dimethylpyrazol-1-yl-methyl)amine, (L2)

A previously reported procedure was used for the synthesis of ligand **L2**.[29]

Step 1: Synthesis of 1-(hydroxymethyl)-3,5-dimethyl-1-pyrazole

Formalin (3.0 mL, 39 mmol) was taken in 20 mL of water. This formalin solution was added dropwise to 3,5-dimethyl-1-pyrazole (3.27 g, 34 mmol) in 30 mL of water/ethanol (1:2, v/v). This reaction mixture was stirred for 2 d at room temperature. The organic part was extracted using chloroform and solvent was subsequently removed under reduced pressure to obtain the crude product. 1-Hydroxymethyl-3,5-dimethyl-1-pyrazole was isolated by crystallization from

dichloromethane/toluene (1:3, v/v) mixture. Yield: 2.60 g (*ca*. 60%). Elemental analyses for $C_6H_{10}N_2O$. Calcd. (%): C, 57.12; H, 7.99; N, 22.21. Found (%): C, 57.02; H, 7.91; N, 22.32. FT-IR (in KBr): 3425, 3156, 2981, 2954, 2851, 1554, 1490, 1465, 1426, 1394, 1307, 1225, 1165, 1070, 1037, 1008, 985, 827, 808, 766 and 704 cm^{-1}. ^{1}H-NMR (400 MHz, $CDCl_3$): $\delta_{ppm,}$ 7.57 (s, 1H), 5.82 (s, 1H), 5.39 (s, 2H), 2.33 (s, 3H), 2.18 (s, 3H). ^{13}C-NMR (100 MHz, $CDCl_3$): $\delta_{ppm,}$ 148.4, 139.9, 106.1, 70.1, 12.9, 10.6. ESI-mass (m/z): Calcd.: 126.15, Found: 127.09 (M+1).

Step 2: Synthesis of *tris*(3,5-dimethylpyrazol-1-yl-methyl)amine

1-(hydroxymethyl)-3,5-dimethyl-1-pyrazole (1.89 g, 15 mmol) and ammonium acetate (0.39 g, 5 mmol) were mixed in 30 mL of acetonitrile. This reaction mixture was stirred for 1 d at room temperature. Then the solvent was dried using rotary evaporator to obtain colourless oil. Pure ligand **L2** was obtained by crystallization from methanol/water (1:1, v/v). Yield: 1.19 g (*ca*. 70%.). Elemental analyses for $C_{18}H_{27}N_7$. Calcd. (%): C, 63.32; H, 7.97; N, 28.71, Found (%): C, 63.56; H, 7.91; N, 28.49. FT-IR (in KBr): 3445, 2926, 1552, 1461, 1422, 1393, 1366, 1344, 1261, 1199, 1142, 1101, 1029, 990, 970, 818, 784, 708, 663, 627, 525 and 459 cm^{-1}. ^{1}H-NMR (400 MHz, $CDCl_3$): $\delta_{ppm,}$ 5.75 (s, 1H), 4.95 (s, 2H), 2.16 (s, 3H), 1.83 (s, 3H); ^{13}C-NMR (100 MHz, $CDCl_3$): $\delta_{ppm,}$ 147.6, 140.1, 105.9, 62.6, 13.3, 9.9. ESI-mass (m/z): Calcd.: 341.232, Found: 342.245 (M+1), 364.228 $[M+Na]^+$.

$[Co^{II}(L2)(CH_3CN)](ClO_4^-)_2$, 3.1

Acetonitrile solution of ligand, **L2** (0.341 g, 1 mmol) was added dropwise to a solution containing cobalt(II) perchlorate hexahydrate (0.366 g, 1 mmol) in acetonitrile. Then this solution was stirred for 3 h at room temperature. The volume of this reaction mixture was reduced to 5 mL and benzene was added to precipitate out the complex, **3.1**. Pink crystals were grown from acetonitrile/benzene mixture by slow evaporation. Yield: 0.525 g (*ca.* 82%).

Elemental analyses for $C_{20}H_{30}N_8O_8Cl_2Co$. Calcd. (%): C, 37.51; H, 4.72; N, 17.50. found (%): C, 37.62; H, 4.70; N, 17.65. UV-visible (CH_3CN): 219 ($\epsilon/M^{-1}cm^{-1}$, 2.23×10^4), 253 ($\epsilon/M^{-1}cm^{-1}$, 1.02×10^4), 304 ($\epsilon/M^{-1}cm^{-1}$, 4.29×10^3), 468 ($\epsilon/M^{-1}cm^{-1}$, 0.95×10^2) and 517 nm ($\epsilon/M^{-1}cm^{-1}$, 1.24×10^2). FT-IR (in KBr): 1554, 1469, 1423, 1393, 1306, 1279, 1248, 1177, 1086, 1056, 1011, 891, 813, 686, 621, 546, 500 and 439 cm^{-1}. ESI-mass (m/z): Calcd.: 499.11 for $[Co(L2)(ClO_4^-)]^+$, Found: 499.14. Magnetic moment: 3.006 BM. Crystal data: $C_{23}H_{33}N_8O_8Cl_2Co$, M = 679.40, triclinic (P -1), a = 12.0617(14), b = 12.3710(15), c = 12.5120(15) Å, α = 100.758(3)°, β = 109.688(3)°, γ = 113.809(3)°, V = 1491.2(3) $Å^3$, Z = 2, D_c = 1.513 g cm^{-3}, μ = 0.814 mm^{-1}, T = 297 K, 5171 reflections, 4826 independent, R(F) = 0.0504 [I>2δ(I)], R(int) = 0.0537, wR(F^2) = 0.1365 (all data), GOF = 1.033.

$[Co^{II}(L2)(NO_3^-)](ClO_4^-)$, 3.2

NO was purged for 5 min to the freshly generated Co(III)-peroxo species at -40 °C in acetonitrile solution with constant stirring. Then this reaction mixture was brought to room temperature and stirred for another 1 h. The color of the solution changed to brown from violet. Excess NO was removed by purging Ar and kept this reaction mixture for crystallization after layering over benzene. The brown needle shaped crystal of complex **3.2** was obtained after 3 d. Yield: 439 mg (*ca*. 70%). Elemental analyses for $C_{18}H_{27}N_8O_7ClCo$. Calcd. (%): C, 38.48; H, 4.84; N, 19.94. Found (%): C, 38.56; H, 4.73; N, 20.07. FT-IR (in KBr): 1555, 1495, 1471, 1384, 1281, 1249, 1103, 1054, 1009, 894, 801, 623 and 438 cm^{-1}. UV-visible (CH_3CN): 293 ($\epsilon/M^{-1}cm^{-1}$, 6.14×10^3) and 519 nm ($\epsilon/M^{-1}cm^{-1}$, 1.35×10^2). ESI-mass (m/z): Calcd.: 462.15, $[Co^{II}(L2)(NO_3^-)]^+$, Found: 462.15. Crystal data: $C_{18}H_{24}N_8O_7ClCo$, M = 558.83, monoclinic (C12/c1), a = 26.450(4), b = 10.5573(15), c = 20.758(3) Å, α = 90°, β = 119.862(3)°, γ = 90°, V = 5026.8(12) $Å^3$, Z = 8, D_c = 1.477 g cm^{-3}, μ = 0.843 mm^{-1}, T = 150 K, 4426 reflections, 3967 independent, R(F) = 0.0445 [I>2δ(I)], R(int) = 0.0513, wR(F^2) = 0.1135 (all data), GOF = 1.071.

3.3.3 Reaction of 3a and NO in the presence of 2,4-di-*tert*-butylphenol

Complex **3.1** was taken in a dry and degassed acetonitrile solution and kept it at -40 °C for 1 h. After that precooled H_2O_2 followed by NEt_3 was added to it. Immediately the color of the solution changed to violet from pink. This indicates the formation of corresponding Co(III)-peroxo intermediate, **3a**. To this cold solution, precooled 10 mL acetonitrile solution of 2,4-di-*tert*-butylphenol was added followed by NO gas. It was then allowed to stirred for 2 h followed by warm up to room temperature. The solvent was dried and 2,4-di-*tert*-butyl-6-nitrophenol and complex **3.3** were purified by using column chromatography.

2,4-di-*tert*-butyl-6-nitrophenol

Yield: 0.263 g (*ca.* 58%). Elemental analyses for $C_{14}H_{21}NO_3$. Calcd. (%): C, 66.91; H, 8.42; N, 5.57. Found (%): C, 66.85; H, 8.35; N, 5.69. FT-IR (in KBr): 2960, 2872, 1617, 1540, 1480, 1460, 1443, 1414, 1363, 1314, 1272, 1235, 1202, 1179, 1139, 1112, 1025, 923, 885, 822, 773, 749, 724, 707, 640, 532 and 513 cm^{-1}. ^{1}H-NMR (400 MHz, $CDCl_3$): $\delta_{ppm,}$ 11.45 (s, 1H), 7.96 (s, 1H), 7.65 (s, 1H), 1.45 (s, 9H), 1.32 (s, 9H). ^{13}C-NMR (100 MHz, $CDCl_3$): $\delta_{ppm,}$ 153.5, 142.4, 140.3, 134.2, 133.0, 119.3, 36.2, 35.0, 31.6, 29.9. ESI-mass (m/z): Calcd.: 251.152, Found: 250.145 (M-1).

$[Co^{III}(L2)(OH^-)](ClO_4^-)_2$, 3.3

Yield: 424 mg (*ca*. 67%). Elemental analyses for $C_{18}H_{28}N_7O_9Cl_2Co$. Calcd. (%): C, 35.08; H, 4.58; N, 15.91. Found (%): C, 35.19; H, 4.53; N, 15.83. FT-IR (in KBr): 3555, 1554, 1470, 1423, 1391, 1304, 1248, 1084, 930, 894, 807, 691, 622 and 441 cm^{-1}. UV-visible (CH_3CN):308 nm ($\epsilon/M^{-1}\,cm^{-1}$, 1.06×10^4), 396 nm ($\epsilon/M^{-1}\,cm^{-1}$, 3.56×10^3), and 525 nm ($\epsilon/M^{-1}\,cm^{-1}$, 1.23×10^2). ESI-mass (m/z): Calcd.: 200.080 (M/2), Found: 200.081.

3.4 Conclusion

A Co(II) complex, **3.1** with tripodal tetradentate ligand framework has been synthesized and characterized spectroscopically. Structural characterization revealed a distorted trigonal bipyramidal geometry around the central metal ion. Complex **3.1** in acetonitrile at -40 °C upon reaction with H_2O_2 in the presence of NEt_3 resulted in the corresponding Co(III)-peroxo intermediate. This intermediate in the presence of NO yielded corresponding nitrate complex, **3.2** *via* the putative formation of Co(II)-peroxynitrite. The formation of Co(II)-peroxynitrite intermediate was evidenced by the characteristic phenol ring nitration test.

3.5 References

1. Goyal, R. K.; Hirano, I. *N. Engl. J. Med*. **1996**, *334*, 1106.
2. Stark, M. E.; Szurszewski, J. H. *Gastroenterology*, **1992**, *103*, 1928.
3. Jaffrey, S. R.; Snyder, S. H. *Annu. Rev. Cell. Dev. Biol*. **1995**, *11*, 417.
4. Bogdan, C. *Nat. Immunol*. **2001**, *2*, 907.
5. Ignarro, L. J. *Nitric Oxide: Biology and Pathobiology*; Ed.; Academic Press: San Diego, **2000**.
6. Fang, F. C. *Nitric Oxide and Infection*; Ed., Kluwer Academic Plenum Publishers: New York, **1999**.
7. Bourassa, J. L.; Ives, E. P.; Marqueling, A. L.; Shimanovich, R.; Groves, J. T. *J. Am. Chem. Soc*. **2001**, *123*, 5142.
8. Lehnert, N.; Kim, E.; Dong, H. T.; Harland, J. B.; Hunt, A. P.; Manickas, E. C.; Oakley, K. M.; Pham, J.; Reed, G. C.; Alfaro, V. S. *Chem. Rev*. **2021**, *121*, 14682.
9. Gantner, B. N.; Lafond, K. M.; Bonini, M. G. *Redox Biology*, **2020**, *34*, 101550.
10. Horst, G.; Marletta, M. A. *Nitric Oxide*, **2018**, *77*, 65.

11. Schopfer, M. P.; Mondal, B.; Lee, D. H.; Sarjeant, A. A. N.; Karlin, K. D. *J. Am. Chem. Soc*. **2009**, *131*, 11304.

12. (a) Pfeiffer, S.; Gorren, A. C. F.; Schmidt, K.; Werner, E. R.; Hansert, B.; Bohle, D. S.; Mayer, B. *J. Biol. Chem*. **1997**, *272*, 3465. (b) Coddington, J. W.; Hurst, J. K.; Lymar, S. V. *J. Am. Chem. Soc*. **1999**, *121*, 2438. (c) Koppenol, W. H.; Bounds, P. L.; Nauser, T.; Kissner, R.; Rüegger, H. *Dalton Trans*. **2012**, *41*, 13779. (d) Lymar, S. V.; Khairutdinov, R. F.; Hurst, J. K. *Inorg. Chem*. **2003**, *42*, 5259. (e) Goldstein, S.; Lind, J.; Merényi, G. *Chem. Rev*. **2005**, *105*, 2457. (f) Molina, C.; Kissner, R.; Koppenol, W. H. *Dalton Trans*. **2013**, *42*, 9898.

13. (a) Schopfer, M. P.; Wang, J.; Karlin, K. D. *Inorg. Chem*. **2010**, *49*, 6267. (b) Ouellet, H.; Ouellet, Y.; Richard, C.; Labarre, M.; Wittenberg, B.; Wittenberg, J.; Guertin, M. *Proc. Natl. Acad. Sci. U. S. A*. **2002**, *99*, 5902. (c) Gardner, P. R.; Gardner, A. M.; Martin, L. A.; Salzman, A. L. *Proc. Natl. Acad. Sci. U. S. A*, **1998**, *95*, 10378. (d) Ford, P. C.; Lorkovic, I. M. *Chem. Rev*. **2002**, *102*, 993. (e) Gardner, P. R.; Gardner, A. M.; Brashear, W. T.; Suzuki, T.; Hvitved, A. N.; Setchell, K. D. R.; Olson, J. S. *J. Inorg. Biochem*. **2006**, *100*, 542.

14. (a) Clarkson, S. G.; Basolo, F. *J. Chem. Soc. Chem. Commun*. **1972**, *11*, 670. (b) Clarkson, S. G.; Basolo, F. *Inorg. Chem*. **1973**, *12*, 1528.

15. (a) Wick, P. K.; Kissner, R.; Koppenol, W. H. *Helv. Chim. Acta*. **2000**, *83*, 748. (b) Wick, P. K.; Kissner, R.; Koppenol, W. H. *Helv. Chim. Acta*. **2001**, *84*, 3057.

16. Thyagarajan, S.; Incarvito, C.; Rheingold, A. L.; Theopold, K. H. *Inorg. Chim. Acta*. **2003**, *345*, 333.

17. Maiti, D.; Lee, D. H.; Sarjeant, A. A.; Pau, M. Y. M.; Solomon, E. I.; Gaoutchenova, K.; Sundermeyer, J.; Karlin, K. D. *J. Am. Chem. Soc*. **2008**, *130*, 6700.

18. (a) Kurtikyan, T. S.; Eksuzyan, S. R.; Hayrapetyan, V. A.; Martirosyan, G. G.; Hovhannisyan, G. S.; Goodwin, J. A. *J. Am. Chem. Soc.* **2012**, *134*, 13861. (b) Kurtikyan, T. S.; Eksuzyan, S. R.; Goodwin, J. A.; Hovhannisyan, G. S. *Inorg. Chem*. **2013**, *52*, 12046.

19. Yokoyama, A.; Han, J. E.; Cho, J.; Kubo, M.; Ogura, T.; Siegler, M. A.; Karlin, K. D.; Nam, W. *J. Am. Chem. Soc*. **2012**, *134*, 15269.

20. Yokoyama, A.; Cho, K. B.; Karlin, K. D.; Nam, W. *J. Am. Chem. Soc*. **2013**, *135*, 14900.

21. Saha, S.; Ghosh, S.; Gogoi, K.; Deka, H.; Mondal, B.; Mondal, B. *Inorg. Chem*. **2017**, *56*, 10932.

22. Yenuganti, M.; Das, S.; Kulbir.; Ghosh, S.; Bhardwaj, P.; Pawar, S. S.; Sahoo, S. C.; Kumar, P. *Inorg. Chem. Front*. **2020**, *7*, 4872.

23. Das, S.; keerthi, A. C. S.; Kulbir.; Singh, S.; Roy, S.; Singh, R.; Ghosh, S.; Kumar, P. *Dalton Trans*. **2023**, *52*, 5095.

24. Samanta, B.; Ghosh, R.; Mazumdar, R.; Saha, S.; Maity, S.; Mondal, B. *Dalton Trans*. **2023**, *52*, 15815.

25. (a) Tran, N. G.; Kalyvas, H.; Skodje, K. M.; Hayashi, T.; Loccoz, P. M.; Callan, P. E.; Shearer, J.; Kirschenbau, L. J.; Kim, E. *J. Am. Chem. Soc*. **2011**, *133*, 1184. (b) Skodje, K. M.; Williard, P. G.; Kim, E. *Dalton Trans*. **2012**, *41*, 7849.

26. Kalita, A.; Kumar, P.; Mondal, B. *Chem. Commun*. **2012**, *48*, 4636.

27. Saha, S.; Gogoi, K.; Mondal, B.; Ghosh, S.; Deka, H.; Mondal, B. *Inorg. Chem*. **2017**, *56*, 7781.

28. Mondal, B.; Saha, S.; Borah, D.; Mazumdar, R.; Mondal, B. *Inorg. Chem*. **2019**, *58*, 1234.

29. Fujisawa, K.; Chiba, S.; Miyashita, Y.; Okamoto, K. *Eur. J. Inorg. Chem.* **2009**,

3921.

30. SMART, SAINT and XPREP, Siemens Analytical X-ray Instruments Inc, Madison, Wisconsin, *USA*, **1995**.

31. (a) Sheldrick, G. M. *Acta Crystallogr. Sect. A Found. Adv.* **2015**, *71*, 3. (b) Sheldrick, G. M. *Acta. Crystallogr. Sect. C Struct. Chem.* **2015**, *71*, 3. (c) Farrugia, L. J. ORTEP-3 for Windows - a version of ORTEP-III with a Graphical User Interface (GUI). *J. Appl. Crystallogr.* **1997**, *30*, 565.

Chapter 4

Reaction of a Co(III)-peroxo Complex of an Asymmetric Tetradentate Ligand with Nitric Oxide: Putative Formation of a Peroxynitrite Intermediate

Abstract

A Co(II) complex, $[Co^{II}(L3)(CH_3CN)](ClO_4^-)_2$, **4.1** having asymmetric tetradentate ligand **L3** [L3 = *N*^{1},*N*^{1}-*bis*((3,5-dimethyl-1H-pyrazol-1-yl)methyl)-*N*^{2},*N*^{2}-dimethylethane-1,2-diamine] has been synthesized and characterized spectroscopically. When complex **4.1** reacted with H_2O_2 followed by NEt_3 in acetonitrile solution at -40 °C, formation of the transient Co(III)-peroxo species, $[Co^{III}(L3)(O_2^{2-})]^+$, **4a** was observed. Addition of NO gas into the freshly generated Co(III)-peroxo species, **4a** in acetonitrile at -40 °C resulted in the corresponding Co(II)-nitrite complex $[Co^{II}(L3)(NO_2^-)](ClO_4^-)$, **4.2**. The reaction is believed to proceed through the formation of a putative Co(II)-peroxynitrite intermediate, **4b**. It was supported by the characteristic phenol ring nitration reaction.

4.1 Introduction

Nitric oxide (NO) is a diatomic heteronuclear gas. It acts as a signaling molecule in mammalian biology and takes part in various physiological processes like neurotransmission, vasodilation, defence immune system etc.[1-6] While a sub-micromolar concentration of NO is necessary for the smooth functioning of these processes.[1-8] Nitric oxide dioxygenase (NOD) enzymes regulate the amount of NO in biological systems. It is proposed that in NOD, a $[Fe^{III}(O_2^-)]$ complex, upon reaction with NO results in biologically atoxic nitrate (NO_3^-). This reaction is proposed to proceed *via* the formation of peroxynitrite intermediate. It decomposes to Fe(IV)-oxo and NO_2 *via* homolytic cleavage of 'O-O' bond of the peroxynitrite which upon recombination give NO_3^- ion.[9-11]

The reaction of NO with superoxo and peroxo complexes of iron, cobalt, and chromium have been shown to involve the formation of a metal-peroxynitrite intermediate.[12-19] The direct evidence for the formation of metal-peroxynitrite is still illusive, due to its short half-life.[6] For example, a $[Fe^{III}(L_a)(O_2^-)]$ complex in the presence of NO resulted in the corresponding $[Fe^{III}(L_a)(NO_3^-)]$ complex, *via* a proposed peroxynitrite intermediate.[10] A peroxo complex of Cr^{IV}, $[Cr^{IV}(12\text{-TMC})(O_2^{2-})(Cl)]^+$ was shown to reacts with NO to form the nitrate complex, $[Cr^{IV}(12\text{-TMC})(NO_3^-)(Cl)]^+$. However, its superoxo analogue, $[Cr^{III}(14\text{-TMC})(O_2^-)(Cl)]^+$ with reaction with NO gives $[Cr^{IV}(14\text{-TMC})(O)(Cl)]^+$ and NO_2. In both the cases, the formation of Cr(III)-peroxynitrite was proposed.[17,18] Kumar group reported a peroxo complex of Ni, $[Ni^{III}(12\text{-TMC})(O_2^{2-})]^+$ which reacts with NO and resulted in Ni(II)-nitrate complex, $[Ni^{II}(12\text{-TMC})(NO_3^-)]^+$.[20] Formation of the Ni(II)-peroxynitrite was proposed in this case. Mn(III)-peroxo complexes, $[Mn^{III}(3PYENMe)(O_2^{2-})]$ and $[Mn^{III}(N3PY)(O_2^{2-})]$ upon reaction with NO yielded the

corresponding Mn(II)-nitrate complexes, $[Mn^{II}(3PYENMe)(NO_3^-)]$ and $[Mn^{II}(N3PY)(NO_3^-)]$, respectively.[21] Formation of the Mn(II)-peroxynitrite intermediates were proposed in these cases. Recently, our group reported two Co(III)-peroxo complexes, $[Co^{III}(Iz)_2(O_2^{2-})]^+$ and $[Co^{III}(L1)_2(O_2^{2-})]^+$ which reacting with NO and resulted in the corresponding Co(II)-nitrate complexes $[Co^{II}(Iz)_2(NO_3^-)]^+$ and $[Co^{II}(L1)_2(NO_3^-)]^+$, respectively. Formation of the corresponding Co(II)-peroxynitrite intermediate was proposed in both the cases.[19,22]

Reaction involving metal nitrosyls and reactive oxygen species like superoxide and peroxide ions are also known to result in the corresponding nitrate/nitrite complexes *via* a peroxynitrite intermediate. For example, non-heme dinitrosyl complex of iron, $[Fe(NO)_2]$ reacts with oxygen molecule and forms nitrate complex.[23,24] A [Cu-NO] complex reacted with H_2O_2 to resulted in the Cu(II)-nitrate complex through a proposed Cu(I)-peroxynitrite intermediate.[25] Co-nitrosyl complexes, $[Co(Cl_4TPP^{2-})(NO)]$ and $[Co(F_8TPP^{2-})(NO)]$ in the presence of H_2O_2 yielded the corresponding $[Co^{III}(Cl_4TPP^{2-})(NO_2^-)]$ and $[Co^{III}(F_8TPP^{2-})(NO_3^-)]$ complexes, respectively. The putative formation of Co(II)-peroxynitrite intermediate was proposed in both cases .[26,27]

This chapter describes a Co(II)-complex, $[Co^{II}(L3)(CH_3CN)](ClO_4^-)_2$, **4.1** upon reaction with H_2O_2 followed by NEt_3 affords Co(III)-peroxo intermediate, $[Co^{III}(L3)(O_2^{2-})](ClO_4^-)$, **4a.** This species in the presence of NO resulted in the corresponding nitrite complex, $[Co^{II}(L3)(NO_2^-)](ClO_4^-)$, **4.2**. Chemical evidence suggests the formation of Co(II)-peroxynitrite intermediate, **4b** during this reaction.

4.2 Results and Discussion

A reported procedure was followed to synthesize the ligand, **L3**.[28] Ligand **L3** was obtained as

colorless oil and characterized using many spectroscopic techniques (Appendix III, Figures **A3.1-A3.4**). The Co(II)-complex, $[Co^{II}(L3)(CH_3CN)](ClO_4^-)_2$, **4.1** was synthesized by stirring the mixture of ligand **L3** and Co(II)-perchlorate hexahydrate in equimolar amount in acetonitrile. It was then characterized spectroscopically as well as structurally (Appendix III, Figures **A3.5-A3.8**). ORTEP diagram of complex **4.1** revealed that the cobalt centre is coordinated to four nitrogen atoms from the ligand **L3** and acetonitrile occupying in the axial position in a distorted trigonal bipyramidal geometry (Figure **4.1**). Perchlorate anions are packed in the crystal lattice near to the cobalt ion.

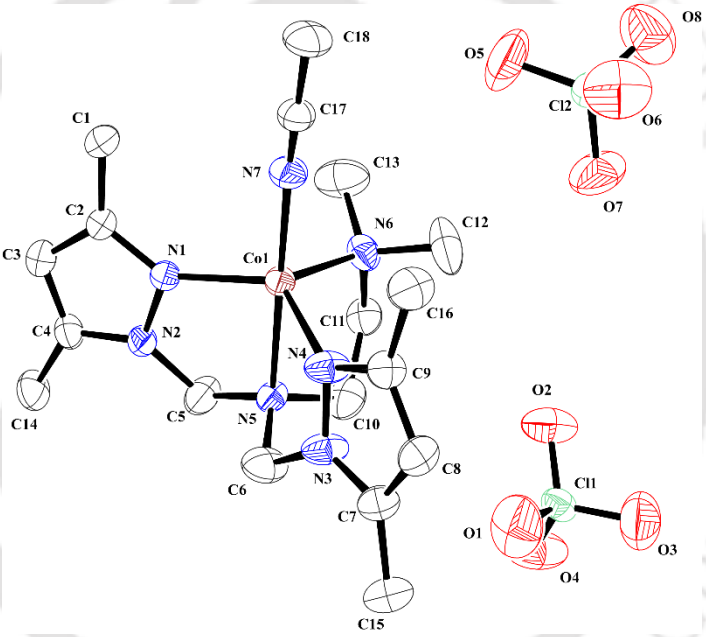

Figure 4.1. ORTEP diagram of complex **4.1** (35% thermal ellipsoid plot, H-atoms are omitted for clarity).

In UV-visible spectroscopy, complex **4.1** absorbs at 520 nm ($\epsilon/M^{-1}cm^{-1}$, 1.24×10^2) and 474 nm ($\epsilon/M^{-1}cm^{-1}$, 0.95×10^2) in acetonitrile solution which are assigned for the *d-d* transition of the cobalt ion. The other lower wavelength transitions are assigned for the intraligand transition (Appendix III, Figure **A3.6**). The X-band EPR spectrum of complex **4.1** in acetonitrile at 77 K displayed a peak at g ~ 4.82 which indicates the +2 oxidation state of cobalt ion (Appendix III, Figure **A3.8**). This value matches with other reported Co(II)-complexes.[22]

In the reaction of complex **4.1** in dry and degassed acetonitrile at -40 °C with 1.5 mole equivalent of H_2O_2 followed by 1 mole equivalent NEt_3 resulted in an unstable intermediate, **4a** (Scheme **4.1**). This intermediate was thermally unstable. During UV-visible spectral studies, **4a** absorbs at 440 nm (Figure **4.2**). This intensity of the absorption band diminishes over time, indicating the unstable nature of the intermediate. This is attributed to the corresponding Co(III)-peroxo species.

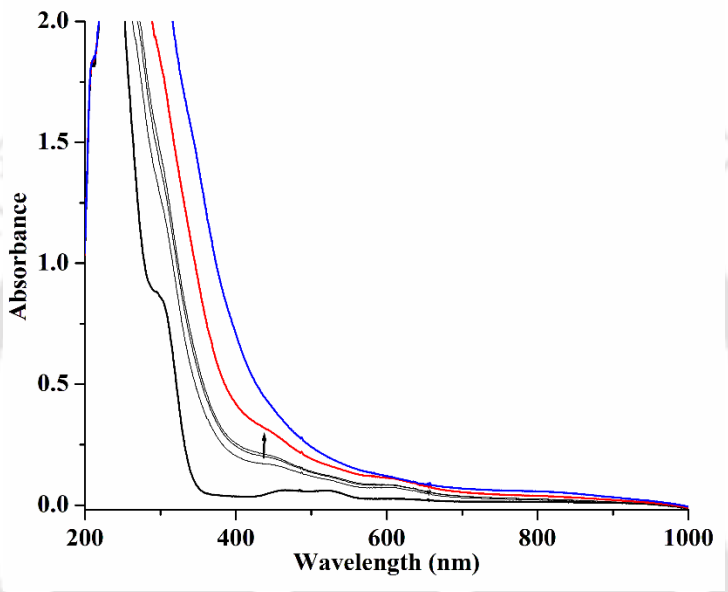

Figure 4.2. UV-visible spectra of the reaction of complex **4.1** with H_2O_2 followed by NEt_3 in acetonitrile at -40 °C [complex **4.1** (black), after the addition of H_2O_2 followed by NEt_3, intermediate **4a** (red)].

The Co(III)-peroxo complexes $[Co^{III}(Iz)_2(O_2^{2-})]^+$ and $[Co^{III}(L1)_2(O_2^{2-})]^+$ were reported to absorb at 452 nm ($\epsilon/M^{-1}cm^{-1}$, 890) and 375 nm ($\epsilon/M^{-1}cm^{-1}$, 856), respectively.[19,22] On the other hand, end-on Co(III)-peroxo complexes were reported to absorb in the range of 485 to 580 nm.[29]

In X-band EPR study after the addition of H_2O_2 followed by NEt_3 to the acetonitrile solution at 77 K of complex **4.1** giving rise to a EPR silent species (Figure **4.3**). This is expected for the formation of a Co(III)-peroxo species, **4a** having low spin Co(III)-centre.

In ESI-mass spectrometry, intermediate **4a** in acetonitrile showed molecular ion peak at m/z

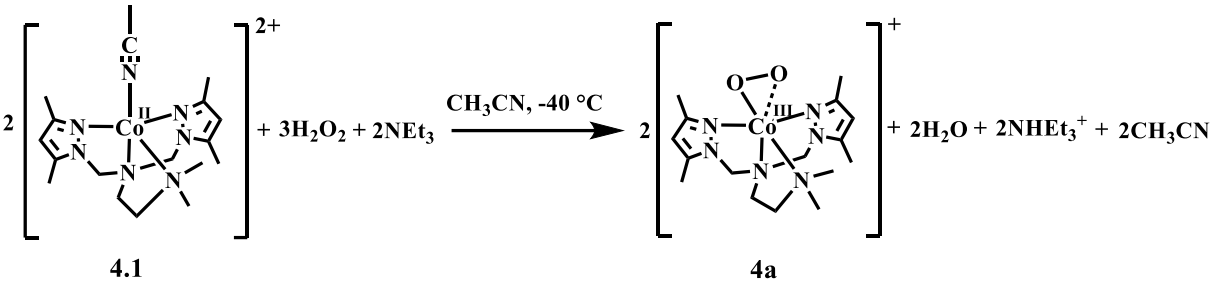

Scheme 4.1. Reaction of complex **4.1** with H_2O_2 followed by NEt_3 in acetonitrile at -40 °C.

395.162 (Figure **4.4**). This corresponds to the mass of $[Co^{III}(L3)(O_2^{2-})]^+$ moiety (Calcd. 395.160). The isotopic distribution pattern is in good agreement with the simulated one.

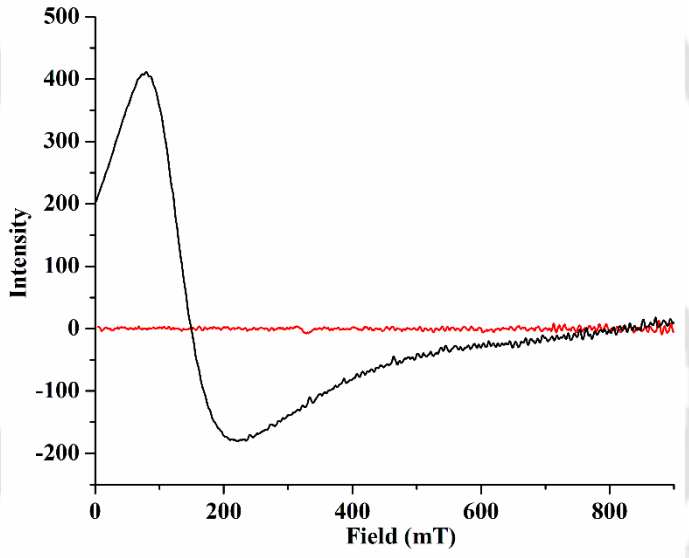

Figure 4.3. X-band EPR spectral monitoring of the reaction of complex **4.1** with H_2O_2 followed by NEt_3 in acetonitrile at 77 K [complex **4.1** (black), after addition of H_2O_2, intermediate **4a** (red)].

When freshly generated Co(III)-peroxo species are made to react with NO in dry and degassed acetonitrile solution at -40 ºC followed by warm up at room temperature, it yielded corresponding nitrite complex **4.2**, $[Co^{II}(L3)(NO_2^-)]^+$ (Scheme **4.2**). Complex **4.2** was isolated as a solid and characterized both spectroscopically and structurally (Appendix III, Figures **A3.9-A3.11**). The ORTEP of complex **4.2** is shown in figure **4.5**. The important bond lengths and bond angles are listed in the appendix (Appendix III, Tables **A3.1-A3.3**). Crystal structure

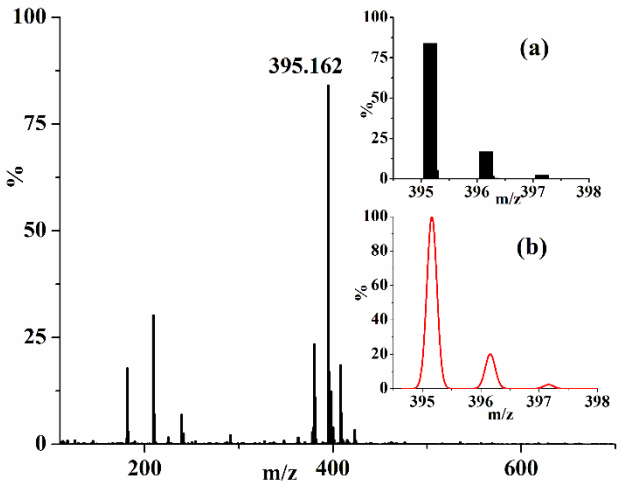

Figure 4.4. ESI-mass spectrum of Co(III)-peroxo intermediate, **4a** in acetonitrile. [Inset: (a) experimental (b) simulated isotopic distribution pattern].

of complex **4.2** confirms that the cobalt center is coordinated to four nitrogen atoms from the ligand and the nitrite group (NO_2^-) in a distorted octahedral geometry (Figure **4.5**). In FT-IR spectrum, complex **4.2** showed a strong signal at 1260 cm^{-1}, which indicates the presence of nitrite (NO_2^-) group in the complex (Appendix III, Figure **A3.9**). This value matches with the reported complexes.[30]

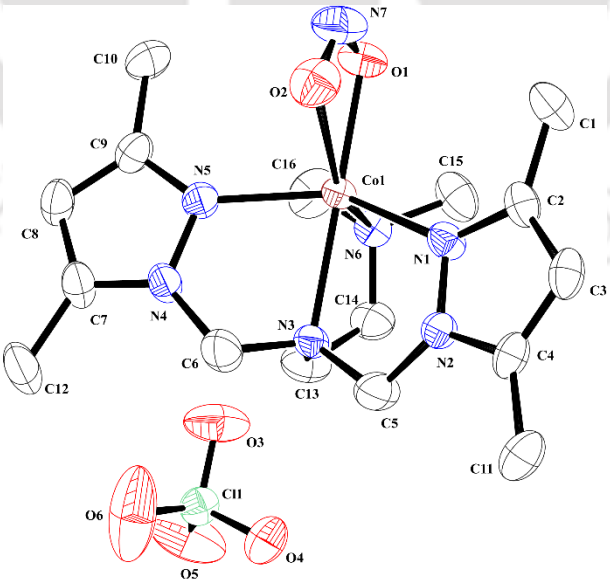

Figure 4.5. ORTEP diagram of complex **4.2** [35% thermal ellipsoid plot, solvent molecule and H-atoms are omitted for clarity].

The final decomposition product, **4.2** obtained after the reaction of **4a** with NO suggest the putative formation of peroxynitrite intermediate during the reaction process. In general, metal-peroxynitrite isomerize at room temperature to the corresponding nitrate (NO_3^-). However, it is also known to decompose to the nitrite (NO_2^-) complex with the release of ½ O_2.[31] The formation of O_2 was confirmed by the alkaline pyrogallol test.

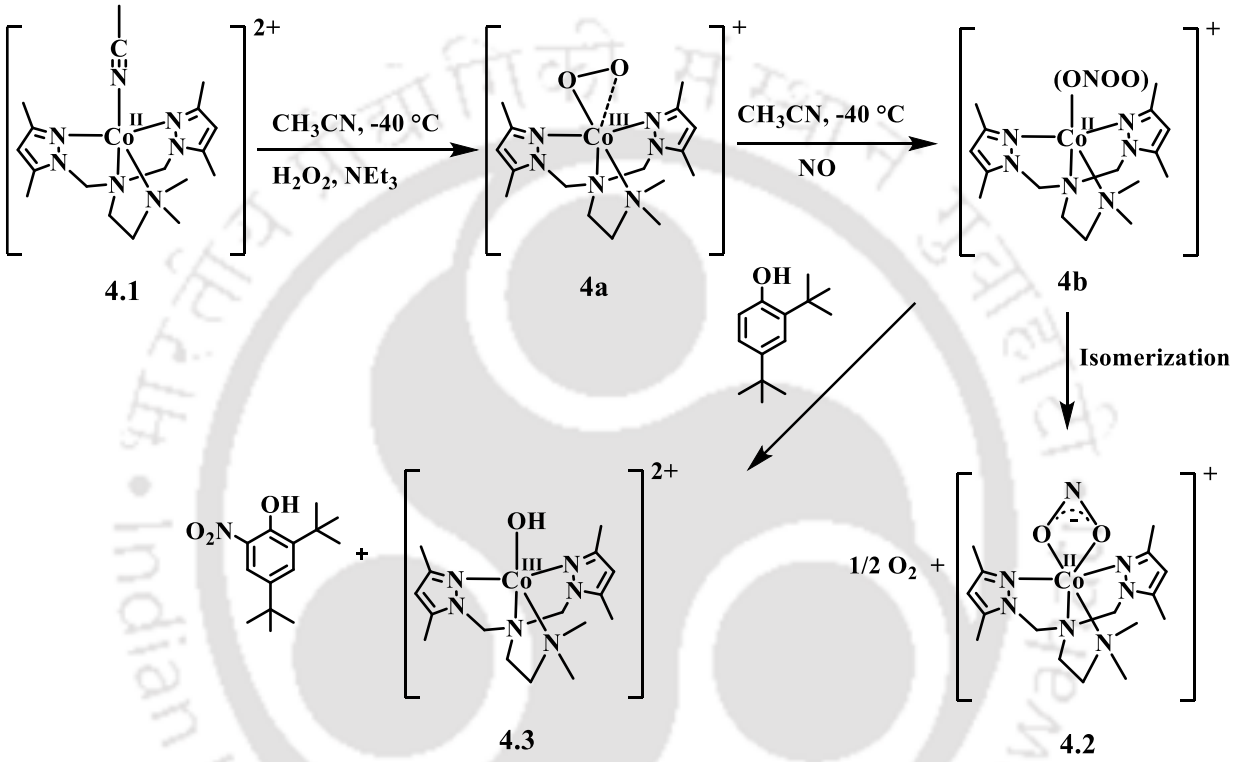

Scheme 4.2. Overall reactions.

Due to the thermal instability of the peroxynitrite intermediate, direct spectral evidence were not found. So, we sought for chemical evidences. When precooled dry and degassed acetonitrile Solution of 2,4-di-*tert*-butylphenol was added to the freshly generated Co(III)-peroxo solution followed by addition of NO, 2,4-di-*tert*-butyl-6-nitrophenol was obtained along with Co(III)-hydroxo product, complex **4.3** (Scheme **4.2**). Both of these products were isolated by column chromatography and characterized spectroscopically (Appendix III, Figures **A3.12-A3.19**). However, when 2,4-di-*tert*-butyl phenol was added after the addition of NO, complex **4.2**

was obtained exclusively with unreacted 2,4-di-*tert*-butylphenol.

4.3 Experimental Section

4.3.1 Materials and methods

All the reagents were purchased from commercial sources and used as it is without further purification unless specified. Acetonitrile was stored over calcium hydride overnight followed by distillation with P_2O_5 under N_2. All the reactions were performed under inert atmosphere except mentioned differently. Deoxygenation of solvents and solutions were effected by consecutive vacuum/Ar purge cycles. UV-visible spectra were taken on an Agilent Cary 8454 spectrophotometer. FT-IR spectra were recorded as KBr pellets or in a KBr cell using a PerkinElmer spectrophotometer. ^{1}H, ^{13}C-NMR studies were recorded using Bruker Avance III on 400 and 500 MHz Varian FT-NMR spectrophotometers. X-band EPR spectra were recorded on a JES-FA200 EPR spectrophotometer with microwave power, 0.998 mW; microwave frequency, 9.14 GHz; and modulation amplitude, 2.

Single crystals were grown from the respective acetonitrile-benzene solutions. The intensity data were collected using a Bruker SMART APEX-II CCD diffractometer, equipped with a fine focus 1.75 kW sealed tube Mo Kα radiation (λ = 0.71073 Å), with increasing ω (width of 0.3° per frame) at a scan speed of 3 s/frame. The SMART software was used for data acquisition. Data integration and reduction were undertaken with SAINT and XPREP software.[32] Structures were solved by direct methods using SHELXL[33a] and refined with full-matrix least-squares on F^2 using SHELXL-2019/1.[33b] Structural illustrations were drawn with ORTEP-3 for Windows.[33c]

4.3.2 Syntheses

[N^1,N^1-*bis*((3,5-dimethyl-1H-pyrazol-1-yl)methyl)-N^2,N^2-dimethylethane-1,2-diamine], (L3)

Ligand **L3** was prepared by stirring a mixture of 1-hydroxymethyl-3,5-dimethyl-1-pyrazole (1.26 g, 10 mmol) and N^1,N^1-dimethylethane-1,2-diamine (0.440 g, 5 mmol) in 30 mL acetonitrile for 3 d at room temperature. Then the solvent was removed using rotary evaporator to obtain the pure colorless oil ligand **L3**. Yield: 0.963 g (*ca*. 63%). Elemental analyses for $C_{16}H_{28}N_6$. Calcd. (%): C, 63.12; H, 9.27; N, 27.61, Found (%): C, 63.25; H, 9.41; N, 27.48. FT-IR (in KBr): 3205, 2951, 2866, 1581, 1555, 1459, 1423, 1378, 1303, 1251, 1226, 1114, 1108, 1030, 979, 931, 779, 669, 662, 626 and 473 cm^{-1}. ^{1}H-NMR (500 MHz, $CDCl_3$): $\delta_{ppm,}$ 2.09 (s, 6H), 2.16-2.19 (m, 14H), 2.71-2.75 (t, 2H), 4.89 (s, 4H), 5.77 (s, 2H). ^{13}C-NMR (125 MHz, $CDCl_3$): $\delta_{ppm,}$147.5, 139.8, 105.8, 65.6, 57.2, 47.1, 45.4, 13.5, 10.9. ESI-mass (m/z): Calcd.: 304.237, Found: 305.439 (M+1).

Complex 4.1, $[Co^{II}(L3)(CH_3CN)](ClO_4^-)_2$

Ligand, **L3** (304 mg, 1 mmol) was taken in 15 mL acetonitrile solution. This solution was added dropwise to 15 mL acetonitrile solution of Co(II)-perchlorate hexahydrate (366 mg, 1 mmol). The reaction mixture was stirred for 4 h at room temperature. Then volume of the mixture was reduced to 5 mL using rotary evaporator and benzene was added to make a layer. After 4 d, pink colored crystal of complex **4.1** was obtained. Yield: 501 mg (*ca*. 83%). Elemental analyses for $C_{18}H_{31}Cl_2N_7O_8Co$. Calcd. (%): C, 35.83; H, 5.18; N, 16.25; Found (%): C, 35.98; H, 5.27; N, 16.13. FT-IR (in KBr): 3381, 1554, 1469, 1425, 1387, 1303, 1276, 1249, 1206, 1100, 1052, 961, 929, 850, 825, 802, 777, 621, 546, 514, 486 and 438 cm^{-1}. UV-visible (CH_3CN): 297 nm (ϵ/M^{-1} cm^{-1}, 2.57×10^4), 474 nm (ϵ/M^{-1} cm^{-1}, 0.89×10^2) and 520 nm (ϵ/M^{-1} cm^{-1}, 0.97×10^2). X-band EPR (CH_3CN, 77 K): g ~ 4.82. ESI-mass (m/z), Calcd. 462.119

$[Co(L3)(ClO_4^-)]^+$; Found, 462.119. Crystal data: $C_{18}H_{31}N_7O_8Cl_2Co$, M = 603.33, monoclinic (P21/c), a = 10.894(2), b = 20.433(4), c = 12.811(3) Å, α = 90°, β = 110.110(5)°, γ = 90°, V = 2677.8(10) $Å^3$, Z = 4, D_c = 1.497 g cm^{-3}, μ = 0.895 mm^{-1}, T = 297 K, 4679 reflections, 4076 independent, R(F) = 0.0473 [I>2δ(I)], R(int) = 0.0558, wR(F^2) = 0.1317 (all data), GOF = 1.076.

4.3.3 Reaction of complex 4.1 with H_2O_2

Complex **4.1** was taken in a dry and degassed acetonitrile solution and kept it at -40 °C for 3 h. To this solution, 1.5 mole equivalent of H_2O_2 was added followed by 1 mole equivalent of NEt_3. Immediately the color of the solution changed from pink to purple. This indicates the formation of the intermediate, **4a**. UV-visible (CH_3CN): 440 nm (ϵ/$M^{-1}cm^{-1}$, 735) and 628 nm (ϵ/$M^{-1}cm^{-1}$, 125). ESI-mass (m/z): Calcd.: 395.160 for $[Co(L3)_2(O_2)]^+$, Found: 395.162.

Complex 4.2, $[Co^{II}(L3)(NO_2^-)](ClO_4^-)$

NO gas was purged to freshly generated Co(III)-peroxo species in acetonitrile solution at -40 °C. This reaction mixture was stirred for 1 h and then kept it at room temperature to obtain the complex **4.2**. Brown color needle shaped crystal was obtained upon layering with benzene to acetonitrile solution of complex **4.2**. Yield 368 mg (*ca*. 72%). Elemental analyses for $C_{16}H_{28}ClN_7O_6Co$. Calcd. (%): C, 37.77; H, 5.55; N, 19.27. Found (%): C, 37.88; H, 5.68; N, 19.13. FT-IR (in KBr): 1551, 1463, 1422, 1391, 1328, 1301, 1260, 1157, 1081, 1051, 1022, 965, 938, 849, 807, 775, 621, 475 and 425 cm^{-1}. UV-visible (CH_3CN): 281 nm (ϵ/M^{-1} cm^{-1}, 1.98 × 10^4) and 494 nm (ϵ/M^{-1} cm^{-1}, 1.14 × 10^2). ESI-mass (m/z): Calcd: 409.163, $[Co^{II}(L3)(NO_2^-)]^+$, Found: 408.168. Crystal data: $C_{16}H_{28}N_7O_6ClCo$, M = 508.83, orthorhombic (P 21 21 21), a = 8.1656(9), b = 10.5914(12), c = 26.227(3) Å, α = 90°, β = 90°, γ = 90°, V = 2268.2(4) $Å^3$, Z = 4, D_c = 1.490 g cm^{-3}, μ = 0.921 mm^{-1}, T = 296 K, 3967 reflections, 3779 independent, R(F) = 0.0473 [I>2δ(I)], R(int) = 0.0558, wR(F^2) = 0.1097 (all data), GOF =

1.111.

4.3.4 Reaction of 4.1 with H_2O_2 and NO in the presence of 2,4-di-*tert*-butylphenol

Complex **4.1** was taken in a dry and degassed acetonitrile solution and kept it at -40 °C for 2 h. To this solution, precooled H_2O_2 followed by NEt_3 was added to afford corresponding Co(III)-peroxo intermediate species. Precooled acetonitrile solution of 2,4-di-*tert*-butylphenol was added to this freshly generated Co(III)-peroxo solution followed by the addition of NO. This reaction mixture was stirred at -40 °C for 3 h. After warming up at room temperature, excess NO gas was removed by purging Ar. Complex **4.3** and 2,4-di-*tert*-butyl-6-nitrophenol were purified using column chromatography.

2,4-di-*tert*-butyl-6-nitrophenol

Yield: 0.263 g (*ca.* 58%). Elemental analyses for $C_{14}H_{21}NO_3$. Calcd. (%): C, 66.91; H, 8.42; N, 5.57. Found (%): C, 66.80; H, 8.31; N, 5.70. FT-IR (in KBr): 2960, 2871, 1617, 1541, 1480, 1459, 1443, 1415, 1363, 1314, 1272, 1234, 1202, 1179, 1138, 1111, 1025, 923, 884, 825, 773, 749, 724, 700, 652, 640, 532 and 512 cm^{-1}. ^{1}H-NMR (400 MHz, $CDCl_3$): $\delta_{ppm,}$ 11.44 (s, 1H), 7.96 (s, 1H), 7.64 (s, 1H), 1.45 (s, 9H), 1.32 (s, 9H). ^{13}C-NMR (100 MHz, $CDCl_3$): $\delta_{ppm,}$ 153.6, 142.5, 140.4, 134.3, 133.1, 119.4, 36.3, 35.1, 31.7, 30.0. ESI-mass (m/z): Calcd.: 251.152, Found: 250.141 (M-1).

Complex 4.3, $[Co^{III}(L3)(OH)](ClO_4)_2$

Yield: 308 mg (*ca*. 52%). Elemental analyses for $C_{16}H_{29}Cl_2N_6O_9Co$. Calcd. (%): C, 33.18; H, 5.05; N, 14.51. Found (%): C, 33.02; H, 5.21; N, 14.37. FT-IR (in KBr): 3545, 1626, 1555, 1465, 1421, 1393, 1295, 1076, 930, 798, 621, 538 and 462 cm^{-1}. UV-visible (CH_3CN): 277 nm (ϵ/M^{-1} cm^{-1}, 1.85× 10^4), 545 nm (ϵ/M^{-1} cm^{-1}, 0.76 × 10^2). ESI-mass (m/z): Calcd.: 181.585, Found: 181.586 (m/2).

4.4 Conclusion

A Co(II)-complex, **4.1** having tripodal tetradentate ligand framework has been synthesized and characterized using spectroscopic technichques as well as structure determination. Complex **4.1** in acetonitrile in the presence of H_2O_2 and NEt_3 at -40 ˚C resulted in the corresponding Co(III)-peroxo intermediate. This intermediate in the presence of NO yielded corresponding nitrite complex, **4.2** *via* the putative formation of Co(II)-peroxynitrite. The formation of Co(II)-peroxynitrite intermediate was evidenced by the chemical test of the phenol ring nitration test.

4.5 References

1. Jaffrey, S. R.; Snyder, S. H. *Annu. Rev. Cell. Dev. Biol*. **1995**, *11*, 417.
2. Bogdan, C. *Nat. Immunol*. **2001**, *2*, 907.
3. Ignarro, L. J. *Nitric Oxide: Biology and Pathobiology*; Ed.; Academic Press: San Diego, **2000**.
4. Fang, F. C. *Nitric Oxide and Infection*; Ed.; Kluwer Academic Plenum Publishers: New York, **1999**.
5. Bourassa, J. L.; Ives, E. P.; Marqueling, A. L.; Shimanovich, R.; Groves, J. T. *J. Am. Chem. Soc*. **2001**, *123*, 5142.
6. Lehnert, N.; Kim, E.; Dong, H. T.; Harland, J. B.; Hunt, A. P.; Manickas, E. C.; Oakley, K. M.; Pham, J.; Reed, G. C.; Alfaro, V. S. *Chem. Rev*. **2021**, *121*, 14682.
7. Gantner, B. N.; Lafond, K. M.; Bonini, M. G. *Redox Biology*, **2020**, *34*, 101550.
8. Horst, G.; Marletta, M. A. *Nitric Oxide*, **2018**, *77*, 65.
9. (a) Pfeiffer, S.; Gorren, A. C. F.; Schmidt, K.; Werner, E. R.; Hansert, B.; Bohle, D. S.; Mayer, B. *J. Biol. Chem*. **1997**, *272*, 3465. (b) Coddington, J. W.; Hurst, J. K.; Lymar, S. V. *J. Am. Chem. Soc*. **1999**, *121*, 2438. (c) Koppenol, W. H.; Bounds,

P. L.; Nauser, T.; Kissner, R.; Rüegger, H. *Dalton Trans*. **2012**, *41*, 13779. (d) Lymar, S. V.; Khairutdinov, R. F.; Hurst, J. K. *Inorg. Chem*. **2003**, *42*, 5259. (e) Goldstein, S.; Lind, J.; Merényi, G. *Chem. Rev*. **2005**, *105*, 2457. (f) Molina, C.; Kissner, R.; Koppenol, W. H. *Dalton Trans*. **2013**, *42*, 9898.

10. Schopfer, M. P.; Mondal, B.; Lee, D. H.; Sarjeant, A. A. N.; Karlin, K. D. *J. Am. Chem. Soc*. **2009**, *131*, 11304.
11. (a) Schopfer, M. P.; Wang, J.; Karlin, K. D. *Inorg. Chem*. **2010**, *49*, 6267. (b) Ouellet, H.; Ouellet, Y.; Richard, C.; Labarre, M.; Wittenberg, B.; Wittenberg, J.; Guertin, M. *Proc. Natl. Acad. Sci*. U. S. A. **2002**, *99*, 5902. (c) Gardner, P. R.; Gardner, A. M.; Martin, L. A.; Salzman, A. L. *Proc. Natl. Acad. Sci. U. S. A*, **1998**, *95*, 10378. (d) Ford, P. C.; Lorkovic, I. M. *Chem. Rev*. **2002**, *102*, 993. (e) Gardner, P. R.; Gardner, A. M.; Brashear, W. T.; Suzuki, T.; Hvitved, A. N.; Setchell, K. D. R.; Olson, J. S. *J. Inorg. Biochem*. **2006**, *100*, 542.
12. (a) Clarkson, S. G.; Basolo, F. *J. Chem. Soc. Chem. Commun*. **1972**, *11*, 670. (b) Clarkson, S. G.; Basolo, F. *Inorg. Chem*. **1973**, *12*, 1528.
13. (a) Wick, P. K.; Kissner, R.; Koppenol, W. H. *Helv. Chim. Acta*. **2000**, *83*, 748. (b) Wick, P. K.; Kissner, R.; Koppenol, W. H. *Helv. Chim. Acta*. **2001**, *84*, 3057.
14. Thyagarajan, S.; Incarvito, C.; Rheingold, A. L.; Theopold, K. H. *Inorg. Chim. Acta*. **2003**, *345*, 333.
15. Maiti, D.; Lee, D. H.; Sarjeant, A. A.; Pau, M. Y. M.; Solomon, E. I.; Gaoutchenova, K.; Sundermeyer, J.; Karlin, K. D. *J. Am. Chem. Soc*. **2008**, *130*, 6700.
16. (a) Kurtikyan, T. S.; Eksuzyan, S. R.; Hayrapetyan, V. A.; Martirosyan, G. G.; Hovhannisyan, G. S.; Goodwin, J. A. *J. Am. Chem. Soc*. **2012**, *134*, 13861. (b) Kurtikyan, T. S.; Eksuzyan, S. R.; Goodwin, J. A.; Hovhannisyan, G. S. *Inorg.*

Chem. **2013**, *52*, 12046.

17. Yokoyama, A.; Han, J. E.; Cho, J.; Kubo, M.; Ogura, T.; Siegler, M. A.; Karlin, K. D.; Nam, W. *J. Am. Chem. Soc*. **2012**, *134*, 15269.
18. Yokoyama, A.; Cho, K. B.; Karlin, K. D.; Nam, W. *J. Am. Chem. Soc*. **2013**, *135*, 14900.
19. Saha, S.; Ghosh, S.; Gogoi, K.; Deka, H.; Mondal, B.; Mondal, B. *Inorg. Chem*. **2017**, *56*, 10932.
20. Yenuganti, M.; Das, S.; Kulbir.; Ghosh, S.; Bhardwaj, P.; Pawar, S. S.; Sahoo, S. C.; Kumar, P. *Inorg. Chem. Front*. **2020**, *7*, 4872.
21. Das, S.; Keerthi, A. C. S.; Kulbir.; Singh, S.; Roy, S.; Singh, R.; Ghosh, S.; Kumar, P. *Dalton. Trans*. **2023**, *52*, 5095.
22. Samanta, B.; Ghosh, R.; Mazumdar, R.; Saha, S.; Maity, S.; Mondal, B. *Dalton Trans*. **2023**, *52*, 15815.
23. Tran, N. G.; Kalyvas, H.; Skodje, K. M.; Hayashi, T.; Loccoz, P. M.; Callan, P. E.; Shearer, J.; Kirschenbau, L. J.; Kim, E. *J. Am. Chem. Soc*. **2011**, *133*, 1184.
24. Skodje, K. M.; Williard, P. G.; Kim, E. *Dalton Trans*. **2012**, *41*, 7849.
25. Kalita, A.; Kumar, P.; Mondal, B. *Chem. Commun*. **2012**, *48*, 4636.
26. Saha, S.; Gogoi, K.; Mondal, B.; Ghosh, S.; Deka, H.; Mondal, B. *Inorg. Chem*. **2017**, *56*, 7781.
27. Mondal, B.; Saha, S.; Borah, D.; Mazumdar, R.; Mondal, B. *Inorg. Chem*. **2019**, *58*, 1234.
28. Driessen, W. L. *J. R. Neth. Chem. Soc*. **1982**, *101*, 441.
29. Wang, C. C.; Chang, H. C.; Lai, Y. C.; Fang, H.; Li, C. C.; Hsu, H. K.; Li, Z. Y.; Lin, T. S.; Kuo, T. S.; Neese, F.; Ye, S.; Chiang, Y. W.; Tsai, M. L.; Liaw, W. F.; Lee, W. Z. *J. Am. Chem. Soc*. **2016**, *138*, 14186.

30. Gogoi, K.; Saha, S.; Mondal, B.; Deka, H.; Ghosh, S.; Mondal, B. *Inorg. Chem*. **2017**, *56*, 14438.

31. Park, G. Y.; Deepalatha, S.; Pulu, S. C.; Lee, D. H.; Mondal, B.; Sarjeant, A. A. N.; Rio, D.; Pau, M. Y. M.; Solomon, E. I.; Karlin, K. D. *J. Biol. Inorg. Chem*. **2009**. *14*, 1301.

32. SMART, SAINT and XPREP, Siemens Analytical X-ray Instruments Inc, Madison, Wisconsin, USA, **1995**.

33. (a) Sheldrick, G. M. *Acta Crystallogr. Sect. A Found. Adv.* **2015**, *71*, 3. (b) Sheldrick, G. M. *Acta. Crystallogr. Sect. C Struct. Chem.* **2015**, *71*, 3. (c) Farrugia, L. J. ORTEP-3 for Windows - a version of ORTEP-III with a Graphical User Interface (GUI). *J. Appl. Crystallogr.* **1997**, *30*, 565.

Chapter 5

Reaction of a Nitrosyl Complex of Co(II)-porphyrin with Hydrogen peroxide: Formation of a Porphyrin Radical Cation

Abstract

A nitrosyl complex of Co(II)-porphyrinate, $[Co^{II}(TTMPP^{2-})(NO)]$, **5.1** having $\{Co(NO)\}^8$ configuration has been synthesized and characterized both spectroscopically as well as structurally. Complex **5.1** in dichloromethane:acetonitrile (1:4, v/v) solution at -40 ºC reacts with H_2O_2 which results in the corresponding nitrite (NO_2^-) complex, $[Co^{III}(TTMPP^{2-})(NO_2^-)]$, **5.2**. Involvement of a Co(III)-peroxynitrite intermediate is proposed during this reaction based on the characteristic phenol ring nitration test. From spectroscopic studies, formation of Co(IV)-oxo species followed by a Co(III)-porphyrin radical complex was observed during the course of the reaction.

5.1 Introduction

Nitric oxide (NO) has been identified as a signaling molecule in mammalian biology. It has been found to control various physiological processes including neurotransmission, vasodilation, immune response etc. For these activities, it is required in sub-micromolar concentration.[1-10] However, overproduction of it leads to the oxidative and nitrosative stress through the formation of reactive nitrogen species like nitrogen dioxide (NO_2) or peroxynitrite ($ONOO^-$).[8] Nitric oxide dioxygenases (NOD) enzyme regulates the level of NO in biological systems. It is proposed that in NOD, $[Fe^{III}(O_2^-)]$ reacts with NO to result in the biologically benign nitrate (NO_3^-) *via* a peroxynitrite intermediate.[11-13] Hence, NO reactivity study towards metal-peroxo or superoxo species is of immense importance for better understanding of this chemistry. Consequently, the reactivity of metal-superoxo/peroxo complexes with NO were studied in small molecule models and the involvement of peroxynitrite intermediate in these reactions was proposed.[14-22] For example, the reaction of a $[Fe^{III}(F_8TPP^{2-})(O_2^-)]$ complex with NO was reported to afford the corresponding nitrate complex, $[Fe^{III}(F_8TPP^{2-})(NO_3^-)]$ *via* a presumed peroxynitrite intermediate.[11] A Cr(IV)-peroxo complex, $[Cr^{IV}(12\text{-TMC})(O_2^{2-})(Cl)]^+$ on reaction with NO was reported to result in the nitrate complex, $[Cr^{IV}(12\text{-TMC})(NO_3^-)(Cl)]^+$.[19] However, the superoxo analogue $[Cr^{III}(14\text{-TMC})(O_2^-)(Cl)]^+$, in similar reaction gives corresponding Cr(IV)-oxo and NO_2.[20] In both the cases, the involvement of Cr(III)-peroxynitrite was proposed.

On the other hand, reaction of metal nitrosyls with superoxide, peroxide ions or dioxygen has also been exemplified which leads to the corresponding nitrate/nitrite complexes *via* a peroxynitrite intermediate. For instance, a non-heme dinitrosyl complex of iron reacts with oxygen and gives nitrate complex.[23] A Cu-NO complex, in

its reaction with H_2O_2 was shown to produce Cu(II)-nitrate complex. Chemical evidence and decomposition product analysis suggest the involvement of Cu(I)-peroxynitrite intermediate in this reaction.[24] In addition, Co-nitrosyl complexes, [Co(Cl_4TPP^{2-})(NO)] and [Co(F_8TPP^{2-})(NO)], in similar reaction result in the corresponding [Co^{III}(Cl_4TPP^{2-})(NO_2^-)] and [Co^{III}(F_8TPP^{2-})(NO_3^-)] complexes, respectively.[25,26] Although, no spectral evidence was observed for the formation of corresponding metal-peroxynitrite intermediate, it was implicated from indirect evidence. A [Mn($F_{20}TPP^{2-}$)(NO)] complex and O_2^-, react to gives [Mn^{III}($F_{20}TPP^{2-}$)(NO_3^-)] through a presumed Mn(III)-peroxynitrite intermediate.[27] In this case, formation of [Mn^{IV}=O] was detected in the reaction medium which was formed after the cleavage of O-O bond of peroxynitrite intermediate. It is to be noted that though the metal-peroxynitrite complexes have been proposed to undergo homolylic cleavage of the O-O bond to result in the corresponding [M^{x+}=O] species and NO_2, examples are very few.[20,27] In addition, the reaction of [Mn($TMPP^{2-}$)(NO)] complex with superoxide has also been exemplified to yield the corresponding [Mn^{III}($TMPP^{2-}$)(OH)] *via* presumed Mn(III)-peroxynitrite intermediate.[28] In this reaction the involvement of [Mn^{IV}($TMPP^{2-}$)(O)] was evidenced in spectroscopic studies.

This chapter describes the synthesis and characterization of a penta-coordinated cobalt-nitrosyl complex, [Co($TTMPP^{2-}$)(NO)], **5.1** having {Co(NO)}^{8} configuration. Upon reaction with H_2O_2, it gives corresponding nitrite complex, [Co^{III}($TTMPP^{2-}$)(NO_2^-)], **5.2**. Formation of the peroxynitrite intermediate is proposed in the course of the reaction based on its characteristic phenol ring nitration test. In addition, spectroscopic analyses suggest the involvement of cobalt(IV)-oxo species followed by the formation of porphyrin radical cation in this reaction. This, in turn, supports the formation of the Co(III)-peroxynitrite intermediate.

5.2 Results and Discussion

Adler's method was followed to synthesize the ligand $TTMPPH_2$, and it was characterized spectroscopically (Appendix IV, Figures **A4.1-A4.4**).[29] The precursor complex, [Co^{II}($TTMPP^{2-}$)], **5.1a** was synthesized by following a reported procedure.[30] Complex **5.1a** was characterized spectroscopically using UV-visible, FT-IR, EPR spectroscopy and ESI-mass spectrometry (Appendix IV, Figures **A4.5-A4.8**). The single crystal X-ray structure of complex **5.1a** shows a square planar geometry around the cobalt centre (Figure **5.1**). The X-band EPR spectrum of the complex **5.1a** shows characteristic signal of low spin Co(II)-centre (Appendix IV, Figure **A4.8**).

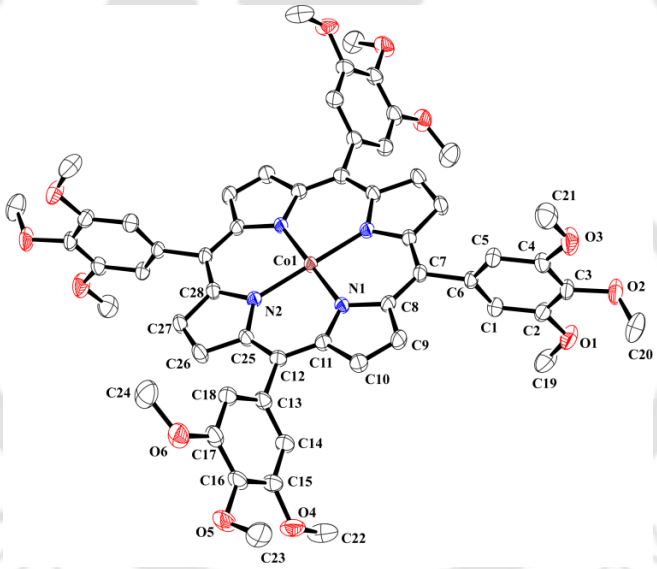

Figure 5.1. ORTEP diagram of complex **5.1a** [30% thermal ellipsoid plot, H-atoms and solvent are omitted for clarity].

The nitrosyl complex [Co($TTMPP^{2-}$)(NO)], **5.1** was synthesized by addition of NO gas in the degassed dichloromethane solution of complex **5.1a**. Complex **5.1** was isolated as red solid and characterized spectroscopically as well as structurally (Appendix IV, Figures **A4.9-A4.12**). The perspective ORTEP view of complex **5.1** suggests that the cobalt center is coordinated to four nitrogen atoms of porphyrin ring and NO group is

bonded axially which results in a square pyramidal geometry (Figure **5.2**). The N-O bond length is 1.218(9) Å and Co-N-O bond angle is 141.6(6)° which match well with the reported complexes.[31,32] The observed metric parameters for complex **5.1** suggest the bent nature of the coordinated nitrosyl moiety (Appendix IV, Tables **A4.1-A4.3**).[20,25-28]

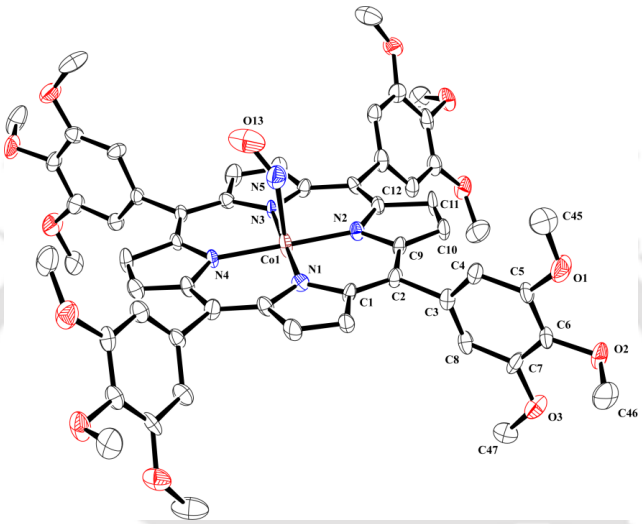

Figure 5.2. ORTEP diagram of complex **5.1** [30% thermal ellipsoid plot, H-atoms and solvent are omitted for clarity].

In the FT-IR spectrum of complex **5.1**, the metal-bound NO stretching frequency appears at 1675 cm^{-1} (Figure **5.3**). Kurtikyan group reported that NO stretching

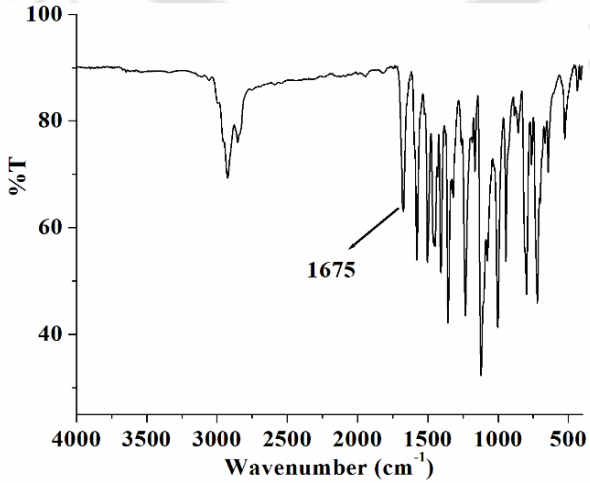

Figure 5.3. FT-IR spectrum of complex **5.1** using ATR probe.

Frequencies of [Co(TPP^{2-})(NO)] and [Co(OEP^{2-})(NO)] complexes, having *meso*-tetraphenylporphyrin and octaethylporphyrin framework, appear at 1689 cm^{-1} and 1675 cm^{-1} (in dichloromethane), respectively.[18] For [Co(F_8TPP^{2-})(NO)], NO stretching frequency appears at 1692 cm^{-1} in KBr.[26] For [Co{T(*p*/*m*-X)PP}(NO)], [where *p*/*m*-X = *p*-OCH_3, *p*-CH_3, *m*-CH_3, *p*-H, *m*-OCH_3, *p*-OCF_3, *p*-CF_3, *p*-CN etc.], it appears in the range of 1681-1695 cm^{-1} in dichloromethane solution.[33]

ESI-mass spectrum of complex **5.1** shows a signal at m/z = 1031.293, which corresponds to [Co^{II}(TTMPP^{2-})] moiety (Calcd. 1031.291) (Appendix IV, Figure **A4.12**). This is attributed to the facile loss of NO group from the apical position of square pyramidal metal-nitrosyls.[25,32] Owing to the antiferromagnetic coupling between NO group and cobalt(II)-centre, complex **5.1** becomes EPR silent (Appendix IV, Figure **A4.11**). As a consequence, it shows well resolved ^{1}H-NMR spectrum confirming the diamagnetic nature of the complex (Appendix IV, Figure **A4.10**).

Complex **5.1** is inert towards dioxygen but it reacts with H_2O_2. The reaction of 1.5 mole equivalent of H_2O_2 with complex **5.1** in dichloromethane:acetonitrile (1:4, v/v) solution yielded the corresponding nitrite complex, [Co^{III}(TTMPP^{2-})(NO_2^-)], **5.2** as the final product (Scheme **5.1**). Complex **5.2** was isolated as solid and characterized spectroscopically and structurally (Appendix IV, Figures **A4.13-A4.17**). The ORTEP diagram of complex **5.2** is shown in figure 5.4. Crystal structure of complex **5.2** has

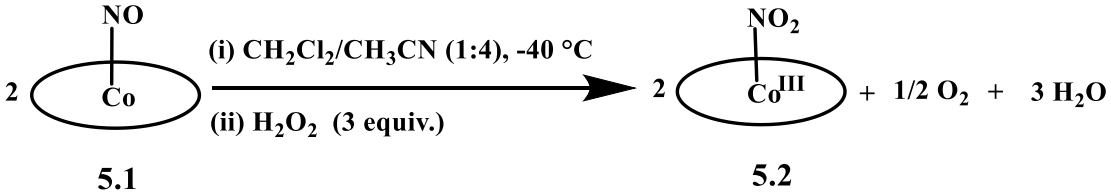

5.1 **5.2**

Scheme 5.1

some intrinsic disorder which could not be resolved even after growing the crystal in different sets. Due to thermal vibration, two oxygen atoms of nitrite (NO_2^-) group occupied in three vibrational positions (Figure **5.4**). FT-IR spectrum of complex **5.2** shows a strong stretching frequency at 1259 cm^{-1}, which confirms the presence of nitrite group (Appendix IV, Figure **A4.13**).[25] The ESI-mass spectrum of complex **5.2** shows a molecular ion peak at m/z = 1077.282 (Calcd. 1077.284 for [Co^{III}(TTMPP^{2-})(NO_2^-)]) (Appendix IV, Figure **A4.16**). The EPR silent nature and well resolved ^{1}H-NMR spectrum of complex **5.2** suggest that the cobalt-centre is in +3 oxidation state (Appendix IV, Figures **A4.15, A4.17**).

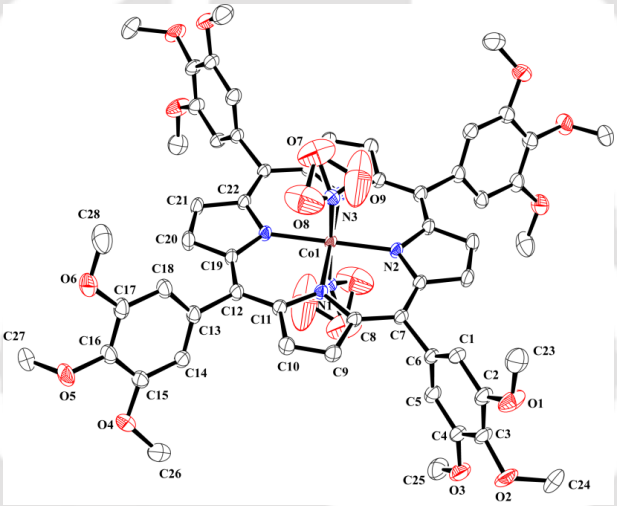

Figure 5.4. ORTEP diagram of complex **5.2** [35% thermal ellipsoid plot, H-atoms and solvent are omitted for clarity].

In UV-visible spectroscopy, complex **5.1** in dichloromethane:acetonitrile (1:4, v/v) solution displays the characteristic soret band at 418 nm and Q band at 537 nm at -40 °C. When precooled 1.5 mole equivalent H_2O_2 was added to the above solution, immediately the soret band and Q band shifted to 434 nm and 543 nm, respectively. This absorption band at 434 nm was further shifted to 458 nm with a quenching of intensity (Figure **5.5**). A new set of absorption bands appeared at 712, 818 and 926 nm

(Figure **5.5**). These are attributed to the decomposition to unidentified multiple products. However, the reaction mixture was allowed to warm-up fast, it yielded complex **5.2** (*vide infra*). This quenching of soret band indicates the formation of a porphyrin radical cation during the course of the reaction.[34] It has been shown earlier that the reaction of metal-nitrosyl with H_2O_2 results in the formation of corresponding peroxynitrite intermediate, which owing to its instability leads to the formation of metal-oxo species and NO_2.[26,27] This metal-oxo species then isomerizes to more stable porphyrin radical cation complex.[34] In the present case, the transient absorptions at 434 nm and 543 nm bands are attributed to the corresponding [Co^{IV}=O] species (Figure **5.5**).

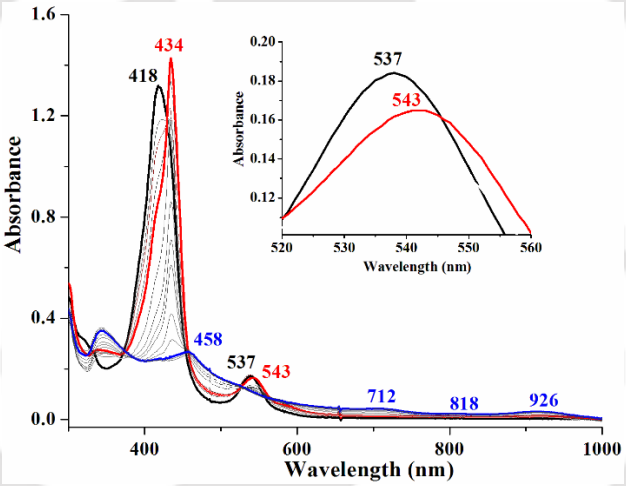

Figure 5.5. UV-visible spectral monitoring of the reaction of complex **5.1** with H_2O_2 [complex **5.1** (black), after addition of H_2O_2 (red), final (blue) in dichloromethane:acetonitrile (1:4, v/v) solution at -40 ºC)].

In addition, the X-band EPR spectroscopic analysis of the frozen reaction mixture of complex **5.1** and H_2O_2 in dichloromethane:acetonitrile (1:4, v/v) solution displays a sharp isotropic signal at g ~ 2.001 which attributes to the formation of a radical species in the reaction mixture (Figure **5.6**). When this reaction mixture was brought to room temperature, the signal was disappeared due to the formation of complex **5.2**. Both [Co^{IV}=O] and NO_2 are formed *via* the decomposition of peroxynitrite intermediate.

These two species are expected to show EPR signals. However, at 77 K temperature NO_2 dimerizes to form a diamagnetic species N_2O_4. So, in this case, sharp isotropic

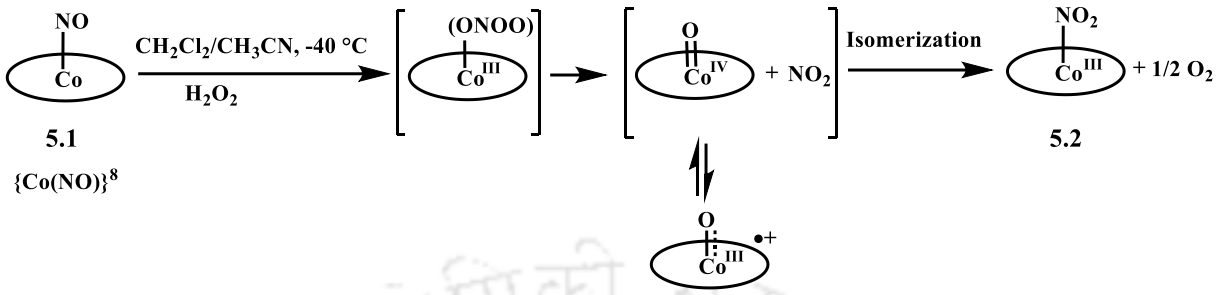

Scheme 5.2

signal at g ~ 2.001 indicates the involvement of [Co^{IV}=O] species during the reaction.[26] Winkler and Gray reported that for a high valent metal-oxo complexes having d^5 metal center, [M^{III}-O$^{\bullet}$] is favorable over [M^{IV}=O] configuration.[35] It is to be noted that the

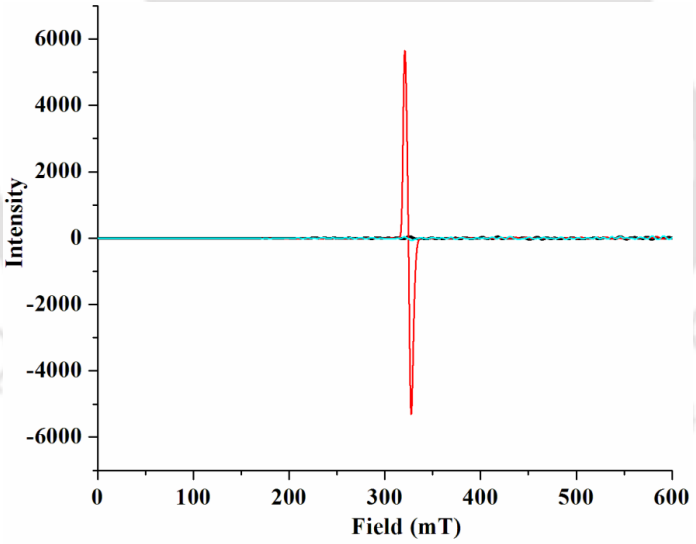

Figure 5.6. X-band EPR spectral monitoring of the reaction of complex **5.1** with H_2O_2 in dichloromethane:acetonitrile (1:4, v/v) solution at 77 K [complex **5.1** (black), intermediate (red) and complex **5.2** (green)].

reaction of [$Co(F_8TPP^{2-})(NO)$] with H_2O_2 resulted in corresponding [$Co^{III}(O)^{\bullet}$] species which in turn confirms the involvement of [Co^{IV}=O] species.[26] Similarly, the

involvement of [Mn^{IV}=O] species was observed in the reaction of [$Mn(F_{20}TPP^{2-})(NO)$] with H_2O_2.[27] In both cases, corresponding nitrate complexes were isolated upon work up. However, in the present case, it was the nitrite complex, **5.2**. In general, metal-peroxynitrites isomerizes at room temperature to the corresponding nitrate (NO_3^-); but in some cases, it has been found to decompose to the corresponding nitrite (NO_2^-) and ½ O_2 (Scheme **5.2**).[36] These decomposition pathways depend on stability of the metal-peroxynitrite intermediate. In the present case, the formation of O_2 was confirmed by alkaline pyrogallol test.

The ESI-mass spectrum of the reaction mixture displays a peak at m/z = 1048.29, corresponding to the [$Co^{III}(TTMPP^{2-})(O)$] unit (Calcd. 1047.21) (Figure **5.7**). Experimental and simulated isotopic distribution patterns are in well accord. This also supports the formation of Co(IV)-oxo species in the reaction medium. An authentic sample was prepared using complex **1a** with *m*CPBA which confirm our assignment (Appendix IV, Figures **A4.18-A4.19**).

Thus, all these spectroscopic studies suggest the formation of a cobalt-oxo intermediate during the reaction which rapidly isomerizes to corresponding porphyrin radical cation.

Due to the transient nature of the proposed [$Co^{III}(TTMPP^{2-})(ONOO^-)$] intermediate, direct spectroscopic evidence was not observed. Hence, phenol ring nitration test has been done to confirm the involvement of metal-peroxynitrite intermediate.[26,27] When H_2O_2 was added to a mixture of complex **5.1** and 2,4-di-*tert*-butylphenol (DTBP) in dichloromethane:acetonitrile (1:4, v/v) solution at -40 °C, formation of 2,4-di-*tert*-butyl-6-nitrophenol was observed along with corresponding cobalt(III)-hydroxide complex, [$Co^{III}(TTMPP^{2-})(OH)$], **5.3** (Scheme **5.3**). These products were isolated by column chromatography and characterized spectroscopically (Appendix IV, Figures **A4.20-**

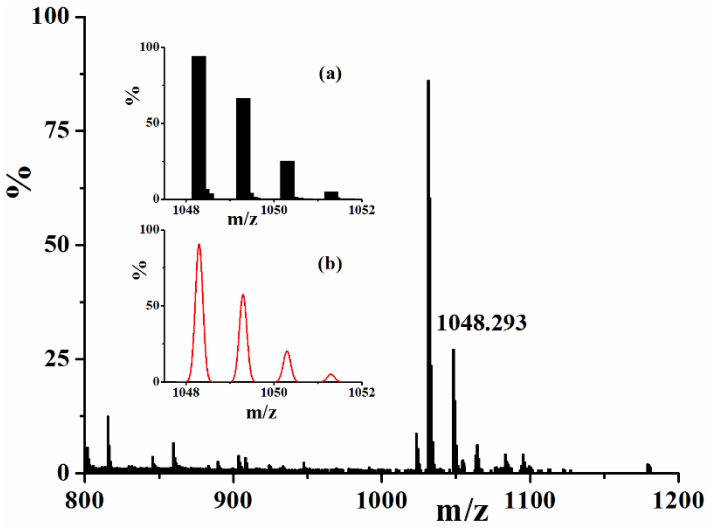

Figure 5.7. ESI-mass spectrum of the reaction mixture of complex **5.1** with H_2O_2 in acetonitrile at -40 °C [Inset: (a) experimental and (b) simulated isotopic distribution pattern].

A4.26). It is to be noted that when H_2O_2 was added to dichloromethane:acetonitrile (1:4, v/v) solution of complex **5.1** followed by 2,4-di-*tert*-butylphenol, no ring nitration product was found. Instead, complex **5.2** was obtained along with unreacted 2,4-di-*tert*-butylphenol.

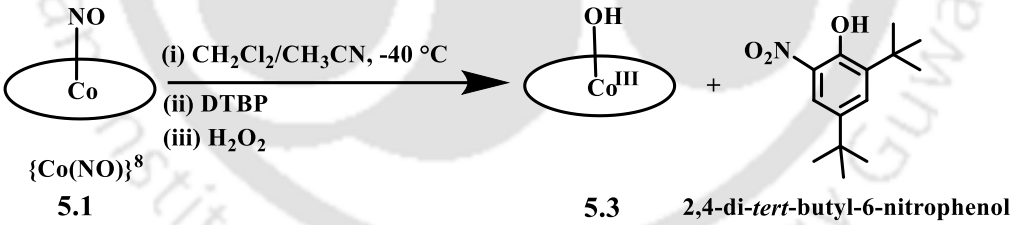

Scheme 5.3

5.3 Experimental Section

5.3.1 Materials and methods

Solvents and reagents were purchased from commercial sources and used as it is unless

mentioned. All reactions were carried out under Ar atmosphere. To remove the oxygen from solvents, repeatedly vacuum/Ar were purged. Dichloromethane was stored under calcium hydride followed by distillation under nitrogen. UV-visible spectra were recorded using Agilent Caray 8454 spectrophotometer. FT-IR spectra were taken in Perkin Elmer spectrophotometer. ^{1}H and ^{13}C-NMR spectra were recorded using Bruker Avance III on a 400 MHz varian FT spectrometer. Elemental analyses were done using PerkinElmer Series II Analyzer. Mass spectra were taken using Q-Tof premier instrument with ESI mode of ionization. EPR spectra were taken using JES-FA200 ESR spectrometer with microwave power, 0.998 mW, microwave Frequency, 9.14 GHz and modulation amplitude, 2.

Single crystals were grown using dichloromethane/methanol solution. Data were collected from Bruker APEX-II CCD diffractometer, equipped with a fine focus 1.75 kW sealed tube MoKα, radiation (λ = 0.71073 Å) at 296 K, at a scan speed of 3 s/frame. APEX-II was used for data acquisition. SAINT and XPREP software were used for data reduction.[37] Structures were solved by direct methods using SHELXL[38a] and refined with full matrix least squares on F^2 using SHELXL-2019/1.[38b] Structural illustration has been drawn with ORTEP-3 for windows.[38c]

5.3.2 Syntheses

5,10,15,20-*tetrakis*(3,4,5-trimethoxyphenyl)porphyrin, [TTMPPH$_2$]

3,4,5-trimethoxy benzaldehyde (5.88 g, 30 mmol) and pyrrole (2.012 g, 30 mmol) were taken in 50 mL propionic acid. The reaction mixture was refluxed for 3 h and kept it overnight at room temperature which results in precipitation. This precipitate was filtered off and washed with warm water followed by hexane to obtained pure ligand (TTMPPH$_2$) as a blue crystalline solid. Yield: 0.16 g (*ca*. 22%). Elemental analyses of

$C_{56}H_{54}N_4O_{12}$. Calcd. (%): C, 68.98; H, 5.58; N, 5.75. Found (%): C, 68.81; H, 5.62; N, 5.70. FT-IR using ATR probe: 2938, 2829, 1579, 1499, 1448, 1404, 1348, 1231, 1181, 1125, 1103, 1001, 976, 921, 848, 802, 761, 738, 719, 640 and 525 cm^{-1}. ^{1}H-NMR (400 MHz, $CDCl_3$): $\delta_{ppm,}$ 8.97 (s, 8H), 7.49 (s, 8H), 4.19 (s, 12H), 3.98 (s, 24H), -2.76 (s, 2H). ^{13}C-NMR (100 MHz, $CDCl_3$*):* $\delta_{ppm,}$ 151.4, 137.9, 137.6, 120.1, 112.9, 61.3, 56.4. ESI-mass (m/z): Calcd.: 974.373, Found: 975.383(M+1).

Complex 5.1a, [Co^{II}($TTMPP^{2-}$)]

Ligand, $TTMPPH_2$ (0.49 g, 0.5 mmol) and cobalt(II) acetate tetrahydrate (1.2 g, 5 mmol) were taken in 1:10 mole equivalent in 50 mL of dimethylformamide and refluxed overnight. This reaction mixture was brought to room temperature and dried in rotary evaporator. The crude mass obtained was subjected to solvent extraction using chloroform/water. Upon drying the chloroform portion *in vacuo*, red mass was obtained. Using column chromatography, pure complex **5.1a** was obtained as red solid. Yield: 0.32 g (*ca*. 60%). Elemental analyses of $C_{56}H_{52}N_4O_{12}Co$. Calcd. (%): C, 65.18; H, 5.08; N, 5.43. Found (%): C, 65.29; H, 5.01; N, 5.58. FT-IR using ATR probe: 3001, 2936, 1579, 1505, 1456, 1404, 1358, 1325, 1230, 1124, 1106, 1075, 1001, 943, 857, 812, 796, 761, 724, 647, 527, 492 and 441 cm^{-1}. UV-visible (CH_2Cl_2): 531 nm (ϵ/M^{-1} cm^{-1}, 2.36 × 10^4) and 413 nm (ϵ/M^{-1} cm^{-1}, 3.18 × 10^5). $\mu_{obs.}$: 1.75 BM. X-band EPR: (CH_2Cl_2, 77 K) g ~ 2.25. ESI-mass (m/z), Calcd. 1031.291, Found, 1031.291, (molecular ion peak). Crystal data: CCDC No. 2336173. $C_{56}H_{52}N_4O_{12}Co$, M = 1031.94, triclinic (P -1), a = 7.879(5), b = 12.946(8), c = 14.269(9) Å, α = 92.022(17)°, β = 103.569(17)°, γ = 91.798(17)°, V = 1412.8(15) $Å^3$, Z = 1, D_c = 1.213 g cm^{-3}, μ = 0.365 mm^{-1}, T = 296 K, 4906 reflections, 4412 independent, R(F) = 0.0783 [I>2δ(I)], R(int) = 0.0865, wR(F^2) = 0.2426 (all data), GOF = 1.147.

Complex 5.1, [Co(TTMPP^{2-})(NO)]

Complex **5.1a** (0.2 g, 0.2 mmol) was taken in dry and degassed dichloromethane solution. NO gas was bubbled to this solution for 5 min. The color of the solution changed to dark red. Excess NO gas was taken out by purging Ar and complex **5.1** was isolated as red solid. Yield: 0.18 g (*ca*. 85%). Elemental analyses of $C_{56}H_{52}N_5O_{13}Co$. Calcd. (%): C, 63.34; H, 4.94; N, 6.59. Found (%): C, 63.25; H, 4.87; N, 6.67. FT-IR using ATR probe: 2925, 1675, 1580, 1503, 1454, 1407, 1357, 1320, 1233, 1166, 1122, 1077, 1003, 945, 858, 799, 762, 721, 644 and 527 cm^{-1}. UV-visible (CH_2Cl_2): 537 nm (ϵ/M^{-1} cm^{-1}, 1.05 × 10^4) and 419 nm (ϵ/M^{-1} cm^{-1}, 1.8 × 10^5). ^{1}H-NMR (400 MHz, $CDCl_3$): $\delta_{ppm,}$ 9.03 (s, 8H), 7.36 (s, 8H), 4.17 (s, 12H), 3.96 (s, 24H). ESI-mass (m/z), Calcd.: 1061.289 for [Co(TTMPP^{2-})(NO)]; Found: 1031.291, for [Co(TTMPP^{2-})]. Crystal data: CCDC No. 2336174. $C_{56}H_{52}N_5O_{13}Co$, M = 1061.95, triclinic (P 1), a = 7.9359(11), b = 12.8765(18), c = 14.309(2) Å, α = 91.942(4)°, β = 104.883(4) (17)°, γ = 91.693(4)°, V = 1411.2(3) Å^3, Z = 1, D_c = 1.250 g cm^{-3}, μ = 0.369 mm^{-1}, T = 296 K, 9842 reflections, 8418 independent, R(F) = 0.0456 [I>2δ(I)], R(int) = 0.0557, wR(F^2) = 0.1219 (all data), GOF = 1.069.

5.3.3 Reaction of complex 5.1 and H_2O_2

Complex **5.1** (0.32 g, 0.3 mmol) was dissolved in dry and degassed dichloromethane:acetonitrile (1:4, v/v) solution and kept at -40 °C. Precooled H_2O_2 (37% v/v in CH_3CN, 0.32 mL) was added to this solution and stirred for 3 h. After warm up at room temperature, this mixture was dried using rotary evaporator to obtained complex **5.2**.

Complex 5.2, [Co^{III}(TTMPP^{2-})(NO_2^-)]

Yield: 0.19 g (*ca*. 58%). Elemental analyses of $C_{56}H_{52}N_5O_{14}Co$. Calcd. (%): C, 62.40; H, 4.86; N, 6.50. Found (%): C, 62.52; H, 4.79; N, 6.62. FT-IR using ATR probe: 2961, 2924, 2855, 1581, 1504, 1455, 1409, 1350, 1259, 1236, 1095, 1010, 794, 722 and 528 cm^{-1}. UV-visible (CH_2Cl_2): 443 nm (ϵ/M^{-1} cm^{-1}, 0.78 × 10^5), 547 nm (ϵ/M^{-1} cm^{-1}, 0.92 × 10^4) and 584 nm (ϵ/M^{-1} cm^{-1}, 0.87 × 10^4). ^{1}H-NMR (400 MHz, $CDCl_3$): $\delta_{ppm,}$ 9.03 (s, 8H), 7.16 (s, 8H), 4.07 (s, 12H), 3.87 (s, 24H). ESI-mass (m/z), Calcd.: 1077.284, for [Co^{III}(TTMPP^{2-})(NO_2^-)]; Found: 1077.282, (molecular ion peak). Crystal data: CCDC No. 2336175. $C_{56}H_{52}N_6O_{16}Co$, M = 1123.96, triclinic (P -1), a = 7.9543(15), b = 12.862(2), c = 14.317(3) Å, α = 87.968(5)°, β = 74.593(5)°, γ = 88.483(5)°, V = 1411.1(5) $Å^3$, Z = 1, D_c = 1.323 g cm^{-3}, μ = 0.377 mm^{-1}, T = 296 K, 4908 reflections, 4312 independent, R(F) = 0.0655 [I>2δ(I)], R(int) = 0.0743, wR(F^2) = 0.1688 (all data), GOF = 1.097.

5.3.4 Reaction of complex 5.1 and H_2O_2 in presence of 2,4-di-*tert*-butylphenol

Complex **5.1** (0.21 g, 0.2 mmol) was taken in degassed dichloromethane:acetonitrile (1:4, v/v) solution and kept at -40 °C. Precooled dichloromethane solution of 2,4-di-*tert*-butylphenol (0.2 g, 1 mmol) was added followed by precooled H_2O_2 (37% v/v in CH_3CN, 0.25 mL). It was then stirred for 1 h at -40 °C. After warm up to room temperature this mixture was dried. 2,4-di-*tert*-butyl-6-nitrophenol and complex **5.3** were purified by column chromatography technique.

2,4-di-*tert*-butyl-6-nitrophenol

Yield: 0.25 g (*ca*. 59%). Elemental analyses for $C_{14}H_{21}NO_3$. Calcd. (%): C, 66.91; H, 8.42; N, 5.57. Found (%): C, 66.83; H, 8.39; N, 5.65. FT-IR using ATR probe: 2960, 2871, 1617, 1539, 1480, 1459, 1443, 1414, 1363, 1314, 1272, 1235, 1202, 1179, 1138, 1112, 1024, 923, 885, 821, 773, 749, 724, 699, 639, 532 and 512 cm^{-1}. ^{1}H-NMR (400

MHz, $CDCl_3$): $\delta_{ppm,}$ 11.43 (s, 1H), 7.94 (s, 1H), 7.63 (s, 1H), 1.43 (s, 9H), 1.30 (s, 9H). ^{13}C-NMR (100 MHz, $CDCl_3$): $\delta_{ppm,}$ 153.1, 142.1, 140.0, 133.8, 132.7, 119.0, 35.9, 34.7, 31.2, 29.5. ESI-mass (m/z): Calcd.: 251.152, Found: 250.160 (M-1).

Complex 5.3, $[Co^{III}(TTMPP^{2-})(OH^{-})]$

Yield: 0.13 g (*ca.* 63%). Elemental analyses for $C_{56}H_{53}N_4O_{13}Co$. Calcd. (%): C, 64.12; H, 5.09; N, 5.34. Found (%): C, 64.24; H, 5.13; N, 5.41. FT-IR using ATR probe: 3434, 2928, 2855, 1580, 1507, 1451, 1411, 1389, 1360, 1327, 1242, 1170,1124, 1006, 945, 815, 765, 720 and 652 cm^{-1}. UV-visible (CH_2Cl_2): 431 nm (ϵ/M^{-1} cm^{-1}, 1.0×10^5) and 541 nm (ϵ/M^{-1} cm^{-1}, 0.75×10^4).

5.4 Conclusion

A Co-nitrosyl complex, **5.1** of $\{Co(NO)\}^8$ configuration has been synthesized and characterized spectroscopically as well as structurally. Complex **5.1** in dichloromethane:acetonitrile (1:4, v/v) solution reacts with H_2O_2 to give $[Co^{III}(TTMPP^{2-})(NO_2^{-})]$ complex, **5.2** as a final product. This reaction is proposed to proceed *via* a $[Co^{III}(TTMPP^{2-})(ONOO^{-})]$ intermediate which is confirmed by characteristic phenol ring nitration test. Spectroscopic studies suggest the involvement of the corresponding porphyrin radical complex which indirectly supports the formation of Co(IV)-oxo intermediate from the homolytic cleavage of O-O bond of the proposed peroxynitrite intermediate.

5.5 References

1. Goyal, R. K.; Hirano, I. *N. Engl. J. Med*. **1996**, *334*, 1106.

2. Stark, M. E.; Szurszewski, J. H. *Gastroenterology*, **1992**, *103*, 1928.
3. Jaffrey, S. R.; Snyder, S. H. *Annu. Rev. Cell. Dev. Biol*. **1995**, *11*, 417.
4. Bogdan, C. *Nat. Immunol*. **2001**, *2*, 907.
5. Ignarro, L. J.; *Nitric Oxide: Biology and Pathobiology*; Ed.; Academic Press: San Diego, **2000**.
6. Fang, F. C.; *Nitric Oxide and Infection*; Ed., Kluwer Academic/ Plenum Publishers: New York, **1999**.
7. Bourassa, J. L.; Ives, E. P.; Marqueling, A. L.; Shimanovich, R.; Groves, J. T. *J. Am. Chem. Soc*. **2001**, *123*, 5142.
8. Lehnert, N.; Kim, E.; Dong, H. T.; Harland, J. B.; Hunt, A. P.; Manickas, E. C.; Oakley, K. M.; Pham, J.; Reed, G. C.; Alfaro, V. S. *Chem. Rev*. **2021**, *121*, 14682.
9. Gantner, B. N.; Lafond, K. M.; Bonini, M. G. *Redox Biol*. **2020**, *34*, 101550.
10. Horst, G.; Marletta, M. A. *Nitric Oxide*, **2018**, *77*, 65.
11. Schopfer, M. P.; Mondal, B.; Lee, D. H.; Sarjeant, A. A. N.; Karlin, K. D. *J. Am. Chem. Soc*. **2009**, *131*, 11304.
12. (a) Pfeiffer, S.; Gorren, A. C. F.; Schmidt, K.; Werner, E. R.; Hansert, B.; Bohle, D. S.; Mayer, B. *J. Biol. Chem*. **1997**, *272*, 3465. (b) Coddington, J. W.; Hurst, J. K.; Lymar, S. V. *J. Am. Chem. Soc*. **1999**, *121*, 2438. (c) Koppenol, W. H.; Bounds, P. L.; Nauser, T.; Kissner, R.; Rüegger, H. *Dalton Trans*. **2012**, *41*, 13779. (d) Lymar, S. V.; Khairutdinov, R. F.; Hurst, J. K. *Inorg. Chem*. **2003**, *42*, 5259. (e) Goldstein, S.; Lind, J.; Merényi, G. *Chem. Rev*. **2005**, *105*, 2457. (f) Molina, C.; Kissner, R.; Koppenol, W. H. *Dalton Trans*. **2013**, *42*, 9898.
13. (a) Schopfer, M. P.; Wang, J.; Karlin, K. D. *Inorg. Chem*. **2010**, *49*, 6267. (b) Ouellet, H.; Ouellet, Y.; Richard, C.; Labarre, M.; Wittenberg, B.; Wittenberg, J.; Guertin, M. *Proc. Natl. Acad. Sci, U. S. A.* **2002**, *99*, 5902. (c) Gardner, P. R.;

Gardner, A. M.; Martin, L. A.; Salzman, A. L. *Proc. Natl. Acad. Sci. U. S. A.* **1998**, *95*, 10378. (d) Ford, P. C.; Lorkovic, I. M. *Chem. Rev*. **2002**, *102*, 993. (e) Gardner, P. R.; Gardner, A. M.; Brashear, W. T.; Suzuki, T.; Hvitved, A. N.; Setchell, K. D. R.; Olson, J. S. *J. Inorg. Biochem*. **2006**, *100*, 542.

14. (a) Clarkson, S. G.; Basolo, F. *J. Chem. Soc. Chem. Commun*. **1972**, 670. (b) Clarkson, S. G.; Basolo, F. *Inorg. Chem*. **1973**, *12*, 1528.
15. (a) Wick, P. K.; Kissner, R.; Koppenol, W. H. *Helv. Chim. Acta*. **2000**, *83*, 748. (b) Wick, P. K.; Kissner, R.; Koppenol, W. H. *Helv. Chim. Acta*. **2001**, *84*, 3057.
16. Thyagarajan, S.; Incarvito, C.; Rheingold, A. L.; Theopold, K. H. *Inorg. Chim. Acta*. **2003**, *345*, 333.
17. Maiti, D.; Lee, D. H.; Sarjeant, A. A.; Pau, M. Y. M.; Solomon, E. I.; Gaoutchenova, K.; Sundermeyer, J.; Karlin, K. D. *J. Am. Chem. Soc*. **2008**, *130*, 6700.
18. (a) Kurtikyan, T. S.; Eksuzyan, S. R.; Hayrapetyan, V. A.; Martirosyan, G. G.; Hovhannisyan, G. S.; Goodwin, J. A. *J. Am. Chem. Soc.* **2012**, *134*, 13861. (b) Kurtikyan, T. S.; Eksuzyan, S. R.; Goodwin, J. A.; Hovhannisyan, G. S. *Inorg. Chem*. **2013**, *52*, 12046.
19. Yokoyama, A.; Han, J. E.; Cho, J.; Kubo, M.; Ogura, T.; Siegler, M. A.; Karlin, K. D.; Nam, W. *J. Am. Chem. Soc*. **2012**, *134*, 15269.
20. Yokoyama, A.; Cho, K. B.; Karlin, K. D.; Nam, W. *J. Am. Chem. Soc*. **2013**, *135*, 14900.
21. Saha, S.; Ghosh, S.; Gogoi, K.; Deka, H.; Mondal, B.; Mondal, B. *Inorg. Chem*. **2017**, *56*, 10932.
22. Samanta, B.; Ghosh, R.; Mazumdar, R.; Saha, S.; Maity, S.; Mondal, B. *Dalton Trans*. **2023**, *52*, 15815.

23. (a) Tran, N. G.; Kalyvas, H.; Skodje, K. M.; Hayashi, T.; Loccoz, P. M.; Callan, P. E.; Shearer, J.; Kirschenbau, L. J.; Kim, E. *J. Am. Chem. Soc*. **2011**, *133*, 1184. (b) Skodje, K. M.; Williard, P. G.; Kim, E. *Dalton Trans*. **2012**, *41*, 7849.

24. Kalita, A.; Kumar, P.; Mondal, B. *Chem. Commun*. **2012**, *48*, 4636.

25. Saha, S.; Gogoi, K.; Mondal, B.; Ghosh, S.; Deka, H.; Mondal, B. *Inorg. Chem*. **2017**, *56*, 7781.

26. Mondal, B.; Saha, S.; Borah, D.; Mazumdar, R.; Mondal, B. *Inorg. Chem*. **2019**, *58*, 1234.

27. Mondal, B.; Borah, D.; Mazumdar, R.; Mondal, B. *Inorg. Chem*. **2019**, *58*, 14701.

28. Mazumdar, R.; Mondal, B.; Saha, S.; Samanta, B.; Mondal, B. *J. Inorg. Biochem*. **2022**, *228*, 111698.

29. Adler, A. D.; Longo, F. R.; Finarelli, J. D.; Goldmacher, J.; Assour, J.; Korsakoff, L. *J. Org. Chem.* **1967**, *32*, 476.

30. Kadish, K. M.; Araullo, M. C.; Han, B. C.; Franzen, M. M. *J. Am. Chem. Soc*. **1990**, *112*, 8364.

31. McCleverty, J. A. *Chem. Rev*. **2004**, *104*, 403.

32. (a) Richter, G. B.; Hodge, S. J.; Yi, G. B.; Khan, M. A.; Ma, T.; Caemelbecke, E. V.; Guo, N.; Kadish, K. M. *Inorg. Chem.* **1996**, *35*, 6530. (b) Enemark, J. H.; Feltham, R. D. *Coord. Chem. Rev*. **1974**, *13*, 339. (c) Richter, G. B.; Legzdins, P. *Metal Nitrosyls*, Oxford University Press: New York, **1992**.

33. (a) Wayland, B. B.; Minkiewicz, J. V.; Abd-Elmageed, M. E. *J. Am. Chem. Soc*. **1974**, *96*, 2795. (b) Fujita, E.; Chang, C. K.; Fazer, J. *J. Am. Chem. Soc*. **1985**, *107*, 7665. (c) Fujita, E.; Fazer, J. *J. Am. Chem. Soc.* **1983**, *105*, 6743.

34. (a) Dey, S.; Sil, D.; Rath, S. P. *Angew. Chem*. **2016**, *128*, 1008. (b) Hong, S.; Pfaff, F. F.; Kwon, E.; Wang, Y.; Seo, M. S.; Bill, E.; Ray, K.; Nam, W. *Angew. Chem*.

Int. Ed. **2014**, *53*, 10403. (c) Ikezaki, A.; Takahashi.; Nakamura, M. *Chem. Commun*. **2013**, *49*, 3098. (d) Ichimori, K.; Nishiguchi, H. O.; Hirota, N.; Yamamoto, K. *Bull. Chem. Soc. Jpn*. **1985**, *58*, 623.

35. Winkler, J. R.; Gray, H. B. *Struct. Bonding* (Berlin, Ger.). **2011**, *142*, 17.
36. Park, G. Y.; Deepalatha, S.; Pulu, S. C.; Lee, D. H.; Mondal, B.; Sarjeant, A. A. N.; Rio, D.; Pau, M. Y. M.; Solomon, E. I.; Karlin, K. D. *J. Biol. Inorg. Chem*. **2009**, *14*, 1301.
37. SMART, SAINT and XPREP, Siemens Analytical X-ray Instruments Inc, Madison, Wisconsin, USA. **1995**.
38. (a) Sheldrick, G. M. *Acta Crystallogr. Sect. A Found. Adv.* **2015**, *71*, 3. (b) Sheldrick, G. M. *Acta. Crystallogr. Sect. C Struct. Chem.* **2015**, *71*, 3. (c) Farrugia, L. J. ORTEP-3 for Windows - a version of ORTEP-III with a Graphical User Interface (GUI). *J. Appl. Crystallogr.* **1997**, *30*, 565.

Conclusion

This thesis broadly covers our endeavor to understand both the reactivity of peroxo complexes of Co(III) with NO in non heme ligand frameworks, L1, L2, L3 and nitrosyl complex of Co(II) with reduced oxygen species, H_2O_2 in heme ligand framework, $TTMPP^{2-}$, respectively. These complexes were synthesized by varying bidentate, symmetric tetradentate, asymmetric tetradentate and square planar ligand framework. The change of reactivity pattern with ligand denticity has been studied. The reactivity of Co(III)-peroxo complexes with NO was discussed in chapters 2-4, following an attempt to mimic the mechanism of the nitric oxide dioxygenase (NOD) enzyme. In every case, formation of putative peroxynitrite intermediate was observed. Efforts were made to identify and characterized the associated intermediates that form during the course of the reaction. For instance, in chapter 2, putative formation of Co(II)-peroxynitrite intermediate was observed using a bidentate ligand framework and finally it isomerizes to the corresponding nitrate complex. In chapter 3 and 4, formation of Co(II)-peroxynitrite intermediates were observed using symmetric and asymmetric tetradentate ligand frameworks, respectively. In case of chapter 3 and chapter 4, different decomposition products were obtained *i.e* corresponding nitrate and nitrite complexes respectively.

On the other way, in chapter 5, a nitrosyl complex of Co(II)-porphyrinate with reduced oxygen species (O_2^{2-}) was explored. Here a Co(III)-porphyrin radical species has been detected after the decomposition of ˈO-Oˈ bond of the Co(III)-peroxynitrite intermediate, which indirectly support the involvement of Co(IV)-oxo species in the reaction. In this case, nitrite complex was obtained as a final decomposition product. We believe that these findings will significantly enhance our current understanding of NOD chemistry and make a substantial contribution to the field of metalloenzyme chemistry. However, despite our best efforts, direct characterization of Co-peroxynitrite intermediate was unsuccessful due to its highly reactive nature.

Appendix I

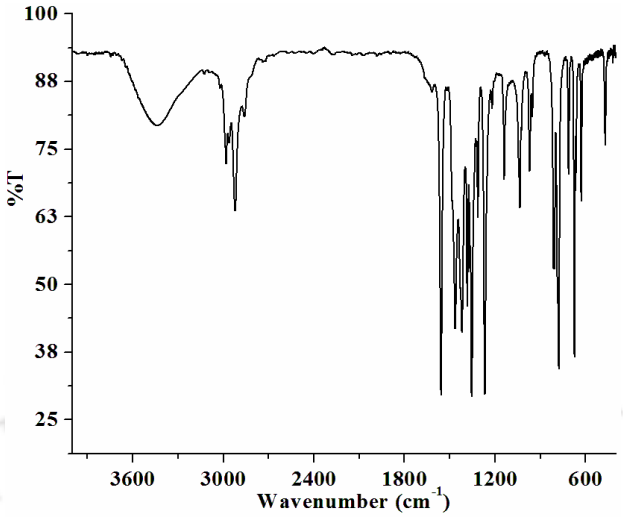

Figure A1.1. FT-IR spectrum of **L1** in KBr.

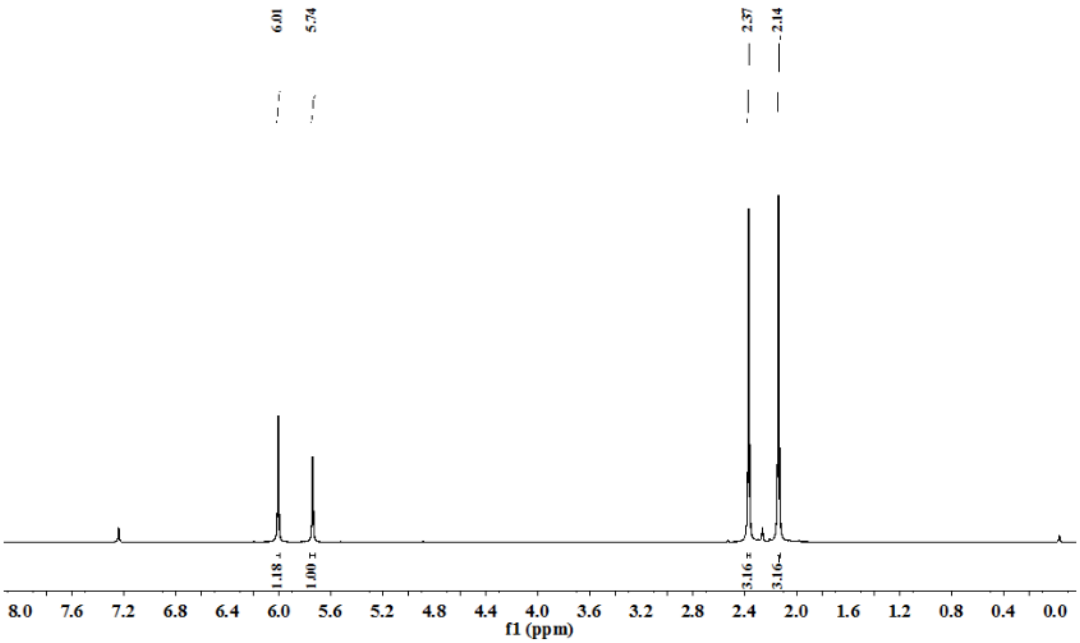

Figure A1.2. ^{1}H-NMR spectrum of **L1** in $CDCl_3$.

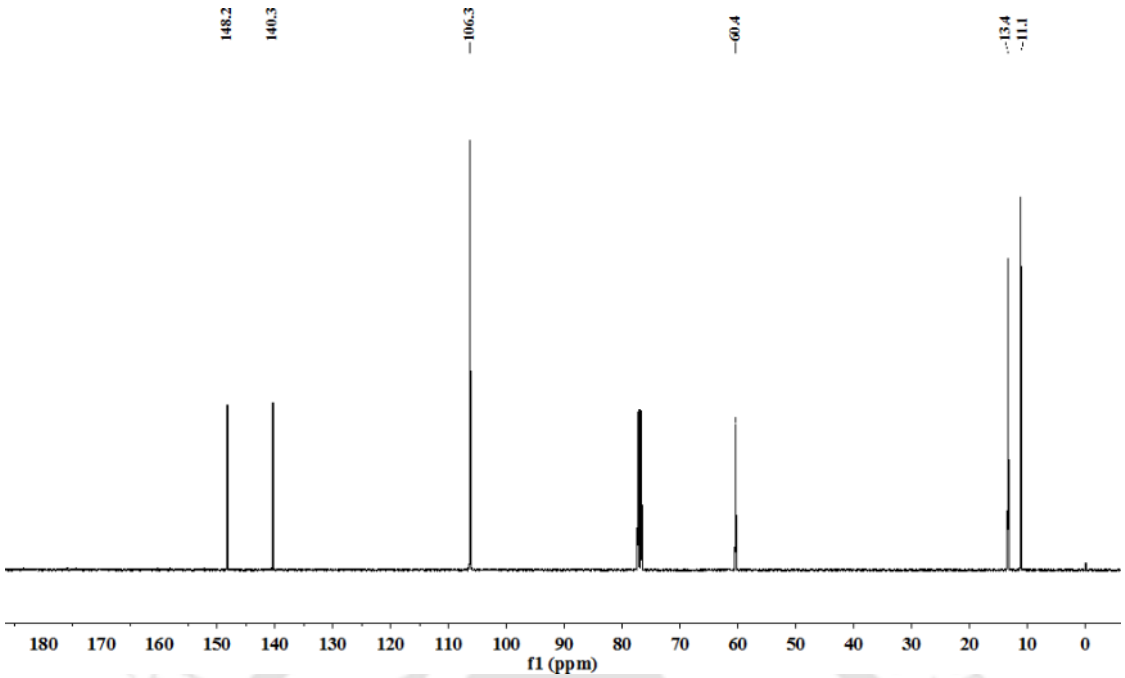

Figure A1.3. ^{13}C-NMR spectrum of **L1** in $CDCl_3$.

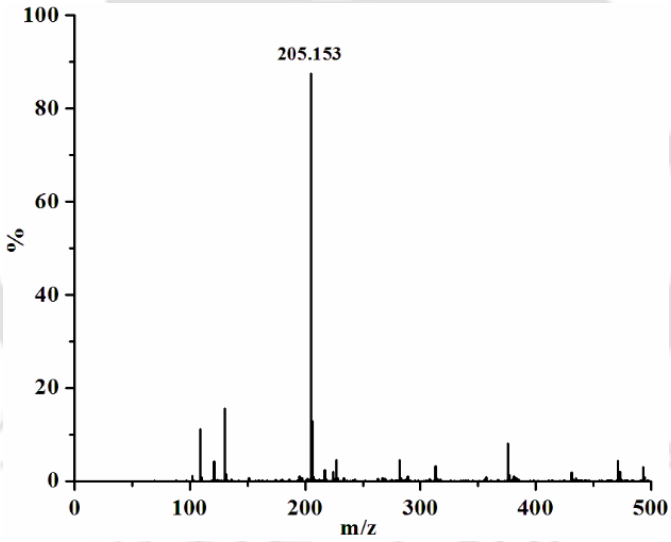

Figure A1.4. ESI-mass spectrum of **L1** in CH_3CN.

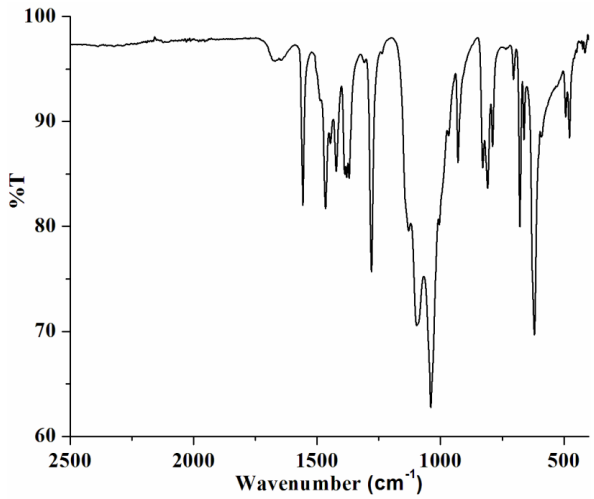

Figure A1.5. FT-IR spectrum of complex **2.1** in KBr.

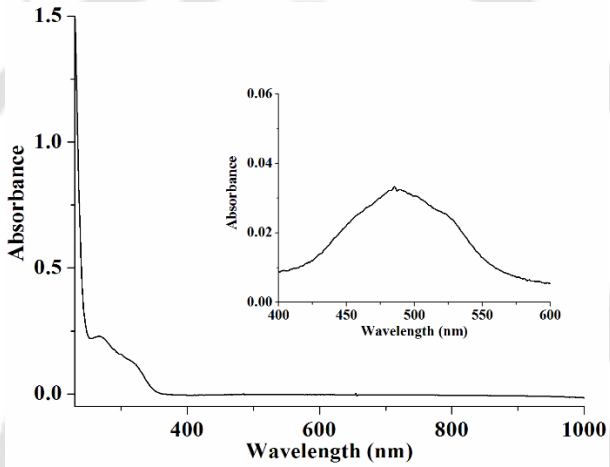

Figure A1.6. UV-visible spectrum of complex **2.1** in CH_3CN at room temperature.

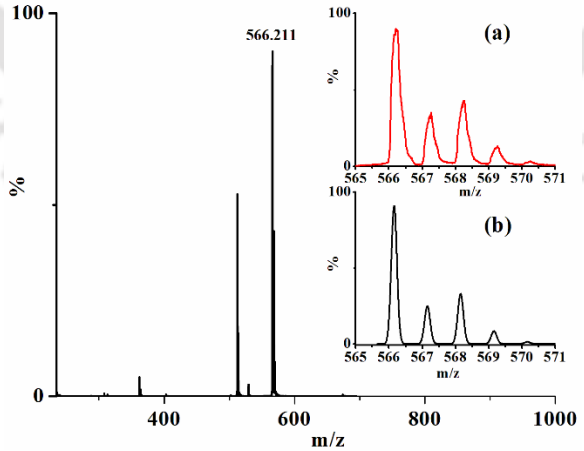

Figure A1.7. ESI-mass spectrum of complex **2.1** in CH_3CN. [Inset: (a) experimental and (b) simulated isotopic distribution pattern].

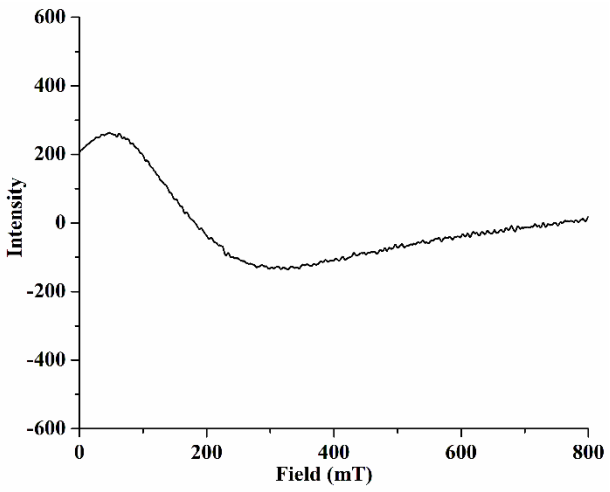

Figure A1.8. X-band EPR spectrum of complex **2.1** in CH_3CN at 77 K.

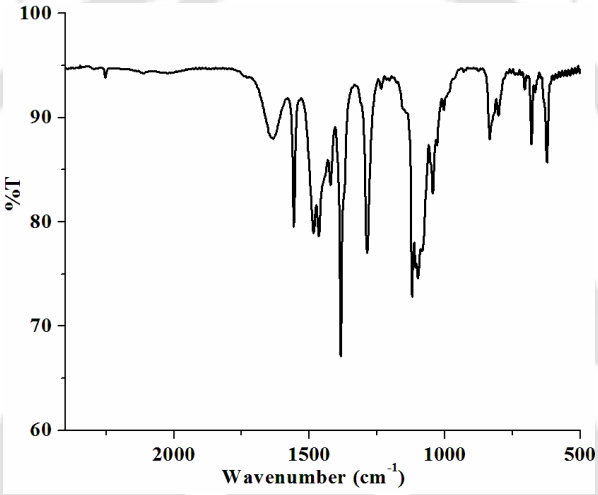

Figure A1.9. FT-IR spectrum of complex **2.2** in KBr.

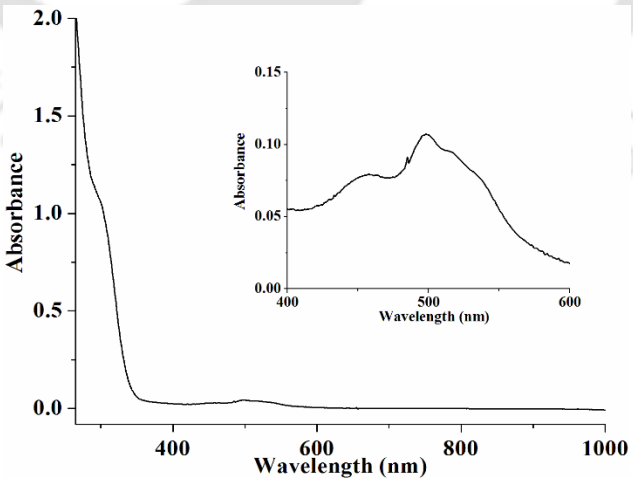

Figure A1.10. UV-visible spectrum of complex **2.2** in CH_3CN at room temperature.

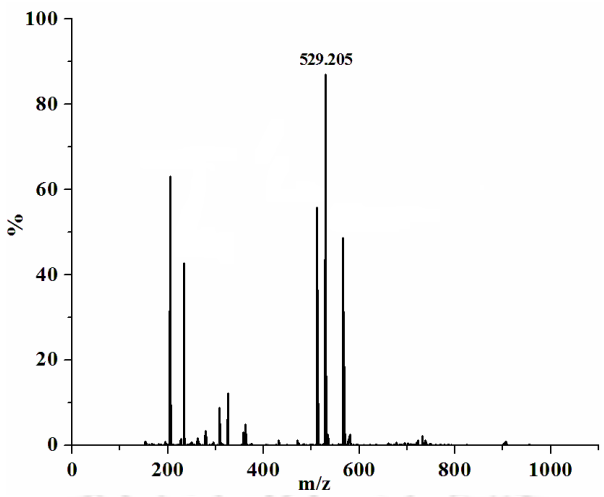

Figure A1.11. ESI-mass spectrum of complex **2.2** in CH_3CN.

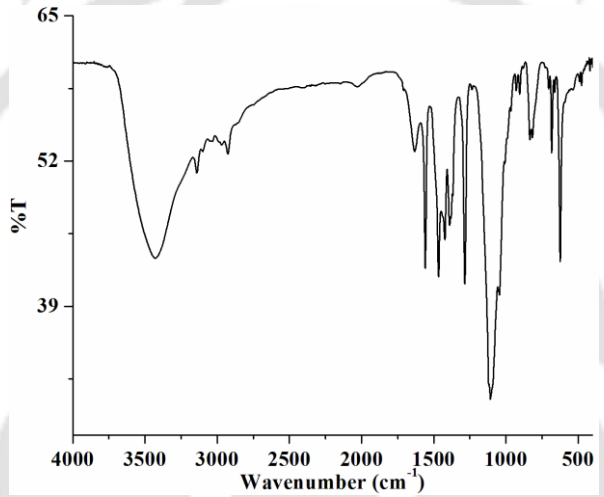

Figure A1.12. FT-IR spectrum of complex **2.3** in KBr.

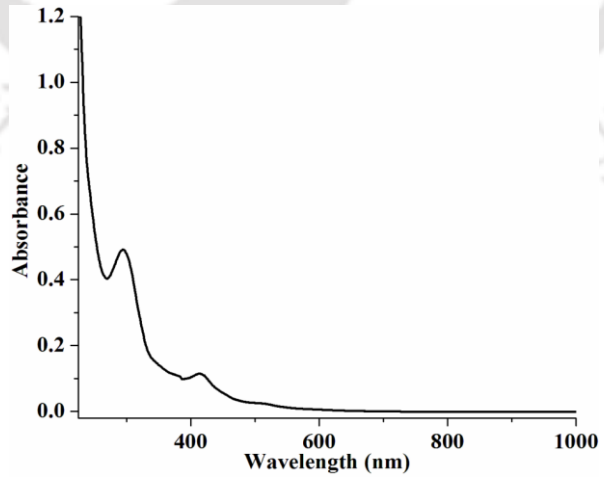

Figure A1.13. UV-visible spectrum of complex **2.3** in CH_3CN at room temperature.

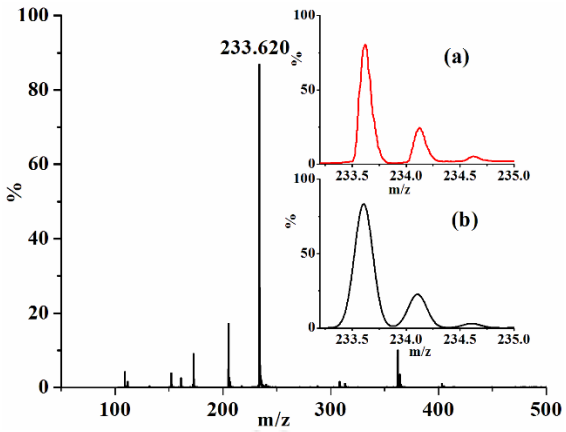

Figure A1.14. ESI-mass spectrum of complex **2.3** in CH_3CN. [Inset: (a) experimental and (b) simulated isotopic distribution pattern].

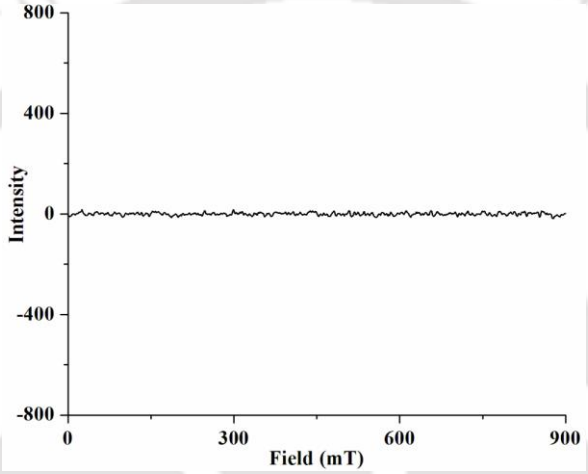

Figure A1.15. X-band EPR spectrum of complex **2.3** in CH_3CN at 77 K.

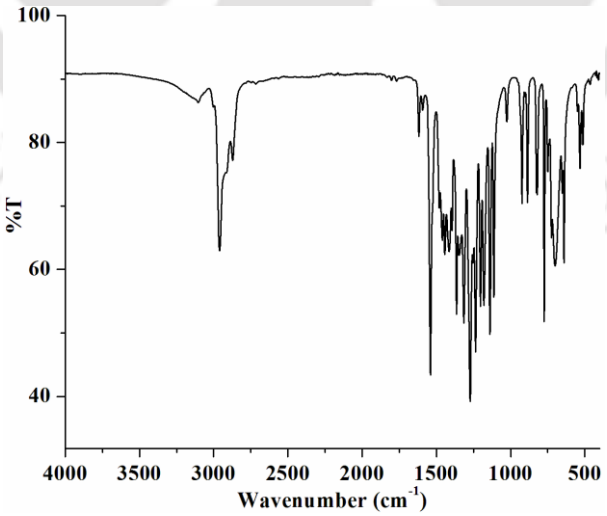

Figure A1.16. FT-IR spectrum of complex 2,4-di-*tert*-butyl-6-nitrophenol using ATR probe.

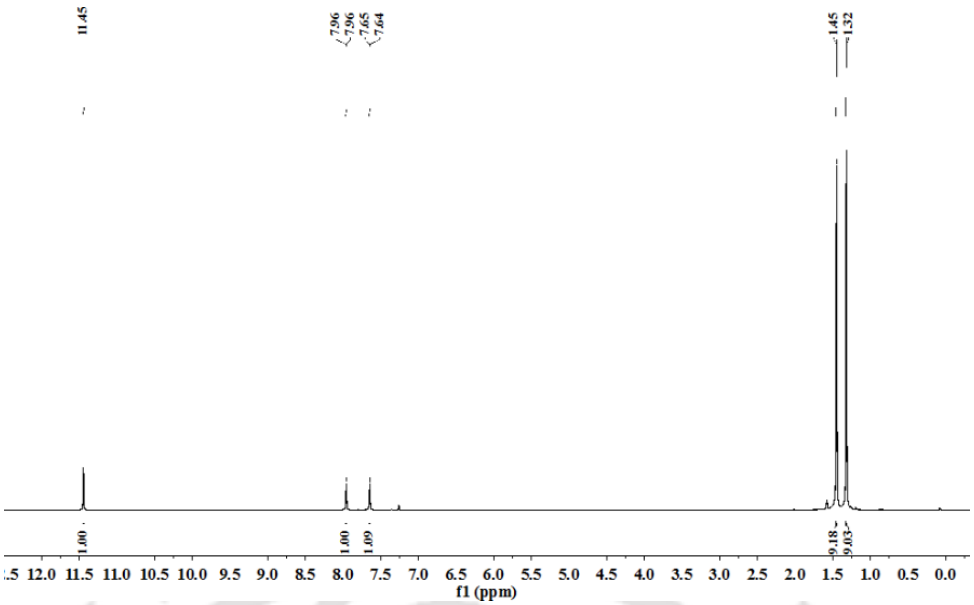

Figure A1.17. ^{1}H-NMR spectrum of 2,4-di-*tert*-butyl-6-nitrophenol in $CDCl_3$.

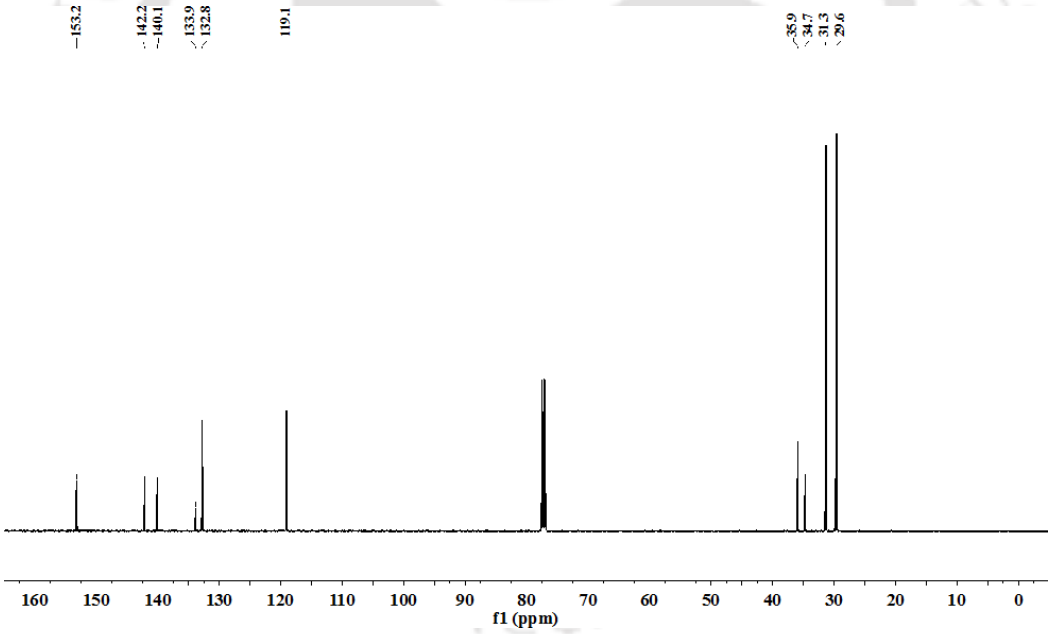

Figure A1.18. ^{13}C-NMR spectrum of 2,4-di-*tert*-butyl-6-nitrophenol in $CDCl_3$.

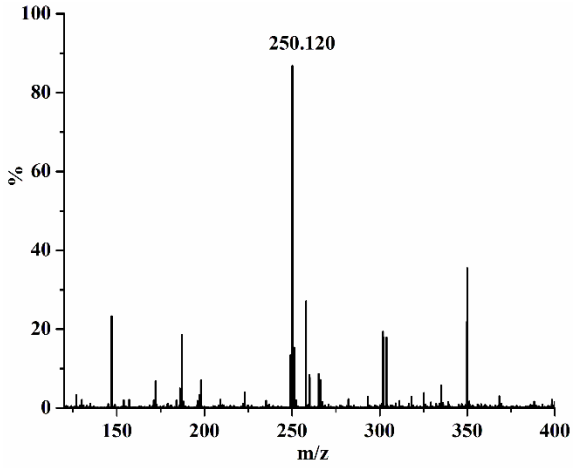

Figure A1.19. ESI-mass spectrum of 2,4-di-*tert*-butyl-6-nitrophenol in CH_3CN.

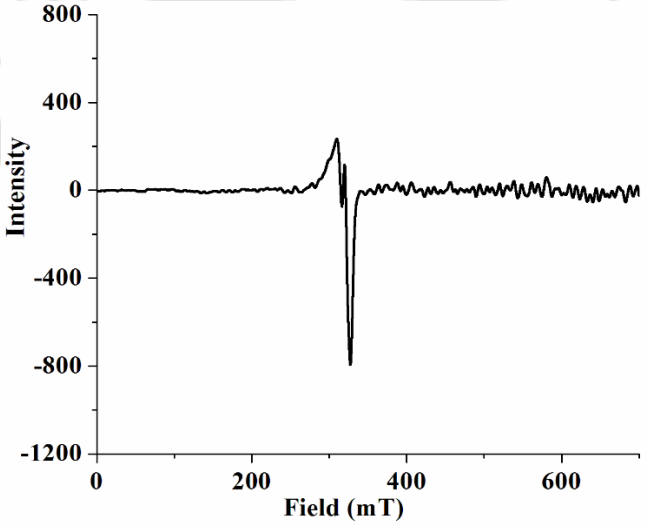

Figure A1.20. X-band EPR spectrum of $[Co^{II}(L1)_2(OH)](ClO_4^-)$ in CH_3CN at 77 K.

Table A1.1: Crystallographic data for complexes **2.1** and **2.2**.

	2.1	**2.2**
Formulae	$C_{22}H_{36}CoN_8O_{10}Cl_2$	$C_{24}H_{35}CoN_{10}O_7Cl$
Mol. Wt	702.42	670
Crystal system	Monoclinic	Monoclinic
Space group	P2(1)/c	P2(1)/c
Temperature/K	296	296
Wavelength/Å	0.71073	0.71073
a/ Å	12.8427(6)	14.7963(8)
b/ Å	12.6406(6)	8.2883(4)
c/ Å	20.2239(9)	25.5819(13)
α/°	90	90.00
β/°	106.4850(10)	94.607(2)

γ/°	90	90.00
V/ Å^3	3148.2(3)	3127.1(3)
Z	4	4
Density/Mgm^{-3}	1.482	1.423
Abs. Coeff. /mm^{-1}	0.778	0.692
Abs. Correction	Multi-scan	Multi-scan
F(000)	1460.0	1396.0
Total no. of reflections	5534	5508
Reflections. $I > 2\sigma(I)$	4352	4464
Max. 2θ/°	24.999	24.999
Ranges (h, k, l)	$-15 \le h \le 15$ $-15 \le k \le 15$ $-24 \le l \le 24$	$-17 \le h \le 17$ $-9 \le k \le 9$ $-30 \le l \le 30$
Complete to 2θ (%)	99	100
Refinement method	Full-matrix least-squares on F^2	Full-matrix least-squares on F^2
Goof(F^2)	1.013	1.102
R indices [$I > 2\sigma(I)$]	0.0560	0.0532
R indices (all data)	0.0736	0.0703
Residual electron density	0.73	0.54

Table A1.2: Selected bond lengths (Å) of complexes **2.1** and **2.2.**

Atoms	**2.1**	**2.2**
Co1-N1	2.136(3)	2.106(3)
Co1-N4	2.130(3)	2.116(3)
Co1-N5	2.118(3)	2.100(3)
Co1-N8	2.126(3)	2.110(3)
Co1-O1	2.206(3)	2.217(2)
Co1-O2	2.180(3)	2.192(2)
N1-N2	1.362(4)	1.368(4)
N3-N4	1.370(4)	1.364(4)
N2-C6	1.441(5)	1.446(4)
N3-C6	1.447(5)	1.447(4)
N9-O1	-	1.260(4)
N9-O2	-	1.263(3)
N9-O3	-	1.228(4)

Table A1.3: Selected bond angles (°) of complexes **2.1** and **2.2**.

Atoms	2.1	2.2
N1-Co1-O1	88.36(12)	160.14(10)
N1-Co1-O2	88.84(13)	101.85(10)
N1-Co1-N4	88.70(12)	88.66(10)
N1-Co1-N8	175.87(13)	97.09(11)
N1-Co1-N5	93.33(12)	96.66(11)
N4-Co1-N5	91.48(13)	95.73(11)
N4-Co1-N8	95.23(12)	172.38(11)
N4-Co1-O1	172.64(12)	87.90(10)
N4-Co1-O2	93.62(14)	86.22(10)
N1-C2-C1	122.5(4)	122.6(3)
N1-C2-C3	109.6(4)	109.2(3)
N1-N2-C4	111.6(3)	-
N2-C4-C3	105.7(4)	106.5(3)
N2-C4-C5	123.0(4)	123.2(4)
N1-N2-C6	119.5(3)	118.6(3)
N2-C6-N3	111.2(3)	110.7(3)
N4-N3-C6	119.1(3)	118.2(3)
N2-N1-Co1	118.7(2)	120.0(2)
N3-N4-Co1	119.7(2)	-
C2-C3-C4	107.5(4)	-
C1-C2-C3	127.9(4)	-
N5-Co1-N8	-	88.59(11)
N5-Co1-O2	-	161.44(10)
N1-Co1-O2	-	101.85(10)
N8-Co1-O2	-	87.70(10)
N4-Co1-O2	-	87.90(10)
N8-Co1-O1	-	85.00(10)
O2-Co1-O1	-	58.41(9)
O1-N9-O3	-	121.8(3)
O2-N9-O3	-	121.2(3)
O1-N9-O2	-	117.0(3)

Appendix II

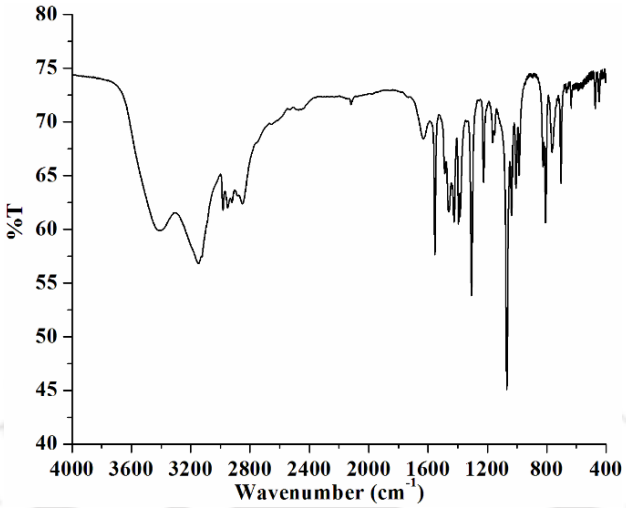

Figure A2.1. FT-IR spectrum of 1-(hydroxymethyl)-3,5-dimethyl-1-pyrazole in KBr.

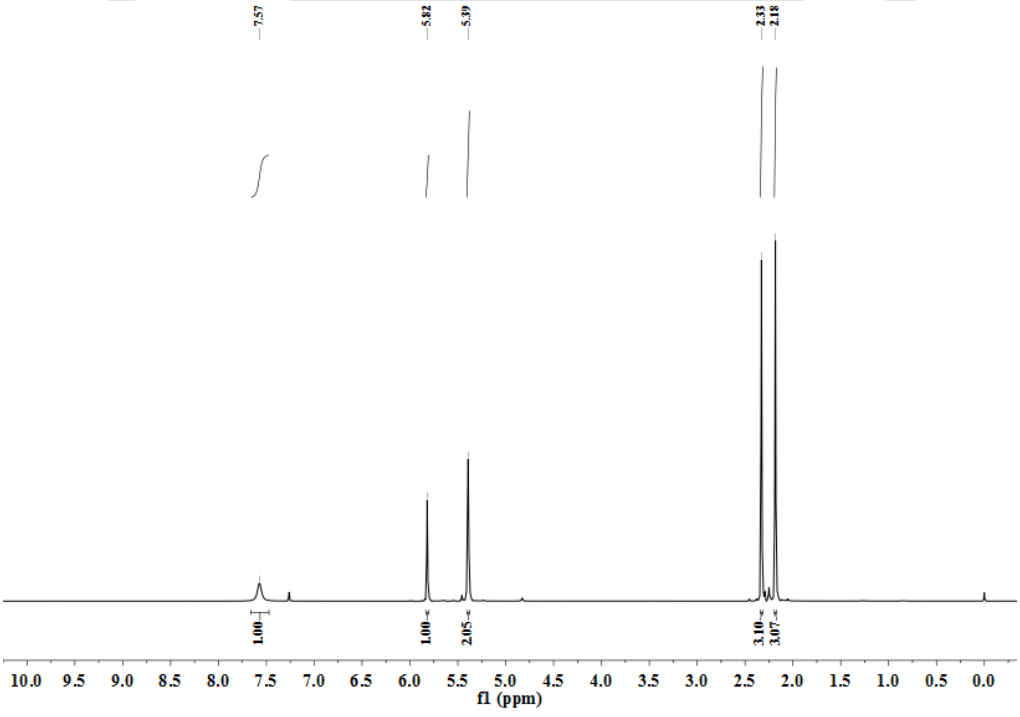

Figure A2.2. ^{1}H-NMR spectrum of 1-(hydroxymethyl)-3,5-dimethyl-1-pyrazole in $CDCl_3$.

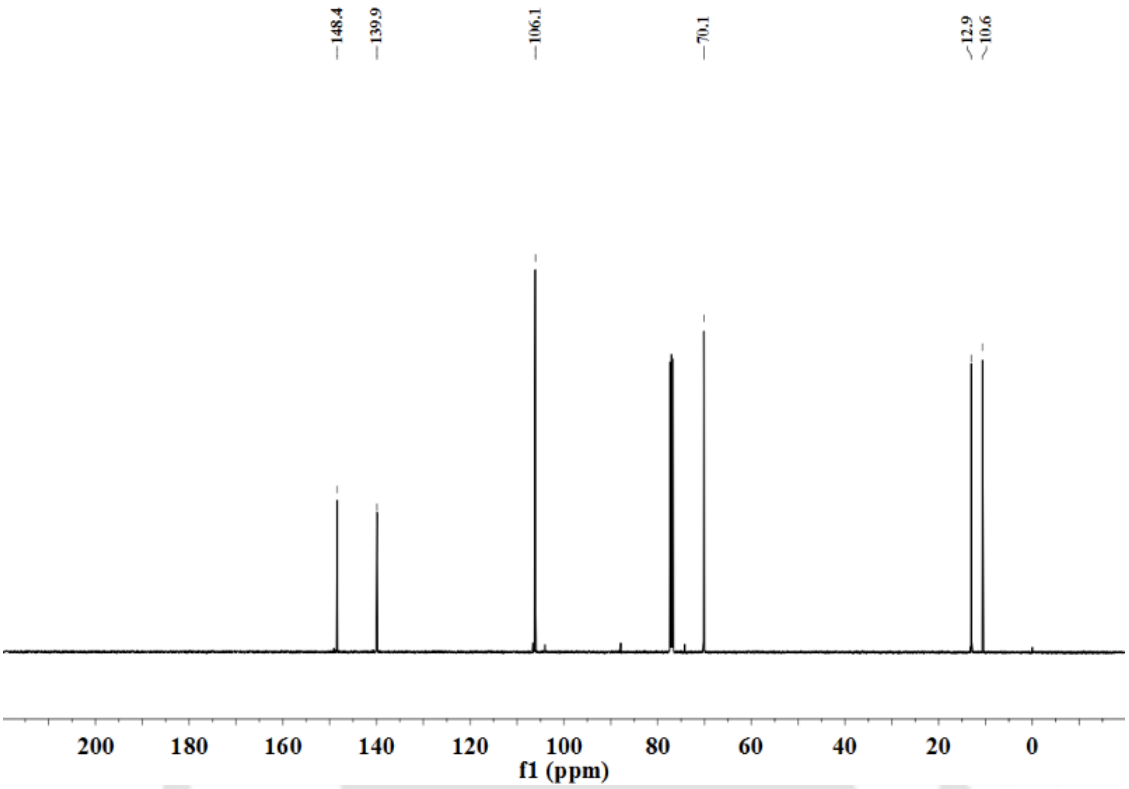

Figure A2.3. ^{13}C-NMR spectrum of 1-(hydroxymethyl)-3,5-dimethyl-1-pyrazole in $CDCl_3$.

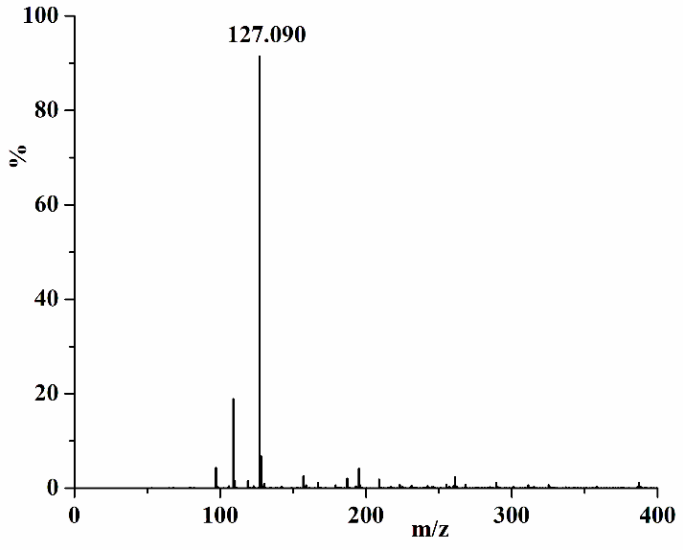

Figure A2.4. ESI-mass spectrum of 1-(hydroxymethyl)-3,5-dimethyl-1-pyrazole in CH_3CN.

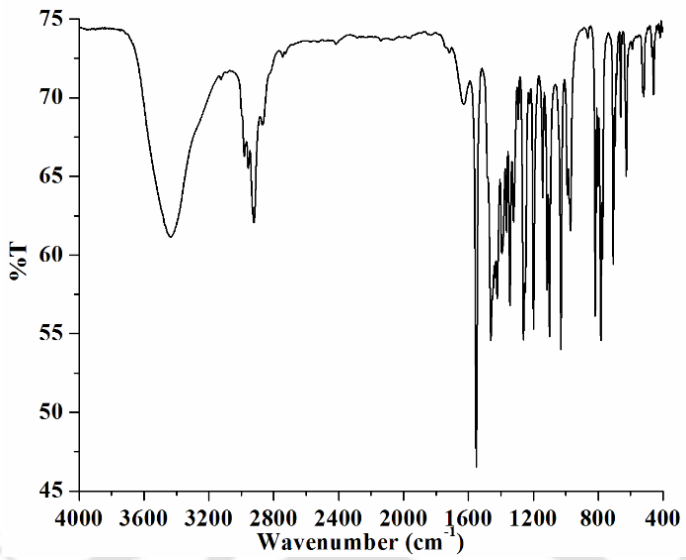

Figure A2.5. FT-IR spectrum of **L2** in KBr.

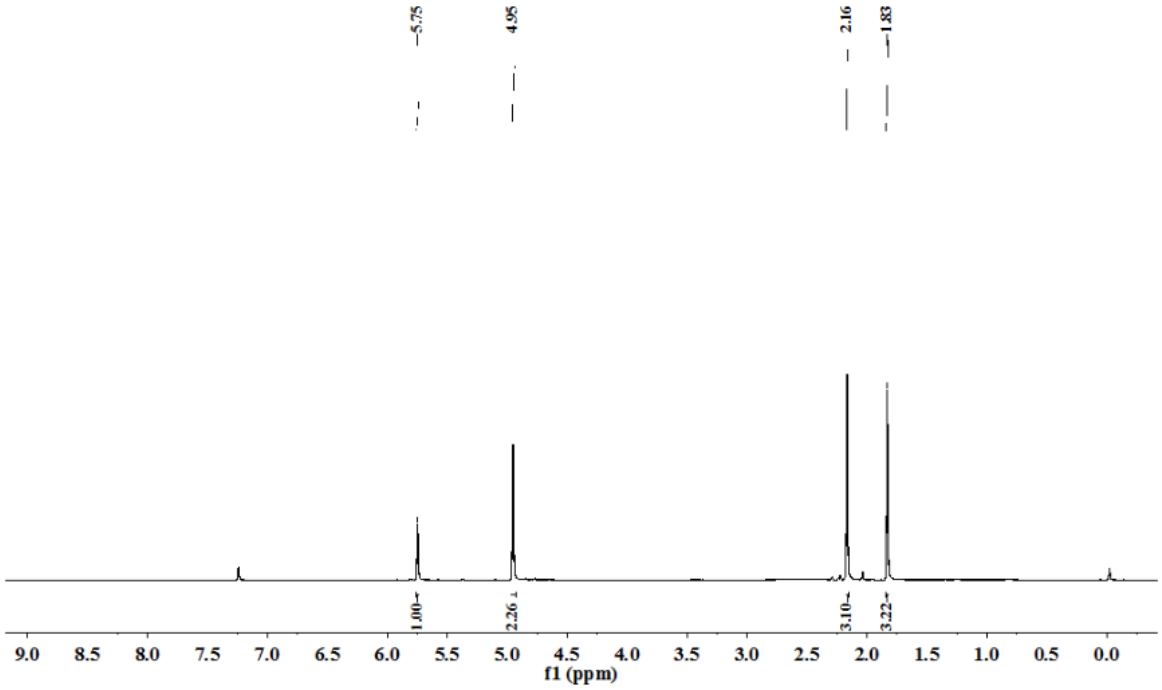

Figure A2.6. ^{1}H-NMR spectrum of **L2** in $CDCl_3$.

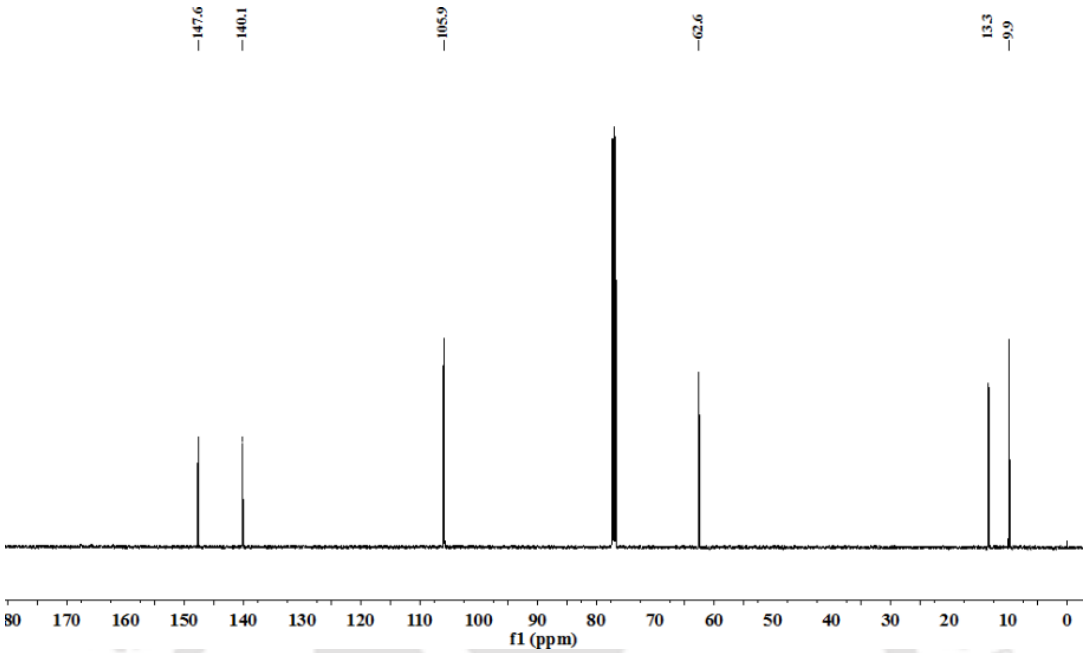

Figure A2.7. ^{13}C-NMR spectrum of **L2** in $CDCl_3$.

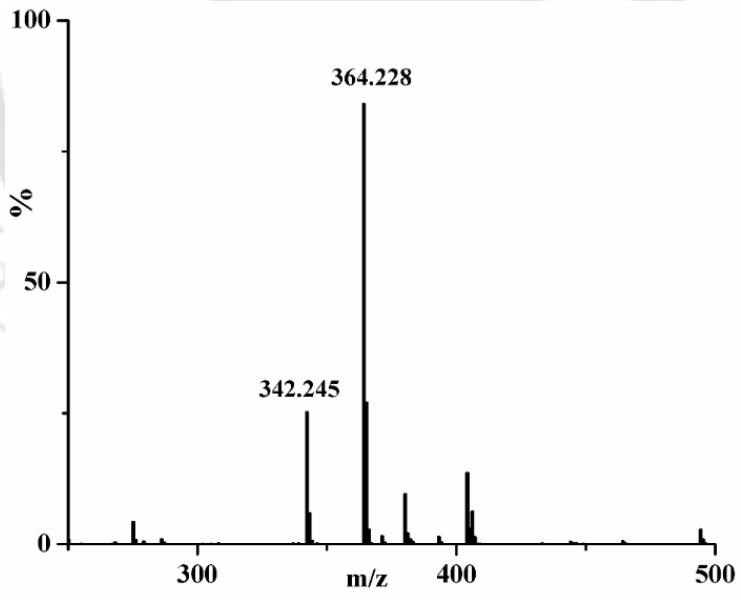

Figure A2.8. ESI-mass spectrum of **L2** in CH_3CN.

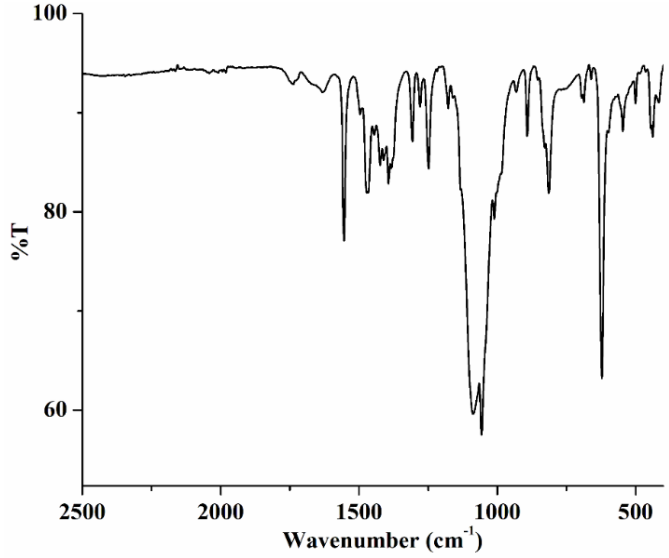

Figure A2.9. FT-IR spectrum of complex **3.1** in KBr.

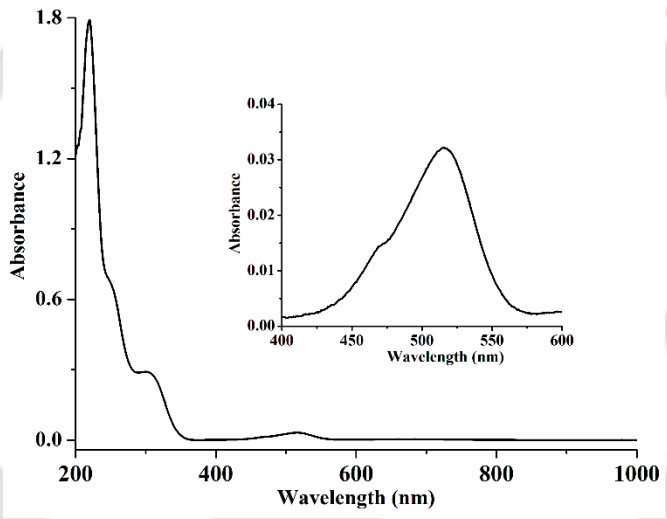

Figure A2.10. UV-visible spectrum of complex **3.1** in CH_3CN at room temperature.

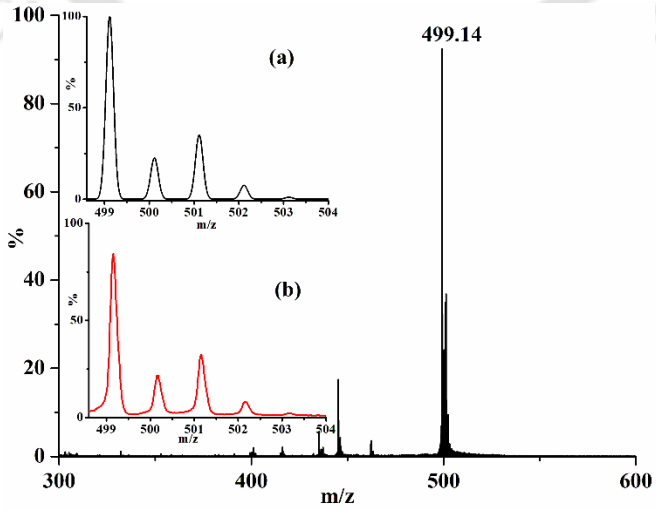

Figure A2.11. ESI-mass spectrum of complex **3.1** in CH_3CN. [Inset: (a) experimental and (b) simulated isotopic distribution pattern].

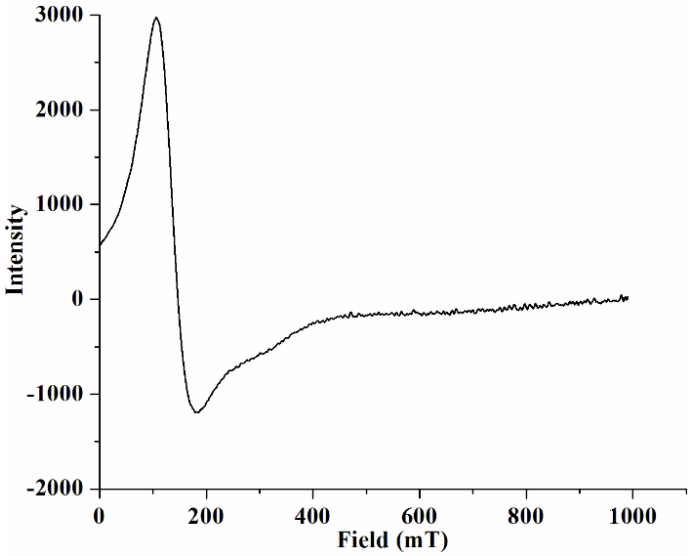

Figure A2.12. X-band EPR spectrum of complex **3.1** in CH_3CN at 77 K.

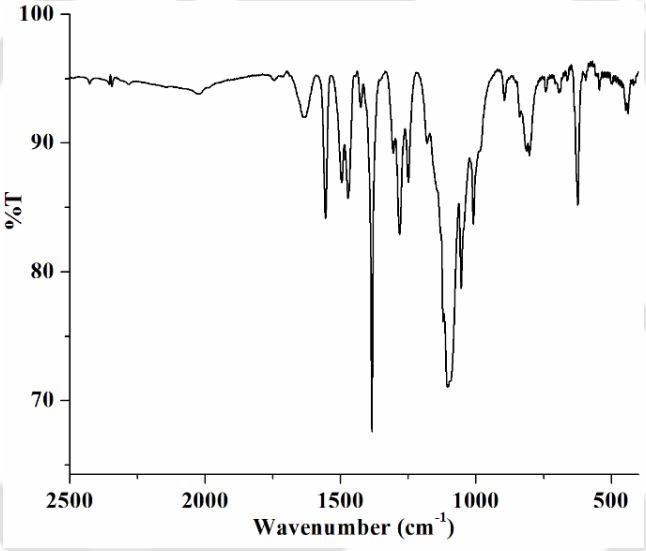

Figure A2.13. FT-IR spectrum of complex **3.2** in KBr.

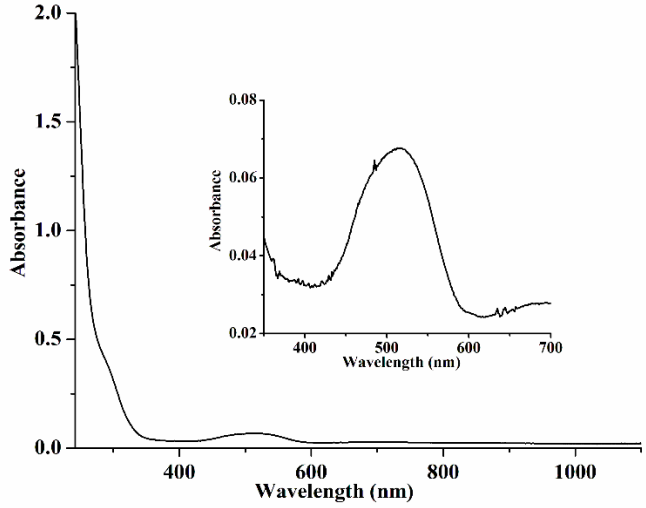

Figure A2.14. UV-visible spectrum of complex **3.2** in CH_3CN at room temperature.

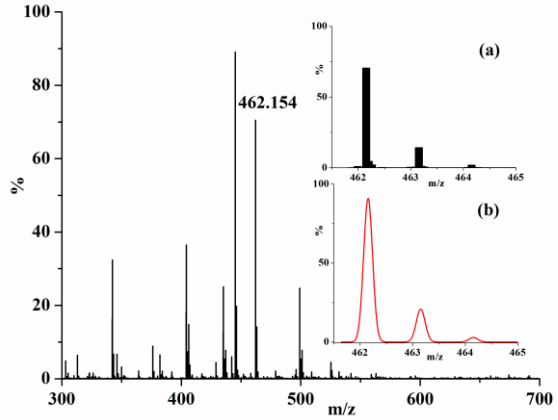

Figure A2.15. ESI-mass spectrum of complex **3.2** in CH_3CN. [Inset: (a) experimental and (b) simulated isotopic distribution pattern].

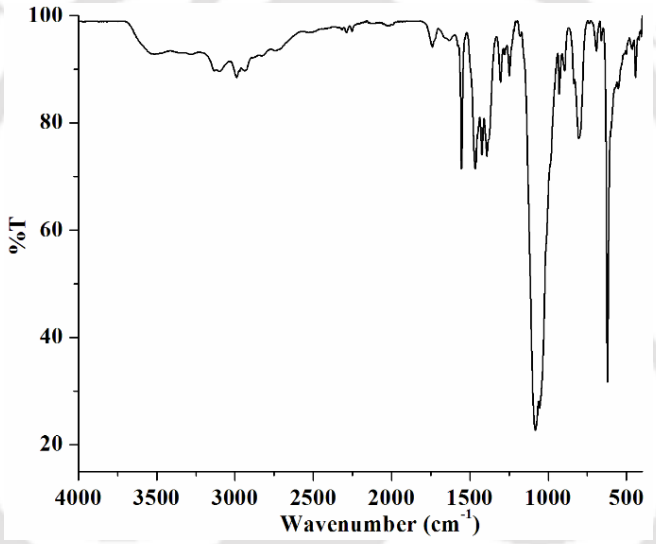

Figure A2.16. FT-IR spectrum of complex **3.3** in KBr.

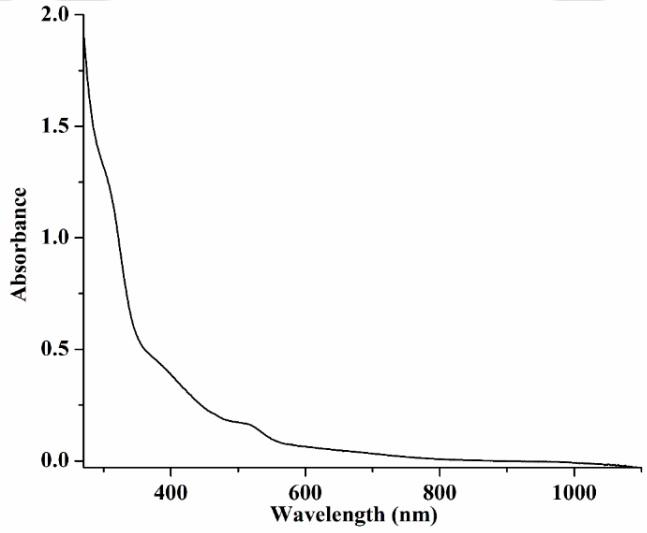

Figure A2.17. UV-visible spectrum of complex **3.3** in CH_3CN at room temperature.

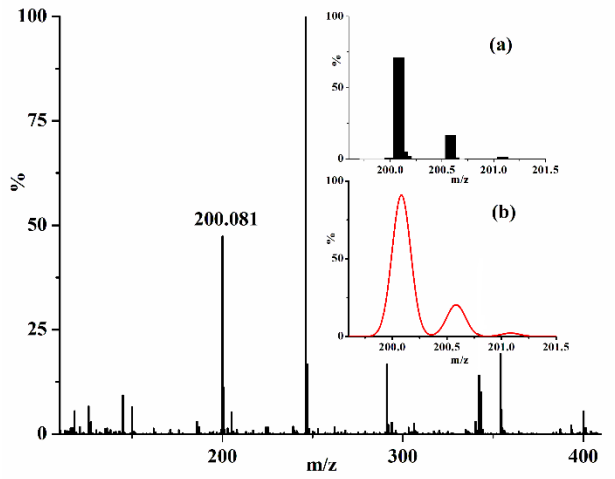

Figure A2.18. ESI-mass spectrum of complex **3.3** in CH_3CN. [Inset: (a) experimental and (b) simulated isotopic distribution pattern].

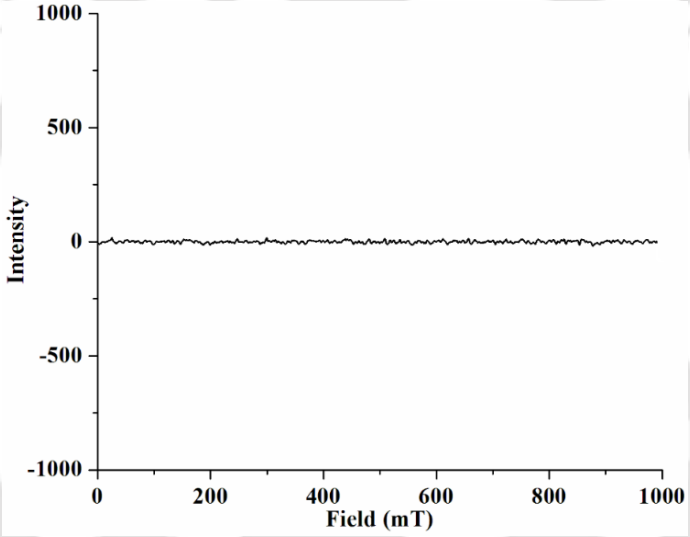

Figure A2.19. X-band EPR spectrum of complex **3.3** in CH_3CN at 77 K.

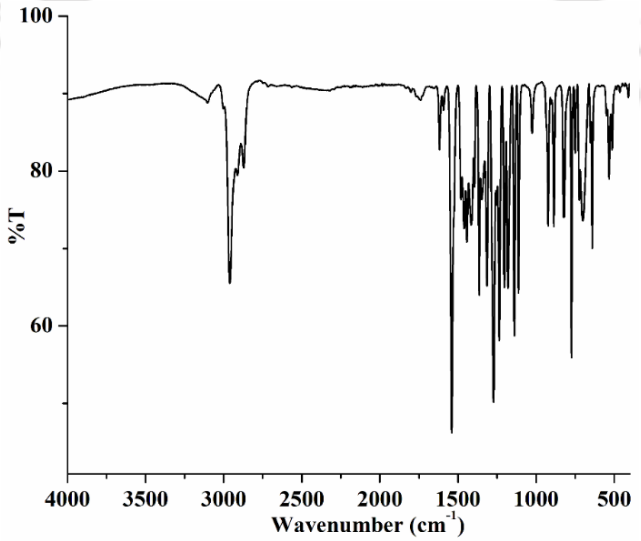

Figure A2.20. FT-IR spectrum of 2,4-di-*tert*-butyl-6-nitrophenol in KBr.

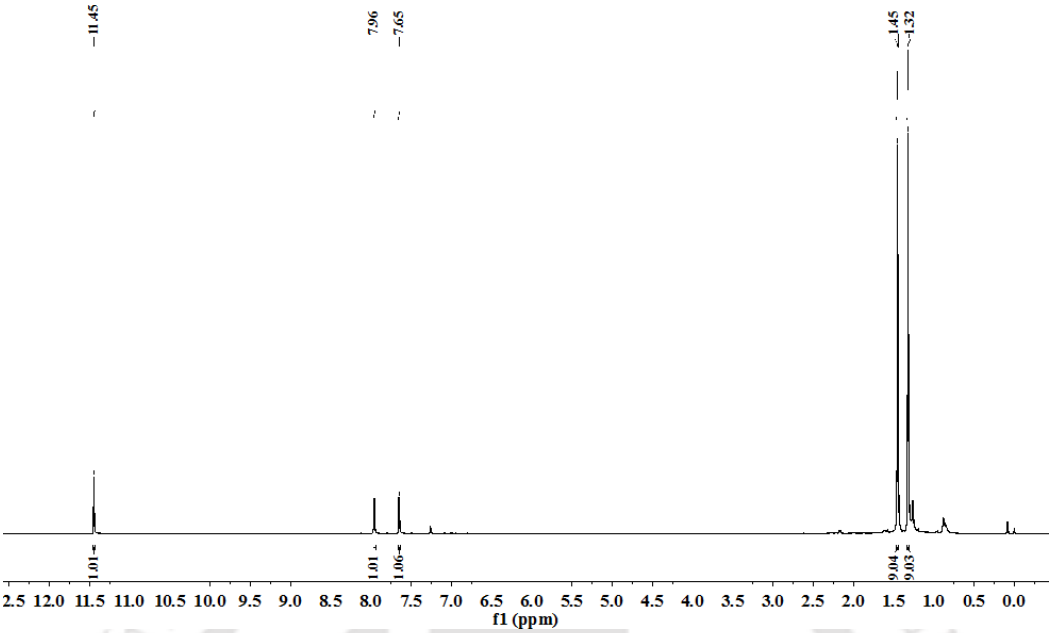

Figure A2.21. ^{1}H-NMR spectrum of 2,4-di-*tert*-butyl-6-nitrophenol in $CDCl_3$.

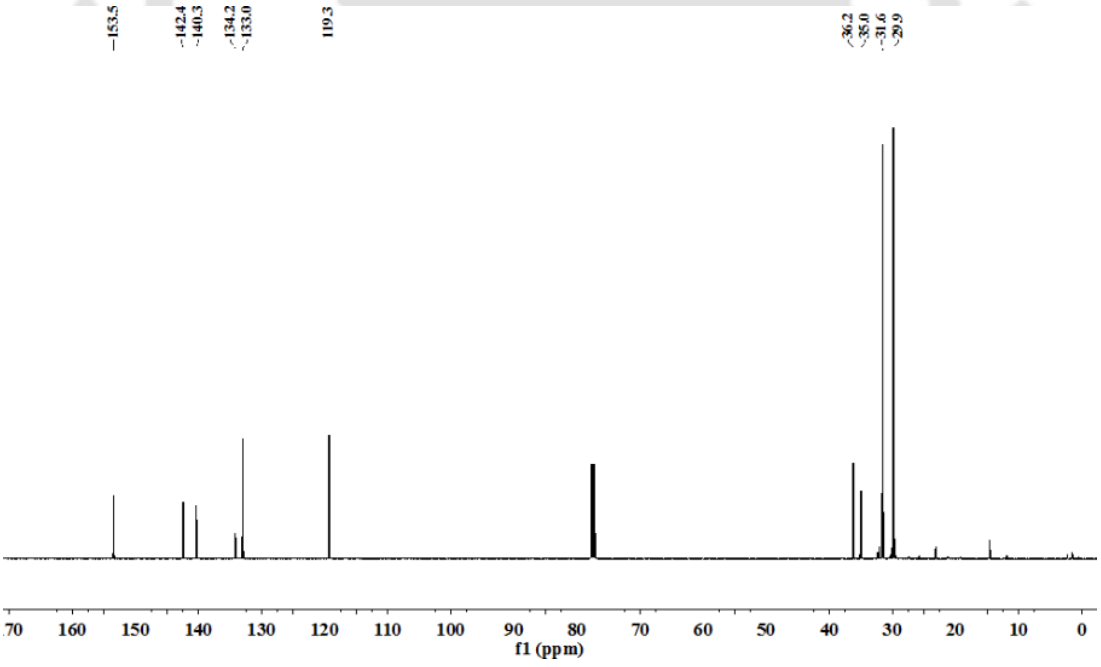

Figure A2.22. ^{13}C-NMR spectrum of 2,4-di-*tert*-butyl-6-nitrophenol in $CDCl_3$.

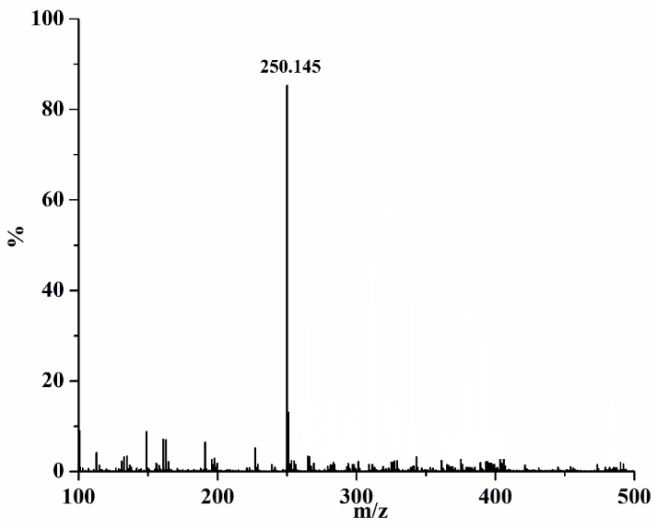

Figure A2.23. ESI-mass spectrum of 2,4-di-*tert*-butyl-6-nitrophenol in CH_3CN.

Table A2.1: Crystallographic data for complexes **3.1** and **3.2**.

	3.1	**3.2**
Formulae	$C_{23}H_{33}CoN_8O_8Cl_2$	$C_{18}H_{24}CoN_8O_7Cl$
Mol. Wt	679.40	558.83
Crystal system	Triclinic	Monoclinic
Space group	P -1	C 1 2/c 1
Temperature/K	297	150
Wavelength/Å	0.71073	0.71073
a/ Å	12.0617(14)	26.450(4)
b/ Å	12.3710(15)	10.5573(15)
c/ Å	12.5120(15)	20.758(3)
α/°	100.758(3)	90
β/°	109.688(3)	119.862(3)
γ/°	113.809(3)	90
V/ Å^3	1491.2(3)	5026.8(12)
Z	2	8
Density/Mgm^{-3}	1.513	1.477
Abs. Coeff. /mm^{-1}	0.814	0.843
Abs. Correction	None	None
F(000)	704.0	2304
Total no. of reflections	5171	4426
Reflections. $I > 2\sigma(I)$	4826	3967
Max. 2θ/°	24.999	24.993

Ranges (h, k, l)	-14 ≤ h ≤ 14 -14 ≤ k ≤ 14 -14 ≤ l ≤ 14	-31 ≤ h ≤ 31 -12 ≤ k ≤ 12 -24 ≤ l ≤ 24
Complete to 2θ (%)	98.3	99.7
Refinement method	Full-matrix least-squares on F^2	Full-matrix least-squares on F^2
Goof(F^2)	1.033	1.071
R indices [$I > 2\sigma(I)$]	0.0504	0.0445
R indices (all data)	0.0537	0.0513

Table A2.2: Selected bond lengths (Å) of complexes **3.1** and **3.2**.

Atoms	**3.1**	**3.2**
Co1-N1	2.025(2)	2.061(3)
Co1-N4	2.018(2)	2.046(2)
Co1-N6	2.023(3)	2.056(3)
Co1-N7	2.260(2)	2.288(2)
Co1-N8	2.045(3)	-
Co1-O1	-	2.040(2)
N1-N2	1.370(3)	1.368(4)
N3-N4	1.366(3)	1.361(3)
N2-C5	1.459(4)	1.559(14)
N7-C5	1.466(3)	1.490(13)
C1-C2	1.491(4)	1.462(5)
C2-C3	1.381(4)	1.388(5)
C3-C4	1.370(4)	1.356(6)
C4-C8	1.493(4)	-
N8-C19	1.126(4)	-
C19-C20	1.451(5)	1.490(4)
O1-N8	-	1.300(4)
N8-O2	-	1.221(4)
N8-O3	-	1.241(4)

Table A2.3: Selected bond angles (°) of complexes **3.1** and **3.2**.

Atoms	**3.1**	**3.2**
N1-Co1-N7	78.27(8)	75.65(9)
N1-Co1-N8	99.97(11)	-
N4-Co1-N7	78.36(8)	77.21(9)
N4-Co1-N1	121.92(9)	130.94(11)

N4-Co1-N6	112.35(10)	107.14(11)
N4-Co1-N8	103.14(11)	-
N6-Co1-N7	78.10(9)	77.60(9)
N6-Co1-N1	113.54(10)	105.89(11)
N6-Co1-N8	102.21(11)	-
N8-Co1-N7	178.15(10)	-
N1-C2-C1	122.5(3)	121.8(3)
N1-C2-C3	109.8(3)	110.0(3)
C3-C2-C1	127.6(3)	128.2(3)
N2-C4-C3	106.1(3)	106.2(3)
N2-C4-C11	-	121.9(4)
N2-C4-C8	122.4(3)	-
N1-N2-C5	118.2(2)	110.1(6)
N2-C5-N7	107.3(2)	100.1(8)
N4-N3-C6	119.3(2)	-
N2-N1-Co1	114.88(16)	116.0(2)
N3-N4-Co1	115.69(17)	115.15(18)
C12-C11-C10	127.9(3)	-
C11-C10-C9	107.0(3)	-
N4-N3-C12	-	111.7(3)
N3-C12-C16	-	122.0(3)
N3-C12-C13	-	106.3(3)
C12-C13-C14	-	106.7(3)
C13-C14-C15	-	128.2(3)
C13-C14-N4	-	109.9(3)
Co1-O1-N8	-	103.42(19)
O1-N8-O2	-	119.0(4)
O1-N8-O3	-	116.6(3)

Appendix III

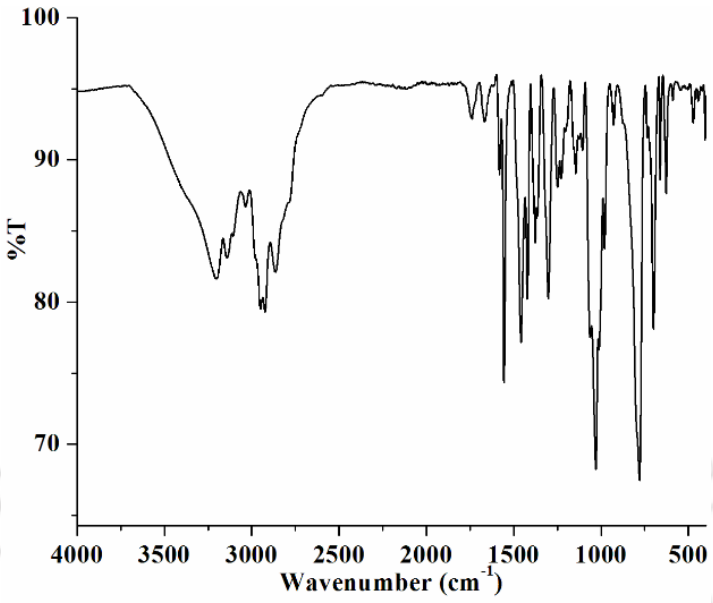

Figure A3.1. FT-IR spectrum of **L3** in KBr.

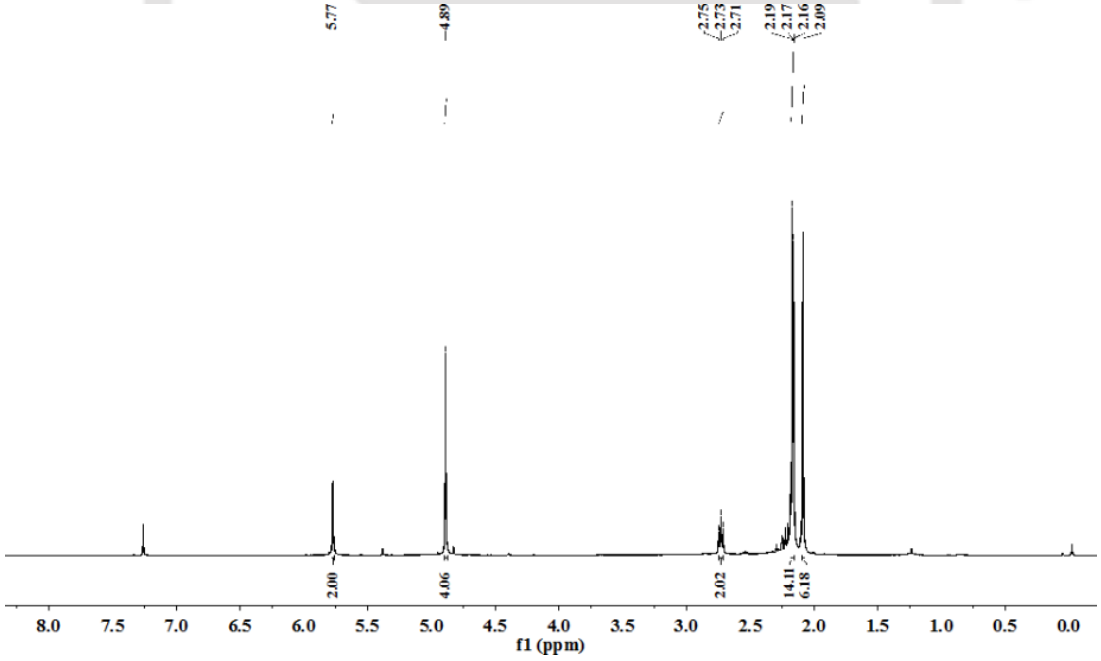

Figure A3.2. ^{1}H-NMR spectrum of **L3** in $CDCl_3$.

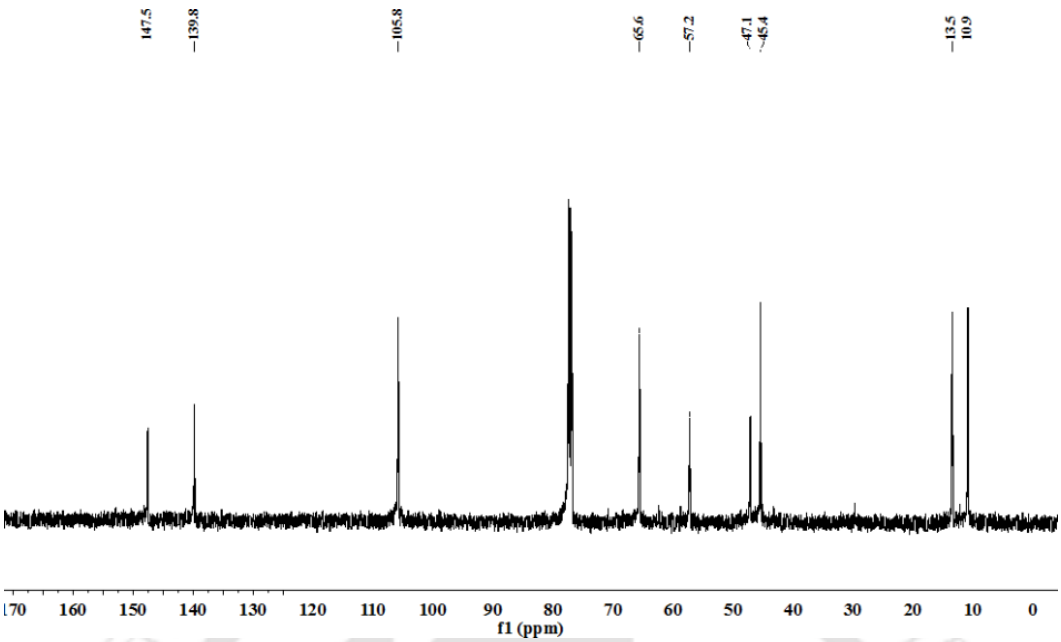

Figure A3.3. ^{13}C-NMR spectrum of **L3** in $CDCl_3$.

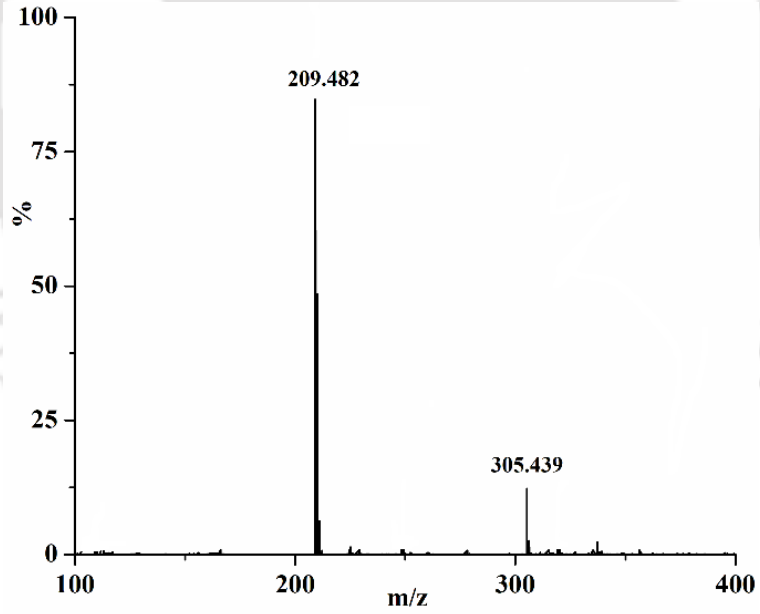

Figure A3.4. ESI-mass spectrum of **L3** in CH_3CN.

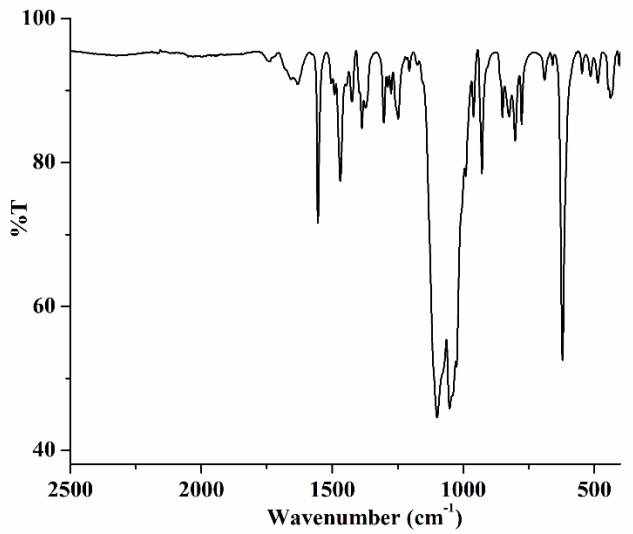

Figure A3.5. FT-IR spectrum of complex **4.1** in KBr.

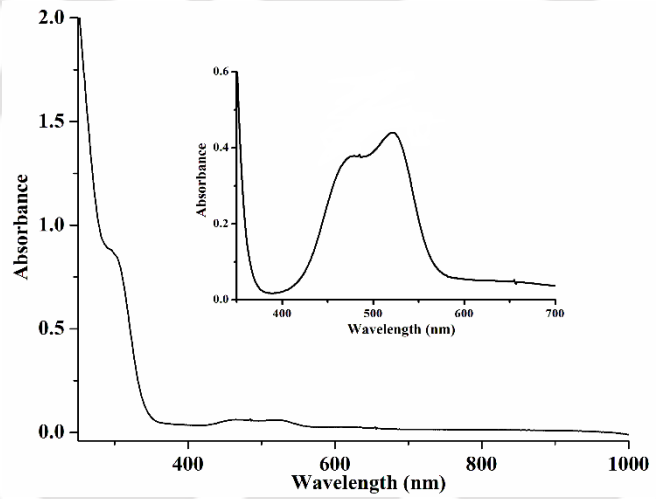

Figure A3.6. UV-visible spectrum of complex **4.1** in CH_3CN at room temperature.

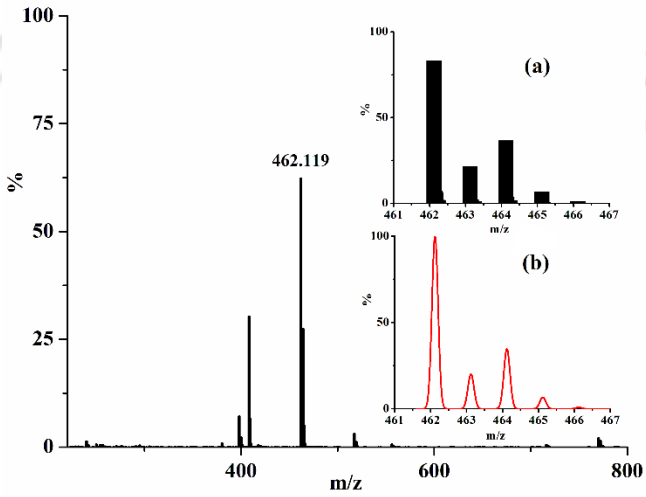

Figure A3.7. ESI-mass spectrum of complex **4.1** in CH_3CN [Inset: (a) experimental and (b) simulated isotopic distribution pattern].

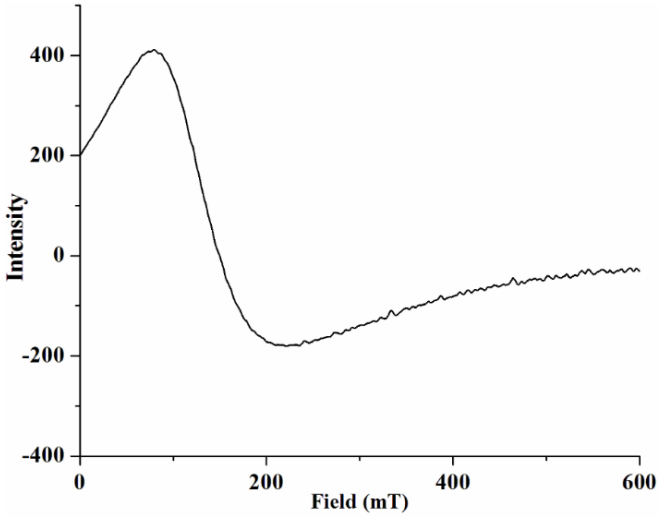

Figure A3.8. X-band EPR spectrum of complex **4.1** in CH_3CN at 77 K.

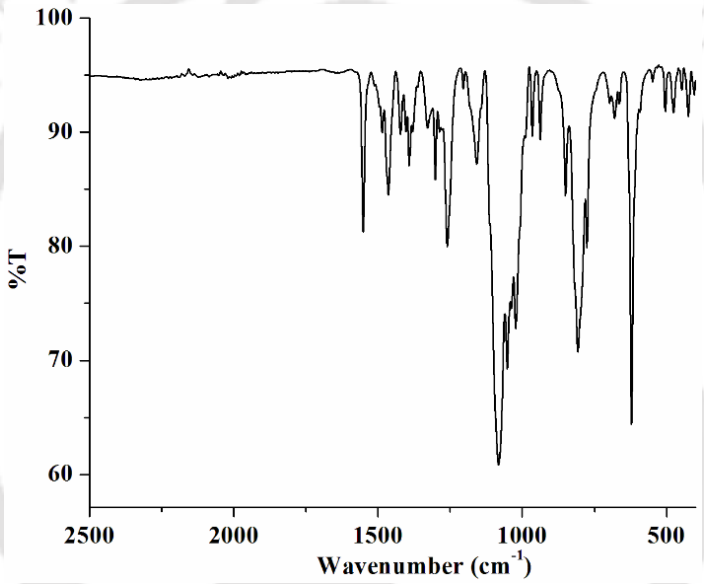

Figure A3.9. FT-IR spectrum of complex **4.2** in KBr.

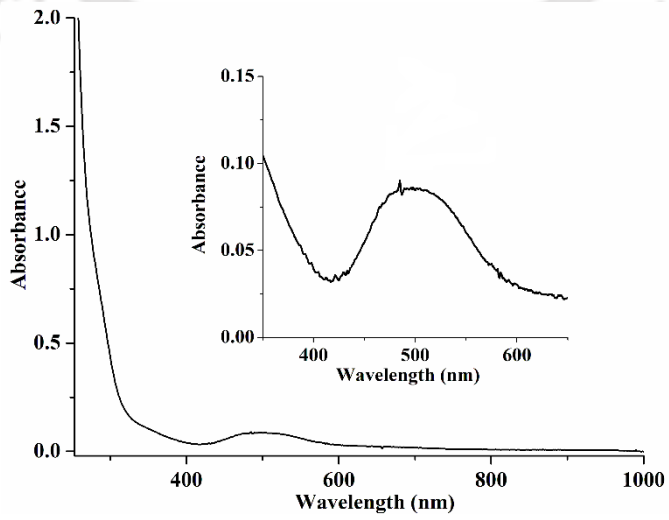

Figure A3.10. UV-visible spectrum of complex **4.2** in CH_3CN at room temperature.

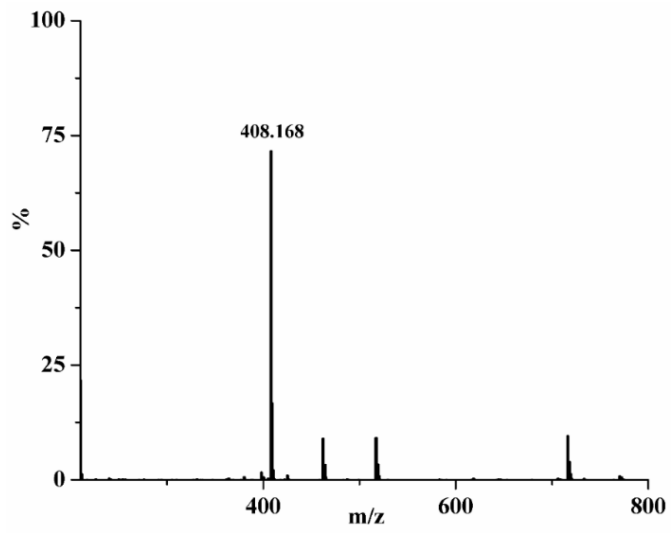

Figure A3.11. ESI-mass spectrum of complex **4.2** in CH_3CN.

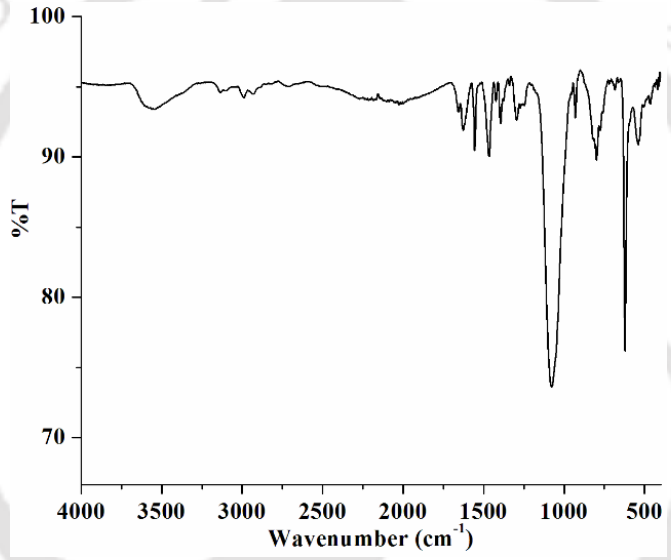

Figure A3.12. FT-IR spectrum of complex **4.3** in KBr.

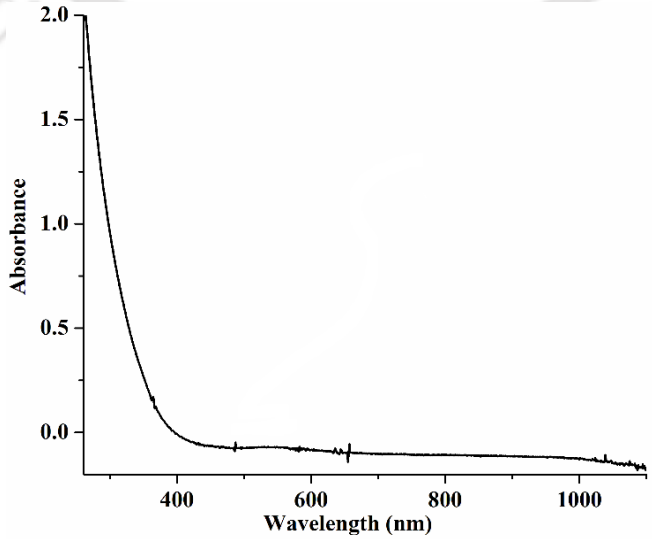

Figure A3.13. UV-visible spectrum of complex **4.3** in CH_3CN at room temperature.

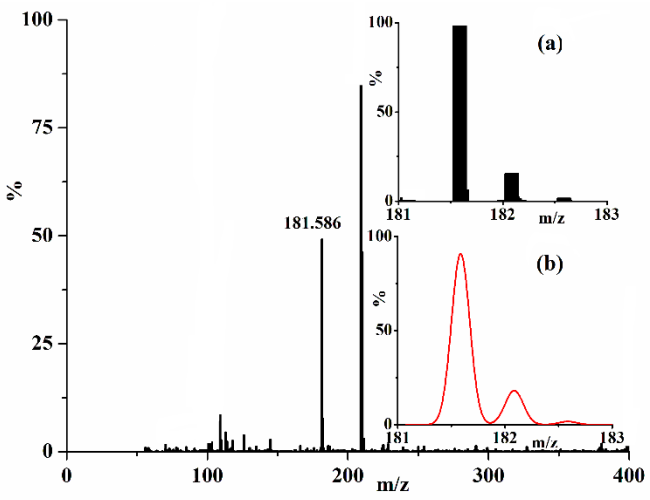

Figure A3.14. ESI-mass spectrum of complex **4.3** in CH_3CN. [Inset: (a) experimental and (b) simulated isotopic distribution pattern].

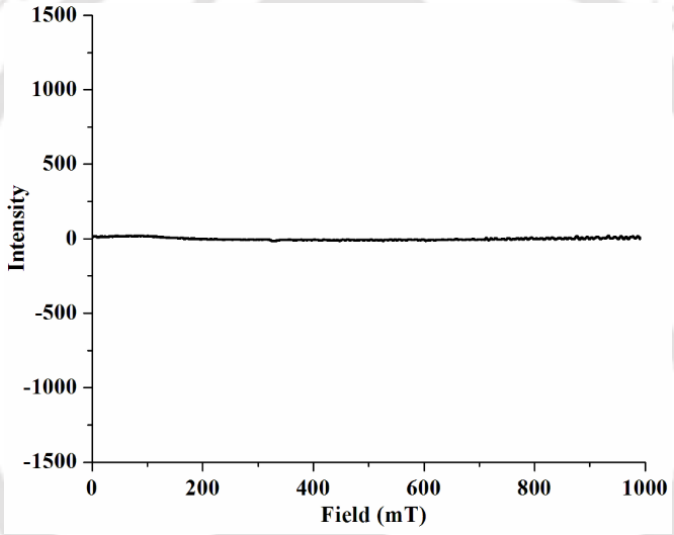

Figure A3.15. X-band EPR spectrum of complex **4.3** in CH_3CN at 77 K.

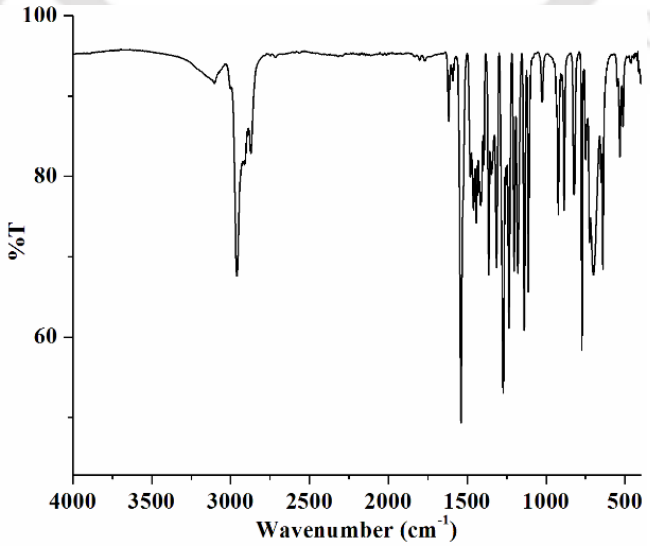

Figure A3.16. FT-IR spectrum of complex 2,4-di-*tert*-butyl-6-nitrophenol using ATR probe.

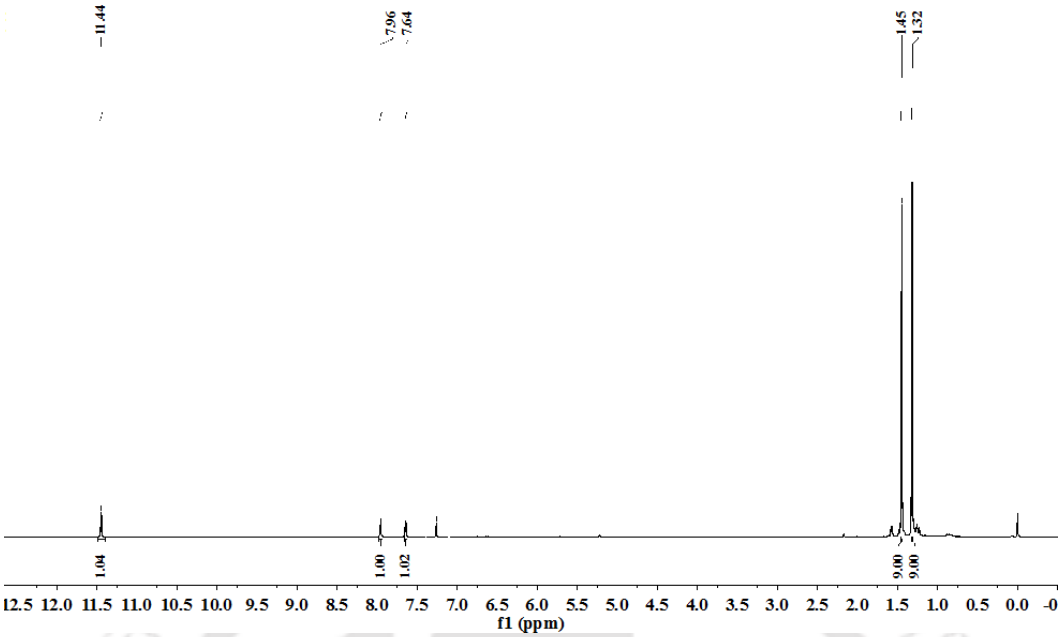

Figure A3.17. ^{1}H-NMR spectrum of 2,4-di-*tert*-butyl-6-nitrophenol in $CDCl_3$.

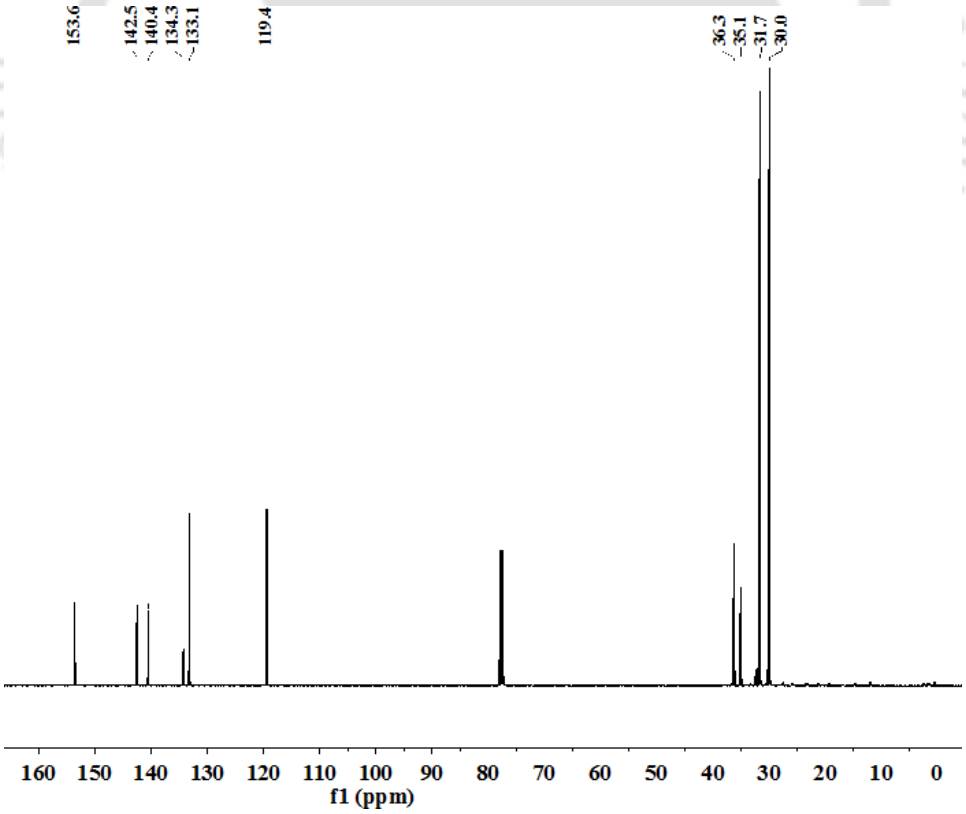

Figure A3.18. ^{13}C-NMR spectrum of 2,4-di-*tert*-butyl-6-nitrophenol in $CDCl_3$.

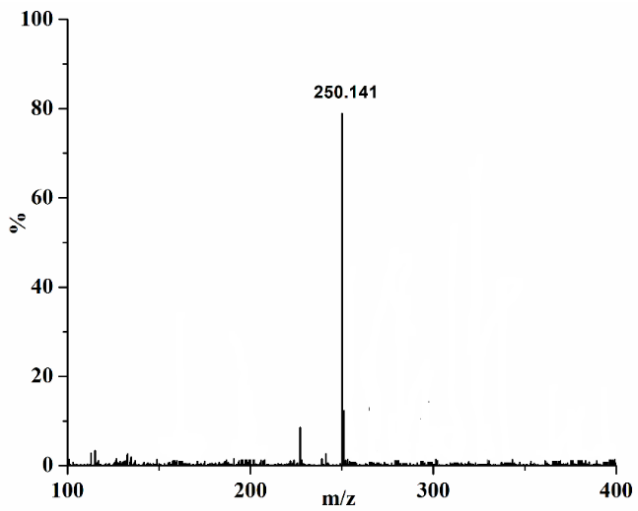

Figure A3.19. ESI-mass spectrum of 2,4-di-*tert*-butyl-6-nitrophenol in CH_3CN.

Table A1: Crystallographic data for complexes **4.1** and **4.2**.

	4.1	**4.2**
Formulae	$C_{18}H_{31}CoN_7O_8Cl_2$	$C_{16}H_{28}CoN_7O_6Cl$
Mol. Wt	603.33	508.83
Crystal system	Monoclinic	orthorhombic
Space group	P21/c	P 21 21 21
Temperature/K	297	295
Wavelength/Å	0.71073	0.71073
a/ Å	10.894(2)	8.1656(9)
b/ Å	20.433(4)	10.5914(12)
c/ Å	12.811(3)	26.227(3)
α/°	90	90
β/°	110.110(5)	90
γ/°	90	90
V/ $Å^3$	2677.8(10)	2268.2(4)
Z	4	4
Density/Mgm^{-3}	1.497	1.490
Abs. Coeff. /mm^{-1}	0.895	0.921
Abs. Correction	none	none
F(000)	1252.0	1060.0
Total no. of reflections	4679	3967
Reflections. $I > 2\sigma(I)$	4076	3779
Max. 2θ/°	24.999	24.987
Ranges (h, k, l)	$-12 \le h \le 12$ $-24 \le k \le 24$ $-15 \le l \le 15$	$-9 \le h \le 9$ $-12 \le k \le 12$ $-31 \le l \le 31$

Complete to 2θ (%)	99.3	99.5
Refinement method	Full-matrix least-squares on F^2	Full-matrix least-squares on F^2
Goof(F^2)	1.076	1.111
R indices [$I > 2\sigma(I)$]	0.0473	0.0398
R indices (all data)	0.0558	0.0428

Table A2: Selected bond lengths (Å) of complexes **4.1** and **4.2**.

Atoms	**4.1**	**4.2**
Co1-N1	2.019(3)	2.081(4)
Co1-N4	2.039(3)	-
Co1-N5	2.231(2)	2.086(4)
Co1-N6	2.073(3)	2.110(3)
Co1-N7	2.047(3)	2.217(2)
N1-N2	1.367(3)	1.368(4)
N3-N4	1.370(4)	1.364(4)
N2-C5	1.471(5)	1.446(4)
N3-C6	1.479(5)	1.447(4)
N3-C7	1.340(4)	1.260(4)
N5-C6	1.469(5)	1.263(3)
N6-C12	1.490(5)	1.228(4)

Table A3: Selected bond angles (°) of complexes **4.1** and **4.2**.

Atoms	**4.1**	**4.2**
N1-Co1-N4	127.25(13)	160.14(10)
N1-Co1-N5	78.09(9)	101.85(10)
N1-Co1-N6	110.81(12)	88.66(10)
N1-Co1-N7	103.09(11)	97.09(11)
N4-Co1-N5	78.55(10)	96.66(11)
N4-Co1-N7	98.48(11)	95.73(11)
N5-Co1-N7	176.84(11)	172.38(11)
N6-Co1-N7	99.37(12)	-
N6-Co1-N5	82.84(11)	-
N1-N2-C5	120.1(3)	87.90(10)
N1-N2-C4	111.5(3)	86.22(10)
N1-C2-C3	109.2(3)	122.6(3)
N1-C2-C1	122.2(3)	109.2(3)
C2-N1-N2	105.8(3)	-
C4-N2-N1	111.5(3)	106.5(3)
C4-N2-C5	125.1(3)	123.2(4)

C7-N3-N4	112.3(3)	118.6(3)
C7-N3-C6	130.7(3)	110.7(3)
C9-N4-N3	104.4(3)	118.2(3)
C11-N6-C12	108.5(3)	120.0(2)
C13-N6-C11	109.4(3)	-
C11-N6-Co1	109.7(2)	-
C12-N6-Co1	108.0(3)	-
C13-N6-Co1	110.7(3)	88.59(11)
C17-N7-Co1	172.7(3)	161.44(10)
C1-C2-C3	128.6(3)	101.85(10)
C2-C3-C4	107.2(3)	87.70(10)
N4-Co1-O2	-	87.90(10)
N8-Co1-O1	-	85.00(10)
O2-Co1-O1	-	58.41(9)
O1-N9-O3	-	121.8(3)
O2-N9-O3	-	121.2(3)
O1-N9-O2	-	117.0(3)

Appendix IV

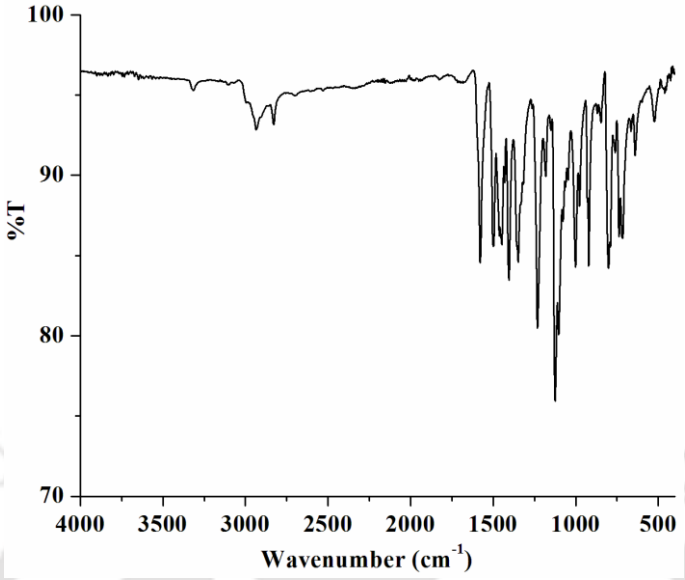

Figure A4.1. FT-IR spectrum of **TTMPPH$_2$** using ATR probe.

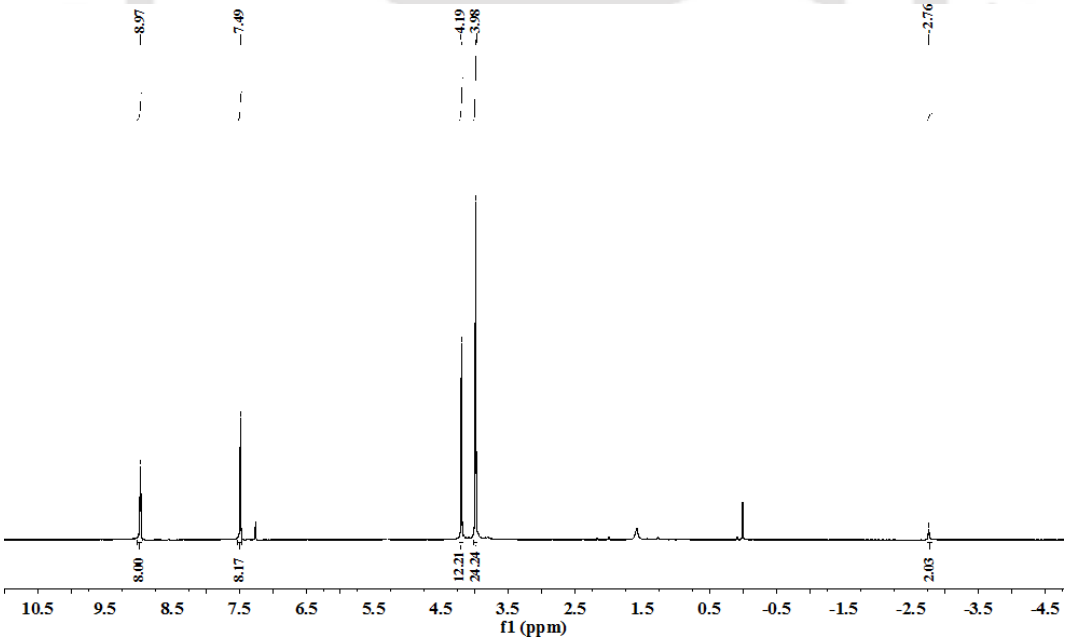

Figure A4.2. ^{1}H-NMR spectrum of **TTMPPH$_2$** in $CDCl_3$.

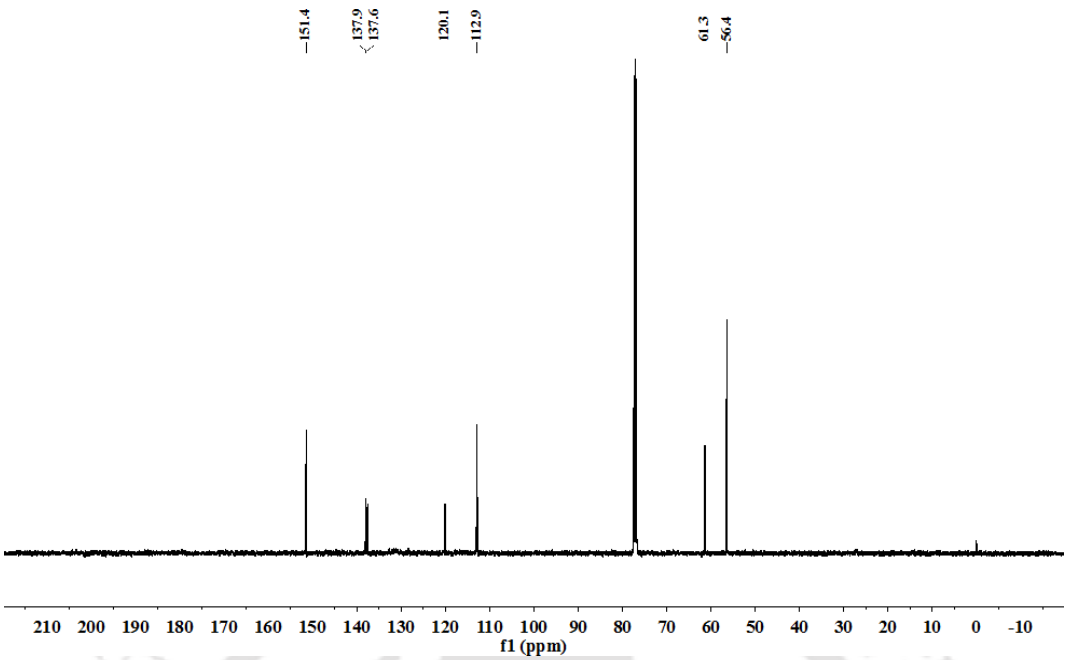

Figure A4.3. ^{13}C-NMR spectrum of **TTMPPH$_2$** in $CDCl_3$.

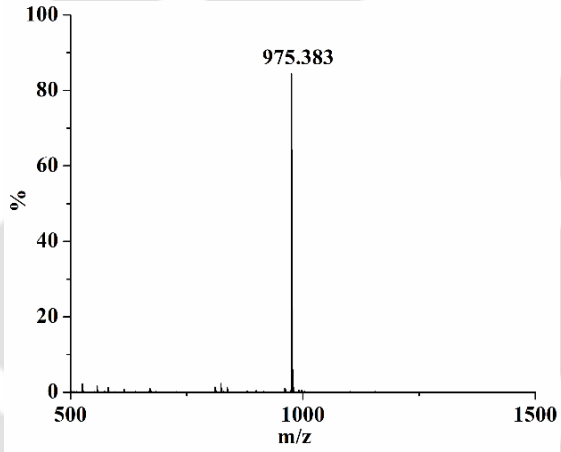

Figure A4.4. ESI-mass spectrum of **TTMPPH$_2$** in CH_3CN.

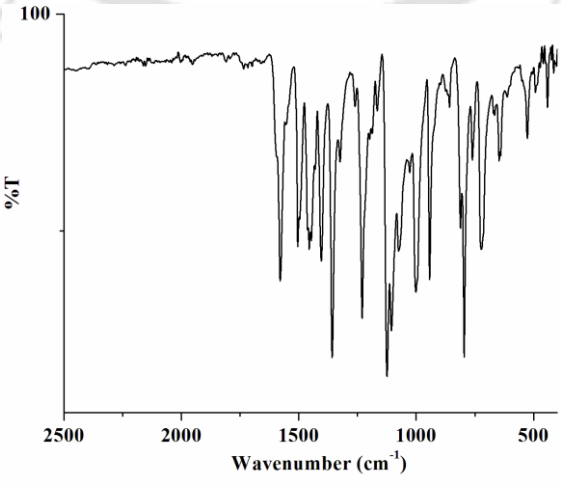

Figure A4.5. FT-IR spectrum of complex **5.1a** using ATR probe.

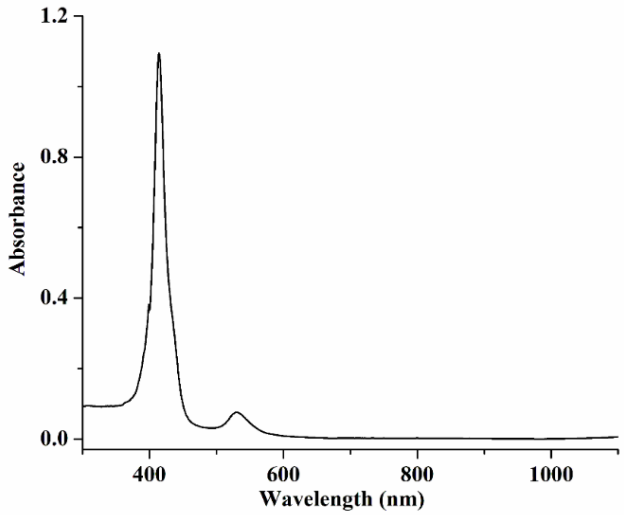

Figure A4.6. UV-visible spectrum of complex **5.1a** in CH_2Cl_2 at room temperature.

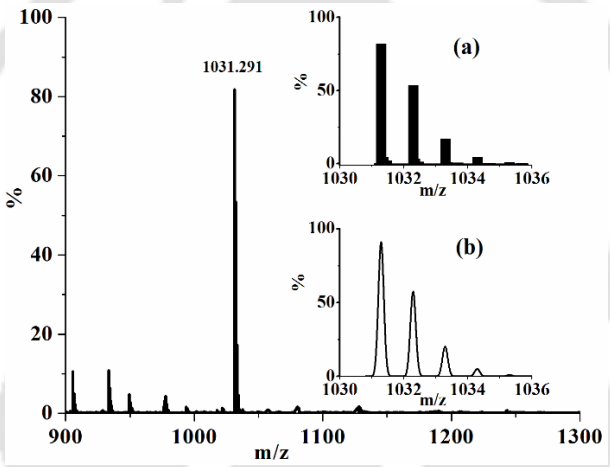

Figure A4.7. ESI-mass spectrum of complex **5.1a** in CH_3CN. [Inset: (a) experimental and (b) simulated isotopic distribution pattern].

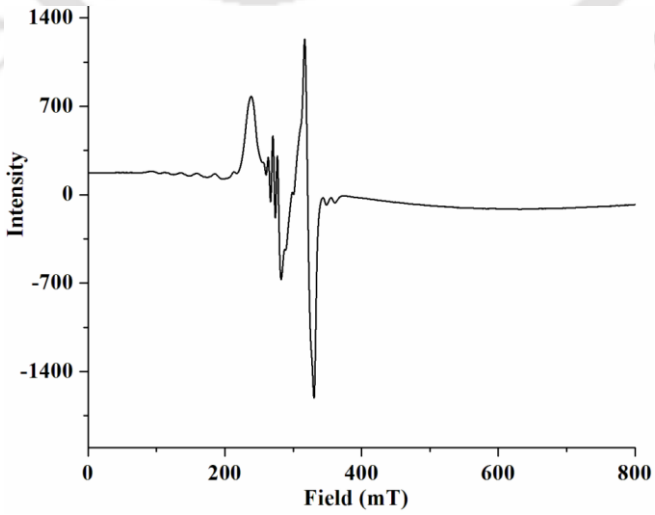

Figure A4.8. X-band EPR spectrum of complex **5.1a** in CH_2Cl_2 at 77 K.

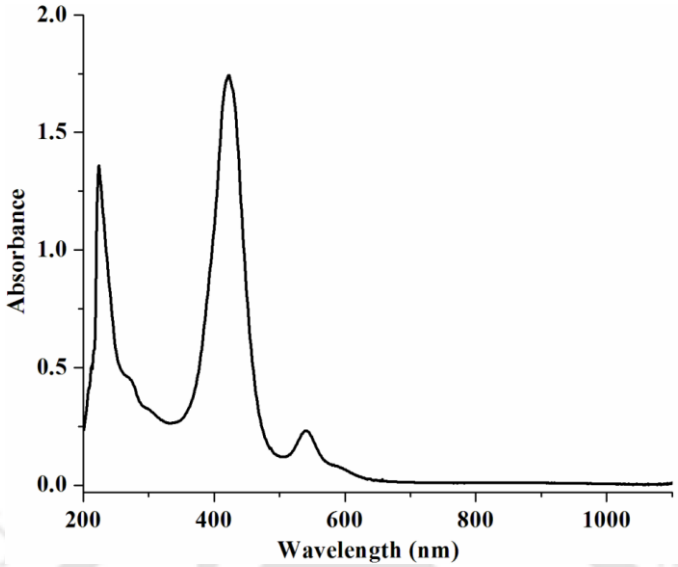

Figure A4.9. UV-visible spectrum of complex **5.1** in CH_2Cl_2:CH_3CN (1:4, v/v) mixture at room temperature.

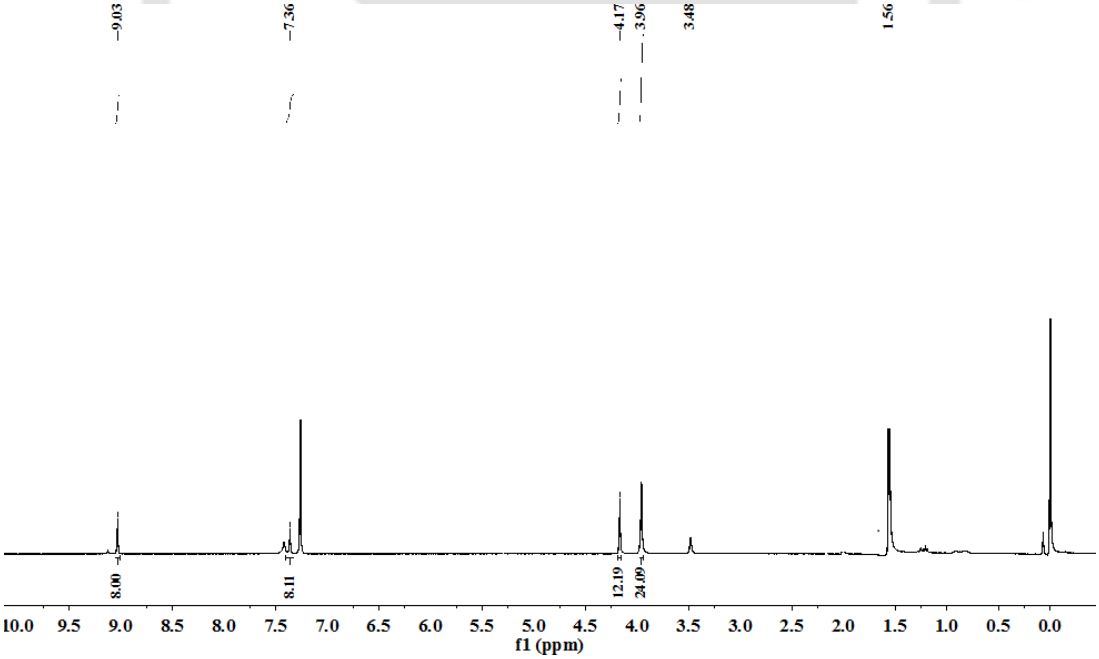

Figure A4.10. ^{1}H-NMR spectrum of complex **5.1** in $CDCl_3$.

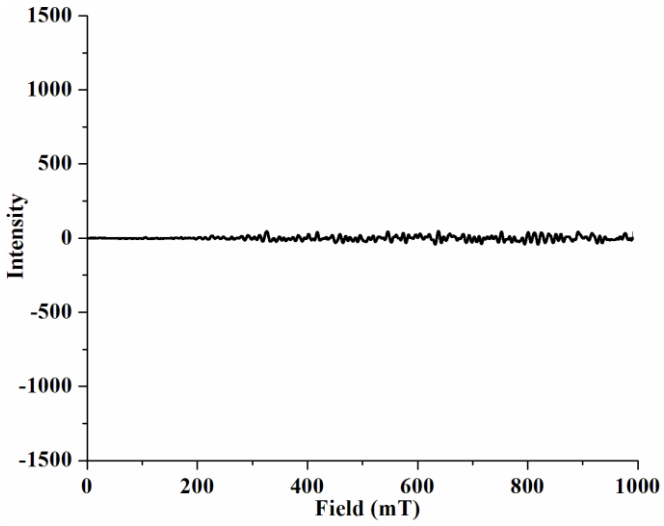

Figure A4.11. X-band EPR spectrum of complex **5.1** in CH_2Cl_2:CH_3CN (1:4, v/v) mixture at 77 K.

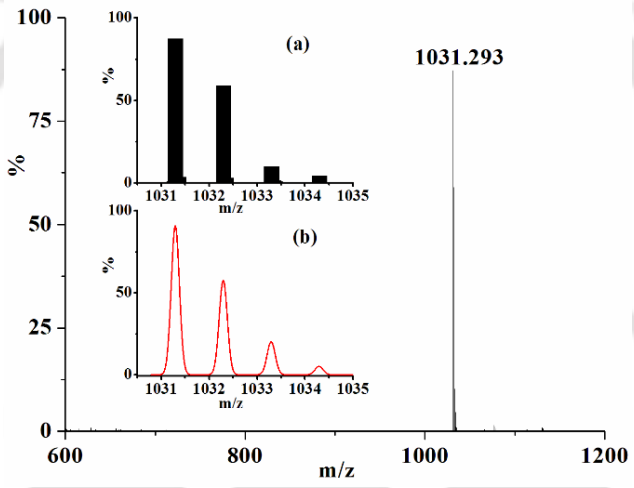

Figure A4.12. ESI-mass spectrum of complex **5.1** in CH_3CN [Inset: (a) experimental and (b) simulated isotopic distribution pattern].

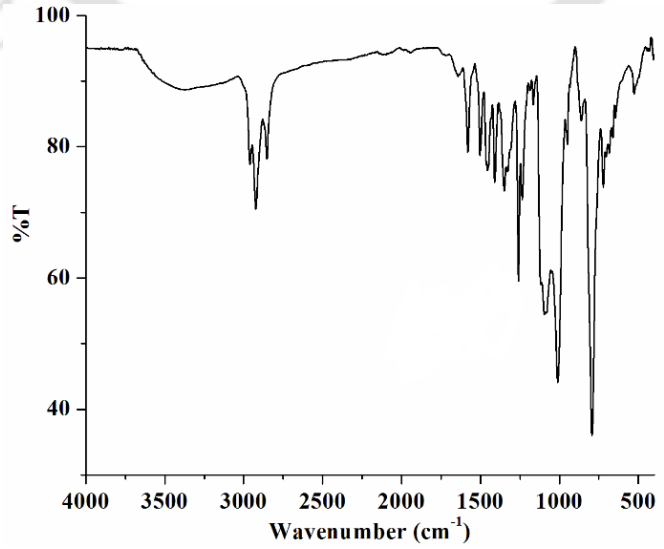

Figure A4.13. FT-IR spectrum of complex **5.2** using ATR probe.

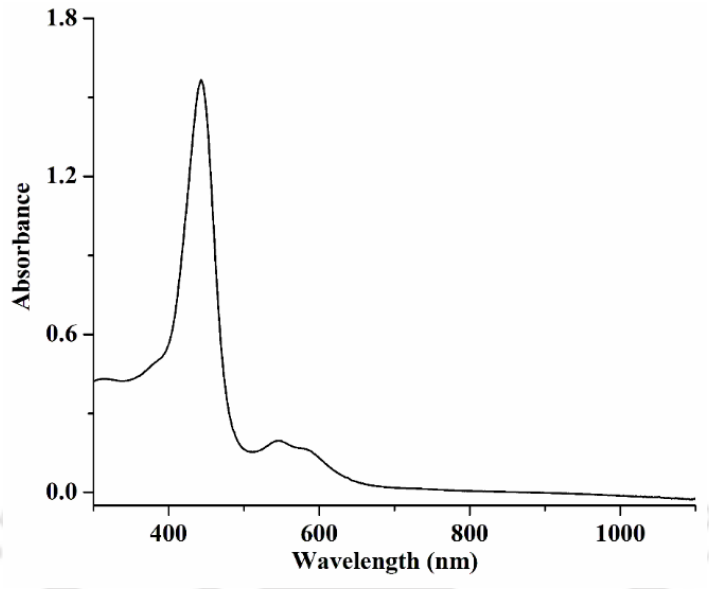

Figure A4.14. UV-visible spectrum of complex **5.2** in CH_2Cl_2 at room temperature.

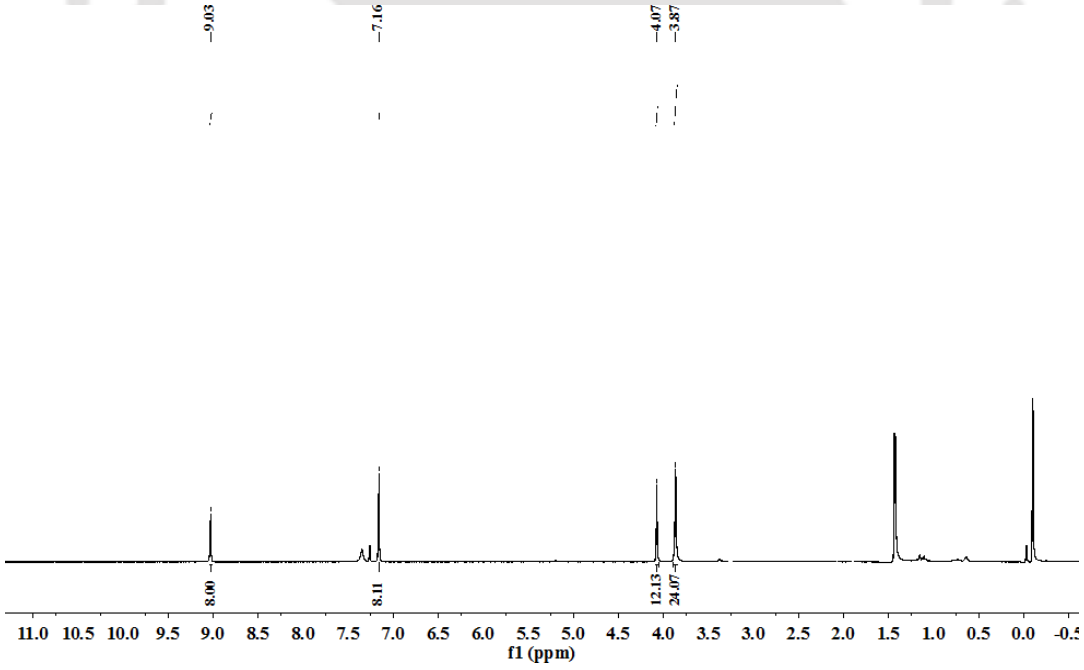

Figure A4.15. ^{1}H-NMR spectrum of complex **5.2** in $CDCl_3$.

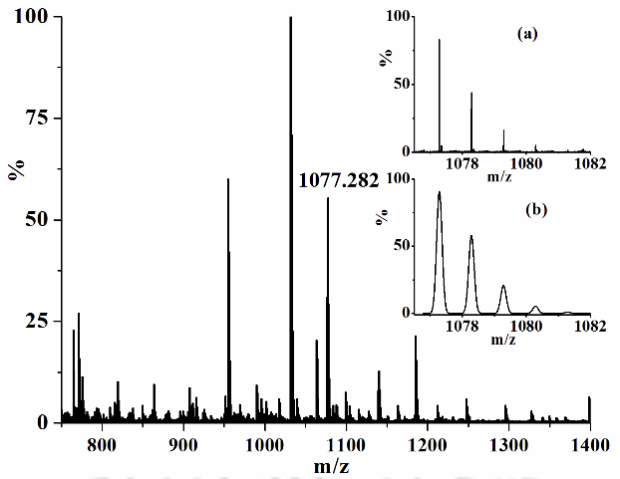

Figure A4.16. ESI-mass spectrum of complex **5.2** in CH_3CN. [Inset: (a) experimental and (b) simulated isotopic distribution pattern].

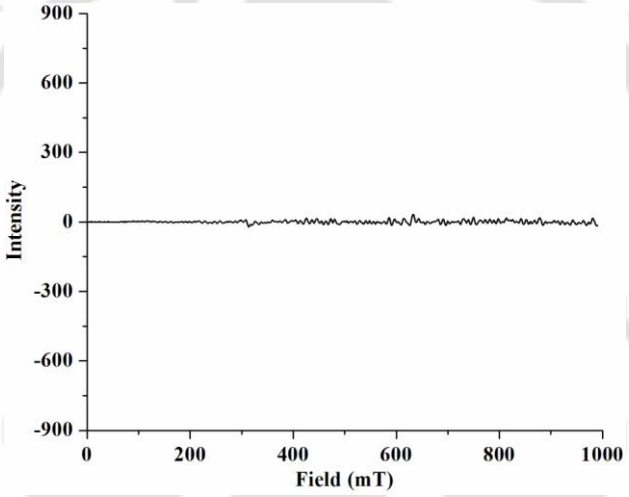

Figure A4.17. X-band EPR spectrum of complex **5.2** in CH_2Cl_2 at 77 K.

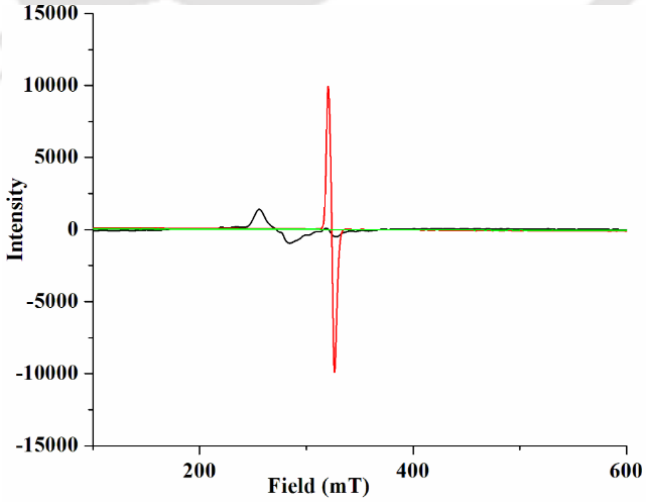

Figure A4.18. X-band EPR spectral monitoring of the reaction of complex **5.1a** with *m*CPBA in CH_2Cl_2:CH_3CN (1:4, v/v) solution at 77 K [complex **5.1a** (black), intermediate (red) and final (green)].

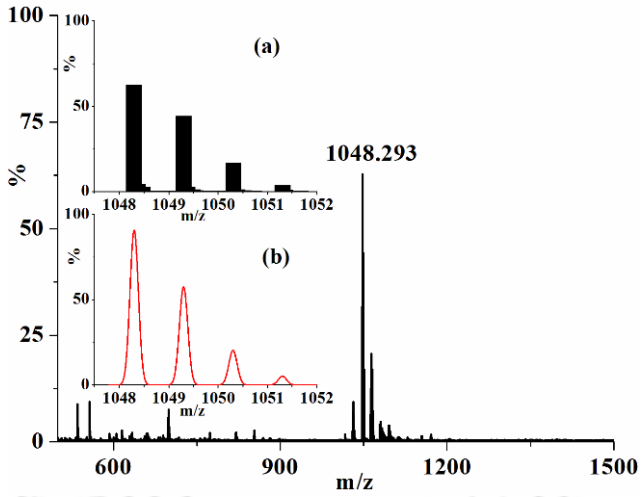

Figure A4.19. ESI-mass spectrum of the reaction mixture of complex **5.1a** with *m*CPBA in acetonitrile at -40 °C [Inset: (a) experimental and (b) simulated isotopic distribution pattern].

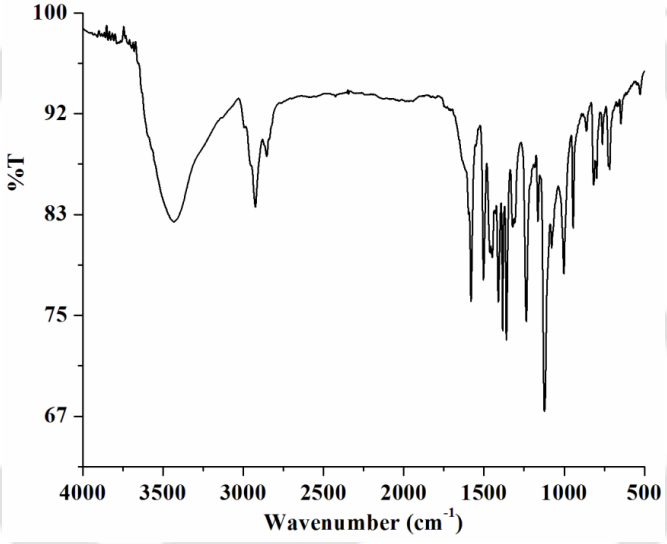

Figure A4.20. FT-IR spectrum of complex **5.3** using ATR probe.

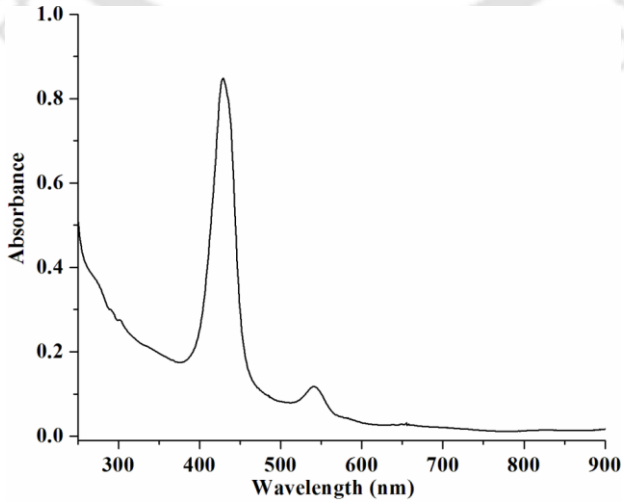

Figure A4.21. UV-visible spectrum of complex **5.3** in CH_2Cl_2 at room temperature.

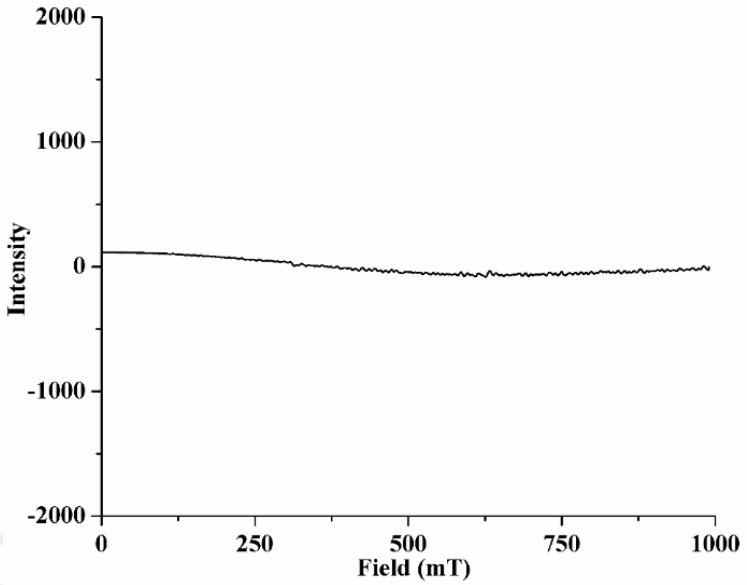

Figure A4.22. X-band EPR spectrum of complex **5.3** in CH_2Cl_2 at 77 K.

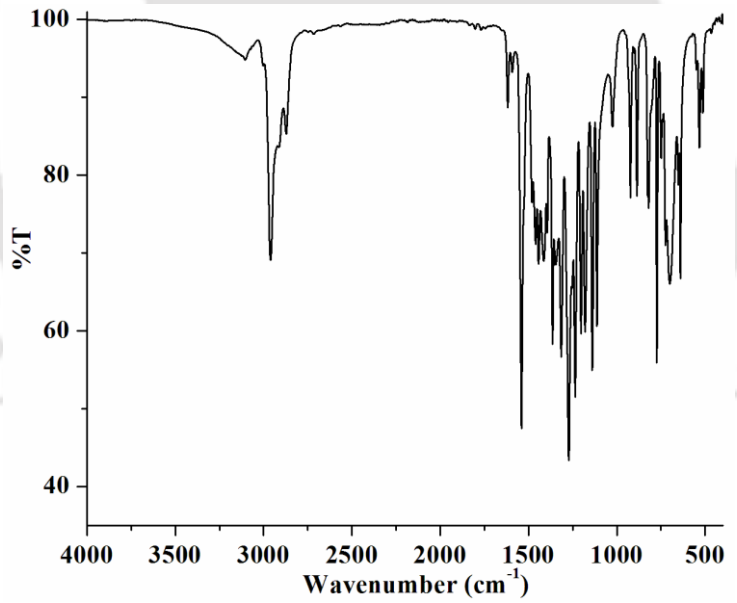

Figure A4.23. FT-IR spectrum of 2,4-di-*tert*-butyl-6-nitrophenol using ATR probe.

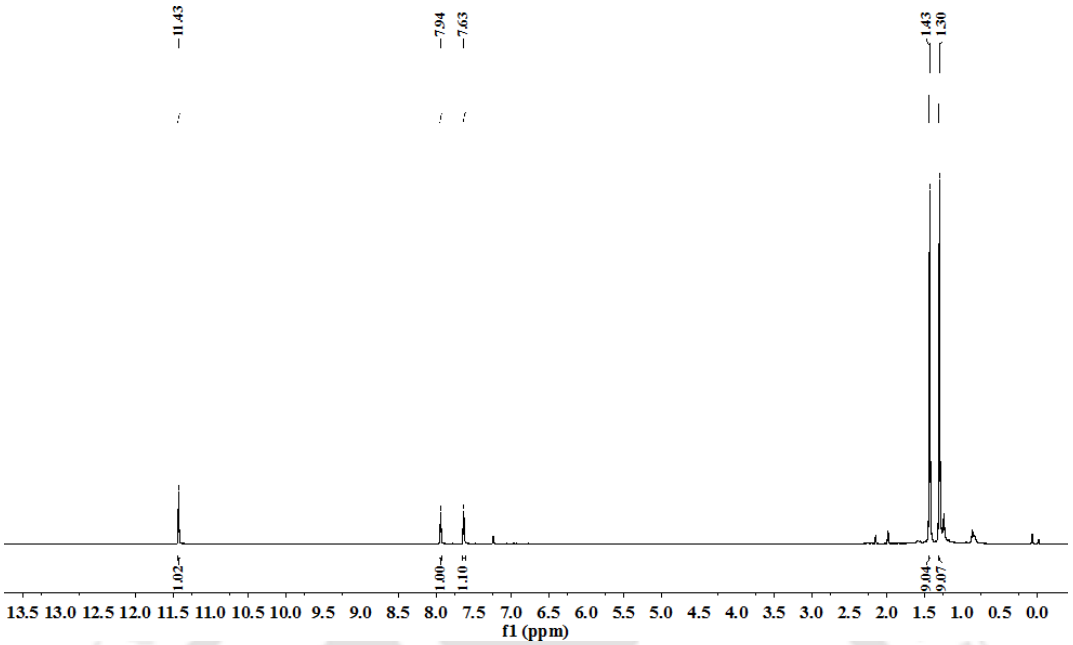

Figure A4.24. ^{1}H-NMR spectrum of 2,4-di-*tert*-butyl-6-nitrophenol in $CDCl_3$.

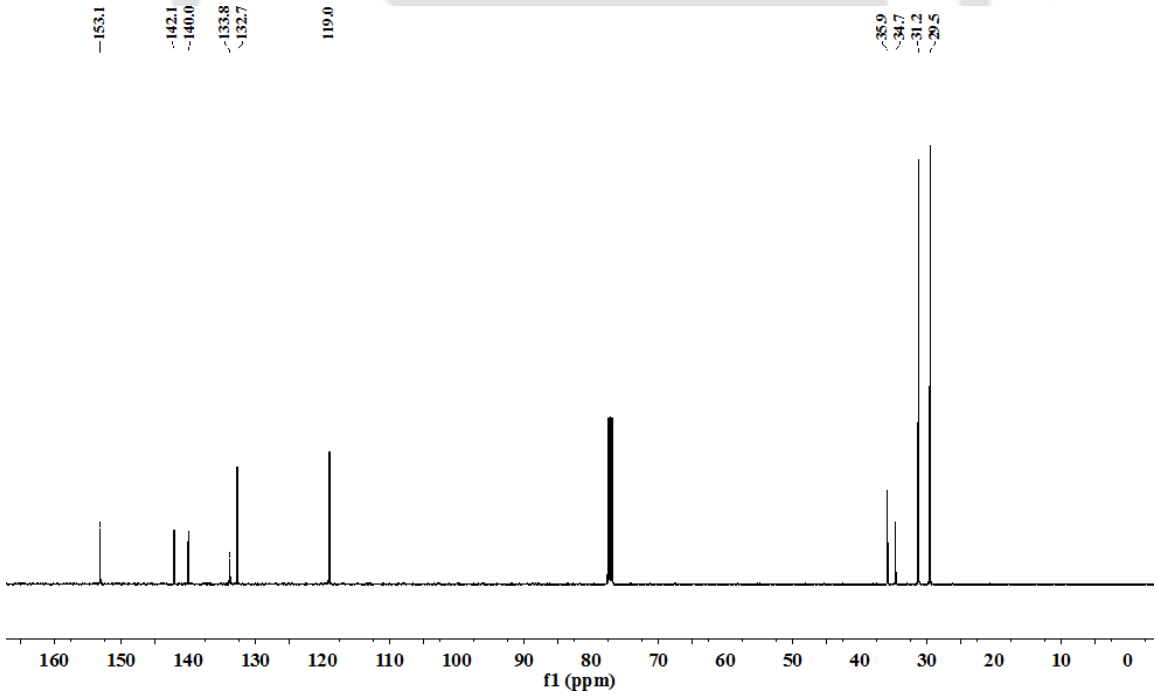

Figure A4.25. ^{13}C-NMR spectrum of 2,4-di-*tert*-butyl-6-nitrophenol in $CDCl_3$.

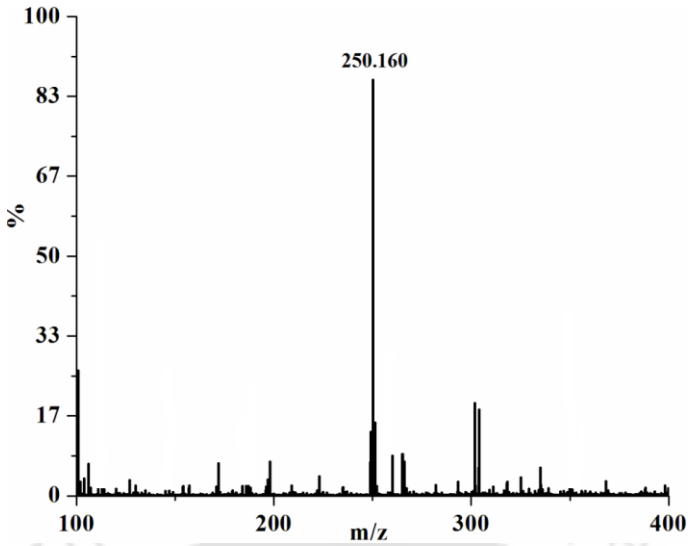

Figure A4.26. ESI-mass spectrum of 2,4-di-*tert*-butyl-6-nitrophenol in CH_3CN.

Table A4.1: Crystallographic data for complexes **5.1a**, **5.1** and **5.2.**

	5.1a	**5.1**	**5.2**
Formulae	$C_{56}H_{52}CoN_4O_{12}$	$C_{56}H_{52}CoN_5O_{13}$	$C_{56}H_{52}CoN_6O_{16}$
Mol. Wt	1031.94	1061.95	1123.96
Crystal system	Triclinic	Triclinic	Triclinic
Space group	P -1	P 1	P -1
Temperature/K	296	296	296
Wavelength/Å	0.71073	0.71073	0.71073
a/ Å	7.879(5)	7.9359(11)	7.9543(15)
b/ Å	12.946(8)	12.8765(18)	12.862(2)
c/ Å	14.269(9)	14.309(2)	14.317(3)
α/°	92.022(17)	91.942(4)	87.968(5)
β/°	103.569(17)	104.883(4)	74.593(5)
γ/°	91.798(17)	91.693(4)	88.483(5)
V/ $Å^3$	1412.8(15)	1411.2(3)	1411.1(5)
Z	1	1	1
Density/Mgm^{-3}	1.213	1.250	1.323
Abs. Coeff. /mm^{-1}	0.365	0.369	0.377
Abs. Correction	Multi-scan	Multi-scan	Multi-scan
F(000)	539.0	554.0	585.0
Total no. of reflections	4906	9842	4908

Reflections. $I > 2\sigma(I)$	4412	8418	4312
Max. 2θ/°	24.999	24.997	24.999
Ranges (h, k, l)	-9≤ h ≤ 9 -15 ≤ k ≤ 15 -16 ≤ l ≤ 16	-9≤ h ≤ 9 -15 ≤ k ≤ 15 -16 ≤ l ≤ 16	-9≤ h ≤ 9 -15 ≤ k ≤ 15 -16 ≤ l ≤ 16
Complete to 2θ (%)	98.5	99.3	98.5
Refinement method	Full-matrix least-squares on F^2	Full-matrix least-squares on F^2	Full-matrix least-squares on F^2
Goof(F^2)	1.147	1.069	1.097
R indices [$I > 2\sigma(I)$]	0.0783	0.0456	0.0655
R indices (all data)	0.0865	0.0557	0.0743

Table A4.2: Selected bond lengths (Å) of complexes **5.1a**, **5.1** and **5.2.**

Atoms	**5.1a**	**5.1**	**5.2**
Co1-N1	1.977(3)	1.973(7)	1.983(3)
Co1-N2	1.976(3)	1.954(7)	1.980(3)
Co1-N3	-	1.971(6)	1.951(4)
Co1-N4	-	1.985(6)	-
Co1-N5	-	2.034(6)	-
N2-C28	1.378(4)	-	-
N2-C25	1.380(4)	-	-
N3-O7	-	-	1.365(9)
N3-O8	-	-	1.096(11)
N3-O9	-	-	0.942(16)
O1-C2	1.373(4)	-	-
O1-C19	1.406(6)	-	-
N5-O13	-	1.218(9)	-
N1-C11	1.384(4)	-	-
N1-C8	1.382(4)	-	-
O2-C3	1.376(4)	-	-
O2-C20	1.408(6)	-	-
C1-C2	1.394(5)	1.351(12)	1.395(5)
C2-C3	1.388(5)	-	1.387(6)
C3-C4	-	-	1.383(6)
C4-C5	-	-	1.396(5)

C5-C6	1.378(5)	-	1.374(5)
C6-C7	1.512(4)	-	-
C6-C1	1.370(5)	-	-

Table A4.3: Selected bond angles (°) of complexes **5.1a**, **5.1** and **5.2**.

Atoms	**5.1a**	**5.1**	**5.2**
N2-Co1-N2	180.0	-	180.0
N2-Co1-N1	89.43(11)	91.2(3)	90.12(11)
N1-Co1-N1	180.0	-	180.00(16)
N2-Co1-N3	-	89.2(3)	89.22(13)
Co1-N3-O7	-	-	129.1(5)
Co1-N3-O8	-	-	116.7(6)
Co1-N3-O9	-	-	118.1(9)
N2-Co1-N4	-	179.1(4)	-
N2-Co1-N5	-	91.0(2)	-
N3-Co1-N1	-	179.4(4)	90.38(13)
N1-Co1-N5	-	92.3(2)	-
N2-C28-C27	110.4(3)	-	-
N2-C28-C27	110.4(3)	-	-
N2-C28-C7	125.5(3)	-	-
N2-C25-C12	125.9(3)	-	-
C2-C1-C6	120.2(3)	-	-
C3-C2-C1	119.8(3)	119.5(7)	-
C4-C3-C2	119.5(3)	120.5(7)	-
C4-C5-C6	118.9(3)	120.0(8)	-
C5-C6-C1	120.7(3)	-	-
C6-C7-C8	119.3(3)	119.4(8)	117.6(3)
C8-C9-C10	107.4(3)	-	-
C9-C10-C11	107.7(3)	-	-
C10-C11-C12	124.9(3)	-	-

List of Publications

(1) "Can a Nitrosyl of a Mn(II)-Porphyrin Complex Release Nitroxyl/HNO?". Mazumdar, R.; Saha, S.; **Samanta, B**.; Mondal, B. *Inorg. Chem.* **2021**, *60*, 18024.

(2) "Reaction of a $\{Co(NO)\}^8$ complex with superoxide: Formation of a six coordinated $[Co^{II}(NO)(O_2^{-})]$ species followed by peroxynitrite intermediate". Mazumdar, R.; Mondal, B.; Saha, S.; **Samanta, B**.; Mondal, B. *J. Inorg. Biochem.* **2022**, *228*, 111698. (Invited article)

(3) "Reaction of a nitrosyl complex of Mn(II)-porphyrinate with superoxide: NOD activity is favoured over SOD activity".

Mazumdar, R.; Saha, S.; **Samanta, B**.; Ghosh, R.; Maity, S.; Mondal, B. *Dalton Trans.* **2023**, *52*, 7917.

(4) "Sixth Ligand Induced HNO/NO^- Release by a Five-Coordinated Cobalt(II) Nitrosyl Complex Having a $\{CoNO\}^8$ Configuration".

Saha, S.; Maity, S.; Mazumdar, R.; **Samanta, B**.; Ghosh, R.; Guha, A.; Mondal, B. *Inorg. Chem.* **2023**, *62*, 17074.

(5) "Reaction of a Co(III)-peroxo complex with nitric oxide: putative formation of a peroxynitrite intermediate".

Samanta, B.; Ghosh, R.; Mazumdar, R.; Saha, S.; Maity, S.; Mondal, B. *Dalton Trans.* **2023**, *52*, 15815.

(6) "Reaction of non-heme iron nitrosyl with dioxygen: Self-killing through NOD-like activity".

Ghosh, R.; Mazumdar, R.; **Samanta, B**.; Saha, S.; Mondal, B. *Inorg. Chem.* (Communicated).

(7) “Reaction of a Nitrosyl Complex of Co(II)-porphyrin with Hydrogen peroxide: Formation of a Porphyrin Radical Cation”.

Samanta, B.; Saha, S.; Ghosh, R.; Maity, S.; Mondal, B. (Communicated).

(8) “Photo-induced nitroxyl anion/HNO release from a nitrosyl complex of Mn(II)-porphyrinate”.

Saha, S.; Maity, S.; **Samanta, B**.; Ghosh, R.; Bhattacharyya, K.; Mondal, B. (Communicated).

(9) “Stable nitrous oxide complexes of Cu(II)”.

Borah, D.; Deka, H.; **Samanta, B**.; Guha, A.; Mondal, B. (Communicated)